Earth Observation for Environmental Monitoring

41st EARSeL Symposium

6th EARSeL Workshop on Developing Countries

13-16 September 2022, Paphos, Cyprus

Symposium Book of Abstracts

Organisers:

About EARSeL

EARSeL is a scientific network of European remote sensing institutes, coming from both academia and the commercial/industrial sector. EARSeL is unique in that it represents the interests of these institutes rather than individuals. Currently, there are about 150 member laboratories.

Every year EARSeL organizes thematic Workshops of Special Interest Groups (SIGs), but the main meeting is the annual Symposium, which aims to indicate the current trends in remote sensing. All scientists, professionals and researchers involved or interested in the themes of the Symposium are strongly encouraged to present papers according to the listed topics.

We warmly welcome you to be part of this exciting event!

ERATOSTHENES Centre of Excellence

A new, autonomous, and self-sustained Centre of Excellence, namely ERATOSTHENES Centre of Excellence of the Cyprus University of Technology (CUT) has been established through the 'EXCELSIOR', H2020 Widespread Teaming Phase 2 project. The newly established centre has been created as a result of upgrading the existing Remote Sensing and Geo-Environment Lab, which has been operating within the Department of Civil Engineering and Geomatics of the Cyprus University of Technology since 2007.

The vision of the ERATOSTHENES Centre of Excellence is to become a world-class Digital Innovation Hub for Earth Observation, space technology and Geospatial Information and to be the reference Centre in the Eastern Mediterranean, Middle East, and North Africa.

The Digital Innovation Hub will create an ecosystem which combines state-of-the-art remote sensing, data management and processing technologies, cutting – edge research opportunities, targeted education services and promotion of entrepreneurship. In order to be dynamic and innovative, the Digital Innovation Hub will be based on two major infrastructures, which are a Satellite Ground Receiving Station and a Ground-based atmospheric remote sensing station. ERATOSTHENES Centre of excellence is paving the way for Cyprus to enter the space arena.

Cyprus University of Technology

The Cyprus University of Technology (CUT) is a public university founded in Limassol in 2003 and consists of six faculties. Times Higher Education World University Rankings for 2018/19 ranked the Cyprus University of Technology in the top 301-350 universities of the world; the University also received the highest score among all universities in Cyprus and Greece. Cyprus University of Technology (CUT) enrolled its first students in 2007. With its orientation towards applied research, the University aspires to establish for itself a role in support of the state and society in their efforts to confront problems, which cover all areas of science and technology. CUT is an advanced University equipped with the most modern infrastructures and technological equipment which makes it possible to be the strongest on the island in research, with specialized units directed by distinguished professionals.

EARSeL 2022 Local Organising Committee

Prof. Diofantos Hadjimitsis, ECoE

Dr. Christiana Papoutsa, ECoE

Ms. Eleni Loulli, ECoE

Mr. Stelios Neophytides, ECoE

Mr. Georgios Leventis, ECoE

Mr. Christos Theocharidis, ECoE

Dr. Kyriakos Themistocleous, ECoE

Ms. Maria Prodromou, ECoE

Dr. Christodoulos Mettas, ECoE

Mr. Evagoras Evagorou, ECoE

Mr. Andreas Christofi, ECoE

Ms. Despina Makri, ECoE

Prof. Phaedon Kyriakidis, CUT & ECoE

Dr. Athos Agapiou, CUT & ECoE

Dr. Chris Danezis, CUT & ECoE

Dr. Evangelos Akylas, CUT & ECoE

Dr. Nicholas Kyriakides, CUT & ECoE

Prof. Andreas Anayiotos, CUT & ECoE

Dr. Kyriacos Neocleous, CUT & ECoE

Dr. Argyro Nisantzi, ECoE

Dr. Marios Tzouvaras, ECoE

Mrs. Heide Bierbrauer, EARSeL

Table of Contents

Keynote Speakers

Prof. Maria Antonia Brovelli

Politecnico di Milano, Italy

Prof. Maria Antonia Brovelli, is a professor of GIS at the Politecnico di Milano (PoliMI), member of the School of Doctoral Studies in Data Science at "Roma La Sapienza" University. She was the Head of the Geomatics Laboratory of PoliMI (1997- 2011) and the Vice-Rector of PoliMI for the Como Campus (2011-2016).

She is the chair of ISPRS WG IV/4 "Collaborative crowdsourced cloud mapping (C3M)"; a former member of ESA ACEO (Advisory Committee of Earth Observation); co-chair of the United Nations Open GIS Initiative, Chair of the UN-GGIM (Global Geospatial Information Management) Academic Network, mentor of the PoliMI Chapter of YouthMappers (PoliMappers). Moreover, she is the Associate Editor of ISPRS International Journal of Geo-Information Responsible for the area of Geospatial Artificial Intelligence.

Dr. Christian Geiss

DFD-DLR, German

Christian Geiss (M'15) received an M.Sc. degree in applied geoinformatics from the Paris Lodron University of Salzburg, Salzburg, Austria, in 2010 and the Ph.D. degree (Dr. rer. nat.) from the Humboldt University of Berlin, Berlin, Germany, in 2014. Since 2010, he is with the German Remote Sensing Data Center (DFD) of the German Aerospace Center (DLR), where he currently is head of the research group "georisks".

His research interests include the development of machine learning methods for the interpretation of earth observation data, multimodal remote sensing of the built environment, exposure and vulnerability assessment in the context of natural hazards, as well as techniques for automated damage assessment after natural disasters.

Prof. Gilberto Camara

National Institute for Space Research, Brazil

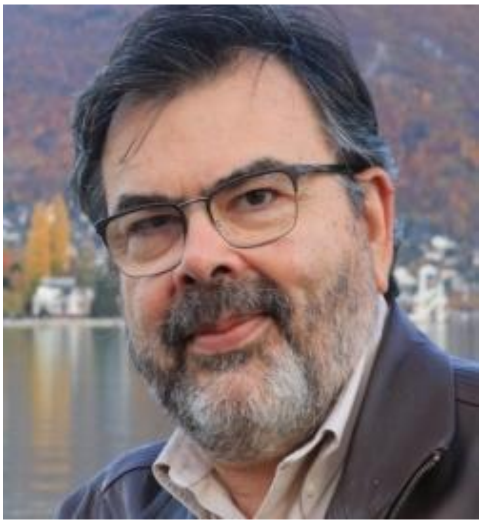

Prof. Dr. Gilberto Camara is a researcher on Geoinformatics and Land Use Change in Brazil's National Institute for Space Research, where he was General Director (2006-2012). He was Director of the Secretariat of the Group on Earth Observations (GEO) from July 2018 to June 2021. Renowned for promoting free access to geospatial data and software and for setting up an efficient satellite monitoring of the Brazilian Amazon rainforest.

In recognition for his works, he was made a Dr. Honoris Causa by the University of Munster (Germany), Chevalier de la Ordre National du Merite of France, and got the Pecora Award from USGS and NASA. His current research interest is in machine learning methods for big Earth observation data analysis.

Prof. Ioannis Gitas

Aristotle University of Thessaloniki, Greece

Prof. Dr. Ioannis Gitas is the Director of the Laboratory of Forest Management and Remote Sensing, Aristotle University of Thessaloniki, Greece and the Chairman of the Aristotle University Forest Administration and Management Fund.

Ioannis, an elected fellow of the Cambridge Philosophical Society, received his PhD and MPhil degrees in GIS and Remote Sensing from the Department of Geography, Cambridge University U.K., and the BSc Hons degree in Forestry and Natural Environment from the Aristotle University of Thessaloniki, Greece. His research has focused on remote sensing and GIS applications in environmental monitoring, with emphasis on forest fire management, land cover/land use mapping and change detection.

Sponsors Session

Long term changes identification and analysis of river deltas and riparian zones using time-series multispectral data

Christos Kontopoulos [12], Dimitra Kitsiou [2], Stavros Chlorokostas [1], Vasiliki Charalampopoulou [1], Nikos Grammalidis [3], Anastasios Tzepkenlis[3]

[1]Geosystems Hellas S.A., Athens, Greece

[2] Dept. Of Marine Sciences, University of the Aegean, Mytilene, Greece

[3]Information Technologies Institute, Center for Research & Technology Hellas, Thessaloniki, Greece

Keywords (5): Remote Sensing, Earth Observation, Coastal Monitoring, Climate Change

The challenge

Coastal riparian zones and river deltas usually demonstrate extreme coastline changes in terms of water extent to inland territories through flood events, low and high tides, the climate and the specific environmental characteristics of an area etc. Nowadays the plethora of Earth Observation assets – data and technological tools - provide a unique opportunity to establish methodological frameworks for the development of efficient and sustainable monitoring solutions upon environmentally fragile regions. In many cases even medium spatial resolutions are deemed adequate to this end, such as Copernicus ESA and Landsat derived data. EPIPELAGIC is a project (project code: T7ΔKI-00160) with the main object and goal of monitoring coastal and riparian zones and ecosystems for their resilience and adaptation to climate change and its effects, by exploiting a variety of data from different sources, for the development of an online Decision Support System platform.

Methodology

EPIPELAGIC's project study corresponds to an area of 762 km^2. It concerns the coastal area of Thermaikos Gulf and includes part of the city of Thessaloniki and the Axios Delta National Park. This park is of high ecological importance and its protection has been included in the Ramsar Convention as a Wetland of International Importance and in the network of Natura 2000 sites. For the scope of monitoring the coastal environment for the full period of the past 20 years, a continuous flow of satellite data and information needed to be available. To this end, all available time series data from three different Landsat missions were selected and specifically Landsat 5TM, 7 and 8. Multispectral datacubes were generated with the exploitation of additional spectral indices (NDVI, NDWI) while additional steps to this task include i) atmospheric correction ii) layer stacking and iii) image clipping to AOI. Each generated scene is classified into two classes through an unsupervised classification via k-means algorithm. Average mean maps for several different periods are generated via the aggregation of each scene - for various different temporal periods. Finally, a forecasting approach was also followed via a dedicated training of a novel LSTM neural network. The network is capable to extract the future state of the coastline as it is feeded with all previous scenes as training samples.

Results

All implemented technical steps that have been carried out and reported through this chapter have been executed through a series of Python-developed functions in a unified script. To this end, Python libraries such as gdal, openCV, rasterio, sklearn, pytorch, pandas etc were widely utilized in this study. The main outputs produced from the timeseries datacubes, are the Yearly Average probability maps for the years 2000 to 2020. Additionally, a set of five-year composite maps has been generated and also their respective change detection maps for every 5year interval in order to extract long-term changes on the coastline environment that are independent from temporal tide and weather related phenomena. The final output of this study concerns the extraction of a coastline's future state derived from an LSTM training methodology. The model successfully predicted the coastline extend for the year 2020 while its comparison with the unsupervised classification result for the same year resulted to great statistical agreement on two different validation procedures with kappa coefficient scores of i) 85.9 % for high variance regions and ii) 91.4% for a 250m coastal buffer zone.

Outlook for the future

In this study we propose a complete methodological framework for the effective monitoring, management and facilitation of decision making on coastal and river riparian zones, such as river deltas. This framework is easily adaptable and can be intergraded to existing solutions as it exploits open access data and methodologies. Multispectral timeseries data of the past 20 years have been analyzed with the use of a simplified Python automated and semi-automated image processing workflows in order to assess a series of change detection maps in coastline environments. Future steps for this study include: i) the application of this methodology on wider and more challenging case studies such as the EPIPELAGIC project case study, ii) the integration of additional EO multispectral data such as Copernicus Sentinel 2 and recently launched Landsat 9, iii) the investigation of different network architectures and the use of ground truth information as an additional validation procedure.

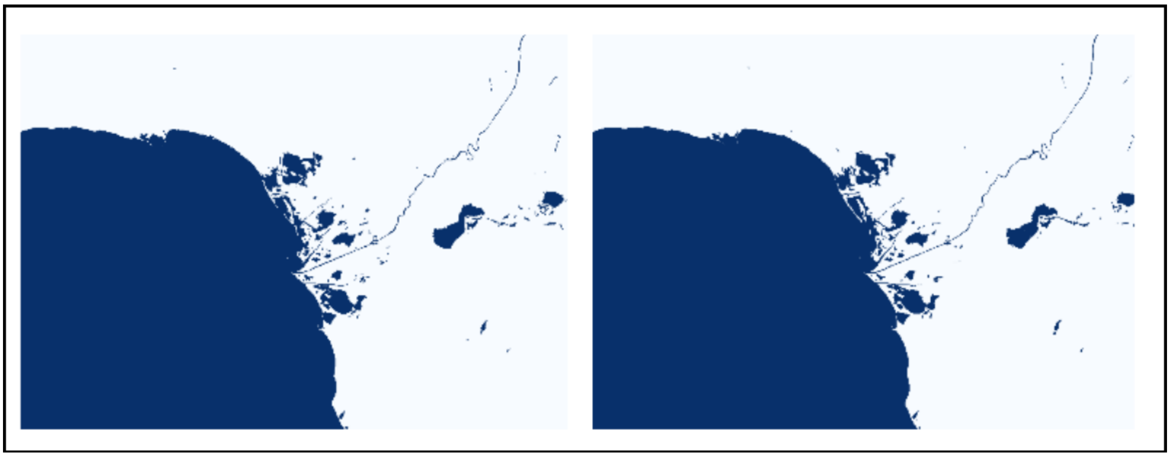

Figure Left - Binary output from unsupervised classification, Right - Binary output LSTM

Addressing the Use of EO and Remote Sensing Technologies to Assess Economic Indicators and Identify Economy Trends - Monitoring Cyprus Economy by Space (Micros)

Christos Kontopoulos [1], Thomas Papakosmas[1], Vasiliki Charalampopoulou [1], Giovanni De Angelis[2], Stelios Zervos[3]

[1]Geomatics (Cyprus) Ltd., Nicosia, Cyprus

[2] Space Systems Solutions (S3) Ltd., Nicosia, Cyprus

[3]Department of Public Works, Ministry of Transport, Communications And Works, Nicosia, Cyprus

Keywords (5): Earth Observation, Remote Sensing, Economy, Statistical data, Correlation analysis

The challenge

In the context of the growing interest for “Space Economy”, policymakers, researchers and private actors operating in economy and finance fields are increasingly interested in how space technologies can be linked to socioeconomic impacts, in order to provide nowcasting and forecasting assessment for the global and local economy. MICROS (ESA funded project-ESA Contract No. 4000136060/21/NL/SC) addresses the use of remote sensing assets and Earth Observation data, combined with econometric models, to assess a series of economic indicators suitable for monitoring economy trends at different geographical scale. This method can potentially provide these near real-time indicators in case of emergencies, where data are not fully reliable, available, or provided with large time delay, filling this temporal gap. Our approach delivers a well-documented correlation analysis between economic statistical data and data derived from EO processing methodologies for Cyprus.

Methodology

Based on end-user requirements feedback given the form of a questionnaire, the application scenarios to be investigated were selected by considering different sectors, but mainly focusing on tourism and trade, which provide a good image for the economic impact of lockdowns, and specifically for Cyprus which relies heavily on its maritime trade and activities.

Due to the strict timeline of the project and considering its nature (i.e. a feasibility study), five easy-to-execute methods were chosen:
1) Ship Detection (SNAP “OOD” algorithm, Sentinel-1 SAR data),
2) Truck (Freight Transport) Detection (Pixel offset exploitation, Sentinel-2 optical imagery, Cypriot Highways),
3) Water Quality Assessment (SNAP “C2RCC” algorithm, Sentinel-2 optical imagery, Chl-a & TSM concentrations in ports),
4) General Night-time Activity (AOI zonal statistics, VIIRS-DNB upward radiance) and
5) Atmosphere Quality Assessment (CAMS re-analysis data, Nicosia).

Free large scale data and open source licences were preferred. For each application and for the respective area of interest investigated, a time series for pre- and post- Covid-19 pandemic was derived, ready to be correlated with economic statistical data.

A development of econometric models was carried out, by linking socio-economic factors and EO satellite data through a correlation analysis, aiming to study the economic patterns (and possible shifts) occuring after the COVID-19 pandemic onset in March 2020.

Results

Final data sets are delivered as monthly aggregated time-series during the lockdown period for the years 2018-2021, ready to be correlated with similar economic statistical data.

The choice of specific pairs of socio-economic parameters and EO observables is based on their relationships from the theoretical economic and empirical analyses. Our analysis focused mostly on datasets and observables, which illustrated the significant changes during COVID-19 pandemic. Utilizing the EO data which showed the best correlation –such as nightlights, see figure-, the economic factors analysed and mostly affected by the pandemic are GDP, tourism activities and associated employment.

Gaps in the time series of some EO parameters prevented the development an econometric model. However, the analysis showed that some significant positive correlations, such as volumes of export vs. the number of ships (proxy for external trade) or GDP vs nightlights (proxy for national economy). A panel data model built also showed a positive correlation between employment vs. nighttime lights mean radiance appears.

Concluding, with all its intrinsic limitations pointed out, it is shown this is a viable approach to obtain proxies for economic activities and build econometric models, not limited to correlations but where possible up to panel data models, with EO data. This is an encouragement to apply this data collection and analysis approach to other realities.

Outlook for the future

Prospect to expand on the main idea of the project is found in various ways, such as translating the Earth Observation data extraction methodologies to seamless automated processes, by utilizing modern open-source tools, and also by integrating additional and more diverse Earth Observation and economic statistical data at different spatial and temporal scales.

Furthermore, the possibility of developing an autonomous platform should be explored, which combines Computer vision (CV) and artificial intelligence (AI) tools with high-resolution satellite imagery to provide a new kind of «fast-data» that can be linked to economic development via fast and reliable economical insights. This prototype service, ready to be accessed by the end user, could be based on Copernicus and contributing data, automatic image processing using AI, statistical modelling and correlation procedures, all integrated in a unified IT platform capable of providing econometric nowcasting and forecasting data.

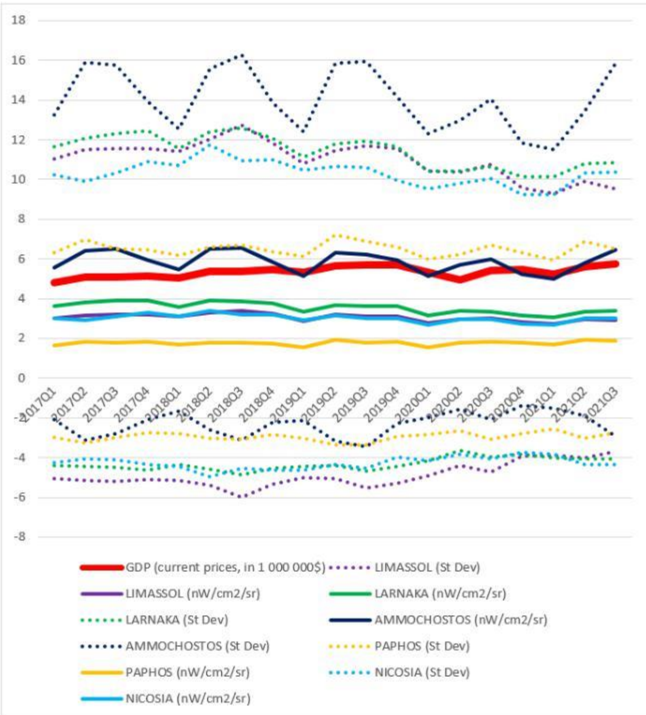

	Overall	Before COVID	After COVID
Limassol	-0,00	0,13	0,06
	(0,995)	(0,675)	(0,903)
Larnaka	-0,15	-0,14	0,18
	(0,526)	(0,648)	(0,725)
Ammochostos	0,25	0,22	0,50
	(0,305)	(0,481)	(0,314)
Paphos	0,41*	0,33	0,61
	(0,079)	(0,269)	(0,196)
Nicosia	-0,00	0,02	0,24
	(0,996)	(0,939)	(0,654)

Figure 1) a) National GDP (current prices, in 100000$) and Nightlights in Cyprus Districts in Q1 2017 – Q3 2021. b) Overall correlation, correlation before (Q1 2017- Q1 2020) and after (Q2 2020 – Q3 2021) COVID-19 pandemic onset for National GDP vs. Nightlights Mean

Radiance in Cyprus Districts. P-value within parentheses. Significance level: *** p<0.01, ** p<0.05, * p<0.1.

Nextland - Next Generation Land Management Services for Agriculture and Forestry

Nuno Grosso[1], Isabelle Piccard[2], Hervé Caumont[3], Luís Filipe Lages[4], David Cordeiro[1], Greg Robson[5], Radoslaw Guzinski[6], Jo Van Brusselen[7], Tord Sorensen[8], Ioannis Manakos[9], Christos Kalogeropoulos[9], Jim Wilson[10], Pieter Janssens[11], Alireza Taravat[12]

[1]Deimos Engenharia, Portugal

[2]VITO, Belgium

[3] Terradue, Italy

[4] Nova School of Business Economics, Portugal

[5]VanderSat Planet, Netherlands

[6]DHI, Denmark

[7]European Forest Institute, Finland

[8]Science and Technology AS, Norway

[9]Centre for Research and Technology Hellas, Greece

[10]SoilEssentials, UK

[11]Soil Service of Belgium, Belgium

[12]Deimos Space UK, UK

Keywords (5): agriculture, forestry, EO services, marketplace

The challenge

The partial success in the uptake of Earth Observation (EO) -based downstream agriculture and forestry products in the last few years relied mainly on approaches focused on national/regional end-users or at most interface institutions that represent interests from wider group of end users. These regional approaches even include at times a vertical integration of EO products with downstream products provided by a specific agriculture and forestry consultancy institution. These methods, while effective at smaller scales, often lead to EO service solutions tailored to the needs of a specific set of end users, with a strong national/regional bias, due to natural associations between EO Service Providers (SPs) and the agriculture and forestry stakeholders within one geographical area. This fragmented ecosystem limits the capability to generalise agriculture and forestry service requirements, leading to a limited scalability to other markets and higher deployment costs.

Methodology

To shift the EO agriculture and forestry service sector from a regional to a global paradigm, Nextland aims to be a reference Online Store for organizations with technological know-how to serve the agriculture and forestry markets. This Online Store will provide business value by being a) a one-stop-shop for added value SPs (AVSPs) and end-users, b) where they can find unique or bundled EO services for their specific needs. These EO services must serve high accuracy and up-to-date information, as well as be rapid-on-demand, highly customizable, and offered at a competitive price. This one-stop-shop aims to facilitate business processes from the SPs' offers towards the EO downstream market and towards the end-users with technological know-how in forestry and agriculture.

The service and online store evolution is driven by yearly cycles that start with the co-design process with users. The first step is to present the status of the services and the online store in webinars. Then the users fill in a form where they select the services they would like and define a first set of requirements for both the services and online store based on their operational needs. The requirements are passed on to the SPs and online store developers and translated into concrete new functionalities. While these new features are being implemented, there is a continuous test, validation, and feedback cycle between users and providers. Throughout the project more users and stakeholders will help to adapt and customize our services to end-users' needs.

Results

NextLand is engaged with 15 users that include stakeholders in the UK, Belgium, Norway, Spain, Finland, Romania, Denmark, Estonia, Bulgaria, France, and the Netherlands. Their requirements were key to the development of NextLand in these 2 last years and this user base will be enlarged over the course of the next year, when NextLand will start commercial activities.

There are 15 services offered by Nextland, all with a high TRL: a) Vegetation Indices; b) Crop type classification; c) Vegetation Water Content; d) Soil Moisture; e) Biomass Production; f) Crop Phenology; g) Anomaly Detection; h) Potential and Actual Evapotranspiration; i) Crop Water Needs; k) Change Detection - Deforestation; l) Forest Fire Burn Scar; m) Forest Density and Statistics; n) Tree Health indices; o) Forest Classification. These services are framed within nine scenarios, defined together with the users and aligned with their operational activities: 1 - Agriculture: a) Improved crop monitoring & yield prediction; b) Support to irrigation; c) Crop planning optimization; d) Early stress / anomaly detection; 2 - Forestry: a) Clearcutting detection; b) Forest inventory support; c) Fire impact & risk assessment; d) Forest health; e) Forest management.

Services are available in an online store where customers can browse and find information about them and be able to parametrise and trigger individual or bundled services. They can also receive services via a dedicated API and have access to a support service.

Outlook for the future

The official launch of the NextLand online store will happen in October 2022 in several online showcase events open to everyone. From that launch onwards, the online store will support the commercial operations of NextLand, following the roles and responsibilities to be defined in a commercial agreement between the different NextLand partners.

This project has received funding from the European Union’s Horizon 2020 research and innovation programme under grant agreement No 776280.

Special Sessions

Wildfires Monitoring

Organizers:

Arnon Karnieli and Manuel Salvoldi

Summary:

Wildfires are a threat to human health and life as well as the environment. Significant damage can be caused to vegetation, animals, and property. In recent years, because of climate change, fires have intensified and increased in frequency. Therefore, different technologies have been developed for detecting and monitoring various aspects of wildfire, including risk assessment, early detection, active fire detection, gas and aerosol emission, smoke penetration, and temporal dynamics of burned areas. Among all technologies, there is a general agreement that remote sensing methods are essential for providing valuable data for detecting, monitoring, interpreting, and responding to wildfires, from local to global scales.

Topics:

- Wildfire Risk Assessment
- Active Wildfire Management
- Vegetation Recovery Following Wildfire
- Wildfire Environmental Concerns (aerosols, greenhouse gasses)

Scientific Committee:

- Arnon Karnieli, Ben-Gurion University of the Negev
- Manuel Salvoldi, Ben-Gurion University of the Negev
- Nicolas Longepe, European Space Agency

Understanding fire dynamics using FRP: the GEO perspective

Simon Jones [1, 2], Konstantinos Chatzopoulos-Vouzoglanis [1], Karin J Reinke [1, 2], Mariela Soto-Berelov [1,2], Chermelle Engel [1, 2]

[1] Royal Melbourne Institute of Technology (Rmit University), Centre for Remote Sensing, School of Science, Melbourne, Australia
[2] SmartSat Cooperative Research Centre, Australia

Keywords (5): Fire radiative power (FRP), GEO, LEO, intercomparison, fire dynamics

The challenge

Fire Radiative Power (FRP) is an important variable in ecosystem and fire science and has been used in the mapping and monitoring of biomass and fire severity (Wooster et al., 2003). FRP has a long history of LEO observations and associated products. For example, MODIS: Giglio et al., 2016, Kaufman et al., 1998, Wooster et al., 2005; Visible Infrared Imaging Radiometer Suite (VNP14IMGTML): Schroeder and Giglio (2021a,b). Although GEO observations have a larger IFOV (as compared to LEO) they offer an enhanced temporal frequency (10-minutes day-night) giving new insights into fire dynamics and behaviour.

This paper seeks to understand the accuracy offered by GEO observations of FRP by intercomparing these to LEO observations. It then details the extra information content of GEO based observations using case studies of synchronous observations for a range of fires, using the criteria of fractional cover, burn severity and area burned.

Methodology

FRP products from the Himawari, MODIS and VIIRS sensors were compared for a range of fires.

Specifically, the LEO MODIS product MOD14/MYD14 (Giglio et al., 2016), and the LEO VIIRS product VNP14IMG (Schroeder et al., 2014) were compared to the GEO Advanced Himawari Imager (AHI) product BRIGHT_AHI product (Engel et al., 2022 in press). Fires from across Australia were assessed using the criteria fractional cover, burn severity and area burned. Since, previous studies indicated a range of agreements between LEO and GEO FRP: Li et al. (2020) and Xu et al. (2021) found good agreement between GOES-13 and GOES-16 and MOD14/MYD14 FRP at a regional level, while Engel et al., (2020) found more modest agreements between their H8 based observations, we decided to interrogate a range of fires using the criteria fire intensity and fractional cover (as a surrogate for canopy obscuration).

Intercomparison was achieved by comparing both fire detection and FRP observations. Both synchronous, i.e. those common to LEO (MODIS / VIIRS) and GEO (H8), and <u>all</u> GEO (H8) observations to all MODIS / VIIRS observations were compared for a range of fires.

Results

Figure 1 shows the first fire detection dynamics for the Black summer fire complex. This fire complex burnt during 2019-2020, the southern hemisphere summer, in south eastern Australia. In total 12.6 million ha of land (mostly forest) burned. Here we compare the BRIGHT_AHI product and MOD14. The spatial and temporal distribution of the fire first detections is similar r=0.77 p=0.95 but the number of potential observations from AHI is far higher (up to 144 per day). Figure 2 shows the integrated FRP and number of hotspots for AHI and MOD14 respectively. The timing of fire activity and associated FRP is more detailed in the AHI dataset. Overall there is good agreement between MOD14 and AHI_BRIGHT for a range of fires while VIIRS is sensitive to a number of smaller and less intense fires (figure not shown).

Outlook for the future

GEO observations of FRP from sensors such as GEOS-x (the Advanced Baseline Imager), Himawari 8/9 (the Advanced Himawari Imager), GE-KOMPSAT 2A (the Advanced Meteorological Imager) all potentially allow for enhanced surveillance of fire dynamics. Such high temporal observations, with accuracies akin to those of MOD14 should enable the development of a new suite of fire severity and combustion completeness products to aide our understanding of ecosystem processes and fire management.

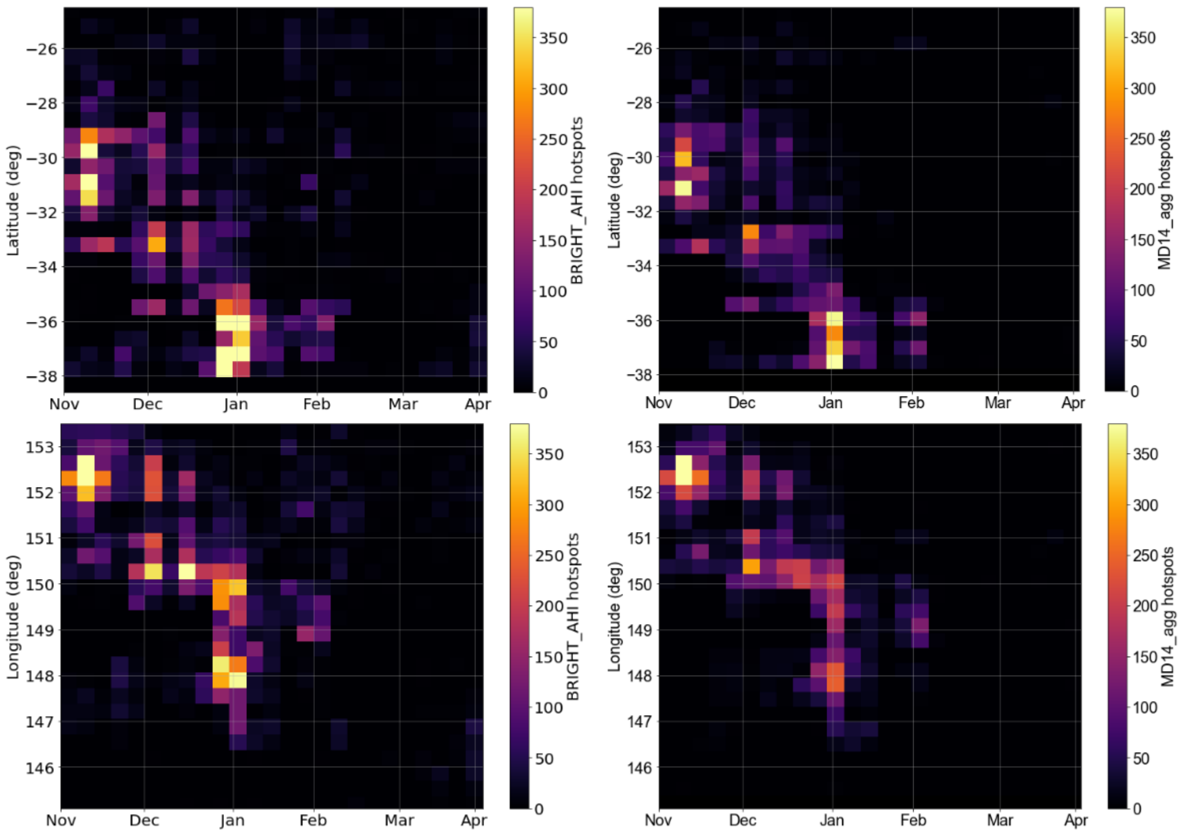

Figure 1 first fire detection dynamics: AHI (left column) and MOD14 (right column), latitude (top row) and longitude (bottom row). Colours represent the number of first detection at each point in time and space.

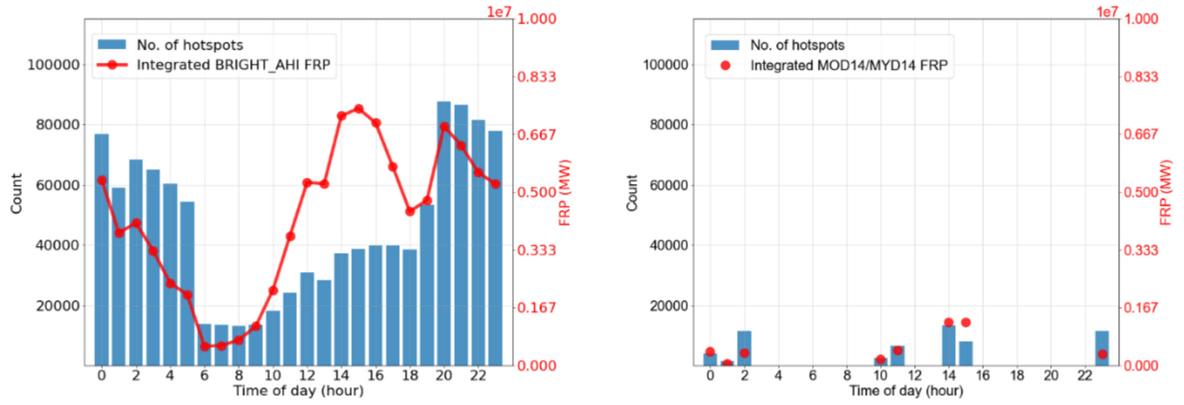

Figure 2 Integrated FRP and number of hotspots: AHI (left panel) and MOD14 (right panel)

Satellite-Based Detection of Potential Post-Fire Regime Shifts in Multiple Dimensions of Ecosystem Functioning

Bruno Marcos[1,2], João Gonçalves[1,2,3], Domingo Alacaraz-Segura[4,5,6], Mário Cunha[7,8], João P. Honrado[1,2,9]

[1] Cibio, Centro De Investigação Em Biodiversidade E Recursos Genéticos, Inbio Laboratório Associado, Campus De Vairão, Universidade Do Porto, 4485-661 Vairão, Portugal

[2] Biopolis Program In Genomics, Biodiversity And Land Planning, Cibio, Campus De Vairão, 4485-661 Vairão, Portugal

[3] Prometheus – Research Unit In Materials, Energy And Environment For Sustainability, Instituto Politécnico De Viana Do Castelo (Ipvc), Avenida Do Atlântico, N.º 644, 4900-348 Viana Do Castelo, Portugal

[4] Iecolab. Interuniversity Institute For Earth System Research (Iista), University Of Granada, Av. Del Mediterráneo, 18006 Granada, Spain

[5] Dept. Of Botany, Faculty Of Sciences, University Of Granada, Av. Fuentenueva, 18071 Granada, Spain

[6] Andalusian Center For The Assessment And Monitoring Of Global Change (Caescg), Universidad De Almería, Crta. San Urbano, 04120 Almería, Spain

[7] Departamento De Geociências, Ambiente E Ordenamento Do Território, Faculdade De Ciências, Universidade Do Porto, 4099-002 Porto, Portugal

8 Institute For Systems And Computer Engineering, Technology And Science (Inesc Tec), Campus Da Faculdade De Engenharia Da Universidade Do Porto, Rua Dr. Roberto Frias, Porto 4200-465, Portugal

[9] Departamento De Biologia, Faculdade De Ciências, Universidade Do Porto, 4099-002 Porto, Portugal

Keywords (5): Resilience, Post-fire recovery, TCT, MODIS, Iberian Peninsula

The challenge

Wildfires can profoundly impact many aspects of ecosystem functioning (matter and energy flows in ecosystems). Changes in fire regimes can decrease ecosystem resilience, leading to regime shifts and ecosystem collapse, exacerbated by environmental changes. Thorough assessments of ecosystem resilience to wildfires are critical to bridging gaps between science, policy, and management. To that end, multi-dimensional satellite-based approaches based on ecosystem functioning offer an integrative view of post-fire resilience, through rapid and quantifiable responses of ecosystems to disturbances, that are more directly connected to ecosystem services. In this study, satellite image time-series were used as surrogates of four key dimensions of ecosystem functioning: primary production, water content, albedo, and sensible heat. Indicators of post-fire recovery were used to detect post-fire regime shifts in each dimension, and to estimate overall multi-dimensional strength-of-evidence.

Methodology

Time-series of Tasselled Cap features (Greenness, Wetness, and Brightness), and Land Surface Temperature were extracted from MODIS products MOD09A1 and MOD11A2 at 500 m, for 2000–2018 (874 images), for all pixels within areas burned (according to MODIS product MCD64A1), in the northwest Iberian Peninsula, in 2005 — a particularly devastating year in this area, coinciding with severe drought. Spurious values (e.g. affected by clouds) were corrected using a Hampel filter. Then, seasonally adjusted time-series and trend components were extracted using Seasonal and Trend decomposition using Loess, and reference intervals were defined from three years before the fire. Next, two post-fire recovery metrics were derived, estimating the time since the fire to: (i) recover to the pre-fire reference levels — "Return-to-Reference Time" (RRT) — i.e., engineering resilience; and (ii) reach stabilization (i.e., change rate lower than a predefined threshold) — "Return-to-Equilibrium Time" (RET) — i.e., ecological resilience. Based on those two metrics, post-fire trajectories were classified into five types: (a) "Return to pre-fire" — equilibrium reached within pre-fire reference interval; (b) "Under-recovery" — stabilized without reaching pre-fire levels; (c) "Over-recovery" — stabilized outside pre-fire levels, after reaching pre-fire levels; (d) "No equilibrium" — pre-fire levels reached, but not stabilized; and (e) "(not detected)" — no recovery detected. Finally, the overall "strength-of-evidence" of potential regime shifts across dimensions was analysed, by counting the number of dimensions (per pixel) corresponding to types (b) or (c).

Results

Overall, most burned pixels were classified as either "Return to pre-fire" (35%–78%) or "(not detected)" (5%–44%), within each dimension of ecosystem functioning (see Figure), suggesting an overall high resilience capacity of ecosystems in the study area. Furthermore, the main effects on primary production, water content, and albedo can be linked to the sudden removal of vegetation. On the other hand, the high percentage of “(not detected)”, and low percentages of “Under-recovery” (2%) and “Over-recovery” (<1%) obtained for sensible heat show that the effects of wildfires on that dimension are mostly transient. Nevertheless, considerable percentages of the studied burned areas exhibited potential regime shifts, with the highest values of “Over-recovery” obtained for primary productivity (13%) and albedo (9%), which may be translating alterations such as land cover conversions, land abandonment, biological invasions, and management operations. On the other hand, the highest values of “Under-recovery” observed for water content (19%) and albedo (15%) may be related to loss of moisture in canopy moisture loss, delayed vegetation mortality, and sometimes persistent increases in the concentrations of impervious, solar radiation-absorbing materials. Finally, the percentages of “No equilibrium”, which may translate to either incomplete recovery or unforeseen interferences on the detection of post-fire inflexion points, were low across dimensions.

Outlook for the future

Overall, our results successfully captured different patterns of post-fire processes in ecosystem functioning, pointing to a high degree of complementarity between different dimensions, and highlighting the added value of such multi-dimensional approaches. We argue that our satellite-based approach based on ecosystem functioning can support an enhanced characterization of ecosystem resilience to wildfires, ultimately upholding potential implications for post-fire ecosystem management. Potential applications include regional-scale, spatially explicit prioritizations for management or conservation purposes, and to support more detailed, local-scale assessments. Furthermore, the proposed approach can be applied in a wide range of geographic and environmental contexts, using data from different satellite-sensor platforms. Validation of results through field-collected data such as spectral readings and aerial (“drone”) imagery could further improve the proposed approach.

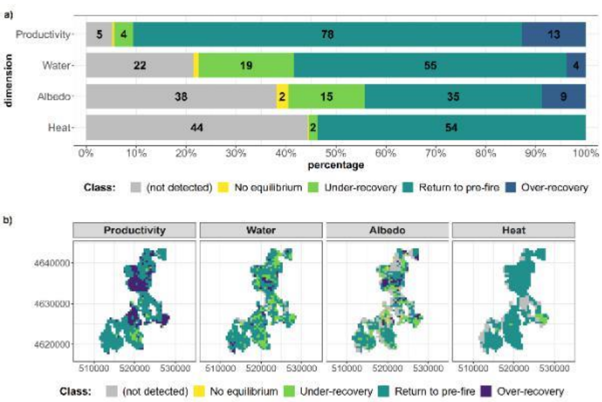

Figure Results for each of the four dimensions of ecosystem functioning considered — primary production (“Productivity”), water content (“Water”), albedo (“Albedo”), and sensible heat (“Heat”): (a) relative frequencies obtained for the five post-fire resilience classes, across all patches burned in 2005 in NW Iberian Peninsula, up until 2018 (note:

numbers in bold are only shown for percentages above 1%); and (b) post-fire recovery and resilience classification map for a selected, illustrative burned area.

Wildfire Damage Assessment Over Arakapas Village in Cyprus Using Sentinel-2 Imagery.

Maria Prodromou[1,2], Kyriacos Themistocleous[1,2], Chris Danezis[1,2], Ioannis Gitas [3], Diofantos Hadjimitsis[1,2]

[1] Department of Civil Engineering And Geomatics, Cyprus University of Technology, Limassol, Cyprus
[2] Eratosthenes Centre of Excellence, Limassol, Cyprus

[3] Department Of Forestry, Laboratory of Forest Management And Remote Sensing, Aristotle University Of Thessaloniki

Keywords (5): fire severity, damage assessment, Sentinel-2, forest fires, earth observation

The challenge

Forest fires are one of the most immediate consequences of climate change affecting forests. Wildfires constitute a critical natural hazard, and they are particularly a threat to human, animal life, and the ecosystem. They lead to land cover change, the disaster of large areas of vegetation, and the contribution of soil erosion. Fires cause significant changes in the structure and the reflection of vegetation as well as to the soil properties that are evident at different wavelengths of the electromagnetic spectrum. Therefore, remote sensing techniques can be used to examine the consequences of fire events.

Mediterranean ecosystems are significantly affected by forest fires as a result of the climate and vegetation present. Cyprus is located in the Eastern Mediterranean, which is an area where forest fires frequently occur, especially during the summer period. Several factors contribute to the increased risk of forest fires, which include prolonged drought, hot summers, strong winds, large slopes of forests and flammable dry vegetation. This study aims to investigate the damage that occurred after the recent fire event near Arakapas village in Cyprus. The fire event started on Saturday, the 3rd of July in the Limassol district near the village of Arakapas, which was finally controlled after less than 24 hours.

Methodology

The methodology is divided into two parts. The first part focus on the burned area estimation and the fire severity. For the first part, a pair of Sentinel-2 images taken before (2/7/2021) and after (27/7/2021) the fire event were used to develop the dNBR (difference Normalized Burn Ratio), which is the most common spectral index for assessing the burn severity and burned area estimation. Furthermore, a cloud masking algorithm based on each sensor's pixel quality assessment band was implemented in order to avoid the probability to have clouds in the study area even though images clear of clouds were selected. For the validation of the fire severity maps, field data was collected for the GeoCBI (Geometrically structured Composite Burn Index) index calculation, which provides a holistic field assessment of fire severity. The second part focuses on the estimation of the short-term regeneration dynamics of vegetation by using monthly time series Sentinel-2 data based on the NBR spectral index. For the purposes of this study, the image processing was performed using custom scripts in the GEE (Google Earth Engine) platform with the JavaScript programming interface. The GEE is a planetary-scale platform for scientific analysis and visualization of geospatial datasets where open-source images acquired by several satellites, including Sentinel-2, Landsat-7, and Landsat-8, are accessible and can be efficiently imported and processed in the cloud without the necessity of downloading the data to local computers.

Results

The area affected by the fire was identified using the dNBR index and the estimated burned area was calculated to be ~40Km^2. The spatial distribution map of the dNBR was classified according to the USGS fire severity levels, where high dNBR values indicate a more severe fire and values near zero and negative values indicate unburned and/or decreased vegetation after the fire. The fire severity map was compared to field measurements of the GeoCBI. Furthermore, the time series shows the general trend of short-term vegetation regeneration dynamics in the study area. Based on the results of the study, the areas characterized by coniferous forest have shown slower recovery than the areas characterized by agricultural land as well as significant areas of natural vegetation that have already begun to recover.

Outlook for the future

The use of spectral indices from Sentinel-2 provides a fast and cost-effective way of monitoring damage from fires and post-fire regeneration. The characterization of the recovery trends provides useful information to forest managers for monitoring and management decisions. The study found significant results regarding the vegetation regeneration dynamics for the burnt area. Further research will include the continuous monitoring of the burnt area. Furthermore, the regeneration dynamics of vegetation for the burnt area will be combined with other related variables, such as fire severity, elevation, land cover etc.

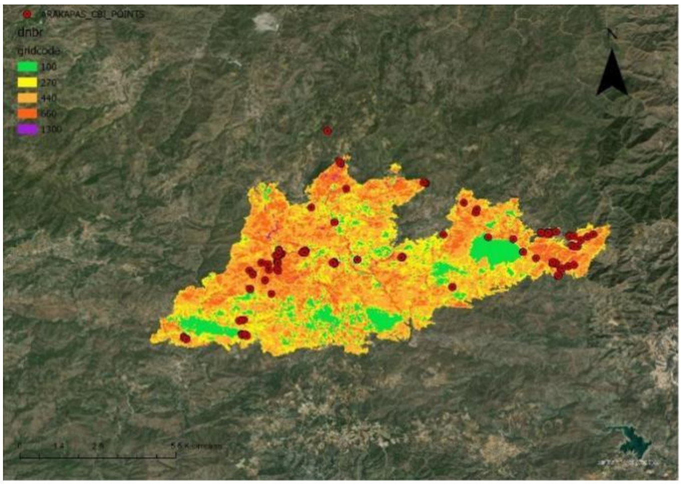

Figure Fire severity mapping using dNBR spectral index on Sentinel-2 images and the field plots for GeoCBI

Acknowledgements

This work has been supported by the project ‘ERATOSTHENES: Excellence Research Centre for Earth Surveillance and Space-Based Monitoring of the Environment-EXCELSIOR’ (https://excelsior2020.eu/) that has received funding from the European Union’s Horizon 2020 research and innovation programme under grant agreement No 857510 (Call: WIDESPREAD-01-2018-2019 Teaming Phase 2) and the Government of the Republic of Cyprus through the Directorate-General for European Programmes, Coordination and Development.

Spatial Consistency Regularized Weakly-Supervised Deep Learning for Wildfire Burned Area Mapping with Low-Resolution

[1]Puzhao Zhang, [1]Yifang Ban

[1]Division of Geoinformatics, KTH-Royal Institute of Technology, Stockholm 11417, Sweden

Keywords (5): Wildfire, Burn areas, Weakly-supervised learning, Spatial Consistency, Inaccurate labels

The challenge

Climate change makes our planet warmer, forest and fuels drier, which may result in more frequent and larger wildfires, and it is critical to quantify wildfire burned areas and carbon release for assessing their environmental impacts. Coarse resolution wildfire burnt areas products have been available on a global scale, such as MODIS 500m and FireCCI 250m monthly burned area products. The open access of Sentinel-1/2 data opens a new era for mapping burned areas at 10-20m resolution. The advances in deep learning make it possible to leverage powerful models that have the capability to handle huge amount of satellite remote sensing data. However, deep learning models often rely on a large amount of accurately labelled data, whereas highresolution or good quality labels are scare in the field of remote sensing. This poses a key challenge: How could we train deep learning models using low-resolution labels to generate medium resolution burned area products? Methodology The proposed weakly supervised learning method for wildfire burned area mapping is presented in Figure 1. Using coarse resolution labels, such as MODIS 500m and FireCCI 250m burned area products, we

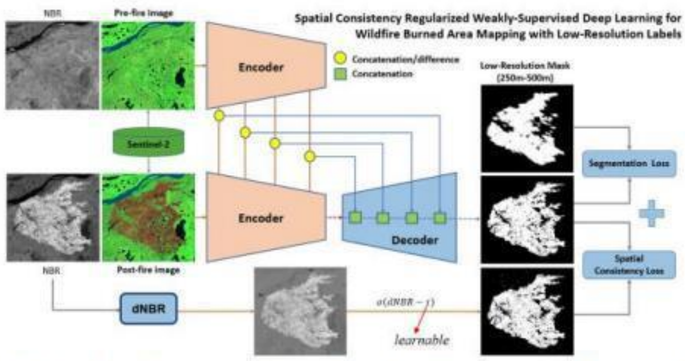

Figure 1: Weakly supervised deep learning for wildfire burned area mapping with coarse labels.

trained deep learning models, including Siamese U-Net to generate 20m spatial resolution burned area products with Sentinel-2 MSI data. Wildfires cause the removal of leaves, branches, and trunks, which would result in a significant decrease in NIR reflectance and an increase in SWIR reflectance, therefore the Normalized burned ratio (NBR) was commonly used to enhance burned areas. For bi-temporal Sentinel-2 images, the pre-fire and post-fire NBR images can be calculated and differentiated to derive the differenced NBR (dNBR), which can highlight the spectral changes caused by wildfires. However, different climate zones or land covers might require different thresholds. Therefore, we introduced a learnable hyperparameter to automatically find the optimal threshold. Then we weighted the spatial consistency loss ( ) and coarse masks-based segmentation loss ( ) to supervise the model learning with another hyperparameter , and the total loss can be written as: = +(1−) +10(−0.1)

Results

We conducted experimental study based on the 2017-2019 wildfires in Canada, Figures 2 and 3 show the effects of the weighting parameter when trained with MODIS 500m labels and FireCCI 250m labels respectively. The best visual results were achieved when = 0.6 on all four example wildfire events. When is too small, significantly more false positive pixels appeared outside the burned areas. If is too large,

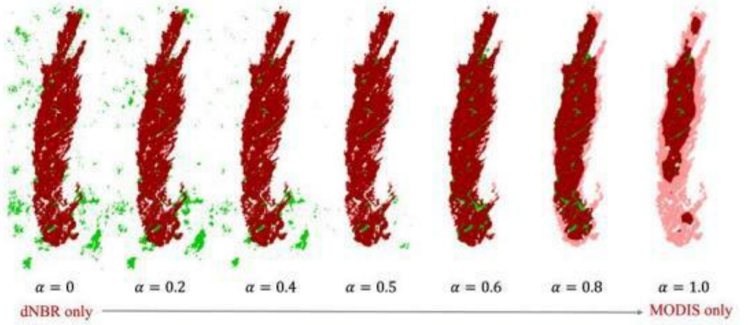

Figure 2: Effects of the weighting coefficient α on wildfire burned area mapping with MODIS labels.

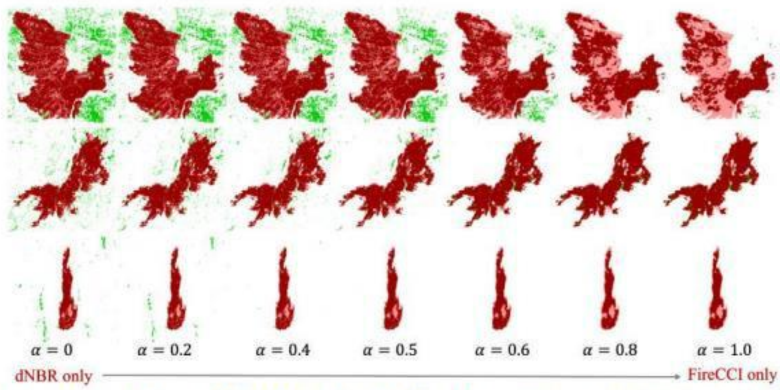

Figure 3: Effects of the weighting coefficient α on wildfire burned area mapping with FireCCI labels.

a lot of details are lost. Therefore, the model reached a good trade-off between keeping spatial details and suppressing noise when = 0.6.

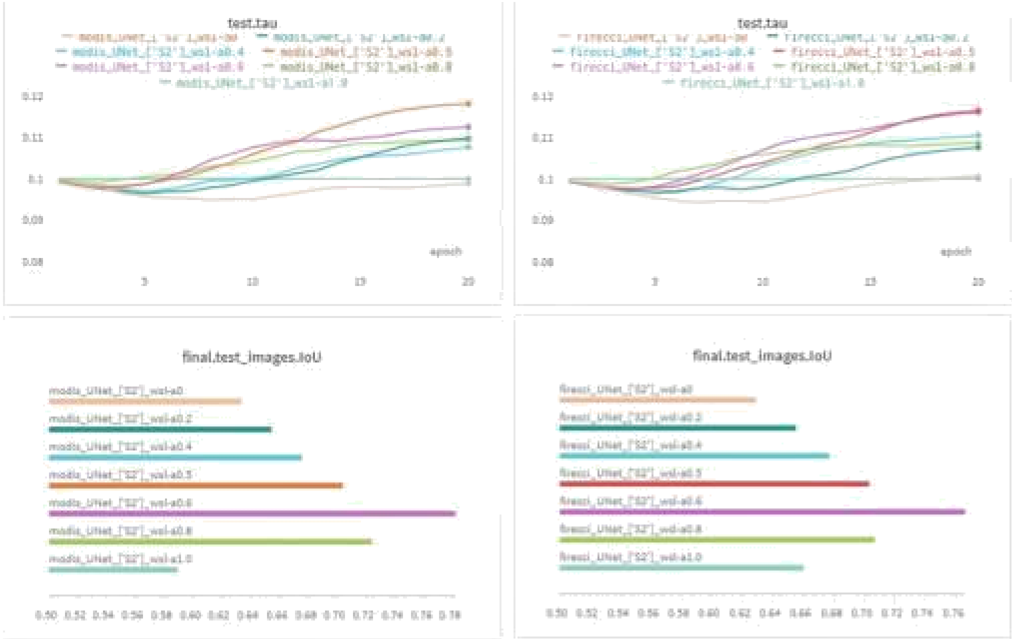

Figure 4: Quantitative results. Left: learned with MODIS labels, right: learned with FireCCI labels.

Figure 4 shows the learning procedure of parameter and quantitative assessment on the effects of , from which we can observe that = 0.6 achieved the highest IoU scores based on MODIS or FireCCI labels. When = 0.5, MODIS and FireCCI masks-based results seem to achieve the same IoU score on the testing set. When = 0.6 0.8, MODIS masks achieved slightly higher IoU score than FireCCI masks based ones. When = 0, i.e., training model only with MODIS or FireCCI labels, FireCCI achieved significantly high IoU, which is reasonable because of its higher spatial resolution.However, it is interesting to see MODIS labels can achieve slightly higher IoU when spatial consistency was introduced.

Outlook for the future

This work demonstrated that introducing spatial consistency loss can significantly boost the wildfire burned area mapping accuracy compared to learning model only based on coarse resolution labels. This is the simplest way to integrate spatial details in input data. We will further investigate other possibilities to exploit spatial prior in medium resolution input data for more accurate burned area mapping. Additionally, the reason needs to be further investigated as to why ended at different dNBR threshold for MODIS and FireCCI based results.

Mapping Wildfire Scares – NDVI vs. NBR vs. AFRI

[1]Arnon Karnieli, [1]Manuel Salvoldi,

[1]The Remote Sensing Laboratory, Jacob Blaustein Institutes for Desert Research, Ben Gurion University (Israel)

Keywords: Burn severity; Change detection; NDVI; NBR; AFRI; RdAFRI; RdNBR; Wildfire; Sentinel-2; Multi-temporal

The challenge

In recent years, wildfires have become serious human and environmental concerns for several reasons. Most importantly, they pose a threat to human life, flora, and fauna, as well as properties and economic losses. Wildfires are considered as one of the worst ecological disturbances to long-term records of vegetation phenology, since land-cover alterations are the basis for the understanding of the biological responses to climate change, such as impacting carbon emissions, at regional to continental scales. It is also worth mentioning the effect of wildfires on biodiversity, plant reproduction, forest succession, habitat quality, hydrologic regimes, and soil characteristics, such as nutrient cycling. For all the reasons mentioned above, different technologies have been developed for detecting and monitoring various aspects of wildfire, including risk assessment, active fire detection, gas and aerosol emission, smoke penetration, and temporal dynamics of burned areas. Among all technologies, there is a general agreement that remote sensing techniques are essential for providing valuable data for detecting, monitoring, interpreting, and responding to wildfires, from local to global scales. The current project strives at developing and using an advanced Earth observation approach for accurate post-fire spatial and temporal assessment shortly after fire events while eliminating the influence of biomass burning smoke on the ground signal. For fulfilling this goal, the Aerosol-Free Vegetation Index (AFRI), Equation 1, which has a meaningful advantage in penetrating an opaque atmosphere influenced by biomass burning smoke, was used. The relative deference AFRI (RdAFRI), equation 2, set of algorithms was implemented at the same procedure commonly used with the Relative deference Normalized Burn Ratio (RdBRN). Similar to the NBR, the Aerosol-Free Vegetation Index (AFRI) is also based on the correlation between the visible-red and the SWIR2 band:

$$= \frac{-0.5 \quad 2}{+0.5} \tag{1}$$

where is the reflectance value of the indicated spectral band— NIR, and SWIR2 (around 2.1 m).

?

Methodology

The study was conducted during nine months when Israel experienced massive pyro-terrorism attacks of more than 1100 fires from the Gaza Strip. 25 Sentinel-2 Level-2A products were selected with cloud coverage inferior to 15%, from 6 April 2018 to 22 December 2018, in order to monitor the study area during the kite and balloon attacks period. The NIR band (B8) and the SWIR2 (B12), at 10 and 20 m spatial resolution, respectively, were used for calculating the relevant spectral indices.

Similar to the procedures developed for the NBR-based set of algorithms, the most intuitive burned

area-mapping indicator consists of an absolute change detection methodology obtained subtracting a

post-fire AFRI image from a pre-fire AFRI image to derive the di erenced AFRI (dAFRI):

(2)

Then, the dAFRI, for two successive images collected in this study, can be formulated as:

$$\mathrm{dAFRI}(i-1,\, i) = \mathrm{AFRI}(i-1) - \mathrm{AFRI}(i), \quad \text{with} \quad i = 2, \cdots, 25 \tag{3}$$

where (i) indicates the i-th image in the database. The dAFRI(i-1, i) can present problems in the cases with low vegetation values for the image taken at (i-1): the absolute change will be small, and the index will not be able to detect the burned area. In order to avoid this issue, the relative differenced AFRI (RdAFRI) was defined as:

$$\mathrm{RdAFRI}(i-1,\, i) = \frac{\mathrm{dAFRI}(i-1,\, i)}{\sqrt{\left|\mathrm{AFRI}(i-1)\right|/1000}}. \tag{4}$$

Positive RdAFRI(i-1, i) values represent a decrease in vegetation cover, while negative values represent an increase in vegetation cover.

The flowchart of the proposed classification algorithm is detailed in Figure 1.

Results

For comparing the performance of the NBR, NDVI, and AFRI indices, a section of the S2 Level-2A image obtained on 10 July 2018, is presented in Figure 2.

The transects represent a common situation when smoke, at different intensities, covers a variety of substrates—cultivated, bare soils, fire scars, and more. The true-color composite image (RGB = 0.665, 0.56, 0.49 m) shows the open fire (light-orange hue), the biomass burning smoke (white hue), as well as burned scars that are a few days old (dark surfaces). The three indices were produced at 10-m spatial resolution, according to Equations (1), (2), and (5), from the surface reflectance values along a cross-section of 2771 m (Figure 6, line A-A). This line was selected since it passes cultivated fields, bare soil, and was overcast by light smoke that characterized the entire region along the whole study period. This line is subdivided into several segments. From pixel 0 to 50 (and similarly from pixel 180 to 190) over the agricultural field where no smoke exists, the AFRI values accurately mimic those of the NDVI, but the NBR values are significantly lower. From pixel 50 to 180, over the bare soil, AFRI values are somehow higher than those of the NDVI. However, the NBR values are negative and much lower. From pixel 180 to 318, under the smoke, the AFRI values of the crops remain at the same high level as in the smoke-clear section, while both the NDVI and NBR produce low values.

While validating with ground observations, the RdAFRI-based algorithms produced an overall accuracy of 87% against the 80% obtained by the RdNBR-based algorithm (table 1 & 2). Furthermore, the RdAFRI maps were smoother than the equivalent RdNBR, with noise levels two orders of magnitude lower than the latter (Figure 3). However, due to different cloud cover on the two consecutive dates, an automatic determination of a threshold level was not possible. Therefore, two threshold levels were considered through visual inspection and manually assigned to each imaging date.

Outlook for the future

Maps of fire scars provide valuable information for studying forestry, agriculture, and penology, as well as climate change. Since Earth observation data are considered to be the most informative means for quantifying the scars, a large variety of space systems have been used for this purpose. Selecting the most appropriate satellite depends on several criteria. Obviously, for the continental to global scales, the large-swath satellites (e.g., NOAA-AVHRR, MODIS) are more suitable. In contrast, for a regional scale, high spatial resolution and narrow swath are preferable. The second criterion is the temporal resolution required for the specific application. The number of fires, burned areas, as well as derived environmental consequences, such as the amount of CO_2 emissions, are usually summed for a monthly, seasonally, or yearly period using the large-swath satellites. However, for fast response and accurate mapping (e.g., for insurance assessment), more frequent images from high-resolution satellites (e.g., Sentinel-2, VEN S, RapidEye, etc.) are essential. Thirdly, the most meaningful spectral index for enhancing the burned signal and differentiating severity levels needs to be identified. Concerning the study objectives, S2 was found to be a suitable satellite due to its characteristics—high spatial resolution of 10 m, high temporal resolution of about five days, and the SWIR bands for computing the AFRI.

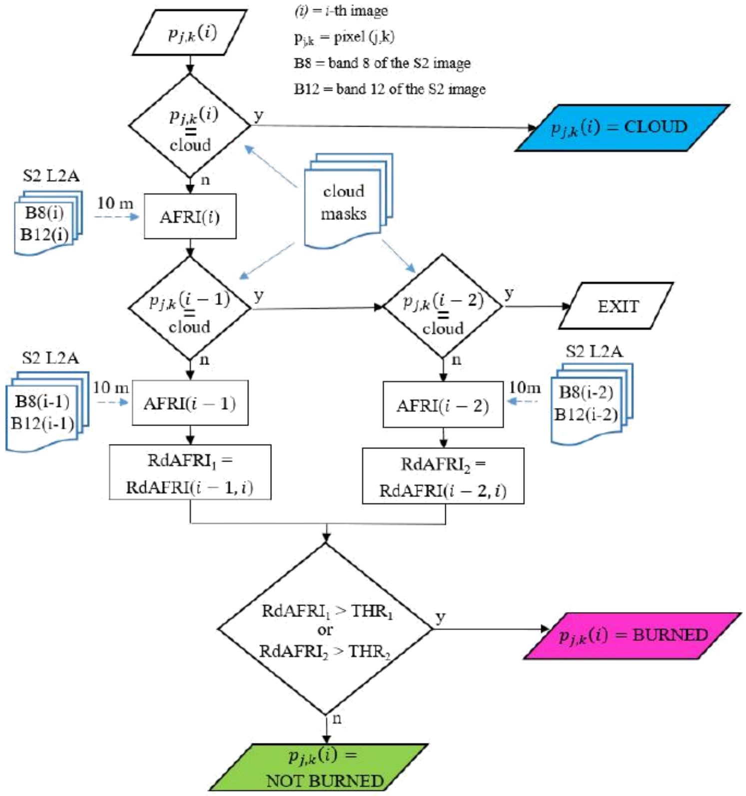

Figure 1. Flowchart of the pixel-based classification algorithm for burned area mapping based on the relative differenced Aerosol-Free Vegetation Index (RdAFRI) and multi-temporal Sentinel-2 Level-2A Level-2A products.

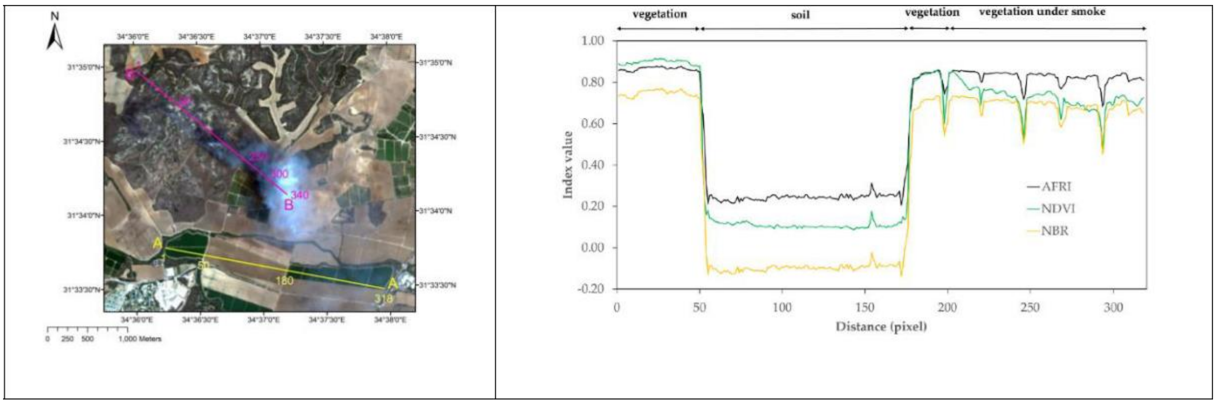

Figure 2. a) A true-color (RGB = 0.665, 0.56, 0.49?m) daily surface reflectance image of the Israeli territory on 10 July 2018. The open fire appears in a light-orange hue, the burn scars are dark, and the smoke is a white hue. b) AFRI, Normalized Difference Vegetation Index (NDVI), and Normalized Burn Ratio (NBR) values along a cross-section on 10 July 2018. The x-axis numbers represent the pixels' distance along line A–A in accordance with Figure 2a).

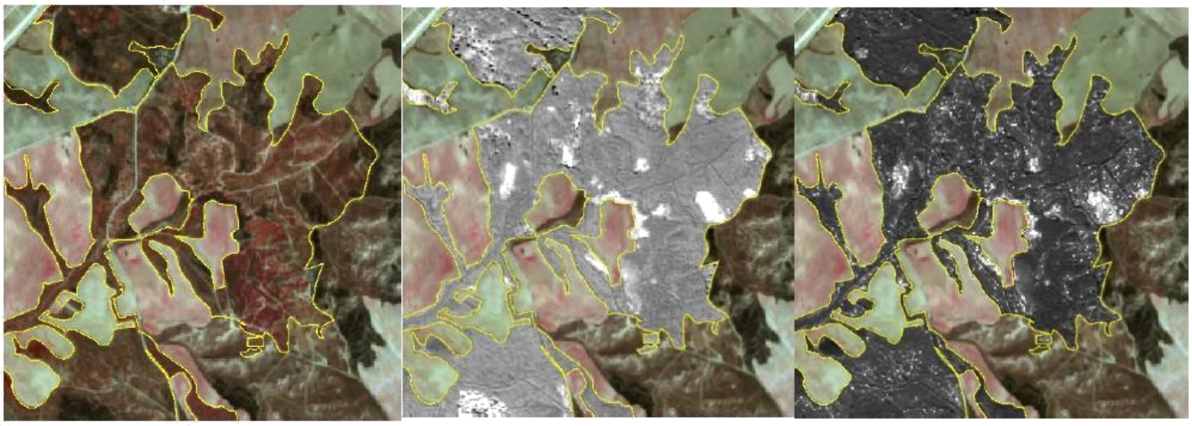

Figure 3. False-color image with the corresponding RdAFRI and RdNBR images.

		Algorithm Classification			
Ground-Truth Data		Burned Area	Not Burned Area	Total	Accuracy
	Burned area	309	151	460	67%
	Not burned area	49	980	1029	95%
	Total	358	1131	-	-
	Overall accuracy	86%	87%	-	87%

Table 1 Confusion matrix for the RdAFRI-based algorithm results

		Algorithm Classification			
Ground-Truth Data		Burned Area	Not Burned Area	Total	Accuracy
	Burned area	300	160	460	65%
	Not burned area	132	897	1029	87%
	Total	432	1057	-	-
	Overall accuracy	69%	84%	-	80%

Table 2 Confusion matrix for the RdNBR-based algorithm results

The implementation of Forest Canopy Density model in Cyprus forests using Landsat-8 and Sentinel-2 satellite data for the assessment of the fire impacts on canopy density

Maria Prodromou[1,2], Kyriacos Themistocleous[1,2], Chris Danezis[1,2], Ioannis Gitas [3], Diofantos Hadjimitsis[1,2]

[1] Department of Civil Engineering and Geomatics, Cyprus University of Technology, Limassol, Cyprus

[2] Eratosthenes Centre Of Excellence, Limassol, Cyprus

[3] Department Of Forestry, Laboratory Of Forest Management And Remote Sensing, Aristotle University Of Thessaloniki, Greece

Keywords (5): Forest Canopy Density, FCD model, Earth observation, Sentinel-2, Landsat-8, forest fires.

The challenge

Tree canopy plays a very important role in forest ecosystems and acts as a regulator, affecting the microclimate and the soil conditions. The density of the forest canopy is associated to the forest development, and it can be used as an indicator of forest degradation. Additionally, forest density is one of the most important parameters used in the design and implementation of programs for forest restoration, especially in cases of areas affected by fires. The main objective of this study is to determine the disturbance that occurred in the canopy density of the Paphos forest, at the Adelphi Forest and Akamas National Forest Park in Cyprus after the fire events that occurred on June 18 and 19, 2016 and on November 13, 2019, for each case study respectively. Cyprus is an area where forest fires frequently occur, especially during the summer period. Evidently, the fact that Cyprus forests cover only 18% of the total area of the island urges a strong need to monitor and protect them.

Methodology

For the purposes of this study, the Forest Canopy Density model (FCD model) was estimated using Landsat-8 and Sentinel-2 satellite imagery in Google Earth Engine (GEE) platform. The FCD model is a combination of four biophysical indices, which are the Normalized Difference Vegetation Index (NDVI), Bare Soil Index (BSI), Shadow Index (SI), and Thermal Index (TI). The FCD model was implemented in each case study before and after the three fire events to estimate the damage to the forest canopy density. Moreover, this study aimed to evaluate the FCD without considering the Thermal Index using Sentinel-2 data, since Sentinel-2 does not offer a thermal band. For the scopes of this study, the calculation of FCD model was carried out in GEE, which is a global-scale platform for scientific analysis and visualization of geospatial datasets. In this platform, the open-source images acquired by several satellites, including Sentinel-2, Landsat-7, and Landsat-8, are accessible and can be efficiently imported and processed in the cloud without the necessity of downloading the data to local computers.

Results

The FCD values for each case study were scaled from 0 to 100 and thereafter divided into three main classes; the first class corresponds to unvegetated areas or areas with very low forest density, whilst the second and third class correspond to medium and dense forest density respectively. The results from the two satellite sensors were validated and compared against each other. The results obtained from Sentinel-2 seem to be very promising and the calculation of the canopy density through this study is achieved at a better resolution than the results derived from Landsat-8.

Outlook for the future

In this study, it was attempted to estimate the FCD using Sentinel-2 data without the TI to map the damage caused from fire. This model was useful for investigating the effects of fire on canopy density. The use of both satellite sensors (Landsat-8 and Sentinel-2) showed similar variations in canopy density changes. Through this study, the Sentinel-2 satellite showed very promising results for the estimation of FCD with better spatial resolution than Landsat 8. Based on this, in cases that a Spatiotemporal analysis is needed to study the forest canopy density changes based on a time series analysis, the combination of Sentinel-2 and Landsat-8 images can be utilized. Our next steps are including a time series analysis for the last 10 years in order to investigate the changes due to fire events on canopy density. Based on the results of this study for the Spatio-temporal analysis to study the forest canopy density changes the combination of Sentinel-2 and Landsat-8 images can be utilized interchangeably.

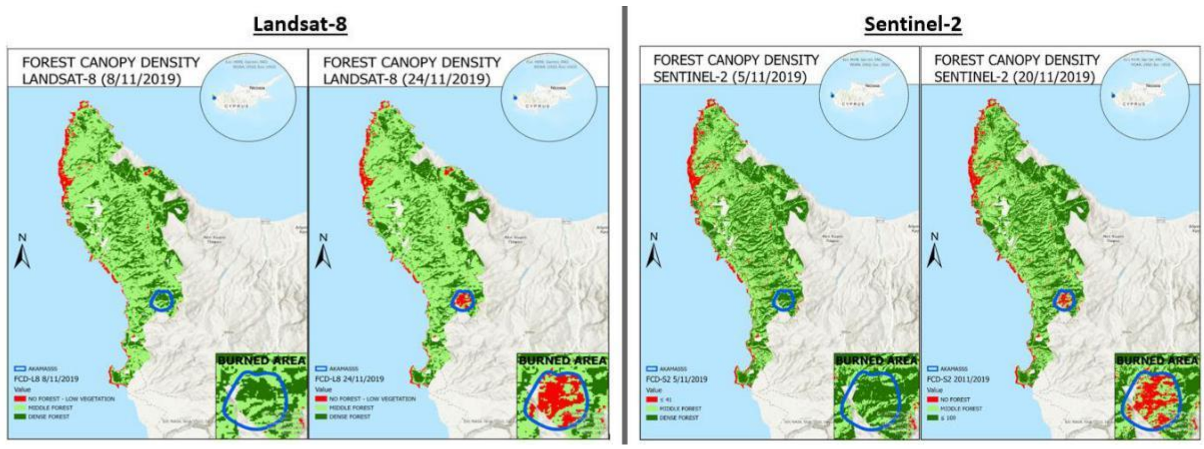

Figure Forest canopy density for the Akamas National Park before and after the fire event using Landsat-8 and Sentinel-2 satellite data

Acknowledgments

This work has been supported by the project 'ERATOSTHENES: Excellence Research Centre for Earth Surveillance and Space-Based Monitoring of the Environment-EXCELSIOR' (https://excelsior2020.eu/) that has received funding from the European Union's Horizon 2020 research and innovation programme under grant agreement No 857510 (Call:

WIDESPREAD-01-2018-2019 Teaming Phase 2) and the Government of the Republic of Cyprus through the Directorate General for European Programmes, Coordination and Development.

EO Education & Training – From Space to Classroom

Organizers:

Alexander Siegmund and Premysl Stych

Summary:

Earth Observation is a key technology to monitor, visualize, analyze, and model changes in earth's surface and a suitable way to better understand the earth system. EO is also a fast-growing economy sector with the need for specialized workforce. Hence national and international organizations and institutions from ESA, NASA, DLR, Universities, and out of school learning places developed programs to integrate EO in lifelong learning from primary, higher to informal education. This session will focus on an international presentation of best-practice-examples, training activities, research results, as well as ongoing and future developments of concepts, methods, and applications of EO Education and Training.

Topics:

- EO Education at schools
- Best Practice for EO Education at Universities & Further Training
- Live demos of innovative EO tools for Education & Training
- Live Demos of Innovative EO Tools for Education & Training
- Results of research studies on EO Education & Training

Scientific Committee:

- Alexander Siegmund, Heidelberg University of Education & Heidelberg University
- Premysl Stych, Charles University, Prague
- Johannes Keller, Heidelberg University of Education
- Amalia Castro Gomes, ESA/ESRIN, Frascati, Italy
- Antonios Mouratidis, Aristotle University of Thessaloniki
- Josef Lastovicka, Charles University, Prague
- Francesco Sarti, ESA/ESRIN, Frascati, Italy

Around The Earth in Less Than 5 Minutes – Exploring Earth Observation Satellites in an Augmented Reality App

Claudia Lindner[1], Henryk Hodam[1], Annette Ortwein[1], Andreas Rienow[1]

[1]Ruhr-University Bochum, Department of Geography, Germany

Keywords (5): secondary education, e-learning, orbits, copernicus,

The challenge

Remote Sensing (RS) has been brought into secondary education in the “Remote Sensing in Schools” (FIS) project since 2007 (Voß et al. 2007). Over the years, a growing number of flash modules was created that dealt with the basics of RS and a variety of applications to topics from geography, but also physics, biology, mathematics, and computer science. Due to the discontinuation of Flash by Adobe in 2020, many of these modules were updated recently (Hodam et al. 2021) to keep up with the times and be useable in web browsers and on current school computers. One of them, a module about satellite systems, was decided to transfer into the “Columbus Eye” Augmented Reality (AR) app (Lindner et al. 2021) and upgrade it significantly.

The main challenge was to transfer a simple animation of a few satellites in a 2D space into a 3D environment in the right balance of realism and simplification. Only very little of the original module could be recycled, mainly the 3D models of 4 satellites.

Methodology

The “Columbus Eye” app is developed in Unity 2019.2 with the Vuforia extension. Vuforia uses image recognition via edge detection on “markers”, which can then be augmented in Unity, overlaying 3D animations, videos, or other information. The user interface (UI) is also implemented in Unity. Custom scripts are written in C#.

The centrepiece of the app is the rotating Earth, 12.7 cm in diameter, taking 288 seconds to complete one rotation, i.e. 1 minute of real time is reduced to 0.2 seconds in the app. It has a day and a night side; the latter being implemented through two masks over the day side that display the night image only in a limited area and shift through a night time image of the Earth at the same speed as the Earth spins underneath. The same masks are applied to the equirectangular map of Earth in the UI where the orbit ground tracks of all visible satellites are displayed. Satellites on geostationary orbits are simply attached to the centre of the spin and only seem to orbit the Earth.

One C# function was developed for the orbital movement of the non-geostationary satellites. The orbital motions in geodetic coordinates were transferred into the cartesian coordinate space of Unity. Since the satellites do not orbit the spinning Earth, but a stationary, immobile centre defined only by the Marker’s position, and the Earth simply turns underneath them, their positions relative to the Earth have to be calculated, too, to display them correctly on the world map.

Results

The AR app, downloadable in the Google Play Store under “Columbus Eye”, accurately depicts the orbits of 11 European satellite constellations, namely the Meteosats, EnMAP (preliminary parameters), RapidEye, TanDEM-X, the ISS, and Sentinels 1-6. The models from Meteosat, EnMAP, RapidEye, and TanDEM-X were transferred from the old Flash module together with the areas of interest, while the Sentinels were re-created in Blender. Each satellite and its ground track can be turned on and off in the UI, the ground track visibility times adjusted and the ground tracks restarted in case the map becomes to cluttered or there are jumps in the tracks after a temporary loss of the Marker.

When tapping on a satellite on the screen, information about the respective satellite is displayed in a separate UI. There, the 3D model can be viewed up close; facts and figures about the satellite, its orbit and sensor are listed; and a short text informs about the satellite’s history and purpose. Additionally, an image taken by the satellite’s sensor is displayed and its content explained. The 5 topics of interest that were previously included in the Flash module were also transferred into the AR app, but no new ones were added. The topics are: DLR, mining in East Africa, the Tohoku tsunami in Japan, weather monitoring in Europe, and the Deepwater Horizon oil leak in the Gulf of Mexico. Tapping on their 3D models displays an image and information text.

Outlook for the future

More satellites can easily be added, however, since most Earth observation satellites are in a sun-synchronous or geostationary orbit, the added value would be limited.

While the other parts of the “Columbus Eye” app are accompanied by worksheets, the satellite systems have no specific worksheet developed alongside. However, they can be used in addition to other material. Another app part deals with, e.g. volcano monitoring using Sentinel-1 and the worksheet even has calculations about the orbit of the satellite which can be visualised in the satellite systems. The part can also be used freely to teach about orbital mechanics and map projections, as the question of why satellites fly in waves comes up rather frequently among students and teachers on workshops and is easily answered in the app.

The “Columbus Eye” app is also scheduled to be published for iOS in the Apple Store soon.

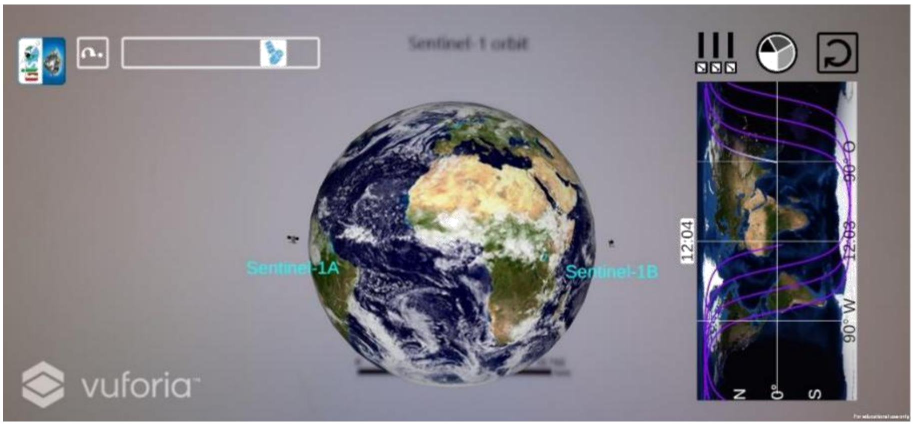

Figure 1 View of the satellite systems app. The Earth is a 3D model slowly turning around while the satellites orbit it. Orbit tracks are displayed on the map to the right.

Developing AND **Testing Explainer Videos on Earth Observation**

Henryk Hodam[1], Andreas Rienow[2], Carsten Juergens[3]

[1] Ruhr University Bochum, Germany

[2] Ruhr University Bochum, Germany

[3] Ruhr University Bochum, Germany

Keywords: education, teaching, eLearning, remote sensing, learning videos

The challenge

Educating the public about the benefits and potentials of remote sensing is becoming more important, as few people are aware of how this technology already affects their everyday lives and how it is going to transform the way we see our planet. There are many ways to enhance the general knowledge of remote sensing principles, including the use of video resources that can be adapted to a variety of teaching scenarios. Over the last decades, numerous studies formed the basis for a set of guidelines on how educational videos can be successful. Based on those we established a workflow for the creation of explainer videos covering the basic concepts of earth observation. While subjectively this workflow yielded learning material that could successfully be integrated in various teaching scenarios, there was yet the need to prove their efficiency before continuing to more complex topics of earth observation like i.e. radar remote sensing.

Methodology

The target groups for these videos are secondary students as well as anyone interested in learning about earth observation. Two of those videos, one on earth observation in general and one on the basics of the electromagnetic spectrum, were used in this research. To test whether or not the workflow leads to effective learning videos and to compare them to traditional text and illustration material derived from those videos, a pre-test/post-test study was undertaken focusing on German pupils in their final year at secondary school as well as first-semester university students. Due to the special circumstances faced during the COVID-19 crisis, this experimental setup used a combination of online questionnaire tools and a web environment. Participants were randomly assigned to a group. An online survey platform was used to administer a pre-test of 12 questions regarding basic remote sensing knowledge in the form of multiple or single-choice questions. After completing the pre-test the participants were redirected to a website that was specifically created to randomly present two videos or a text and illustration version of the content separated into chapters. Pre and post-test data were compared using t-Test and ANCOVA to determine if the material had a significant effect on the participants and how the effects of the video (n=26) group compare to the text and illustration group (n=30).

Results

A t-test run on the pre-test and post-test results of the video group showed a significant difference (F=(1,25), p=0.00) indicating that the videos did succeed in conveying basics facts on remote sensing.

Also, a t-test was admitted on pre-test and post-test results of the text/illustration group also indicating a significant difference (F=(1,29), p=0.00)

To evaluate whether the groups differ under the assumption of baseline equality an ANCOVA was applied. Its results show no significant difference in the video and text/illustration group (F (1,53)=3,342, p=0,073).

Outlook for the future

It has been shown that the established production process leads to successful video learning material. Because no significant difference between the video and the text/illustration group was found, it is important to point out, that before the substantial effort of creating videos of a high production value is made, it is necessary to consider the future field of application for the learning resource. Assessing what kind of learning video meets the requirements of the intended application is crucial since the amount of production effort may quickly become disproportional to the intended outcome. Motivated by the possibility to present complex topics in a concise format that proved to be applicable in very different teaching scenarios and can be easily disseminated we continued our efforts and extended the range of topics to applied remote sensing as well as the basics of radar remote sensing. The presentation will present the basic concept as well study results. Also, examples from the ongoing work will be shown.

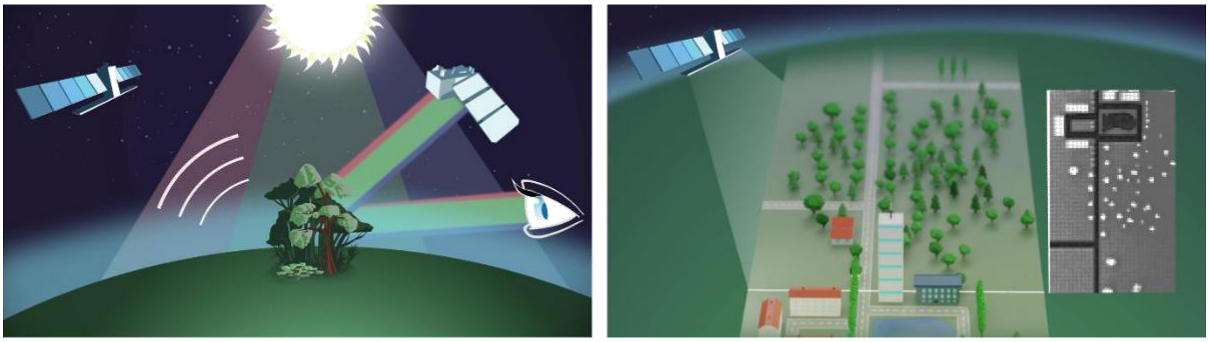

Figure 1 Exemplary Screenshots taken from recent Explainer Video on radar remote sensing

Potentials of the App BLIF: Explorer for Location-based Use of Satellite Imagery to Foster Remote Sensing in Schools

Johannes Keller[1], Mario Blersch[1], Christian Plass[1], Alexander Siegmund[1,2]

[1] Department of Geography – Research Group for Earth Observation (Rgeo), Heidelberg University of Education, Germany

[2] Heidelberg Center for The Environment (Hce) & Institute of Geography, Heidelberg University, Germany

Keywords: Earth Observation, Remote Sensing, Education & Training, location-based learning

The challenge

Earth observation provides important data to analyse, model, visualize, and evaluate environmental changes. Due to the growing importance of this technology for the labour market, science, and society, it should be introduced to students at an early stage. Ground truth data collected by students is necessary to support them in understanding abstract visualizations such as false-color composites. The mobile app "BLIF:Explorer", developed at the Department of Geography – Research Group for Earth Observation (rgeo), Heidelberg University of Education, enables students to collect ground truth data, visualize satellite imagery, and carry out location-based learning. Through this, students can deal with local topics such as biodiversity loss, agriculture, and forestry in the context of the Sustainable Development Goals (SDGs). In order to be used in schools, the app must work on different operating systems (iOS, Android, tablet, smart phone), needs an offline-mode, and must have a high usability. Therefore, the challenge was to design an app which combines all necessary functions with an appealing and simple screen design. The aim of this study was to evaluate the usability off the app with students.

Methodology

To analyse the usability of the app, a school project was developed with materials for grade 10 students. Based on existing usability tests, a new questionnaire was developed and 12 items to measure the intrinsic motivation of the students were added. The project days were carried out with 3 classes (n = 52) in March 2022. After receiving initial input and instructions on how to use the app, the students solved several tasks independently. To better understand their work processes and identify problems with the app, they were observed during their tasks and afterwards filled out the usability questionnaire.

Results

Usability tests and observations showed that the students had no problems to solve given tasks with the app (Figure 1 a). They were able to navigate in the field, collect location-based data in form of pictures, and use different layers such as the vegetation index (NDVI) or false-colour images. To do so the students required a minimum amount of guidance and were able to solve technical problems within their learning groups. Throughout their work with the app, students stated to have been highly motivated (Figure 1b).

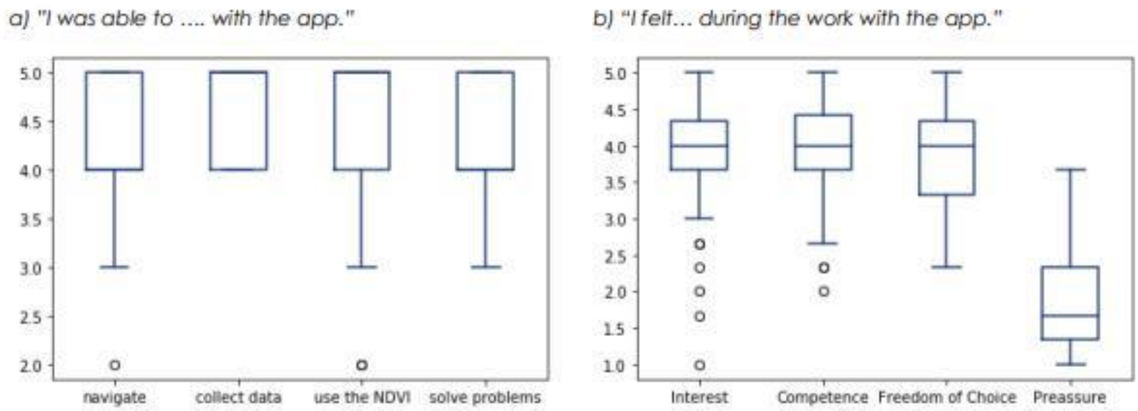

Figure 1 a) Usability of the app (*n* = *52*). b) Four dimensions of intrinsic motivation of students during the work with the app (*n* = *50*). Scale: 1 = "strongly disagree", 5 = "totally agree" for all items.

Outlook for the future

The results show that students can use all functions of the app and are motivated during the work. We conclude that the screen design off the app was simple while appealing. This work shows that the app "BLIF:Explorer" is a good tool to combine satellite imagery with field work to teach students environmental topics as well as the potentials and constrains of remote sensing. In a next step, support material for teachers will be created. This will enable them to independently use the app in their classes and instruct their students themselves.

The European Perspective: Earth Observation for Education (EO4Edu)

[1]Annette Ortwein, [1]Henryk Hodam, [1]Claudia Lindner, [1]Kilian Staar, [1]Andreas Rienow

[1]Ruhr-University Bochum, Germany

Keywords: Education, Earth observation, augmented reality, MOOC, Intercultural exchange

The challenge

With satellite imagery, the world can be observed without adhering to administrative or perceived boundaries on the ground. Nevertheless, earth observation resources for school education often focus on a specific use case within a country or small region, although education can benefit greatly from comparing local, regional, and global phenomena. At the same time, many European countries experience a similar lack of high-quality and easy-to-use resources for applying and integrating remote sensing and GIS tools in their school curricula.

Methodology

The ERASMUS+ project EO4Edu strives to overcome these challenges by including partner schools and universities from four different countries, jointly developing teaching resources for including Earth observation topics in primary and secondary schools across Europe. In a baseline survey conducted in Greece, Czech Republic, Wales, and Germany, potential topics, needs, and the use of earth observation methods and imagery in classrooms was assessed. Simultaneously, the potential of including earth observation in curricular topics were determined on a country-by-country basis. Combining both baseline assessments, common topics across Europe were identified and used as a reference for resource development. While the university partners develop educational apps and videos, and simplify earth observation methods and methodology to an extent that they can be used by pupils, the schools design lesson plans and use cases for their specific context while providing feedback, evaluating, and proposing additional content.

Results

Within the project, several resources covering a broad range of remote sensing and earth observation topics are under development. For example, the University of Bochum illustrates the principles and developments of land use and land cover change in video format using animations and satellite imagery, whereas the topics floods and volcanoes can be explored by the children themselves through an augmented reality app. Regional use cases from all four countries accompany these global introductory learning materials, providing an opportunity to compare the local situation to other European countries. First tests of these resources and their accompanying example lesson plans for different grades and class sizes in the Czech and German partner schools show great potential for adaptation and use in multiple educational settings as part of modern earth observation education for the benefit of pupils all over Europe.

Outlook for the future

The project partners will continue to develop and refine teaching resources, and test as well as adapt these materials to various settings from primary to secondary schools. All resources will be translated into the project languages English, Welsh, Czech, Greek, and German, and will be made publicly available through the project's website. As part of intercultural exchange, class visits will take place, sensitizing pupils for living and learning together in Europe.

"From Space To Classroom" Using Esa's Climate Change Initiative Educational And Training Resources

Eirini Politi[1], Suhyb Salama[2], Catherine Fitzsimons[3], Norman Fomferra[1], Tonio Fincke[1], Carsten Brockmann[1]

[1]Brockmann Consult Gmbh, Germany

[2] University OF Twente, The Netherlands

[3] National Centre For Earth Observation, University Of Leicester, United Kingdom

Keywords (5): Climate Change Initiative, Knowledge Exchange, Educational Resources, Training Material, CCI Toolbox

The challenge

ESA's Climate Change Initiative (CCI) has realised the full potential of long-term global EO archives as a timely contribution to the Essential Climate Variables (ECVs) required by the UN Framework Convention on Climate Change. In recent years, a plethora of satellite derived ECV datasets have been developed, covering land, water and atmospheric variables, and these are made available to users via the free and open CCI Open Data Portal (ODP). Despite the R&D advances of the CCI programme and its numerous outputs, until recently specific educational resources were not centrally developed, rather they were being generated on an *ad hoc* basis by projects outside of CCI. In part to fill this gap, the CCI Knowledge Exchange (KE) project was launched in late 2019. Aiming overall to coordinate and harmonise access and easy uptake of CCI ECV and cross-ECV products by various user communities and the public, efforts also included the development of a series of Educational and Training Resources.

Methodology

A thorough curriculum analysis was conducted in 2019-2020 across Europe and educational levels, from primary to tertiary, to guide the development of the CCI KE Educational Resources. Having identified 22 climate-related topics across STEM curricula, 10 narratives were shortlisted based on occurrence and cross-curricula coverage to form the basis of 10

Education Resource Packs (ERPs) tailored to primary (8-11 years old) and secondary (11-16 years old) school students. These narratives also guided the development of a Tertiary Training Kit (TTK) tailored for under- and postgraduate students. The TTK makes use of the CCI Toolbox (Cate): a cloud-based environment for climate data visualisation, analysis and processing, and includes a suite of resources from reference documentation and tutorials to lessons and exercises for skills development. Building and expanding on the TTK, a Summer School and Massive Open Online Course (MOOC) were also developed aiming to equip students, scientists and scholars with the skills to understand climate change and analyse EO-based climate data. Developed by experts in Education, the CCI KE Educational and Training Resources cover key aspects necessary to meet STEM curricula in relation to the climate, and use appropriate language for each age group they aim to target. The role and benefits of long-term monitoring from space to understand the Earth's climate has been a core theme across all those resources.

Results

Originally produced in English, the 10 ERPs were also translated in Dutch, French, Spanish and German, and can be downloaded from a dedicated 'Educate' section of the CCI website: https://climate.esa.int/en/educate/. They include themes such as the water and carbon cycles, biodiversity and habitat loss, the ozone hole, rising sea level and ice melt, among others (Figure). Up to date, the ERPs have been downloaded by more than 1200 unique users. The TTK lectures, presentations and assignments in English as well as information on the Summer School and MOOC can also be found on the CCI website.

Outlook for the future

While one of the main objectives of the CCI KE Educational and Training Resources is to support topics taught in STEM curricula across education systems (ERPs) and teach analytical skills and techniques to manipulate ECV data using Cate (TTK, Summer School and MOOC), this suite of resources also helps to promote the CCI programme and its outputs through educating different age groups. Future work includes wider promotion aiming to increase uptake, while feedback received through various dedicated channels can steer potential future developments. Interaction with teacher associations and educators could facilitate integration of these open-access resources to curricula and taught modules across various education levels. As Cate evolves and the CCI Open Data Portal continues to expand and be the host of the latest CCI datasets and long-term CCI data archive, these educational resources can prove a powerful means to bring the public and young scholars closer to the data.

Figure Ten Education Resource Packs developed under ESA's Climate Change Initiative (CCI) Knowledge Exchange (KE)

Promoting The Benefits of Earth ObservatION IN SECONDARY AND HIGHER EDUCATION IN CYPRUS

Maria Prodromou[1,2], Eleni Loulli[1,2], Christiana Papoutsa[1,2], Christos Theocharidis[1,2], Antonis Hadjiantonis[3], Diofantos G. Hadjimitsis[1,2]

[1] ERATOSTHENES Centre OF Excellence, Limassol, Cyprus

[2] Department OF Civil Engineering AND Geomatics, Faculty OF Engineering AND Technology, Cyprus University OF Technology, Limassol, Cyprus
[3] Cyprus Research AND Innovation Centre (CYRIC), Nicosia, Cyprus

Keywords (5): space education, secondary education, questionnaires

The challenge

Remote sensing along with its features and applications can be described as a channel that can provide immense opportunities for secondary and higher education. It presents an interdisciplinary approach, because it involves a combination of aspects of different fields, such as Geography, Mathematics, Physics, Biology, Computer Sciences, and requires various tasks and skills. Essentially, Remote Sensing comprises an interdisciplinary component that enables students to use cross-linked thinking to deal with a range of curriculum-specific topics in a problem-solving manner. In natural science classes like Mathematics, Physics or Computer Sciences, the basic principles of Remote Sensing can be introduced, while in Geography or Biology, which are considered as applied sciences, satellite data can be analysed for further comprehension. In applied sciences classes, the teacher can pose environment related questions to be answered by students using Remote Sensing data. This paper presents the importance and potential of promoting the benefits of Earth Observation, when implemented in secondary education schools, as well as higher education institutions in Cyprus.

Methodology

Since 2007, the ERATOSTHENES Research Centre at the Cyprus University of Technology supports schools participating in national and European research competitions. One of the aims of the 'EXCELSIOR' project and ERATOSTHENES Centre of Excellence (ECoE) is to support students during their first contact with research, science and technology and encourage them to become young researchers. This can be achieved through presentations, seminars, workshops, science cafes and the researcher's night. For the purposes of this study, presentations to numerous schools in Cyprus were conducted to inform students about the Earth Observation and the use of Copernicus Program. Before and after each presentation was conducted, the researchers handed out questionnaires to the students as well as to their teachers in order to find out the existing knowledge of the students about space education. In particular, the questionnaires asked the students for information about their knowledge around space technologies, satellite data and space services.

Results

The presentations took place in various classes in different schools around Cyprus. There, we had the opportunity to present to students of the age between 11 and 18 years old, and to teachers of different ages coming from different professional backgrounds. Based on the analyses of the demographics of our audience, including both students and teachers we found out that the majority of the students had an average knowledge of the space-related terms before listening to our presentation. Additionally, the students showed an interest in attending educational seminars on Earth Observation and in working with space technologies, already before listening to our presentation. After the presentation, the answers to our questionnaire showed an overall improvement of the students' knowledge in the field of space technologies and remote sensing. Particularly, almost half of the students were confident about what space technologies, satellite data and space services are. Most of the students also expressed that they are confident to describe what the European Space Agency (ESA), the Copernicus Program and its services, as well as the science of remote sensing are.

Outlook for the future

Over the past years, the benefits of Earth Observation were promoted in the secondary and higher education in Cyprus. In secondary education this was achieved through presentations, handout questionnaires, workshops, meetings, competitions, seminars, science cafes and participation in researcher's nights. In higher education, we used remote sensing in the curriculum of engineering courses both on undergraduate and postgraduate level, workshops, seminars using on-line platforms or conventional methods. Preliminary results regarding the effectiveness of each educational method have been demonstrated for both secondary and higher education in Cyprus. The campaign is still ongoing and aims to increase awareness and encourage students of secondary education to engage with Earth Observation and space-related topics.

The authors acknowledge the ‘EXCELSIOR’: ERATOSTHENES: EXcellence Research Centre for Earth Surveillance and Space-Based Monitoring of the Environment H2020 Widespread Teaming project (www.excelsior2020.eu). The ‘EXCELSIOR’ project has received funding from the European Union’s Horizon 2020 research and innovation programme under Grant Agreement No 857510, from the Government of the Republic of Cyprus through the Directorate General for the European Programmes, Coordination and Development and the Cyprus University of Technology.

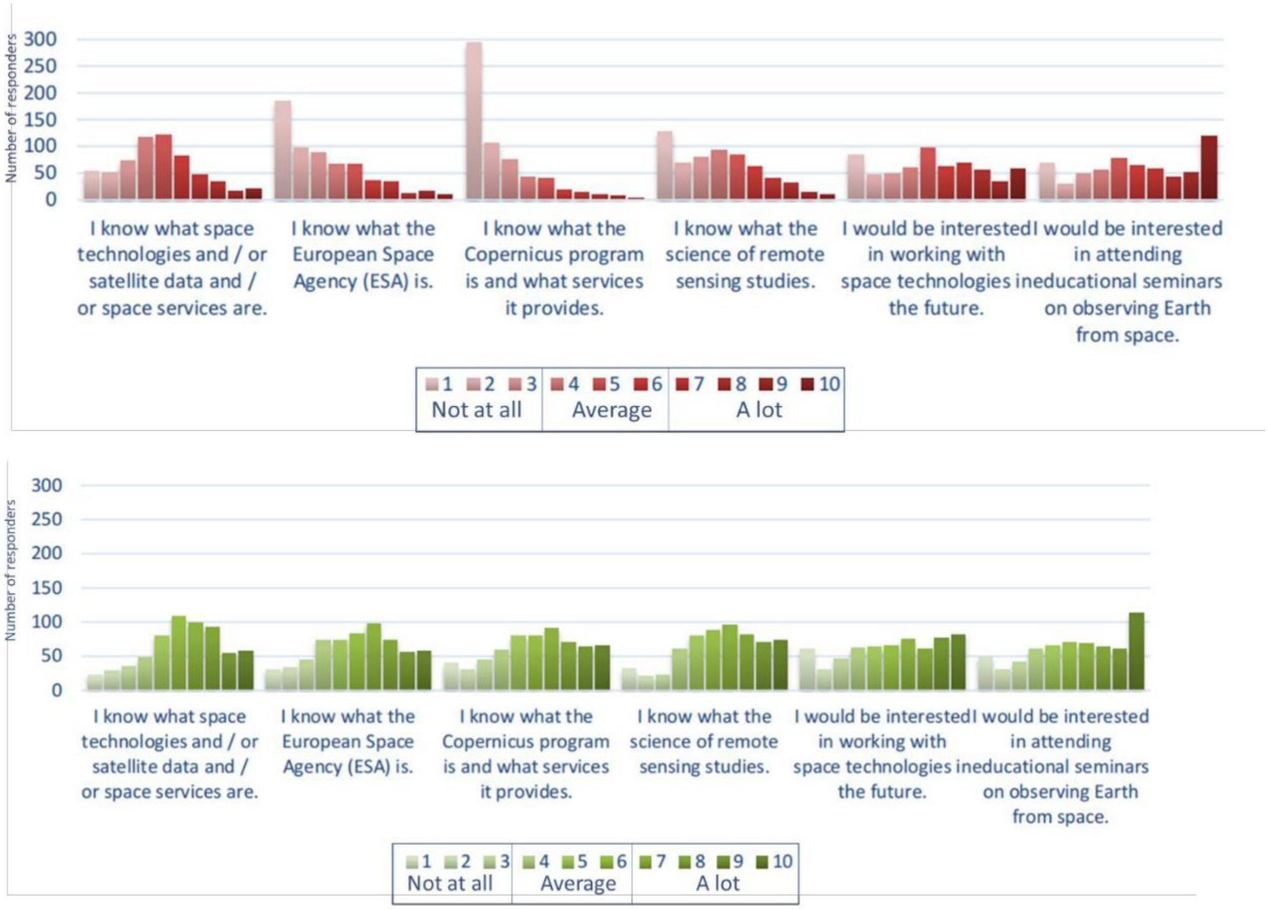

Figure (a) Answers of Students before the presentation (b) Answers of Students after the presentation

Poster(s)

Advanced Training Course on Remote Setting For Educators At The Junior Academy Of Sciences Of Ukraine.

Svitlana Babiichuk[1], Olga Tomchenko[2], Natalia Kobliuk[1]

[1] National Center "Junior Academy Of Sciences Of Ukraine", Kyiv, Ukraine,

[2] State Institution "Scientific Centre For Aerospace Research Of The Earth Of The Institute Of Geological Sciences Of The National Academy Of Sciences Of Ukraine", Kyiv, Ukraine

Keywords (5): remote sensing, science education, Junior Academy of Sciences of Ukraine, training course for educators, education.

The challenge

Remote Sensing (RS) and Geographic Information Systems (GIS) belong to the fields of science education, which have been actively promoted by the Junior Academy of Sciences of Ukraine (hereinafter referred to as the "JASU"). This is driven by the current need for the introduction of satellite imagery analysis not only in research but also in education. Since the students already use, directly or indirectly, the results of satellite imagery analysis and GIS-based image processing in their everyday life (electronic maps to find the best route, online resources to analyse the current environmental situation of the locality, Google Earth, etc.), and analysis of satellite data gathered by man-made satellites has become an integral part of current research in Earth sciences, it is, therefore, necessary to engage RS scientists in teaching science and provide advanced training for the JASU educators in Remote Sensing.

Methodology

The special course consisted of 16 online sessions and included lectures and hands-on activities based on the use of EO Browser, ArcGIS Online, Google Planet Earth, and other resources. During the course, participants learned how to use the images collected by Sentinel and Landsat family satellites in a variety of research, including climate, hydrology, forestry, agriculture, etc. In particular, the course covered the following topics: detection of consequences of fires, monitoring of volcanic activity, monitoring of water bodies and air pollution, changes in agricultural lands and loss of forest resources, analysis of the anthropogenic impact of amber mining on landscapes, etc.

The special training course included:

1. information (promotional) webinar to present the special training course;
2. following the closure of registration for the course, initial testing of registered course participants was held to assess their baseline level of knowledge;

3. intensive training sessions (theory and hands-on activities) within the framework of the special course;
4. a final closing conference, at which the course participants presented their independent projects developed using the acquired skills;
5. final tests to evaluate the course efficiency;
6. interviewing participants in half a year to evaluate the effectiveness of acquired knowledge use in their classroom practices.

Results

When replying to the question, "What do you think is the most difficult in mastering the techniques of satellite imagery processing?", more than half of the participants stated the lack of appropriate education in the processing of satellite imagery. In addition, 22.9% of participants pointed to outdated technical equipment.

When replying to the question, “What areas of research are you interested in?”, most participants mentioned landscape science, hydrology, climatology and ecology, etc.

Upon completion of the course, the participants shared their opinions on the educational disciplines in which it is advisable to use satellite images. Here are some quotes from participants:

- "For almost all topics in Geography course, even in History classes";
- “Inland waters and water resources, soils and soil resources”;
- “Terrain forms, air mass circulation, and interaction of a man and nature”.

Six months after the course, we conducted an interview. One question of the interview was: «How often have you used EO Browser for personal purposes and in classroom practice? », most participants replied that they used satellite technology in the educational process. In particular, a teacher from the Kyiv Lyceum said that she used satellite images as illustrations to the teaching certain topics, including amber mining. In higher education institutions, teachers used satellite-based monitoring of the Earth more in research than in educational activity.

Outlook for the future

According to the final survey data, 92% of the special course participants would like to improve their knowledge of the RS fundamentals through the analysis of satellite images in QGIS, so we plan to hold such a course ("Analysis of Satellite Images in GIS") by the end of 2021 and determine its effectiveness based on interviewing and questionnaire surveys. Visual support also has a significant impact on the quality of the educational process, so one of the promising areas for improving special course is the production and release of short thematic videos about satellite monitoring of certain phenomena or processes using remote sensing tools.

Land Cover & Land Use Remote Sensing Techniques and Applications for Effective Climate Action

Organizers:

Gregory Giuliani and Birgitta Putzenlechner

Summary:

Land Cover and Land Use (LCLU) is on the 14 Global Fundamental Geospatial Data Themes driving Sustainable Development. Incredible progress has been made in analyzing Big Data for better land monitoring. However, Land Cover characterization remains a major source of inconsistency and there is a lack of comparability between existing products. Numerous challenges remain to achieve the vision of transforming EO data into actionable knowledge by lowering the entry barrier to massive-use Big Earth Data analysis and derived information products. Consequently, it is crucial to support the development of effective means to build socially robust, transparent, accessible, replicable, and reusable knowledge, to generate decision-ready products based on Land Use & Land Cover data. In particular, the thematic expansion/intensification of ECVs and their impact assessment of LCLUC could be worth considering for several reasons.

The current situation is that research on the intercomparison of diverse ECVs is still at its infancy while impact assessment of LCLUC regarding biogeophysical effects using ECVs is gaining importance to assess and understand global change. As satellite-derived ECVs become more available, they will also be used to analyze LULCC effects. Therefore, knowledge and integration of the uncertainties of individual ECVS will be of great importance. Ultimately, LCLU remote sensing is critical to contribute to applied research using powerful geospatial and statistical analyses with the objective to serve as a source of "actionable" and timely early warnings of emerging issues and environmental change, and related multi-scale assessments, based on scientific data, indicators, and real-time information, and helping to catalyze "evidence-based" responses. To reach this objective, we think that a paradigm shift is essential moving from traditional data-centric approaches to information- and knowledge-centric approaches. To fully realize the value chain of EO data, the Data-Information-Knowledge-Wisdom (DIKW) paradigm can facilitate evidence-based decision-making processes and inform us about Earth's limits. Therefore, exploring how best to apply DIKW on LCLUC would be valuable.

Topics:

- New methods for generating LCLU products
- Ecological or biophysical impact assessment of LCLUC
- Innovative tools and solutions to work with EO Data Cubes for LULC mapping
- Integration of in-situ observations for LCLU analysis
- Data quality, reliability and uncertainty of LCLU products

Scientific Committee:

- Gregory Giuliani, University of Geneva
- Birgitta Putzenlechner, University of Goettingen Georg-August
- Martin Kappas, University of Goettingen Georg-August
- Ioannis Manakos, CERTH/ITI/GR
- Birgit Kleinschmit, TU Berlin

An automated approach to habitat mapping on a rehabilitation peatland using google earth engine

Richa Marwaha[1], Stuart Green[2], Matthew Saunders[1]

[1] Trinity College Dublin, Department of Botany, Ireland

[2] Teagasc food research centre, Spatial analysis unit, Ireland

Keywords: SENTINEL-2, RAPIDEYE, PEATLANDS, REHABILITATION, HABITATS

The challenge

In Ireland, peatlands cover approximately 21% of land area, however 85% of these have been degraded through extraction for fuel and horticulture, and conversion to agriculture and forestry. These processes require peatland to be drained and drainage of peatlands can cause them to act as a carbon source but rehabilitation through rewetting can reduce carbon emissions and ultimately return the systems to a carbon sink while providing additional ecosystem services such as supporting biodiversity and water regulation. Cavemount is a raised bog in County Offaly in Ireland and was an active peat extraction site for around 45 years. Industrial peat extraction ceased in 2015 and the process of rehabilitation began by blocking the drains and rewetting the site to allow for natural vegetation colonisation. The main aim of this work is to use the earth observation techniques to develop a change detection methodology to monitor ecological succession over time and to evaluate the success of the rehabilitation programme.

Methodology

Ground truth survey data from 2010 (when the wetland was an active peat extraction site) and a new post rewetting remote expert survey mapped vegetation communities. The validation data for 2010 was collected by Bord Na Móna by field visits and for 2021, airborne imagery with 0.5m resolution. Satellite data used included RapidEye (2010) and Sentinel-2 images (2021). RapidEye was resampled to 10 m to match the spatial resolution of Sentinel-2 and same vegetation indices were used NDVI, EVI and NDWI. A machine-learning algorithm-random forest, was used to measure the spatiotemporal changes in land use before and after peat production was stopped. It is expected that in the long-term the Cavemount wetland will become a carbon sink following the rehabilitation process and therefore it is important to form a baseline and monitor the seasonal and annual changes in vegetation and hydrology. An automated approach was developed in the google earth engine (GEE) to develop a change detection methodology post re-wetting using the satellite data. In this work, the random forest model was used to map the habitats on the site. The input to the random forest included all the spectral bands along with 3 additional spectral indices.

Results

The effect of rewetting activities is illustrated by the succession of vegetation and reduction in bare peat area from 3.36 to 0.81 sq. km. The overall accuracy of the habitat for 2010 was 83% and for 2021 was 75%. The site in 2010 was under extraction and the majority of land cover was bare peat followed by Betula pubescens. After the rewetting process in 2015, some key habitats have developed on the site. For 2021, 2 the dominant vegetation communities included- Betula pubescens, Eriophorum angustifolium, Ulex europaeus, Calluna vulgaris, Phragmites australis, Typha latifolia and Juncus effusus. The Figure 1 depicts the change detection output showing the changes from bare peat to various habitats. The results obtained using the random forest were validated using the latest field data. The vegetation communities can be characterized into two distinct categories relating to the hydrology of the site, wet and dry. The dry vegetation communities include- Betula pubescens, Ulex europaeus, Calluna vulgaris and Juncus effusus whereas the wet category includes- Phragmites australis and Typha latifolia. Eriophorum angustifolium is found in both wet and dry conditions. The site is on the trajectory toward becoming a carbon sink. These habitat maps will be used as a baseline to monitor the rehabilitation in the future.

Outlook for the future

The objective of this work was to map the vegetation communities using machine learning with spectral bands and vegetation indices from satellite data which were validated by the ground truth data. The methodology will be transferrable to any wetland with similar vegetation communities. It can also help to identify the extent of the progress of the rehabilitation process. There was a misclassification when vegetation occurred in mosaic with bare peat or in mosaic with water because of 10 m resolution of Sentinel-2 which can be solved using higher resolution images such as PlanetScope or drone images. The future work of the project is to build a model to estimate net ecosystem exchange (NEE) using Satellite data and the flux data from an eddy covariance tower on the site. The habitat maps derived from this work will be used to upscale the NEE and will be validated by the flux tower data. Finally, the land-use and the upscaled carbon flux data will give improved estimates of greenhouse gas (GHG) dynamics for inclusion in national emission inventories for key land-use classes on the wetland sites.

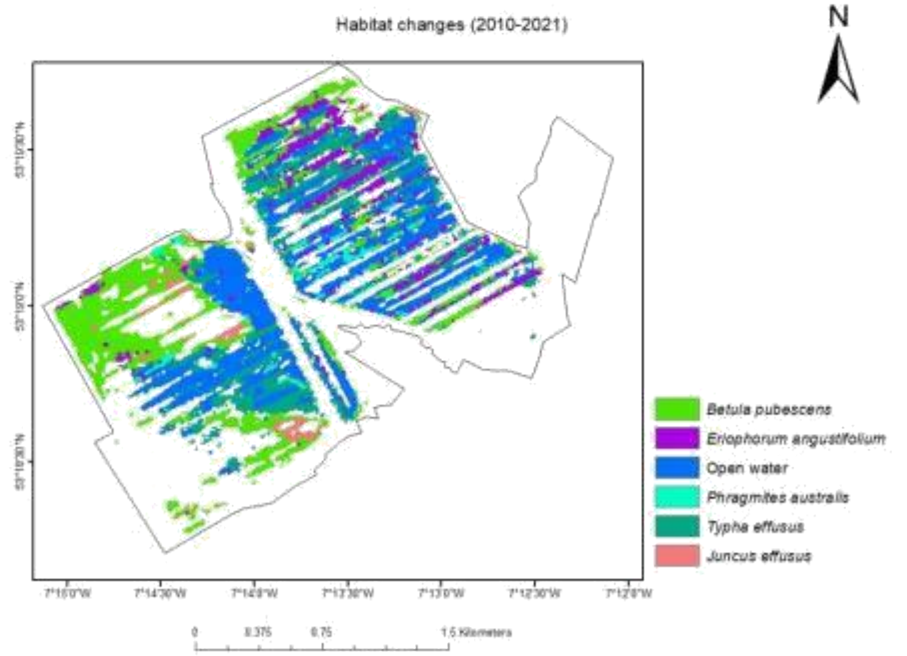

Figure 1 Change detection map showing change of bare peat to various habitats

Random Forest and Convolutional Neural Networks classification of LULUCF using Sentinel-2 data in Czechia

Gabriel Antonio Carneiro[1], Jan Svoboda[2], Přemysl Štych[3], Joaquim João Moreira De Sousa[4]

[1,4] University of Trás-os-Montes e Alto Douro, Department of Engineering, Vila Real, Portugal [1,4] INESC-TEC, Porto, Portugal

[2,3] Charles University Faculty of Science, Department of Department of Applied Geoinformatics and Cartography, Czechia

Keywords: LULUCF, Random Forest, Convolutional Neural Networks, Sentinel-2, Czechia

The challenge

Land Use, Land-use Change and Forestry (LULUCF) is a greenhouse gas inventory sector that evaluates greenhouse gas changes in the atmosphere from Land Use and Land-use change. LULUCF contributing to about 23% of anthropogenic emissions of carbon dioxide, methane and nitrous oxide. Areas of all LULUCF classes (Forest Land, Cropland, Grassland, Wetlands, Settlements and Other Land) and Land-use changes between them are annually collected by each contributing state and sent to the IPCC. LULUCF report is mostly based on official records. An implementation of remote sensing data in LULUCF reporting is still very limited.

This study contributes this problematic and brings an approach based on two methods of classification the LULUCF classes using Sentinel-2 data in the selected regions in Czechia.

Methodology

The methods of classification are based on Random Forest and Convolutional Neural Networks and were tested in two Czech NUTS-2 units using Sentinel-2 data collected in 2018. LULUCF classes were classified. For classification purposes, a mosaic was created using the median in the cloud-based platform Google Earth Engine (GEE). The resulting mosaic consisted of all Sentinel-2 bands in 10 and 20 m spatial resolution. Altitude values derived from SRTM and NDVI variance values were also included in the classification.

RF classification is applied in GEE. In terms of classification method and an evaluation of the accuracy, a combination of these parameters for Random Forest was tested: The Number of Trees (NT), the Variables per Split (VPS) and the Bag Fraction (BF). A total of 450 combinations of selected parameters were tested.

CNN classification is applied to data at desktop using python script. A total of 6 CNN models were trained, varying the size of their input, the loss function used to train them, and the depth of the feature extractor of each one. Mowing windows of sizes 5x5, 7x7, and 65x65 were considered in this study. Four CN architectures were trained in this work, two small networks based on 2D Convolutions, one small network based on 3D Convolution, and one big network (more than 20 layers). The 2D Max Pooling was employed to reduce the data dimension, while the Batch Normalization is used aiming to reduce the overfitting during the training.

Results

For validation purpose number of 2200 points were generated with stratified sampling method in one preliminary classification. The class of each validation point were checked using available resources (LPIS, aerial images, in-situ etc.).

The highest accuracy of Random Forest classification was achieved with overall accuracy = 89.1% and Cohen's Kappa = 0.84 using this combination of parameters: NT = 150, VPS = 3 and BF = 0.1. From point of view input bands, the altitude derived from SRTM and NDVI variance were the most significant for classification in terms of Gini importance.

The best result by CNN classifications was achieved with Extended architecture, slide-window of size 7x7 and Focal Loss function with an overall accuracy = 88 %. It shows that the small models are capable of classifying the LULUCF classes. However, the general performance is still lower than that achieved by Random Forest classification. Compared to the random forest, this method takes much more time for counting the result using CPUs.

Outlook for the future

The developed RF method is based on the classification of Sentinel-2 data using the Random Forest classifier in the cloud-based platform GEE. This seems to be very promising for the systematic implementation of EO data in LULUCF. CNN method is not yet implemented to the GEE, but this method is perspective bringing accurate results.

The following research steps should focus on the possibilities of combining satellite data (Sentinel-2) and cadastral data with the maximum exploitation of the advantages of individual data sources for the purposes of time-compatible LULUCF reporting. For this reason, it is necessary to focus on the evaluation and validation of LULUCF within a longer period and assess the accuracy of the changes. The cloud-based classification method, which would be using the standardized data (Copernicus data) and would be applicable in many countries around the world, could bring significant progress in the use of EO data in LULUCF.

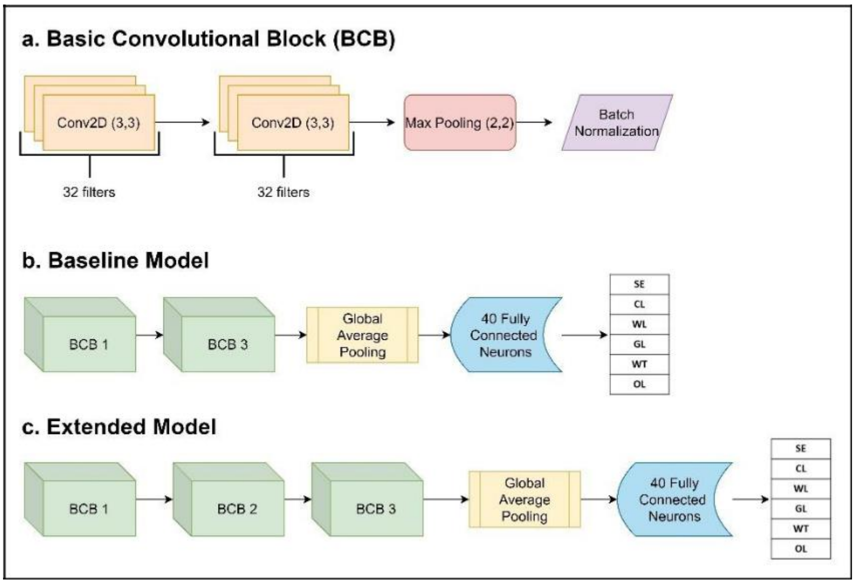

Figure 1 Small 2D Convolution's Architectures used in this study. The a) Basic Convolutional Block is the basis from the feature extractor of the b. Baseline Model and the c. Extended Model. Both de models are connected to the fully connected part using a global average pooling.

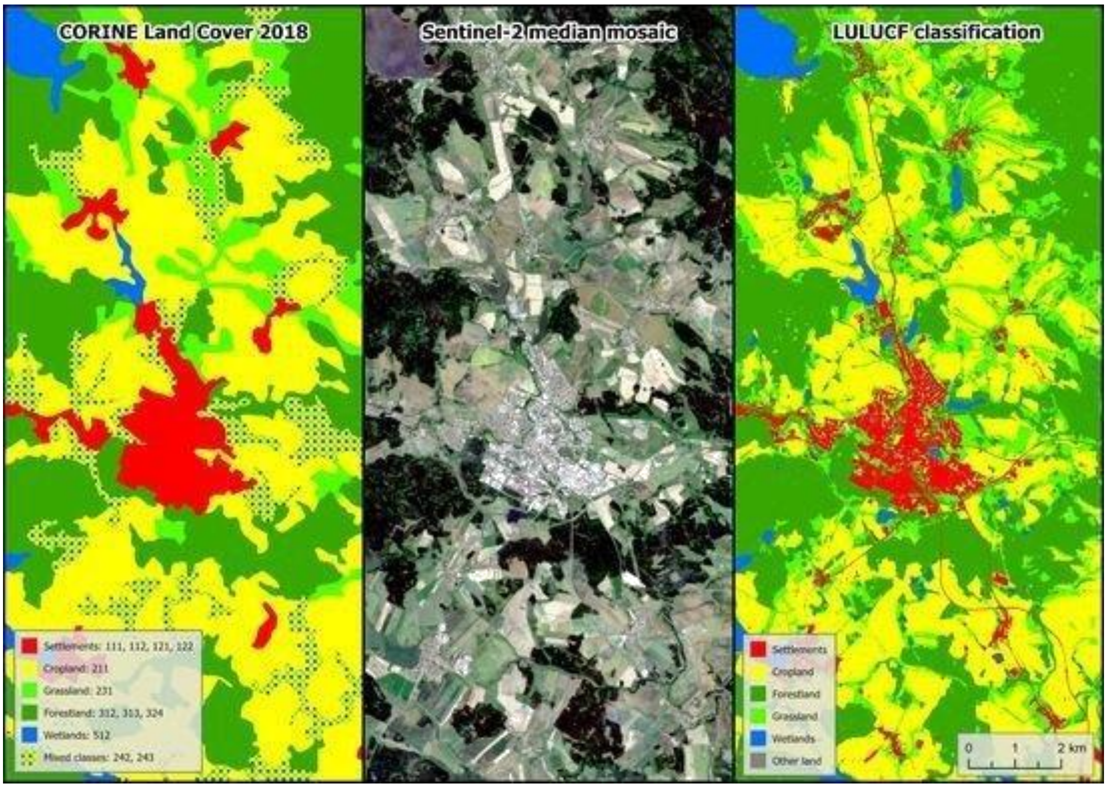

Figure 2 Comparison of CLC 2018 dataset, median mosaic a RF classification

Performance Analysis of Pixel-Based and Object-Oriented LULC Classification in Google Earth Engine Using Multi-Temporal Sentinel-2 Imagery

Suzanna Cuypers[1], Korneel Hoebeke[1], Sander Bracke[1], Andrea Nascetti[1,2], Maarten Vergauwen[1]

[1] KU Leuven, Department of Civil Engineering, Geomatics Section, Belgium

[2] Polytechnic University of Bari, Department of Civil, Environmental, Land, Building Engineering and Chemistry DICATECh, Italy

Keywords (5): LULC, PIXEL-BASED, OBJECT-ORIENTED, MULTI-TEMPORAL IMAGERY, RANDOM FOREST

The Challenge

Land Use and Land Cover (LULC) mapping has been widely investigated over the last decade. The recent availability of dense satellite image time series and the accessibility to cloud processing platforms such as Google Earth Engine (GEE) have unlocked new possibilities for developing LULC classification strategies.

The objective of this research is to explore machine learning processing pipelines in GEE and their accuracy for LULC mapping based on multi-temporal Sentinel-2 (S2) imagery. We compare two machine learning classifiers and investigate the effect of different sets of input features such as S2 spectral bands, vegetation indices, and temporal analysis on the classification results. We also compare a pixel-based (PB) and object-oriented (OO) approach to compute the input features. We investigate the effect of the spectral and temporal indices as well as the performance of the different classification strategies.

Methodology

The reference dataset used for this study is “MiniFrance”, provided by the 2022 IEEE GRSS Data Fusion Contest with 12 LULC classes. Firstly, the reference data collection is imported in GEE and the available labelled areas are sampled using a stratified sampling strategy obtaining a total of 500 reference points per class. 80% of these samples are used as training data and the other 20% as validation data. Subsequently, a composite median cloud-free image is created merging one year of S2 images. Several spectral indices (e.g., NDVI, NDBI, NDWI, EVI etc.) are used to characterize the seasonal variation of the spectral information using harmonic models. The reason for investigating the time-dependency of spectral indices is to highlight the temporal features that are useful to classify land cover, such as crops which exhibit an annual trend in their reflectance pattern. The classification is performed by two different strategies: PB and OO. In the OO method the features are calculated in three steps. Simple Non-Iterative Clustering (SNIC) segmentation provides the necessary spatial object clusters. A Gray Level Co-Occurrence Matrix (GLCM) computes the textural indices, and a Principal Component Analysis (PCA) is used to reduce this textural information into one more informative band. The classification is performed using two classifiers, i.e., a random forest (RF) and support vector machine (SVM). Both RF and SVM yield an overall accuracy (OA) and a confusion matrix for the input bands.

Results

Several tests on various input feature combinations show that the RF classifier obtains an accuracy of around 4 to 8% higher than SVM. Subsequently, the variable importance in the RF algorithm is tested. Figure (a) showcases the variable importance histogram for all S2 bands and the NDBI bands with the corresponding temporal index variables. From this figure, the potential of including the multi-temporal data becomes evident showing that most of the temporal variables exceed all other bands. Oval accuracies drop up to 2% when the time-series analysis is not performed. Excluding high resolution imagery results in a 3-4% performance drop for the OO method. Depending on the used bands and the chosen region of interest, the OA fluctuates between 60 and 70%.

Figure 1 (b) shows the OA and mean Intersection over Union for the optimal datasets for each method. The most accurate classification is achieved with the OO method using S2 and the Normalized Difference Built-up Index (NDBI) bands without temporal data. The overall accuracy of this classification is 70.1%. The larger errors are related to the confusion between urban land cover and between vegetation classes.

Outlook for the Future

The classification will improve by choosing an optimal combination of the input variables, as well as finetuning the RF classifier hyperparameters. We expect adding S1 SAR data will improve detection of the urban class. Abandoning underrepresented or redundant classes could also resolve incorrect classifications. Furthermore, we will assess the classification results by calculating the IoU for each of the reference tiles and investigating the accuracy of the produced land cover maps in the different areas. We will also further investigate the performance of the trained model from the training regions to unseen areas for testing the model's generalisability. When an accurate LULC mapping method is achieved, this method can be expanded to investigate LULC changes.

(a)

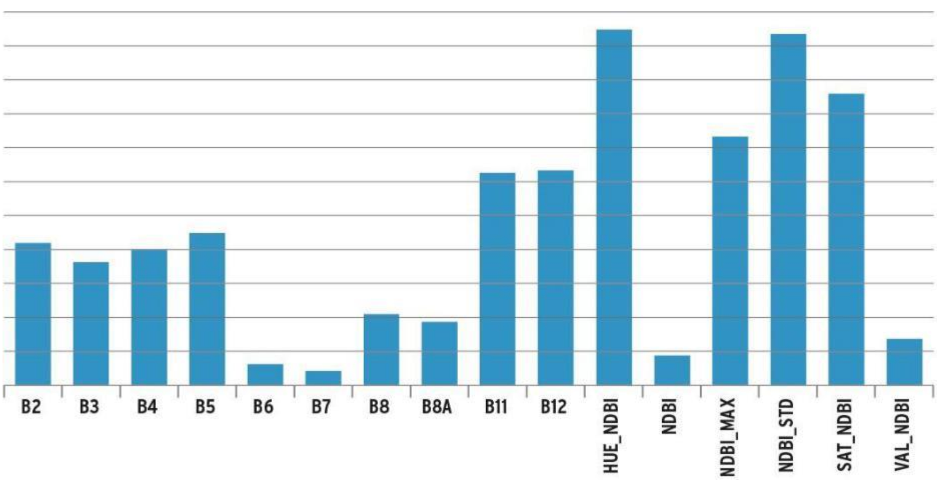

(b)

Optimal dataset			OA	MIoU
Nantes	PB	NDVI (max, std, hue, sat), NDBI (std, hue), GRVI (max, mean, hue, sat), B2, B3, B5, B7, B8, B11, B12, HR imagery (R, G, B)	76.63 %	53.65 %
	OO	NDBI (max, std, mean), B2, B3, B4, B5, B11, B12, HR imagery (R, G, B)	77.31 %	54.18 %
Nice	PB	NDVI (max, hue, sat), NDBI (std, hue), BSI (sat), GRVI (mean, std, hue, sat), B4, B5, B7, B8, B11, B12	71.54 %	57.91 %
	OO	NDBI (max, std, mean), B2, B5, B7, B8, B12, HR imagery (R, G, B)	76.44 %	63.18 %

Figure (a) RF variable importance histogram for S2, NDBI and **(b)** Overall Accuracy (OA) and mean Intersection over Union (MIoU) for the optimal input dataset.

Agricultural Land Use Forecasting – Preliminary Results for a Case Study in the Paphos district, Cyprus

Stelios Neophytides[1,2], Phaedon Kyriakidis[1,2]

[1] ERATOSTHENES Centre of Excellence, Cyprus
[2] Cyprus University of Technology, Cyprus

Keywords (5): Crop yield, Climate Crisis, Earth Observation (EO), Machine Learning, Food Security

The challenge

Agriculture is one of the biggest and most important industries in Cyprus and worldwide. Crop yield estimation, in particular, underpins planning strategies to fulfill projected demands of human population under the constraints of food security. As agricultural land use (ALU) is one of the main parameters controlling crop yield, realistic forecasts regarding future ALU are essential for sustainable growth, particularly in light of the current Climate Crisis. As an example, warmer air temperatures have already affected the duration of the growing season in various parts of the world. In some parts of the Mediterranean area, extreme heat and water stress during the summer months might lead to the cultivation of summer crops during winter instead. Against this backdrop, the principal objective of this research is to forecast ALU distribution for years 2050 and 2100 in the Paphos district on the island of Cyprus, a region that underwent significant ALU changes due to growing population and economic development over the last decades.

Methodology

To build a forecast algorithm, one typically works with past changes, trying to establish links between changes on successive dates, and then forecast these changes in the future. To accomplish such a task, we designed a forecast model combining Markov Chain (MC) and Cellular Automata (CA). MC is a probabilistic model for transitions from one state to another according to certain rules. A Cellular Automaton models the spatial distribution of these changes. In combination, the Markov Chain Model and Cellular Automata form a dynamic model in time and space, powerful in predicting transition dynamics among several LU classes. More specifically, we use the TerrSet2020 software (Land Change Modeller) to develop our CA-MC model and forecast ALU for 2050 and 2100. The most important step in developing this forecast model is the estimation of transition probabilities between Land Use classes for successive timestamps of the past. For this study, LU transition probabilities were computed for the Paphos province for three dates (1990, 2015, 2020) using Earth Observation (EO) data and Machine Learning (ML). The spatial distribution of LU was estimated for the three dates of interest using a supervised classification model base on Landsat 5TM and 8TM data, as well as a NASA Digital Elevation Model (DEM). For classification, the cloud platform of Google Earth

Engine (GEE) was used, as it is becoming a standard tool for the Earth Observation community when dealing with Big Earth Data.

Results

The very first step of our work was the development of Land Use maps for the Paphos area for different years. Land Use supervised classification was performed using the Random Forest (RF) classification algorithm for the years 1990 and 2015*. For 1990, an overall accuracy of 92,10% and a Kappa coefficient of 88,77% were achieved, whereas, for 2005, those statistics were 92,97% and 89,23%, respectively. The largest number of misclassified pixels corresponds to the urban class for both years, and to the fallow Land Use class for 1990 and the agriculture Land Use class for 2015. The calculated area (in km^2) for agricultural land in 1990 was 62.262 and for 2005 was 76.9266. Losses of 0.44% to water bodies, 6.5% to afforested areas 31.39% to urban areas and 6.6% transformed to fallow land in 2005, 0.29% of the forest transformed into an agricultural area, 3.57% changed also to agriculture as the 11.47% of Urban Areas. Agricultural land exchanges maps are generated using Terrset2020, the same as Persistence Map and Changes Map. In the table below one can find Markov Chain derived transition probabilities for Land Use for 2050 and 2100.

From Agricultural Land To:	**2050**	**2100**
Water Bodies	0.096	0.0128
Afforested Areas	0.0548	0.0325
Agricultural Land	0.2376	0.1355
Urban Areas	0.3428	0.3122
Fallow Land	0.3552	0.5285

Outlook for the future

Work is underway towards further optimization of the classification model to achieve more accurate Land Use maps. Most important is the development of a Markov Chain Cellular Automata model to forecast Agricultural Land Use all over Paphos and Cyprus in general. Spatially explicit ALU forecasts will be subsequently combined with crop growth and yield models developed under future climate projections for the region. By the end of the year 2100, the impacts of ALU changes might be more significant than climate change itself. The rise of the Climate Crisis forces the research community to monitor and investigate these critical subjects for the continuation of humanity.

The authors acknowledge the 'EXCELSIOR': ERATOSTHENES: EXcellence Research Centre for Earth Surveillance
and Space-Based Monitoring of the Environment H2020 Widespread Teaming project (www.excelsior2020.eu). The

‘EXCELSIOR’ project has received funding from the European Union’s Horizon 2020 research and innovation
programme under Grant Agreement No 857510, from the Government of the Republic of Cyprus through the
Directorate General for the European Programmes, Coordination and Development and the Cyprus University of Technology.

Adaptability of Inundation Mapping in Service of the Water Utilities: the Case of Giaretta Lake and Brenta River

Ioannis Manakos[1], Afroditi Kita[1], Francesco Zaffanella[2], Sofia Papadopoulou[1],
Lisa Napolitano[2]

[1] Centre for Research and Technology Hellas, Information Technologies Institute, Greece

[2] Autorità di bacino Distrettuale delle Alpi orientali (AAWA), Italy

Keywords: inundation mapping, multispectral data, radar data, fusion, hydroperiod

The challenge

Earth Observation data, especially spaceborne ones, contribute significantly in the study, analysis and preservation of wetland ecosystems by providing continuous monitoring of the fluctuation of open surface water bodies’ extent. This supports a more accurate estimation of the hydrological cycle through time. Various methodologies have been introduced relying on satellite multispectral and radar imagery. Main requirement is the performance stability across habitats and areas. Thus, the applicability of the approach to further sites than the one, where the methodologies have been developed, is of high importance. In this context, this study aims to investigate the adaptability of the workflows developed in H2020 ECOPOTENTIAL project, namely WaterMasks [1: doi.org/10.3390/rs10060910 & 2: doi.org/10.3390/rs11192251] and Hydroperiod, in Giaretta wetland, which comprises the Italian pilot area of the H2020 WQeMS - “Copernicus assisted Water Quality emergency Monitoring Services” project (funded by the EU’s H2020 RIA programme under Grant Agreement No 101004157).

Methodology

WaterMask inundation mapping is based on an unsupervised local thresholding approach, which exploits the light interaction with open surface water and land. The area of interest is classified into inundated (open water and water vegetation class) and non-inundated (land). WaterMask utilises Sentinel-2 (S2) L2A products to automatically detect thresholds in the following three alternative combinations of input bands: SWIR-1 (Band 11) {Alt1}, product of SWIR-2 (Band 12) and NIR {Alt2}, product of SWIR-1 and NIR (Band 8) {Alt3}. Splitting thresholds are detected with minimum entropy thresholding (MCET) or Otsu’s algorithm [1]. Totally nine alternatives were applied to the area of interest, and the best one emerged through a validation process, in which Google Earth images combined with Very High Resolution data and local knowledge about the water level were used to create the ground reference layers. Furthermore, the annual hydroperiod map was produced out of the

WaterMasks's derived maps. Consistent temporal resolution (avoiding non favourable atmospheric conditions) was maintained by employing a machine learning approach [3: https://doi.org/10.1080/22797254.2019.1596757], which exploits fused information from Sentinel-1 (S1) and S2 imageries. Results were then juxtaposed against previous relevant works to retrieve indications between best performing alternative combinations and land cover (landscape) synthesis of the selected area of interest (e.g. land cover elements' distribution). 2 Brenta River Giaretta Lake

Results

The performance of WaterMask in Giaretta open surface water reservoir supported the series of excellent estimations across various areas. Donana in Spain [1], Kerkini [4: doi:10.5220/0010555700480055] and Polyphytos [to be announced] in Greece reached best overall accuracies using the SWIR-1 or SWIR-2 and the MCET algorithm, i.e. 97.5%, 97.16%, and 99.2%, respectively. The best results for Camargue in France[2] reached an overall accuracy of 92.9%, when the product of SWIR-1 and NIR was used together with the Otchu threshold detection algorithm. Indications had related misclassifications with shadowing in the landscape, wave effects and varying structure of the emerged vegetation [2]. The presence of the riverbed in Giaretta's study area synthesis, in conjunction with the fine detailed meandering between the water channel and the sediment depositions, seem to contribute to a relatively lower on average best performance by using the product of SWIR-1 and NIR algorithm (94,9% - see Figure 1). The formation of numerous fine scale sequential landscape patches generates a series of land water transition effects. Monitoring of the flooding regime is timely enhanced with the fusion approach, which shows similarly accurate results [3]. Finally, presence of water over 2% at all times across the area of interest guarantees the presence of expected histogram patterns across the S2 bands used for the analysis. A detailed discussion based on maps will be presented.

Outlook for the future

WQeMS H2020 project aims to expand its services for the users to be able to access and obtain water quality features or maps illustrating the land water transition zone for an open surface water reservoir that are interested in. An up-to-date inundation map may effectively inform and warn water utilities or protected area managers about the possible additional load of materials entering the aboveground aquifer in case of flooding or the increment of the chemical compounds' concentration in case of evaporation and drought. Further elements of consideration for future work are the possibility of enhancing the detectability through S1 imagery analysis and increasing the capacity of registering submerged vegetation. Especially the latter contributes significantly to the water quality balance of the water reservoir.

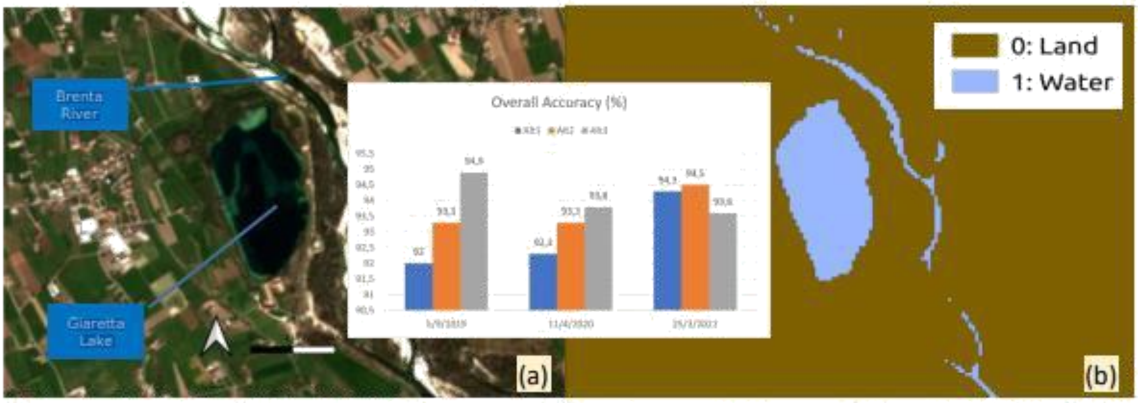

Figure 1. (a) True colour image of the Giaretta lake and surroundings on 24-03-2021. (b) Inundation map of the area of interest derived with the WaterMask module.

Poster(s)

Evaluation of open-source data and remote sensing techniques for spatially explicit very high-resolution soil sealing information in North-Rhine Westphalia (Western Germany)

Jan-Philipp Langenkamp[1], Christian Daniel[1], Andreas Rienow[1]

[1] Ruhr-University Bochum, Institute of Geography, Germany

Keywords: soil sealing, aerial imagery, Sentinel-2, OBIA, convolutional neural network (CNN)

The challenge

With the introduction of ALKIS, the official real estate cadastre information system for Germany, all federal states replaced their previous real estate cadastre records - the automated real estate map (ALK) and the automated real estate book (ALB) - in December 2015. The migration to ALKIS led to a break in the official land statistics. These circumstances affected the vital estimation of the soil sealing degree as an indicator of urbanization. There is a need for less susceptible methods to detect soil sealing that can spatially keep up with the official in situ data. Our study aims to develop a remote sensing-based method network that forms a counterpart to the official in situ data collection to provide time-independent soil sealing information. For this purpose, we focus on the federal state of North Rhine-Westphalia (NRW). Our study is financed by the State Office for Nature, Environment, and Consumer Protection NRW.

Methodology

In our study, we focused on freely accessible data. Therefore, we considered official aerial imagery due to its high spatial resolution (0,1m/ pixel), Sentinel-2 satellite imagery due to their temporal and spectral resolution, and official geodata as a federal-wide information basis. Our region of interest for this study is the heterogeneous metropolitan city of Wuppertal. For object-based approaches, we used the software eCognition Developer for pixel-based approaches, we used Google Earth's Engine (GEE). For our purpose, we defined the classes impervious surfaces such as e.g., buildings and roads, and pervious surfaces. In these two classes, we sampled our training data. In our first approach, we classified aerial imagery with a convolutional neural network based on spectral bands to interpret the feasibility of this method for our task. In our second approach, we performed both pixel-based and object-based Random Forest classification on both aerial imagery and Sentinel-2 satellite imagery, as it is known to be robust for large-area land cover classification. Besides spectral bands, we calculated various spectral indices as inputs for Random Forest classification. Additionally, we calculated various temporal composites in order to optimize results from the pixel-based approach in GEE. In our third approach, we fused aerial imagery with official geodata before Random Forest classification to oppose disturbing factors such as canopy or shadow areas in the imagery.

Results

The results provide information on pervious and impervious surfaces in our region of interest based on aerial imagery and Sentinel-2 satellite imagery with accuracies exceeding 80 %. For validation, we selected 100 samples per class based on aerial imagery by stratified random sampling. According to our results, object-based Random Forest classification of aerial imagery provides the highest accuracy within the approaches with an accuracy of 91, 5 %. The data fusion with official geodata optimized this result by up to 92 %. With this method, the pixel-based Random Forest classification reached an accuracy of 91, 5 %. This result also applies to object-based Random Forest classification of Sentinel-2 satellite imagery. For this case, we provided an accuracy of 96 %. Although, the pixel-based Random Forest classification of Sentinel-2 satellite imagery has a lower accuracy of 94% the consideration of temporal composites improved the result up to 95%. Accordingly, the object-based classification approaches on different spatial resolutions allow accurate estimation of soil sealing. Furthermore, the data fusion of official aerial imagery and official geodata is a suitable method to optimize classification results.

Outlook for the future

However, there is a dilemma between the high spatial but low temporal resolution of the official aerial imagery and the low spatial but high temporal and spectral resolution of the Sentinel-2 satellite imagery. Furthermore, due to its spatial resolution, there is a need to overcome the high processing times of aerial imagery. Accordingly, our goal for the future is to combine the benefits of both official aerial imagery and Sentinel2 satellite imagery to build a robust method to provide gapless estimations of soil sealing for the official land statistics in NRW. Further, it is our goal to create an accessible solution that can easily be integrated into the data infrastructure of NRW to provide an independent counterpart to the public in situ data collection. For this purpose, we are working on a reference classification based on official aerial imagery that can be updated annually both retrospective and prospective via Sentinel-2 satellite imagery using linear spectral unmixing.

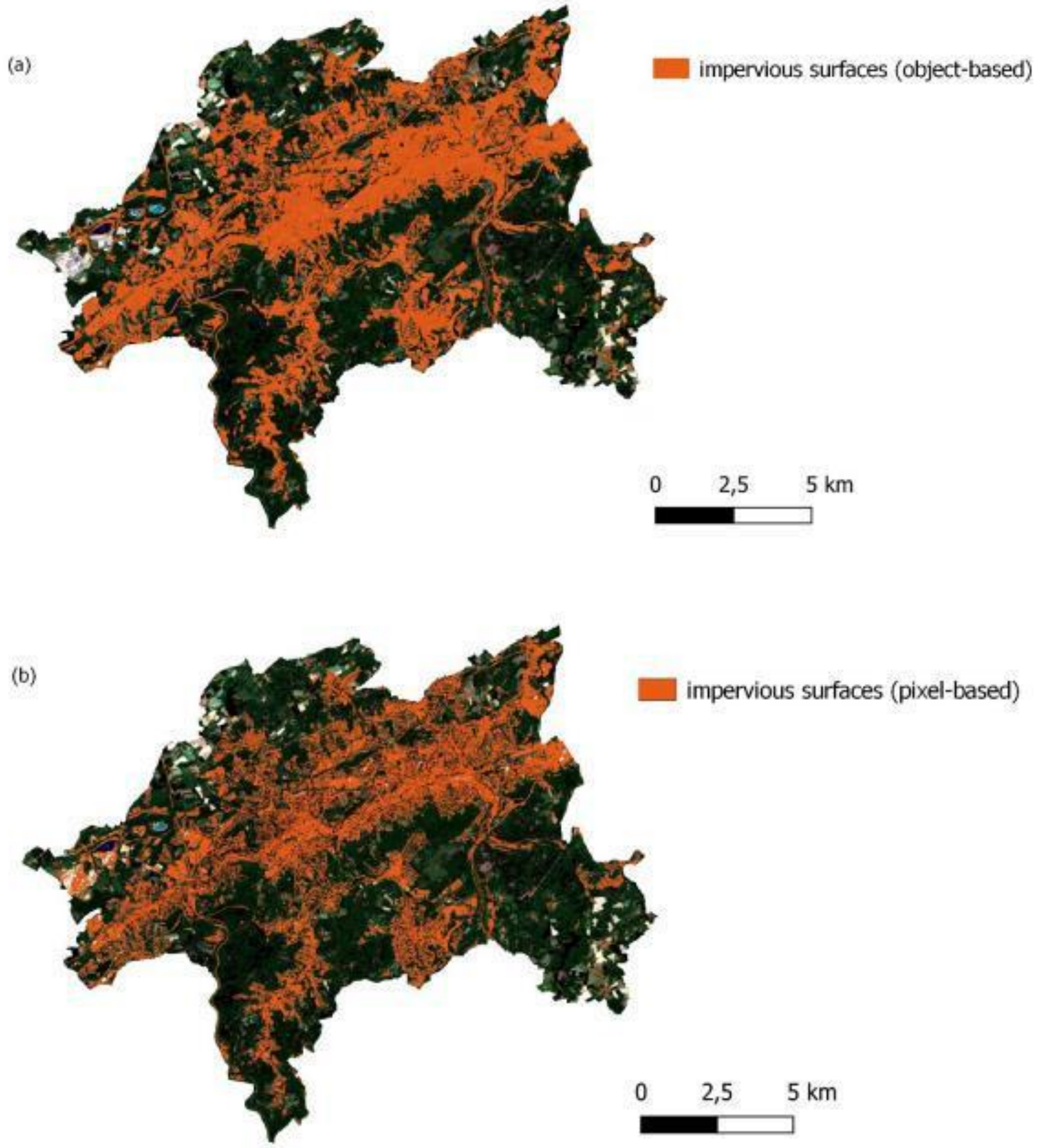

Figure (a) Wuppertal: Random Forest classification on Sentinel-2, object-based (b) Wuppertal: Random Forest classification on Senitnel-2, pixel-based

A Long-Term Spatiotemporal Analysis of Biocrusts Across A Diverse Arid Environment: The Case of the Israeli-Egyptian Sandfield

Klil Noy[1], Noa Ohana-Levi[1,2], Natalya Panov[1], Micha Silver[1], Arnon Karnieli[1]

[1] The Remote Sensing Laboratory, French Associates Institute For Agriculture And Biotechnology Of Drylands, The Jacob Blaustein Institutes For Desert Research, Ben-Gurion University, Sede Boker Campus, 84990, Israel
[2] Independent Researcher, Ashalim, 85512, Israel

Keywords (5): Crust Index, Time-series clustering, Long-term trend, Landsat, Remote sensing

The challenge

Spatiotemporal data can be analyzed using spatial, time-series, and machine learning algorithms to extract regional biocrust trends. Analyzing the spatial trends of biocrusts through time, using satellite imagery, may improve the quantification and understanding of their change drivers. The current work strives to develop a unique framework for analyzing spatiotemporal trends of the spectral Crust Index (CI), thus identifying the drivers of the biocrusts' spatial and temporal patterns.

Methodology

To fulfill this goal, CI maps, derived from 31 annual Landsat images, were analyzed by applying advanced statistical and machine learning algorithms. A comprehensive overview of biocrusts' spatiotemporal patterns was achieved using an integrative approach, including a long-term analysis, using the Mann-Kendall (MK) statistical test, and a short-term analysis, using a rolling MK with a window size of five years. Additionally, temporal clustering, using the partition around medoids (PAM) algorithm, was applied to model the spatial multi-annual dynamics of the CI. A Granger Causality test was then applied to quantify the relations between CI dynamics and precipitation.

Results

The findings show that 88.7% of pixels experienced a significant negative change, and only 0.5% experienced a significant positive change. A strong association was found in temporal trends among all clusters ($0.67 \leq r \leq 0.8$), signifying a regional effect due to precipitation levels ($p < 0.05$ for most clusters). The biocrust dynamics were also locally affected by anthropogenic factors (0.58 > CI > 0.64 and 0.64 > CI > 0.71 for strongly and weakly affected regions, respectively).

Outlook for the future

A spatiotemporal analysis of a series of spaceborne images may improve conservation management by evaluating biocrust development in drylands. The suggested framework may also by applied to various disciplines related to quantifying spatial and temporal trends.

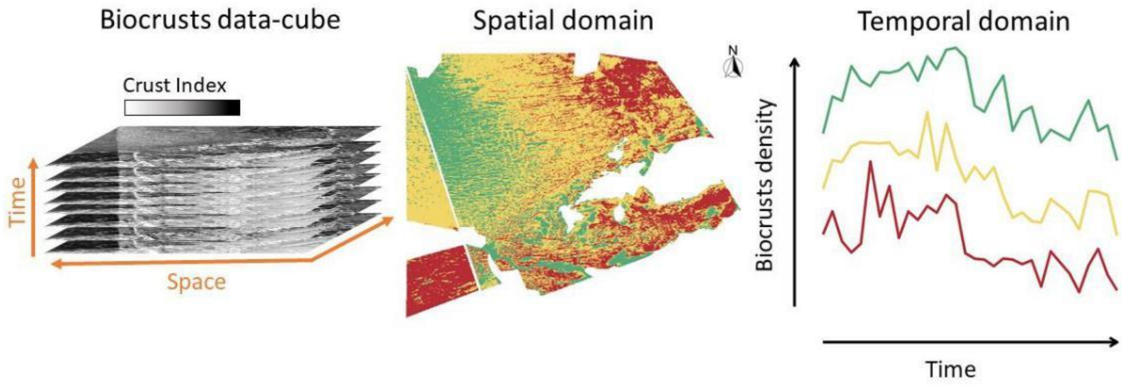

Figure: Graphical abstract

Joint exploitation of Sentinel-1 and Sentinel-2 temporal composites for land cover and crop type mapping

Giorgos Begkos, Christina Karakizi, Konstantinos Karantzalos

National Technical University of Athens, Remote Sensing Laboratory, Greece

Keywords: Classification, SAR, Random Forest, Google Earth Engine

The challenge

Accurate and regularly updated land cover mapping arises as essential for several scientific communities, but also for public and regional authorities in terms of supporting decision making, planning, and natural resources management. Regular monitoring and mapping plays also a key role for agricultural areas, given the projected population growth and dietary changes in many of the fastest growing regions in the world. At the same time open data policies are delivering an unprecedented volume of satellite imagery data with an increasing level of detail and accuracy, while also posing significant challenges, concerning data handling, storage and processing. Recent studies have demonstrated the effectiveness of the combined use of SAR data along with optical imagery, for land cover and crop-type mapping tasks. To this end, in this work, we assess the synergistic use of Sentinel-2 and Sentinel-1 temporal composites for land cover and crop type mapping, on the Google Earth Engine Platform.

Methodology

The mapping experiments were applied on two Sentinel-2 tiles: 34SEJ and 35TLF in central and northeast Greece respectively (Figure 1a). All available Sentinel-2 L2A images with less than 20% cloud cover corresponding to one agricultural year i.e., from November 2018 to November 2019, were used to create three-month composites based on the median reflectance values of seven spectral bands and four spectral indices. Three-month composites for the same period were created based on the mean and the standard deviation values, derived from the corresponding Sentinel-1 GRD IW products in dual polarimetry (VH&VV), after the application of additional corrective/normalizing steps. A Random Forests classifier was applied for the classification of 35 land cover classes, including 18 crop types, which were specifically defined to depict the Greek landscape. Reference data used for the classification experiments, derived from a national database created in the NTUA Remote Sensing Laboratory through intensive photo-interpretation and annotation procedures, in-situ data collection and the integration of external data sources. Several combinations of classification features, i.e., multispectral optical, radar and additional ancillary information from elevation and thematic data, were employed on various experiments. The different features' contribution was assessed based on the derived classification results while the impurity-based feature importance was computed using the Gini index.

Results

The standard metrics of Overall Accuracy, User's Accuracy and Producer's Accuracy were calculated to evaluate the classifier performance for each experiment. Per class F-measure (F1) scores were also calculated as the harmonic mean between User's and Producer's Accuracy. In addition, the average F1 from all classification categories was calculated, as a single-number indicator of each experiment's efficiency, comparable to Overall Accuracy, but without the bias of class sample size. Experimental results in all cases reached high Overall Accuracy rates (exceeding the 86% mark for the 35TLF tile and 90% for the 34SEJ) and Average F1 scores (exceeding 68% and 78% respectively). In particular, when classification was performed using the Sentinel-2 composites, the Overall Accuracy rates reached 86% and 91% for tile 35TLF and 34SEJ, with average F1 rates of 75% and 81% respectively. When appending the Sentinel-1 composites as well, OA rates increased by 2-3% whereas average F1 scores by 3- 6%. The highest accuracy rates were recorded when combining optical, SAR and ancillary data, especially for the crop classes, reaching OA rates and average F1 scores of 90% and 82% for the northern 35TLF tile and 94% and 86%, respectively, for the central 34SEJ one. Nevertheless, the use of ancillary data along with the Sentinel-2 temporal composites produced competitive results (OA differed less than 2%) to the full set of features.

Outlook for the future

In overall, the experimental results and their evaluation demonstrated the efficiency of the proposed approach achieving high overall accuracy rates, while analysis on the variation of accuracy metrics when using different classification schemes highlighted the discriminative capacity of the different classification features. The expansion of the proposed methodology at the country scale could set the basis towards operational national land cover and crop type map production at regular time intervals, for supporting national and European actions, initiatives and mapping programs, such as the CORINE Land Cover inventory and the EU Common Agricultural Policy partnership.

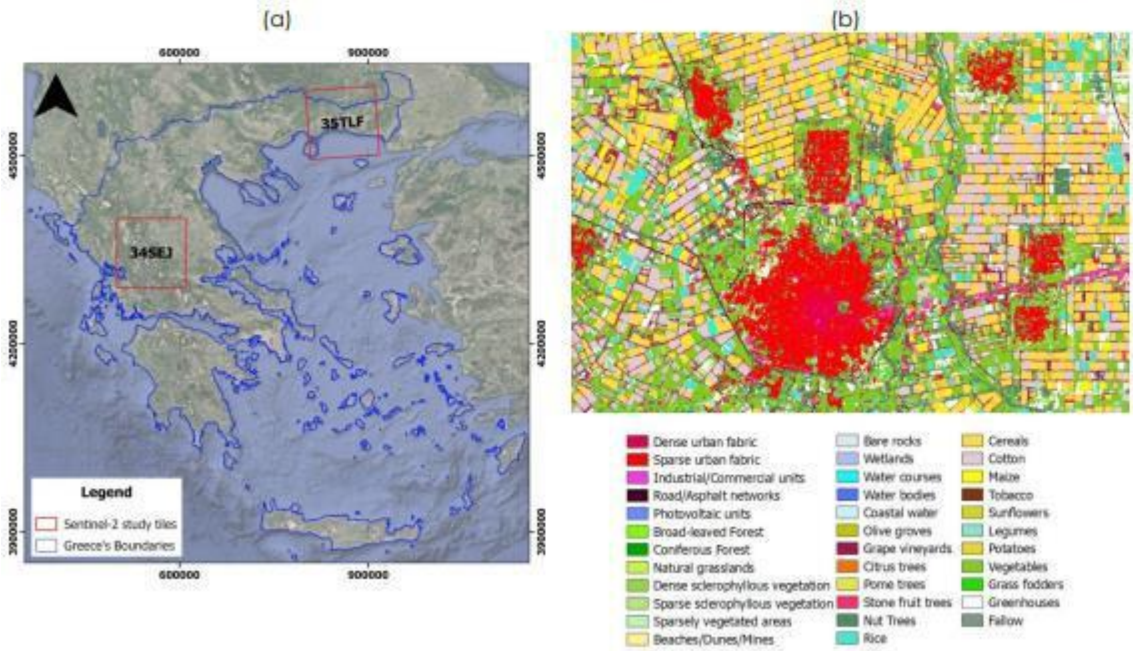

Figure 1.(a) The footprint of the selected for study Sentinel-2 tiles in Greece and (b) part of the predicted land cover and crop type map around the Karditsa city in central Greece.

Local Climate Zone Mapping for Climate Mitigation and Adaption

Benjamin Bechtel[1] , Matthias Demuzere[1] , Jonas Kittner[1] , Panagiotis Sismanidis[1] Gerald Mills[2]

[1] Urban Climatology Group, Department of Geography, Ruhr-University Bochum, Bochum, Germany

[2] School of Geography, University College Dublin, Dublin, Ireland

Keywords: Local Climate Zones, WUDAPT, Climate Mitigation, Climate Adaptation, Urban Form

The challenge

Urban areas are critical for climate action. First of all they are main sources of greenhouse gases and traffic emissions, electricity consumption, and space heating. Second, they are vulnerable towards climate related risks due to high concentrations of people, infrastructure, and stressors. Third, they generate climate related risks due to their modification of the natural surfaces such as urban overheating and flooding. Thus, cities need to be in focus of both mitigation and adaptation efforts. Studying the interactions of cities and the atmosphere is urgent, since urban structures tend to be very persistent once build, meaning wrong design decisions today can likely not be corrected for many decades. Despite this relevance, state of the art global climate models typically lack urban representation, often due to a mismatch in grid resolution and complexity of the processes in the urban canopy and boundary layers, but also the lack of a fit for purpose representation of urban structures.

Methodology

Remote Sensing has the potential to contribute the provision of detailed, timely, and consistent information on urban areas. However, this potential is currently not fully exploited. According to a review from Zhu et al. (2019) Urban Remote Sensing limits itself to case studies and methodological advancements, lacking comprehensive perspectives and diversity. They suggest strategic directions including more details on urban heterogeneity as well as form and structure. To fill some of these gaps, we created a global map of Local Climate Zones (LCZ) (Demuzere et al., 2022). LCZ are a generic description of urban and rural landscapes at local scales of 100s of m to kms (Steward and Oke 2012). They have proven useful in various contexts as physically-based simple and generic description of urban structures and their heterogeneity including a set of physical parameters (Ching et al. 2018). Over the past years the WUDAPT-method (Bechtel et al., 2015) was adapted and improved to be applied on to global scale. First, the LCZ Generator (Demuzere et al., 2021) was launched to 1) allow automated LCZ map creation in the cloud and 2) to extend the collection of training area samples from around the world. Combining local processing with Python's scikit-learn and the power of google earth engine cloud processing, a Random Forest classifier was trained on 30 selected earth observation features using the collected training samples. A 50x bootstrapping approach was used for accuracy assessment generating a classification probability map and deriving the final map using the modal value of all classifications.

Results

LCZ mapping has become very popular both in the Urban Climate and Remote Sensing and Image Analysis (e.g. Yokoya et al. 2018) communities. In this contribution we present the latest developments in 2 (Style: Footer) the field, in particular the first global LCZ map (Figure 1, Demuzere et al. 2022) and its potential applications in climate mitigation and adaption. Its quality is assessed using a bootstrap cross validation alongside a thematic benchmark for 150 selected functional urban areas using independent global and open-source data on surface cover, surface imperviousness, building height, and anthropogenic heat (not shown).

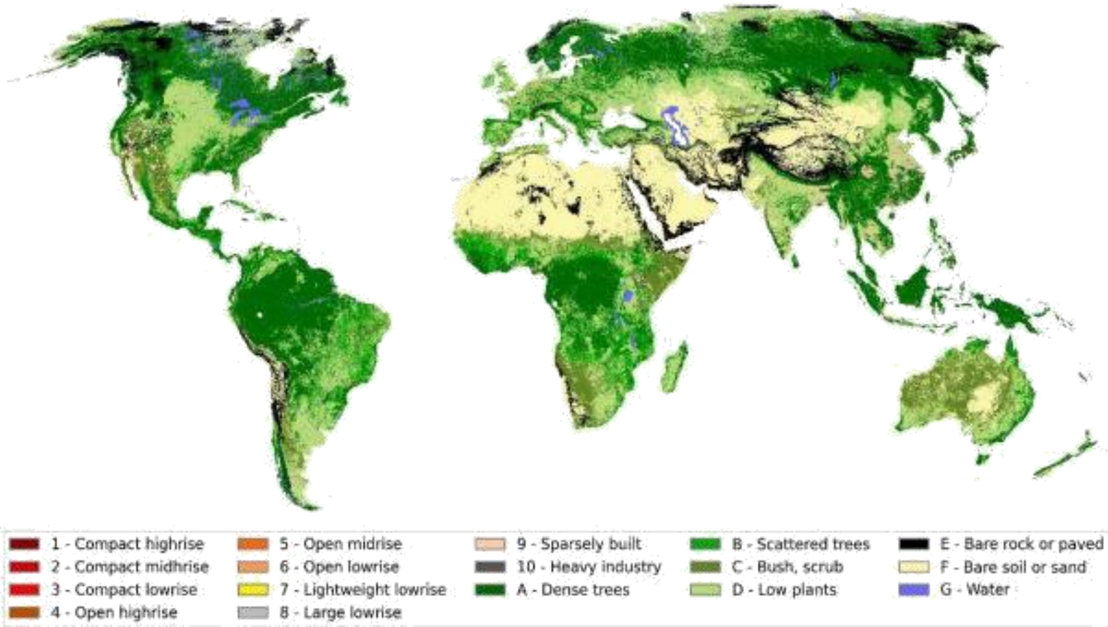

Figure 1: Global Map of Local Climate Zones (Demuzere et al. 2022)

Outlook for the future

As each LCZ type is associated with generic numerical descriptions of key urban canopy parameters that regulate atmospheric responses to urbanization, the availability of this globally consistent and climaterelevant urban description is an important prerequisite to create evidence-based climate-sensitive urban planning policies and to support model development. Work is e.g. ongoing to introduce the global LCZ map as a default urban surface description in the Weather and Research Forecasting (WRF) model, as the LCZ information provides added value when modeling (urban) land-atmosphere interactions (e.g. Patel et al., 2022). In addition, the global map of LCZs can also be used as a framework to examine city-based mitigation and adaptation options at a continental scale, by combining the LCZ data with other publicly available geographic datasets on projected climate changes, topography, population, greenhouse gas emissions, etc., to provide a large-scale evaluation of urban risk and responses.

Time Series Satellite Data For Urban Thermal Environment Changes Analysis Over Bucharest Metropolitan City

Maria Zoran[1], Roxana Savastru[1], Dan Savastru[1], Marina Tautan[1]

[1] National Institute Of R&D For Optoelectronics, Itc Department, Bucharest-Magurele, Romania

Keywords: urban thermal environment*,* Heat wave, Urban Heat Island, biogeophysical variables, Romania

The challenge

The rapid urbanization and the increase in global urban population significantly affects the land surface temperature for major cities worldwide. A better understanding of spatiotemporal changes of the land surface temperature provides accurate insights into global issues such as climate change, urban thermal environment, and energy consumption. This remote sensing-based study aims to investigate the spatiotemporal variations of air temperature T and land surface temperature (LST) over Bucharest metropolitan city in Romania related to summer heat waves (HW) in synergy with urban heat island (UHI) phenomena under global warming. This study considered spatiotemporal changes in the urban and peri-urban land cover and land surface properties as well as in the atmospheric abundance of greenhouse gases and aerosols, and surface solar irradiance which alter the energy balance of the climate system.

Methodology

Remote sensing data from Landsat TM/ETM+/OLI, MODIS Terra/Aqua and NOAA AVHRR, SENTINELs, GOES and SEVIRI sensors with different accuracy due to sensor and satellite specifications (e.g., spatial resolution, orbital frequency, spectral band) have been used to assess urban land cover– temperature interactions change over 2000 - 2022 period. Time series of Thermal InfraRed (TIR) satellite remote sensing data in synergy with meteorological data (air temperature, relative humidity, rate of precipitation, wind speed intensity, surface solar irradiance, etc.) have been applied mainly for analysing land surface temperature (LST) patterns and its relationship with surface landscape characteristics, assessing urban heat island (UHI), and relating urban land cover temperatures (LSTs) and urban heat fluxes. Vegetation abundances and percent impervious surfaces were derived by means of linear spectral mixture model, and a method for effectively enhancing impervious surface has been developed to accurately examine the urban growth.

Results

The air (T) and land surface temperature (LST), key parameters for urban climate research, were analysed in relation with land surface albedo and Normalized Difference Vegetation Index (NDVI) at city level. Based on these parameters, the urban growth, Urban Heat Island (UHI) effect and the relationships of LST to other bio geophysical parameters have been analysed. The correlation analyses revealed that, at the pixel-scale, T and LST possessed a strong positive correlation with percent impervious surfaces and negative correlation with vegetation abundances at the local and regional scale, respectively. Was also analysed UHI phenomenon during extreme heat waves events. Our results suggest that monthly mean UHI intensity is between 1.07^{O}C and 6.12 ^{O}C, and the most intense UHI occurs in day-time in the summer period during heat waves periods. This study found that different urban/peri-urban zones and landscapes bring diurnally and seasonally different contributions to the local and regional thermal environment. City land cover was the most important contributor to increases in regional LST. Vegetation had a clear cooling effect as the normalized vegetation difference index (NDVI) increased during summer periods. Bucharest showed the highest changes in daytime UHI under HW at 2.05 ^{O}C, due to the low convection efficiency in compact high-rise building, while nighttime UHI was highly influenced by heat storage and anthropogenic heat release.

Outlook for the future

Given the ability to define land cover characteristics at the city levels based on attributes such as physiognomy, horizontal and vertical structure of built environment, vegetation phenology and leaf morphology, direct parameterisation of new models and urban thermal environment mapping using time series of new satellite remotely sensed data can enhance the ability to characterize and monitor the derived biogeophysical parameters. Knowledge of urban thermal environment through air and land surface temperature spatio-temporal monitoring as well as heat fluxes variation within a city is of prime importance to the study of urban climate and human–environment interactions.

Acknowledgements: This work was supported by the Romanian Ministry of Research, Innovation and Digitalization, through Program 1- Development of the national research-development system, Subprogram 1.2 - Institutional performance - Projects to finance the excellent RDI, Contract no. 18PFE/30.12.2021, and Program NUCLEU Contract 18N/ 08.02.2019 Act Adit. Nr. 15 /2022

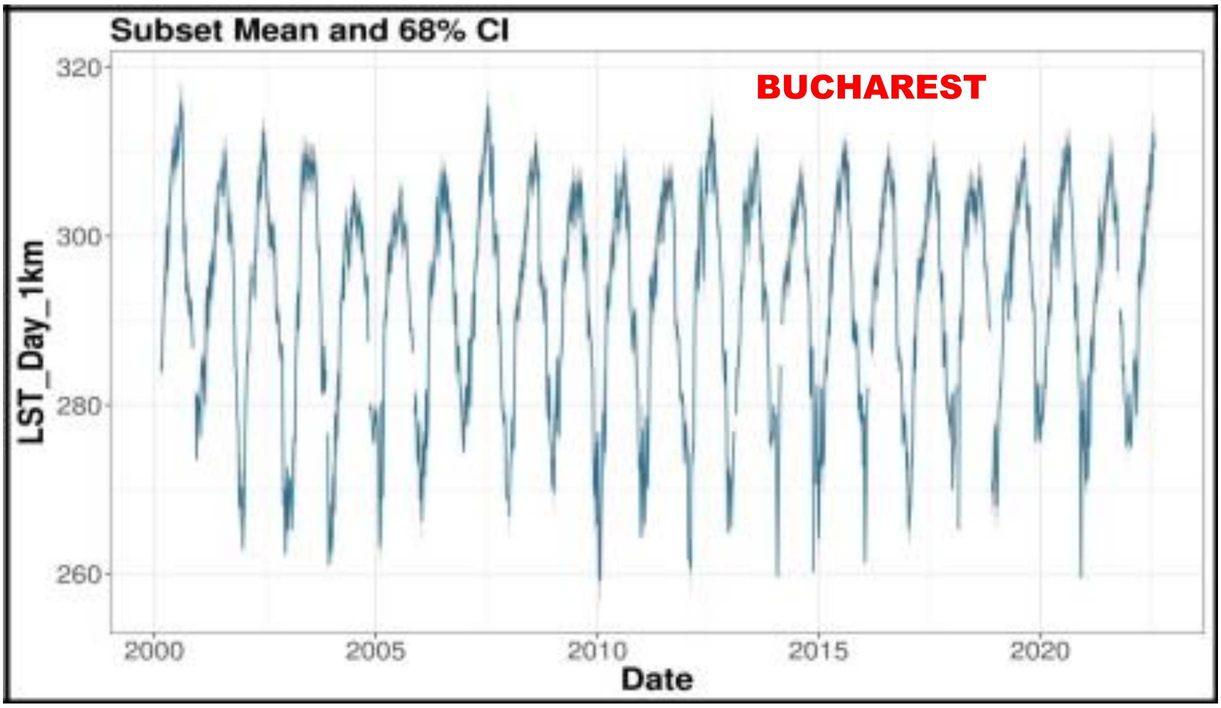

Figure 1. MODIS Terra LST variation between 2000- 2022 years over Bucharest test site

New trends in Geological Remote Sensing

Organizers:

Konstantinos Nikolakopoulos, Christian Mielke and Aggeliki Kyriou

Summary:

Geological Remote Sensing has become ever more important for the scientific and, in the last years, the commercial world. The academic achievements of remote sensing in geology have grown into fully commercialized applications. Dozens of start-up and SME companies have been founded throughout the world offering remote sensing services in diverse topics: Geological Mapping, Tectonic Geology, Mine Monitoring, Hydrogeology, Geomorphology, Geohazards (Landslides, Floods, Earthquakes). Geological remote sensing can offer accurate solutions in scales from 1/100 up to 1/100.000. The session will allow researchers to present the state-of-the-art methods, to make public the opinions and the ideas, get information, find partners and generally relying on the community, to share and to give solutions to many of our common problems.

Topics:

- Geological Mapping
- Mineral Exploration
- Mine Monitoring
- Hydrogeology
- Geomorphology
- Geohazards (Landslides, Floods, Earthquakes)

Scientific Committee:

- Konstantinos Nikolakopoulos, University of Patras
- Christian Mielke, GFZ-Potsdam
- Aggeliki Kyriou, University of Patras
- Olga Sykioti, National Observatory of Athens
- Friederike Koerting, HySpex
- Issaak Parcharidis, Harokopeio University

Creation Of High-Precision 3D Reference Point Clouid Using UAV And TLS Data, Within "PROION" Project.

Konstantinos Nikolakopoulos[1], Aggeliki Kyriou[1], Athanassios Ganas[2], Yiannis Maroufidis[3], Vassiliki (Betty) Charalampopoulou[3], Theodoros Athanasopoulos[4]

[1]University of Patras, Department of Geology, 26504 Patras, Greece

[2]National observatory of Athens, Athens, Greece

[3]Geosystems Hellas S.A, 11632 Athens, Greece

[4]ES Systems, 19442 Koropi-Athens, Greece

Keywords: monitoring, infrastructure, UAV, TLS

The challenge

Climate change has emerged as a global challenge with serious consequences for both humans and environment. In this context, infrastructure monitoring constitutes a vital issue, that requires the development of reliable cost-effective systems, in which remote sensing data, field measurements and advanced methods are integrated. "PROION" is a research project, focused on the development of a platform for the continuous monitoring of high priority infrastructure (public infrastructure, dams, bridges, etc.) in a highly -tectonically and seismically- active area. The project is financially supported by the European Union and the Hellenic government. The monitoring procedure is based on the integration of instrumental and remote sensing measurements along with fuzzy logic network methods and machine learning algorithms, aiming at generating an innovative decision-making and support tool.

Methodology

In more detail, measurements are derived by three-axis accelerometers, Global Navigation Satellite System (GNSS) receivers and Persistent Scatterer Interferometry. These measurements are validated using high-precision reference representations extracted by Terrestrial Laser Scanning (TLS) surveys and Unmanned Aerial Vehicle (UAV) campaigns. The current work focuses on the description of the generation procedure of these representations. An electric vertical take-off and landing (eVTOL) was utilized for the execution of the repeated UAV campaigns over the selected sites. The obtained imagery was processed into Agisoft Metashape according to the SfM photogrammetry. High resolution orthophotos (Figure 1a) and DSMs with sub-centimetre accuracy, were created. On the other hand, a Leica ScanStation P50 was used for the execution of TLS surveys. Each area of interest was scanned using the appropriate number of scan stations for full coverage, while the processing of the collected TLS data was performed into Leica Cyclone software. The correct registration of the scans obtained by the different scan positions in each area of interest, constituted the primary step of the processing. The registration error was calculated lower than 5mm.

Results

The high-precision representations arising from either UAV campaigns or TLS surveys, are used to monitor and detect topographic changes at the investigated areas and to calibrate and evaluate the results of the other data types. It is worth mentioning that monitoring procedure requires the performance of repetitive UAV and TLS surveys throughout the selected sites. Regarding TLS surveys, the proper alignment of the 3D representations constitutes an important step of the processing. The alignment was performed through the identification of common points between the point clouds. The assessment of the accuracy of the generated representations, derived from UAV and TLS data, is performed using precise GNSS measurements. In more detail, the evaluation is based on the computation of root mean square error (RMSE) as well as the implementation of Cloud-to-Cloud comparison approaches.

Outlook for the future

"PROION" project is in an early stage, in which repetitive UAV campaigns and TLS surveys covering the areas of interest are taking place and the collected data is processed appropriately. Deformation maps of each area of interest are created as final outputs of the monitoring process. In a later phase, the deformation maps will be analysed using fuzzy logic network methods and machine learning algorithms. Finally, useful information on the current and future state of each infrastructure will be provided. Acknowledgments: We acknowledge funding by the project PROION "Multiparametric microsensor monitoring platform of the Enceladus Hellenic Supersite" co-financed by Greece and the European Union. Figure 1. (a) Reference 3D representation of a dam, generated by UAV data, and (b) Reference 3D representation of a building, created by TLS data.

SAR-based Automated Unsupervised Rapid Mapping of Land Surface Changes after Volcanic Eruptions in Indonesia

Aiym Orynbaikyzy[1], Simon Plank[1], Sandro Martinis[1], Arum Tjahjaningsih[2], Rido Dwi Ismanto[2], Farikhotul Chusnayah[2], Imam Santoso[2], Suwarsono[2], M. Rokhis Khomarudin[2], and Yenni Vetrita[2]

[1]German Remote Sensing Data Center (DFD), German Aerospace Center (DLR), Germany

[2] Research Organization for Aeronautics and Space, National Research and Innovation Agency (BRIN), Indonesia.

Keywords: change detection, unsupervised, SAR, Sentinel-1, volcanic eruptions.

The challenge

More than one billion people live within <100 km distance from an active volcano (Freire et al., 2019). With the population growth rate above the global average, it is expected that the human concentration around active volcanoes will strongly increase. This also increases the vulnerability, where lowermagnitude volcanic eruptions can lead to catastrophic outcomes

(Mani et al., 2021). Rapid mapping of the affected areas after effusive or explosive volcanic eruptions are crucial for the management of the first response actions and the understanding of the scale of the hazard. In this study, we propose an automatic, unsupervised change detection procedure for mapping land surface change after volcanic eruptions using time-series data of the Synthetic Aperture Radar (SAR) sensor Sentinel-1, supported by preevent clear-sky multispectral imagery of Sentinel-2. Recent eruptions of Indonesian volcanoes – Semeru and Sinabung - were selected as study cases.

Methodology

The unsupervised change detection workflow consists of three main parts: input feature generation, super-pixel segmentation and region growing (Figure 1). For each volcanic eruption event, the closest (in the time dimension) post-event and five pre-event Sentinel-1 scenes, and more than ten pre-event Sentinel-2 scenes are used. Sentinel-2 data was used to calculate the Normalized Difference Vegetation Index (NDVI).

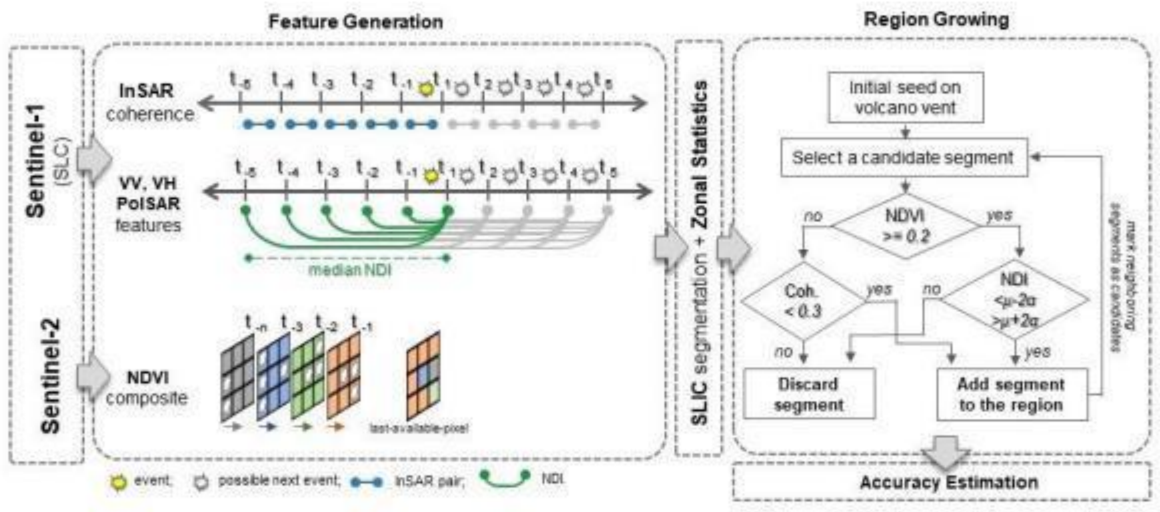

Figure 1. Change detection workflow.

First, the input features such as NDVI composite, radar backscatter intensity and polarimetric SAR (PolSAR) features were calculated. The last-available-pixel composite of NDVI was generated to separate vegetated sites from non-vegetated ones. For mapping changes on non-vegetated sites during and after a volcanic eruption, we used the Interferometric SAR (InSAR) coherence information. As for vegetated sites, we tested the multi-date Normalized Difference Index (mNDI) of SAR backscatter intensity (VH and VV) together with polarimetric features (i.e. entropy, alpha and anisotropy). mNDI was calculated using one, three and five pre-event images. For multi-date mNDI, median reducer over bands was applied. The scikit-image implementation of the Simple Linear Iterative Clustering (SLIC) super-pixel segmentation algorithm was used for segmenting input images using a single set of parameters across all study sites. The last step, a region growing procedure, starts with initial seeds placed on active volcanic vents. Based on the last-available-pixel NDVI composite the segment is evaluated if it is vegetated or non-vegetated. For non-vegetated segments, which are often around the vents of active volcanoes, the empirically selected median InSAR coherence threshold of 0.3 is used to define the segment's change status. For vegetated segments, we tested single features and combinations of mNDI based on radar intensity and polarimetric features. Since calculated NDIs follow a normal distribution, everything outside two standard deviations was considered as a change.

Results

The unsupervised land surface change detection method was tested on two very active Indonesian volcanoes with several major explosive eruptions in the last years. Figure 2. Illustrates the mapping results of two events at Semeru Volcano and at Sinabung Volcano that both took place in 2021. The reference data were created using visual evaluation of pre- and post- event Sentinel-1 and Sentinel-2 scenes. The highest accuracy estimates (Intersection over Union – IoU, dice coefficient - dice) were received when radar backscatter was used alone for detecting changes in vegetated sites (Semeru: IoU – 0.77, dice – 0.63; Sinabung: IoU – 0.81; dice – 0.68) and three or five pre-event scenes were used to calculate NDI. The usage of only polarimetric features resulted in substantially lower accuracies at Semeru Volcano (IoU – 0.27, dice – 0.16), but not at Sinabung Volcano mapping case (IoU – 0.76, dice – 0.61).

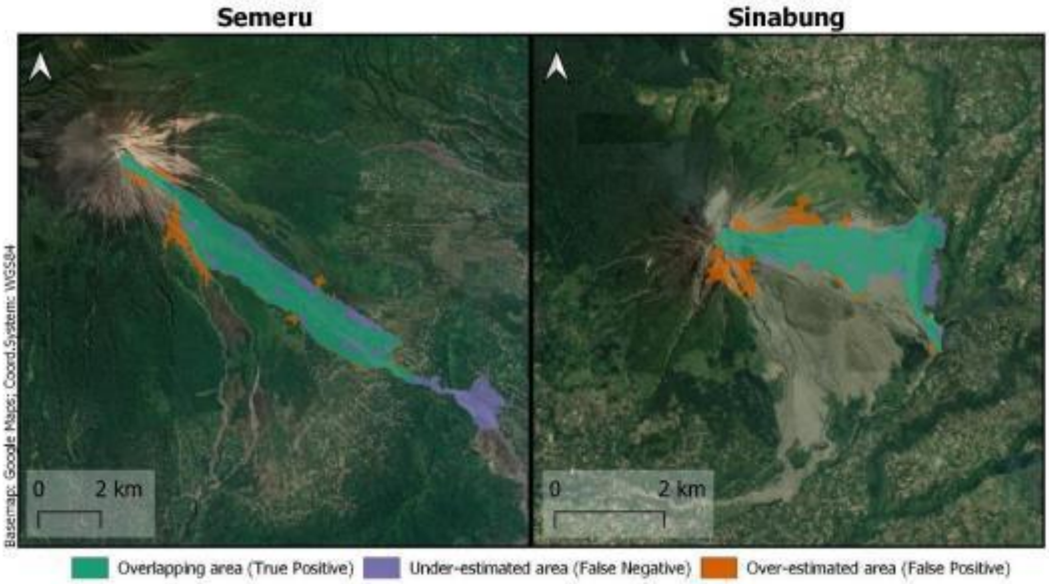

Figure 2. Change detection results of eruptions (left) at Semeru Volcano on 6th of December, 2021 and at (right) Sinabung Volcano on 2nd of March, 2021.

Outlook for the future

In the future, analysis of Sentinel-2 post-event time-series data is planned for an improved understanding of the nature of the change and its severity. In addition, for defining additional seed points, information from infrared sensors about the thermal volcanic activity will be used for an improved location of active volcanic vents. Also, testing the method on other study sites is planned.

Satellite-Based Monitoring of An Active and Fast-Moving Landslide Using Psi And Dinsar Analysis: The Case Study Of Pissouri Village In Cyprus

Kyriaki Fotiou[1,2], Dimitris Kakoullis[2], Marina Pekri[3], Diofantos G. Hadjimitsis[4], George Melillos[2], Chris Danezis[1]

[1]Cyprus University Of Technology, Department Of Civil Engineers And Geomatics, Cyprus
[2]Eratosthenes Centre Of Excellence, Cyprus

Keywords: Active landslide, earthquake, displacement monitoring, PSI, DInSAR, Pissouri, Cyprus

The challenge

The devastating consequences of the active landslide that occurs in Pissouri village in Limassol, Cyprus, in the last few years, has determined the necessity to provide a holistic displacement monitoring analysis of the area using satellite-based techniques. Following the consecutive evacuation of the collapsed houses, in 2017, the Cyprus government intensified ground-based observation campaigns, including geotechnical drilling investigations and geophysical excavations, to determine the geological and geotechnical suitability of the area. Nevertheless, the increased cost and the limited spatial scope offered by conventional techniques do not enable a wide area investigation of the village and the broader area of interest. This study presents the preliminary findings of a spaced-based monitoring analysis carried out by means of Differential Interferometry (DinSAR) and Persistent Scatterer Interferometry (PSI) using the newly found CyCLOPS strategic infrastructure unit's equipment.

Methodology

The rationale of the current methodology is the combination of three (3) main components for monitoring the displacements in the area of interest (AOI). The first component concerns the PSI analysis and includes the quantification and analysis of persistent scatterers. The number of persistent scatterers was computed in three main stages; (a) the identification of as many scatterers as possible in the AOI, (b) extraction of potential scatterers with minimum value of coherence equal to 0.60, based on building density in the village and (c) isolation of the final scatterers that correspond to collapsed houses and critical infrastructures in every pixel. The processing and analysis of Copernicus Sentinel-1 data, covering a timespan ranging from June 2017 to April 2022, were implemented by using the Sentinel Application Platform (SNAP), the Stanford Method for Persistent Scatterers (StaMPS/MTI), and the 'snap2stamps' python workflow, creating a time-series sequence over the passing years. As a secondary factor, a time-series of the rainfall from 2017-present is also used. Finally, data regarding the seismicity of the area were also used to examine the landslides' triggering factors. Eventually, the combination of the aforementioned information will assist the derivation of conclusions regarding the stability of the AOI.

Results

Following the above methodology, three (3) main results were extracted and imported in a GIS environment. Initially, PSs and their vertical displacements in mm/year and their statistics were computed. The epoch 01/12/2019 was selected as the master image to enable geometric and interferometric co-registration of the dataset with respect to a common frame (master image). A significant number of Persistent Scatterers was identified. The displacements rates reach up to a few cm/year. Note that significant displacements were seen pre- and post- earthquake occurrences. In every earthquake phenomenon (as shown in Figure 2), the most affected areas were studied further. Another important finding was that the majority of displacements and infrastructure damages occurred systematically during winter. This conclusion was derived by studying the rainfall time series. Finally, the results were combined and presented in suitable maps, to visualize the behaviour of displacements from 2017 to date.

Outlook for the future

In the framework of the 'CyCLOPS' (INFRASTRUCTURES/1216/0050) strategic infrastructure unit activities, three cutting-edge continuously operating high-rate GPS/GNSS reference stations, weather stations, and tilt-meters, have been deployed in the AOI. Concordantly, an electronic transponder (ECR) has been co-located with one of the GNSS Stations. ECR devices represent the latest development in the field of SAR, replacing the conventional Corner Reflectors. The next step involves the integration of space and ground-based techniques for monitoring the displacements in Pissouri village in a most concise and reliable fashion and form an early warning mechanism for geohazards in Cyprus.

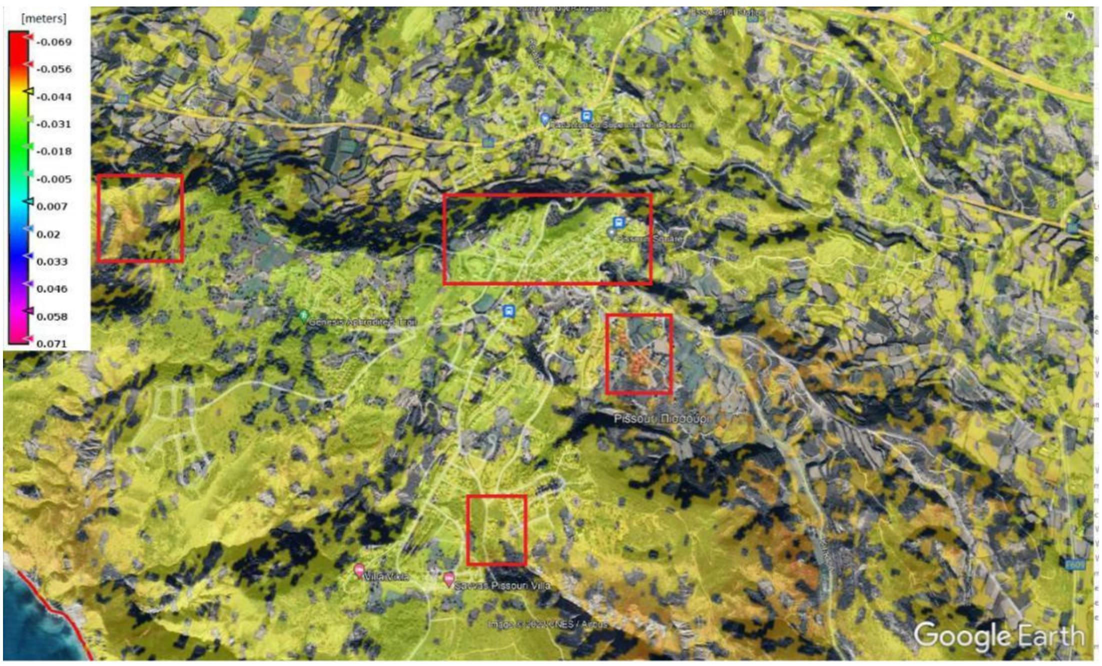

Figure 2: Displacements in Pissouri Area, Cyprus, after the earthquake in 12/01/2022 through DinSAR process, as presented in Google Earth

Acknowledgments

The authors would like to acknowledge the ‘CyCLOPS’(RIF/INFRASTRUCTURES/1216/0050) project (www.cyclops.cy), which is funded by the European Regional and Development Fund and the Republic of Cyprus through the Research and Innovation Foundation in the framework of the RESTART 2016-2020 programme.

The authors would like to acknowledge the ‘EXCELSIOR’ H2020 Teaming project (www.excelsior2020.eu). This paper is under the auspices of the activities of the ‘ERATOSTHENES: Excellence Research Centre for Earth Surveillance and Space-Based Monitoring of the Environment’ – ‘EXCELSIOR’project that has received funding from the European Union's Horizon 2020 research and innovation programme under Grant Agreement No. 857510 and from the Government of the Republic of Cyprus through the Directorate General for the European Programmes, Coordination, and Development.

Seismic Activity Monitoring and Surveillance Of Active Geotectonic Region Vrancea In Romania Via In-Situ And Geospatial Data

Maria Zoran[1], Roxana Savastru[1], Dan Savastru[1], Marina Tautan[1]

[1] National Institute of R&D for Optoelectronics, ITC Department, Bucharest- Magurele, Romania

Keywords: Earthquake Precursors, Satellite Remote Sensing, Lithosphere-Atmosphere-Ionosphere Coupling Model, Crustal Deformation, GPS Data

The challenge

Vrancea, active geotectonic region in Romania, one of the riskiest seismic areas in Europe, spans diverse topography features, several active faults, and present-day crustal deformation. Due to significant physical/ chemical changes which take place in the earthquake preparation zone prior to moderate and major earthquake events, satellite data may record anomalies of different electromagnetic and non-electromagnetic earthquake precursors, while GPS/GNSS observations may record the local deformation precursors. This work is based on the retrospective analysis of several geophysical observations to search for possible lithosphere-atmosphere-ionosphere coupling effects in the preparatory phase of moderate and strong earthquakes recorded in Vance zone for 2012-2021 period. However, the investigation of the seismo-associated phenomena from space is a challenge for the present and near future Earth observation and earthquake forecasting.

Methodology

In Vrancea zone, strong earthquakes with focal depths of ≥70 km will likely occur in the future. Anomaly recognition established criteria were specified explicitly, and the predicted earthquake attributes included time, location, and magnitude. Several retrospective and prospective correlation analyses and new developed algorithms of earthquake forecasting using remote sensing data have been applied for pre-seismic anomalies recognition of different geophysical observables. A global earthquake dataset for moderate and strong historical deep earthquakes data of moment magnitude Mw≥4.0 in Vrancea zone (**Fig.1**) recorded between 2012-2022 years was established as the baseline for statistical analysis against various geophysical parameters and anomaly detection methods. This study consists of a multi parametric approach over different observables from ground and space: the land and atmospheric parameters (land surface temperature-LST, surface latent heat flux -SLHF, and air surface temperature- AT) anomalies, investigated on the basis of time-series NOAA AVHRR and MODIS Terra/Aqua satellite and in-situ data analysis. Ground surface deformations have been detected through analysis of radar satellite Sentinel 1 and high quality in-situ GPS monitoring data.

Results

The detected changes show strong evidence of coupling between lithosphere-atmosphere-ionosphere associated with the Vrancea's earthquakes. For some analysed earthquakes, starting with ten days up to one week prior to a moderate or earthquakes a transient thermal infrared field rise appeared in SLHF (tens of W/m^2) and AT (2-10C^o) values higher than the normal, function of the magnitude and focal depth, which disappeared after the main shock. We apply a methodology that allows to detect subtle, localized patio-temporal fluctuations in hyper-temporal, geostationary-based geophysical parameters data and statistically evaluate our findings with respect to distance from epicenter and temporal coincidence with earthquakes. Ground vertical surface displacements presented on interferometric deformation map are in the range of 4-5 cm for uplifts and subsidence. Since the variations of the solar and geomagnetic indices follow a normal behavior during the whole period of the observed anomalies between 3 and 10 days before the earthquake, it can be concluded that multi-precursors analysis is very useful to detect the possible Lithosphere- Atmosphere-Ionosphere Coupling (LAIC) effects. The results for seismic precursors monitoring of this study could be integrated for continuous and distributed monitoring and surveillance of earthquake hazard/risk in Romania due to Vrancea source, having a high impact on the seismicity monitoring for SDGs as well for Natural Hazard Directive in the EU.

Outlook for the future

As mechanism of earthquakes is very complex, based on new geospatial sensors data new anomaly detection approaches need to be developed and verified, considering also local and regional pre-signal anomalies patterns in different seismically active regions. Synergy use of geospatial, geophysical, and geological information is revealing new insights for Vrancea zone seismicity understanding in Romania. With new geospatial observation data, accurate seismic activity monitoring and surveillance of active geotectonic areas offers significant socioeconomic benefits and improvements to forecasting capability are imperious needed.

Acknowledgements: This work was supported by the Romanian Ministry of Research, Innovation and Digitalization, through Program 1- Development of the national research-development system, Subprogram 1.2 - Institutional performance - Projects to finance the excellent RDI, Contract no. 18PFE/30.12.2021, and Program NUCLEU Contract 18N/ 08.02.2019 Act Adit. Nr. 15 /2022

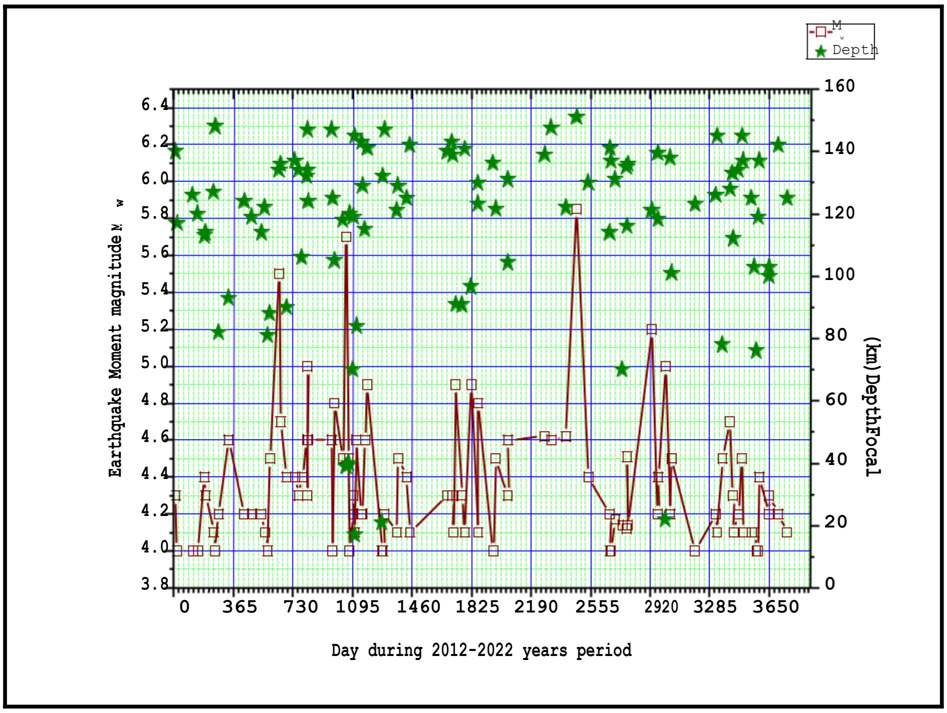

Figure 1 . Recorded earthquakes of moment magnitude Mw≥4 in Vrancea area between 2012-2022 years.

Potentiality of landslide detection in open-pit mines using satellite-based techniques: The case study of Vasiliko Open-Pit Mine in Cyprus

Marinos Avgousti[1,2], Kyriaki Fotiou[1,2], Dimitris Kakoullis[1,2], Chris Danezis[1,2]

[1]Cyprus University of Technology, Department Of Civil Engineers And Geomatics, Cyprus
[2]Eratosthenes Centre Of Excelence, Cyprus

Keywords: Open-pit mines, landslides, limestone, Sentinel-1, DInSAR, Cyprus

The challenge

Monitoring and identifying geohazards in open-pit mines, such as surface deformation, is critical in all planning and development operations stages. Landslides are considered the most dangerous natural hazard in the mining industry. The ability to monitor and predict surface deformations in mining activities could significantly improve and contribute to safety operations and, thus, protect against loss of life, severe injuries, equipment damages, or sustained production losses. On January 9th, 2018, the most severe landslide of all years occurred in Vasiliko open-pit mine in Cyprus. As it is well known, the integrated use of Differential Interferometry (DInSAR) is among the most effective methods to monitor geohazards, such as landslides. The objective of this study is to investigate the possibility of detecting and monitoring large- or small-scale landslides in open-pit limestone mines, using the Sentinel-1 constellation.

Methodology

In the framework of this research, the DInSAR technique was used. Totally eight (8) Sentinel-1A images were processed in Sentinel Application Platform (SNAP) before-and-after the event, covering a time interval from December 2017 to February 2018. Specifically, regarding the Sentinel-1A scenes acquired by the 167 relative orbit number, the satellite passed over Vasiliko Open Pit mine in descending acquisition mode. The VV polarization was chosen as the most favourable mode for monitoring landslides using Sentinel-1 images. The processing was divided into two independent workflows. Initially, the procedure of the extraction of a coherence map with units 0-1, was followed. As a secondary objective, the displacements in the Line of Sight (LoS) and the vertical displacements in the area of interest (AOI) were computed through the phase differences. Consequently, the combination of these two components yields the magnitude of the landslide along the vertical (1D) and horizontal directions (W-E).

Results

Following the above methodology, a preliminary assessment of the ability of Sentinel-1 to detect the landslide at Vasiliko open pit mine, was carried out. As shown in Figure 1, the range of the landslide can be estimated to 25 m along the N-S direction and 20 m along the

E-W direction. Regarding the coherence values, a time-series stack was created in order to visualize and compare the values in the AOI. Indeed, nearby the landslide's dates (30/12/2017-23/1/2018), the coherence values tend to zero, almost covering the entire AOI, as shown in Figure 1. Preliminary results concerning the computed surface displacement in LoS and vertical component were estimated as well.

Outlook for the future

In the framework of the 'CyCLOPS' (INFRASTRUCTURES/1216/0050) strategic infrastructure unit activities, one (1) cutting-edge continuously operating high-rate GPS/GNSS reference station, weather station, and tilt-meter, has been deployed in the Vasiliko Quarry. Concordantly, two (2) corner reflectors have been installed 4 km northest of the Vasiliko open-pit mine, at Asgata Village. Corner Reflectors can be used as reference points, due to their backscattering stability in the time domain. The next step involves the integration of space and ground-based techniques for monitoring the impact of natural hazards at Vasiliko open-pit mine in a most concise and reliable fashion and form an early warning mechanism for related incidents in Cyprus.

(a) (b)

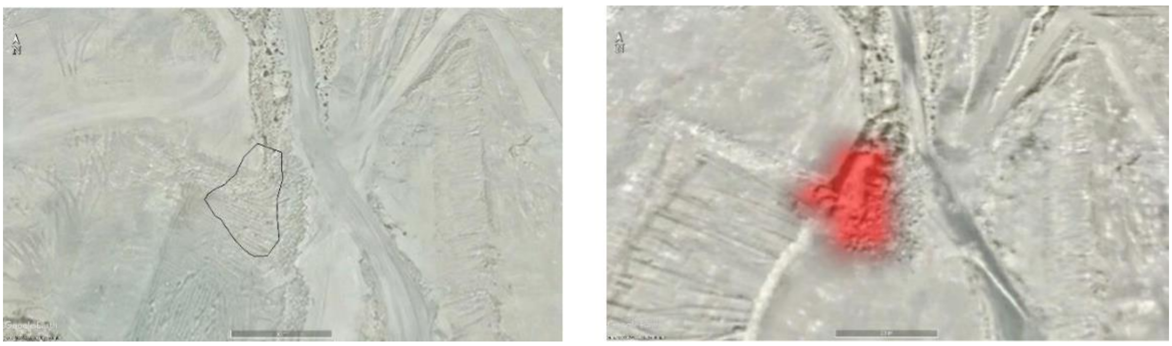

Figure 3: A Snapshot from the initial DinSAR processing. (a) An image obtained from google earth illustrating the AOI in 2017 and (b) the hazardous AOI in 2018. The red colour indicates the vertical displacement after the landslide through DinSAR process.

Acknowledgments:

The authors would like to acknowledge the 'CyCLOPS' (RIF/INFRASTRUCTURES/1216/0050) project, which is funded by the European Regional and Development Fund and the Republic of Cyprus through the Research & Innovation Foundation in the framework of the RESTART 2016 – 2020 programme.

The authors would like to acknowledge the 'EXCELSIOR' H2020 Teaming project. This paper is under the auspices of the activities of the 'ERATOSTHENES: Excellence Research Centre for Earth Surveillance and Space-Based Monitoring of the Environment': 'EXCELSIOR' project that has received funding from the European Union's Horizon 2020 research and innovation programme under Grant Agreement No. 857510 and from the Government of the Republic of Cyprus through the Directorate General for the European Programmes, Coordination, and Development.

Poster(s)

Using remote sensing data with machine learning to predict distribution of red-listed forest species

Xi-Lillian Pang[1], Stefanos Georganos[2], Ulla Mörtberg[1], Yifang Ban[2]

[1] KTH Royal Institute of Technology, Department of Sustainable Development, Environmental Science and Engineering, Sweden

[2] KTH Royal Institute of Technology, Department of Urban Planning and Environment, Sweden

Keywords (5): Biodiversity, Red-listed species, Remote sensing, Machine learning, Forest ecosystems

The challenge

Essential Biodiversity Variables (EBVs) have been developed during the last decades. A critical aspect of EBVs is aiming to capture biodiversity changes. So far, six classes of EBVs have been defined but is still in development, while some variables are still rather conceptual. Due to the complexity of biodiversity, traditional biodiversity monitoring programs and ecological field studies have been seen as insufficient and spatially uneven. At the same time, biodiversity change is often detected when damage is already irreversible, such as when species become locally or regionally extinct. As such, it is imperative to improve our understanding on how natural and anthropogenic drivers determine the spatial and temporal trends of biodiversity. Researchers and decision-makers are currently constrained by the lack of data and indicators to make EBVs operational. In this work, we focus on the potential of remote sensing and machine learning as tools to bridge these gaps and advance our capabilities to understand biodiversity processes.

Methodology

The case study area is Sweden, with research scope of Swedish forest ecosystems. From the European Union's satellite infrastructure and NASA, we select a wide-suit of remotely sensed (RS) derived indicators related to forest species diversity such as: Forest (f.ex. Forest-Cover, Top-of-Canopy, and Burnt-Area); Soil and Surface (f.ex. Surface-Albedo, Leaf-Area-Index, Vegetation-Index, Surface-SoilMoisture, Soil-temperature, etc) and Climate data (such as Air and Precipitation). To understand what the key drivers and their synergistic interactions on species distribution are, we use state-of-the-art machine learning and deep learning approaches to investigate the relationships between the various indicators and occurrence rate (Red-listed species data).When links are established and the key drivers are identified, we work on the analysis of anthropogenic drivers vs nature drivers and recall the gaps of current EBVs development. At the same time, we build a prediction tool based on how speciesdistribution responds to environmental variables to predict the distribution of red-listed species related to natural and man-made driving factors at the national level.

Results

• Ranking on importance of environmental variables regarding to species occurrence • Primary impact factors that affect species richness • Distinguishman-made drivers vs. natural drivers • Response curves of each variable to species occurrence/richness • Synergic effects of individual variables as alliances • A tool box to predict red-listed species distribution

Outlook for the future

The research work will help improve our capabilities to track critical changes of biodiversity at early stages, and further fortifying the use of RS as a rigorous tool to do so. And help to fill the gaps between operational indicators and EBVS. Future studies will include comparison studies on other case study area, to check how environmental variables react on red-listed species distributionand species richness. How different the rankings of variables' importance are, and what are the reasons for the differences.

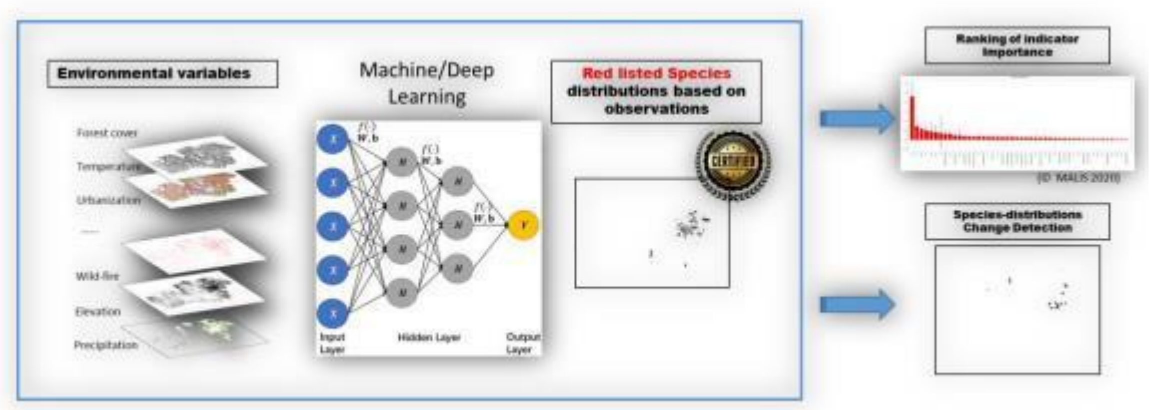

Figure - Research framework (source: Xi-Lillian Pang)

The Valuable Usage of The Multitemporal Data To The Rate Of Shoreline Change Determination In Sandy Beaches

Dionysios N. Apostolopoulos[1], Konstantinos G. Nikolakopoulos[1]

[1]University Of Patras, Department Of Geology, G.I.S & Remote Sensing Laboratory, Greece

Keywords (5): GIS, Shoreline, Multitemporal, EPR, LRR

The challenge

Sandy beaches are subject to pressures of natural phenomena such as wind, waves, tides, etc. It is important, in such beaches, the rate of the coastline changes to be able to determinate efficiently. Nowadays remote sensing applications have proven to be particularly useful and effective in monitoring and measuring physical parameters as well as in extracting statistical conclusions. The success of these methods is even greater when high-resolution data are used. The aim of the current study is to determinate the more reliable index, among the End Point Rate (EPR) and the Linear Regression Rates (LRR), provided by the (Digital Shoreline Analysis System (DSAS) tool developed for the ArcGIS software, for shoreline change measuring. The sandy coastal area of Prokopos lagoon, situated in the Achaia Prefecture, Greece, was used as test site.

Methodology

High-resolution orthomosaics were acquired through the Ministry of Rural Development and Food, and the Greek Cadastre for the years of 1945, 1996, and 2008. In addition, three sets obtained by the declassified CORONA top-secret military archive, for the years of 1965, 1968, and 1975 with spatial resolution up to 4 meters were orthorectified and georeferenced to Hellenic Geodetic Reference System of 1987 (Greek Grid). Moreover, aerial photographs were collected at scale 1/30,000 obtained from different missions (1960, 1971, and 1987) by the Hellenic Military Geographical Service (HMGS), while a scene of Worldview-2 imagery (0.50-m spatial resolution) of the year 2018 was used.

All images were cloud free, while the tide height throughout the year is estimated at 0.00 m to ± 0.10 m, which is quite negligible to affect the shoreline extraction process.

In a Geographic Information System (G.I.S) environment, using the wetted boundaries that where visible in the images, we digitized all the relative shorelines and a baseline was drawn onshore manually, while transects were set every 30 m along the coast.

The LRR and the EPR statistical models computed for the period of 1945 - 2018 and the results were compared between them as well as to the EPR provided by the intermediate periods 1945-1960, 1960 – 1971, 1971 – 1987, 1987- 1996, 1996 – 2008, and 2008 – 2018.

Results

The result shows that the EPR corresponds to the absolute annual rate of change of the coastline only in the case where two consecutive coastlines are examined (oldest and newest). In any other case the EPR transformed to a statistical indicator, the uncertainty of which increases as the years between the available coastlines increase. For this reason, the EPR change rate is not suitable to be used to describe future shore changes.

On the other hand, the LRR corresponds to the statistical annual rate of shoreline change, calculated using all the available shoreline positions, providing results different to the EPR. It is calculated using a least square regression line from all the shoreline positions along each transect. The inclination of the line is the linear regression rate. The LRR become more reliable as many shorelines are available. It is obvious that the more evenly distributed the coastlines, the better and more reliable the rate of change provided by the LRR. In addition, the LRR has the advantage to could be used to express the future rate of change with satisfactory accuracy only in cases where high correlation between the EPR and the LRR rates emerged. It was proved that the LRR is more reliable index than the EPR in case of multitemporal datasets, while both tools yield the same results in the case where two consecutive coastlines are examined. Moreover, the LRR is susceptible to outlier effects and tends to underestimate the rate of change relative to the EPR.

Outlook for the future

As many data is now collected daily from both, aerial and satellite images, as well as from images from UAV's, in the future there will be a plenty of data available to consider the shoreline evolution in a coastal area. The LRR index could be an efficient and easy-to-use statistical tool which accurately give the rate of change of the coastline for a period but also for the future under some restrictions.

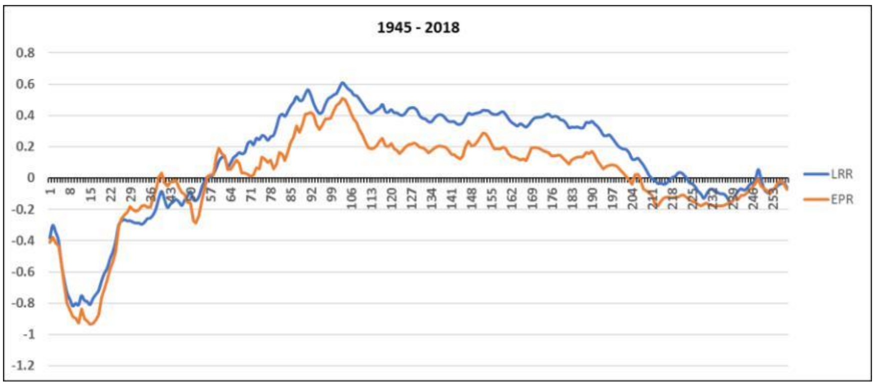

Figure Comparative LRR and EPR Rates along the Prokopos Lagoon sea-zone for 1945-2018 period

Earth Observation for Water Resources Management in the Eastern Mediterranean Middle East North Africa (EMMENA) Region

Organizers:

Diofantos Hadjimitsis, Gunter Schreier, Haris Kontoes, Albert Ansmann, George Komodromos, Christiana Papoutsa, Silas Michaelides, Kyriakos Themistocleous and Vincent Ambrosia

Summary:

Throughout the past decades, the EMMENA region faces climatic extremes due to the climate crisis. Particularly, the decrease of precipitation makes the region highly vulnerable to droughts. The increased frequency and intensity of droughts results in various problems to the environment, the economy, and the agricultural sector. The need for fresh water obliges many countries to place unprecedented pressure on water resources, therefore sustainable water resources management presents a vital issue in the EMMENA region. Aligning with the needs in the region, the ERATOSTHENES Centre of Excellence, in the framework of the EXCELSIOR H2020 Project, has defined sustainable water resources management as one of the five application domains to excel. The challenges associated with climate variability and change include the availability and use of freshwater, water shortages, water mismanagement, water quality, the use of water for irrigation, agricultural failure, land desertification, coastal zone management, etc. Remote sensing tools provide spatially and temporally explicit information on earth's processes and contribute significantly in managing risks and reducing impacts of natural disasters. Thus, the use of remote sensing techniques is considered of great importance in sustainable water resources management.

Topics:

- Droughts
- Climate Change
- Desertification
- Hydrology
- Soil Degradation
- Irrigation
- Smart Techniques

Scientific Committee:

- Diofantos Hadjimitsis, Cyprus University of Technology & ERATOSTHENES Centre of Excellence
- Gunter Schreier, German Aerospace Center
- Haris Kontoes, National Observatory of Athens
- Felix Bachofer, German Aerospace Center
- Christiana Papoutsa, Cyprus University of Technology & ERATOSTHENES Centre of Excellence
- Silas Michaelides, Cyprus University of Technology & ERATOSTHENES Centre of Excellence
- Kyriacos Themistocleous, Cyprus University of Technology & ERATOSTHENES Centre of Excellence
- Vincent Ambrosia, NASA

Comparison Of Rainfall Rate Retrieval Algorithms Using Ground-Based Radar Data, Intended for Drought Monitoring In Cyprus

Eleni Loulli[1,2], Johannes Bühl[3], Silas Michaelides[1], Athanasios Loukas[4], Diofantos G. Hadjimitsis[1,2]

[1]ERATOSTHENES Centre of Excellence, Cyprus

[2]Cyprus University of Technology, School of Engineering and Technology, Department of Civil Engineering and Geomatics, Cyprus

[3]Leibniz Institute for Tropospheric Research (TROPOS), Germany
[4]Aristotle University of Thessaloniki, Greece

Keywords: XBand radar, GPM DPR, rainfall rate retrieval, precipitation monitoring, drought monitoring

The challenge

Drought is the phenomenon of rainfall deficit compared to its long-term mean and affects a large area for a certain time period. It is a multidimensional phenomenon that starts imperceptibly, advances slowly and cumulatively, and its consequences show up gradually. Weather-based parameters and indices are usually applied to monitor drought, but such methods are often insufficient for the estimation of the temporal and spatial drought features. Existing research on the phenomenon of drought in Cyprus is limited to in-situ monitoring. The dependence of drought monitoring solely on in-situ data constitutes a significant risk for decision makers and stakeholders, as in case of technical damages, or remote areas of interest, drought monitoring may be inadequate or impossible. Remotely sensed data yield continuous, digital and spatially explicit information on earth's processes and present a vital tool in overcoming the aforesaid risk.

Methodology

This study employs data from the NASA's Global Precipitation Measurement (GPM) Mission and from the two ground-based radars of the Department of Meteorology (DoM) to estimate the distribution of precipitation over Cyprus. The ground-based radar data employed in this study are located in Rizoelia (Larnaca district) and Nata (Paphos district). Each station is composed of an X-Band, Doppler, dual-polarization radar that provide continuous information on the estimation of rainfall and hydrometeor classification. As the radar data are provided in raw format, some initial pre-processing conversion was done. Using the given range, azimuth and elevation of the radar, we estimated the height and the distance of each cell. Additionally, the reflectivity data are converted to a linear scale. The DPR (Dual-frequency Precipitation Radar) aboard of GPM is applied in order to compare the rainfall rate at the ground with a spatial resolution of 5-25 km for 120 km wide swath. For the present study, we used the precipRate dataset that is provided in the solver (SLV) module, which presents the rainfall rate. The two datasets are interpolated on a universal grid with pre-defined dimensions. Then, the polarimetric radar variables (horizontal reflectivity ZH, vertical reflectivity ZV, differential reflectivity ZDR and the specific differential phase shift KDP) are applied in various rainfall retrieval algorithms and compared to the precipitation rate derived from the GPM satellite.

Results

Figure 1 presents the preliminary results for the example of December 12th, 2019, 07:50. As shown, the Marshall-Palmer equation and the Standard Z_H-R relation for X-band by Kalogiros et al. (2006) yield rainfall rates that are comparable to the rainfall rate that is given by the GPM satellite. In fact, the Standard Z_H-R relation for X-band seems to provide higher precision in terms of spatial distribution, whereas the Marshall-Palmer equation seems to provide better results in terms of quantitative accuracy. It is important to mention that these relations are compared to the precipRate product of GPM satellite that is considered as an accurate and reliable product, because it is already calibrated. From the GPM data, the bin that is right above the earth ellipsoid is taken into consideration (h=0-125m).

Outlook for the future

The rainfall rates presented in this work are derived from the reflectivity values of the XBAND radar. Nevertheless, these reflectivity values need to be adjusted based on the characteristics of the area. The main target in future work is to adjust the reflectivity measures and re-calculate the rainfall rates based on the adjusted reflectivity in order to come up with more precise results.

The overall outcome will contribute to the development of an automated tool for the estimation of the precipitation budget over the area of Cyprus. The automated tool will be enhanced with auxiliary data (such as evaporation rate, temperature, evapotranspiration, etc) in order to be reliable and accurate for drought monitoring in the Eastern Mediterranean region.

The authors acknowledge the 'EXCELSIOR': ERATOSTHENES: EXcellence Research Centre for Earth Surveillance and Space-Based Monitoring of the Environment H2020 Widespread Teaming project (www.excelsior2020.eu). The 'EXCELSIOR' project has received funding from the European Union's Horizon 2020 research and innovation programme under Grant Agreement No 857510, from the Government of the Republic of Cyprus through the Directorate General for the European Programmes, Coordination and Development and the Cyprus University of Technology.

The authors acknowledge also the Department of Meteorology of the Republic of Cyprus for the provision of the XBAND radar time-series.

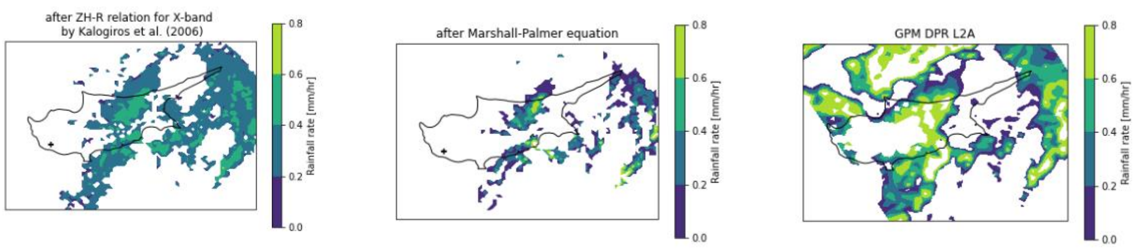

a) b) c)

Figure 1 (a) Rainfall rate after the Standard Z_H-R relation for X-band by Kalogiros et al. (2006) [mm/hr] (b) Rainfall rate after the Marshall-Palmer equation [mm/hr] (c) Rainfall rate derived from the GPM DPR satellite [mm/hr]

Remote sensing-based algorithm for monitoring water quality of inland water bodies

Gordana Jakovljević[1], Miro Govedarica[2], Flor Alvarez-Taboada[3]

[1] University of Banja Luka, Department of Geodesy, Bosnia and Herzegovina

[2]University of Novi Sad, Department of Computing and Control Engineering, Serbia

[3] University of Leon, Department of Mining Engineering, Spain

Keywords: water quality parameters, remote sensing, neural network, Sentinel 2, Landsat 8

The challenge

Access to clean water has become a critical issue worldwide due to urbanization, growing population, intensive industrial development and climate change increasing water stress and pollutant loads into the freshwater ecosystem. Water quality describes the water properties in terms of biological, physicchemical and hydro morphological characteristics. Traditionally, the monitoring of water quality is based on in-situ sampling and laboratory analysis which is a resource and time-intensive process. Taking that into account the discrete observation lacks sufficient and effective information for sustainable management and decision making. Therefore, there is an increasing need to develop a capacity to monitor water quality at large spatial and temporal scales. Remote sensing technologies and recent advantages in cloud computing and machine learning can be used to provide monitoring of water bodies in a more efficient manner.

Methodology

The spectral characteristics of water are functions of the hydrological, biological, and chemical characteristics of water. Therefore, the amount of radiation at various wavelengths reflected from the water surface can be used directly or indirectly to detect different water quality parameters. Optical remote sensing monitoring of Water Quality Parameters (WQP) is based on the comparison between surface reflectance and correspondent in-situ measurement. We used a 22-year long time-series of available atmospherically corrected Landsat (Landsat 5, Landsat 7, and Landsat 8) and Sentinel 2 satellite images and publicly available in-situ measurements collected in the TransNational Monitoring Network (TNMN) for monitoring six WQPs including chlorophyll-a (chl-a) (biological parameters) and Suspended Solids (SS), Turbidity, Total Nitrogen (TN), Total Phosphorus (TP), and Dissolved Oxygen (DO) (Physicochemical parameters). The TNMN provides an overall view of pollution and long-term trends in water quality in major rivers of the Danube River Basin (extent (EPSG: 4326): (41.85, 8.05):(50.45, 30.55)) by monitoring water quality at 101 stations 12 times per year. The relationship between WQP concentration and surface reflectance was modeled by using an Artificial Neural Network (ANN). The input layer of ANN is defined based on Pearson correlation while the final network architecture is fixed by using a trial-and-error approach. The data set and NN architecture were defined for each WQP. All data sets were split at 80% for training and 20% for validation. To avoid data overfitting, early stopping method was applied. The performance of the developed workflow was evaluated using Root Mean Square Error (RMSE) and normalized RMSE.

Results

According to the results, the highest accuracy was obtained for DO (RMSE: 0.09; nRMSE: 0.57%) and SS (RMSE: 8.50; nRMSE: 0.97%). The ANN model produced nRMSE of 2.89% and 2.73% for nitrate and phosphor concentration, respectively. The lowest accuracy was reported for chl-a (nRMSE 3.68 %). Both the analysis and size of the training dataset as well as the produced accuracy indicate that the accuracy of ANN is strongly influenced by the size of the training dataset. The accuracy assessments and nRMSE values show that remote sensing data are suitable for monitoring water quality. The trained models were used to predict the concentration of WQP for each pixel. Results of prediction were classified into five classes. (I class – blue, II class – green, III class – yellow, IV class – orange, V - red). The ranges of each class (Table 1.) were defined in line with local legislation. The spatial distribution of WQP in Belgrade, Serbia and were presented in Figure 1. Based on a visual inspection of the derived results, it could be assumed that hot spots of pollution are related to the areas of the cities and in this perspective, cities may be considered the major sources of pollution. The DO concentration in the Danube decreases along its flow across Serbia. The highest SS concentration was in small rivers and wetlands. The visual inspection shows a high correlation between TP and SS. Moreover, the visual inspection shows that chl-a concentration is highest at river banks and decreases in the center of the river Table 1. Legislation values for classification of water body status Class/Parameter Chl-a DO [mg/l] SS TN TP I 0-25 8.5> 0-10 250 80 >15 >1

Outlook for the future

Remote sensing technologies with continuous data acquisition and data availability in real and near realtime have greater potential to support water resource management and the decision-making process. However, the water quality operational monitoring using remote sensing data is still limited for the selected case study. This is mostly due to a lack of technical expertise and knowledge to understand the possibilities and limitations of remote sensing technology, lack of established methodologies, and complex processing needs. Moreover, the current methodology for the collection of in-situ data limits the application of remote sensing for water quality monitoring. In order to address those limitations, it is recommended to use the sensors for automatic monitoring for integration with remote sensing data. Taking that into account, future research should be directed toward establishing a clearly defined methodology for in-situ data collection and remote sensing data processing.

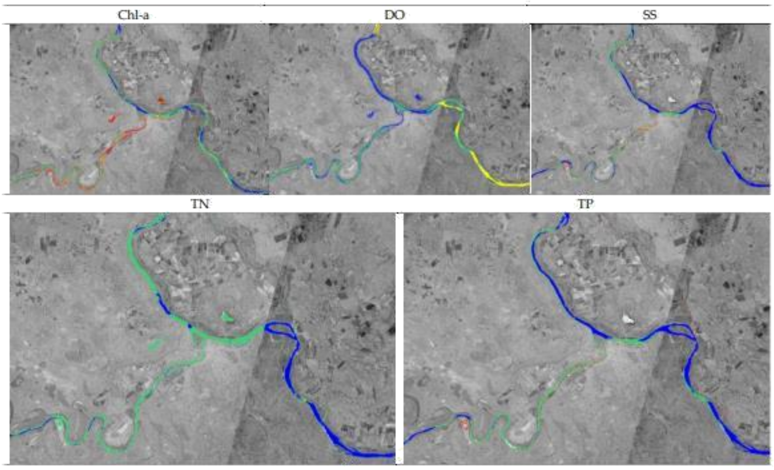

Figure 1 Visual inspection of water quality monitoring results

Deriving strong rain hazard risk maps from geo-mophology Deriving strong rain hazard risk maps from geo-mophology

[1]Thomas Krauß, [1]Veronika Gstaiger

[1]DLR, German Aerospace Center, Münchener Str. 20, 82234 Wessling, Germany

Keywords (5): strong rain, hazard-risk-maps, digital surface models, climate-change

The challenge

In the last summer a long-time stationary rain event struck parts of western Germany leading to massive floodings especially in the Ahr valley. Such long-term stationary weather conditions get actually more and more frequent and can lead to long extreme heat or massive continuous rainfall as shown in a study of the Potsdam-Institut für Klimafolgenforschung (PIK) last year (Rousi, E., Selten, F., Rahmstorf, S., Coumou, D. (2021): Changes in North Atlantic atmospheric circulation in a warmer climate favor winter flooding and summer drought over Europe. - Journal of Climate, 34, 6, 2277- 2295. https://doi.org/10.1175/JCLI-D-20-0311.1). The flood of the Ahr revealed that the existing modelling for flood probabilities is not sufficient. Possible causes may be the comparatively short observation period of the underlying measurements, missing historical data or the dynamics of climate change are not taken into account. For this reason, our approach is based on simulations of individually adapted worst case scenarios to derive possible effects of heavy rainfall more generally and over a wide area just based on satellite data and digital elevation models. So it's a simplified model which can be adapted and applied fast to regions all over the world – especially regions with only sparse available data.

Methodology

In the last years we developed a methodology for classification of strong rain dangers depending only on the terrain. It is based on 10 years events of a German insurance company and digital elevation models (DEMs) in resolutions starting from 2.5 m derived from the Indian Cartosat satellite up to 90 m (SRTM). The final method is based on the terrain positioning index with parameters, resolution and type of DEM calibrated using the available insurance data. These strong rain danger maps estimate a worst case scenario by not taking into account local drains since those are mostly blocked by leaves and branches at such sudden events. But these maps are only based on the local situation and do not consider water coming from other areas. So we developed an additional component including water-run-off from up-stream areas. In the presented study we calculate the maximum run-off for each point of a whole water catchment area (see fig. 1) assuming a massive strong rain event and the following flash flood. For each position in the run-off-map a local height profile perpendicular to the flow direction is calculated and filled up with the maximum estimated water volume at this position. This is depicted in fig. 2, right. There a blue "wall" is shown across the river profile representing the volume covered by the calculated run-off volume at this point of the river. These cross sections along the river in a valley gives the water levels for the maximum possible run-off for a given strong rain event.

Results

The result of the presented method is a map containing the flood outlines depending on the assumed rainfall (see fig. 2, left). But since some part of the rain will drain away and not contribute to the run-off this is also a worst case estimation. The results are compared to aerial imagery acquired on 2021-07-16 – two days after the flooding struck the Ahr valley –, flood-masks derived from Sentinel-1 imagery and Copernicus damage assessment maps. Based on this reference imagery, measurements and estimations of water gauge levels the effective flood level of the catchment was calculated and the simulation was calibrated and adapted to the observed water levels which led to a reasonable prediction of the flood extends. A second result of the presented method is a color coded danger map (see fig. 2, right). The colors represent areas which will be covered by 10 cm or higher water level depending on the rain-fall over the up-stream catchment of each point.

Outlook for the future

The presented method will be operationalized and cross-checked with other observed strong-rain events all over the world to generate a system for a danger classification due to strong rain all over the world. Figure 1 left: 3D view of calculated catchment of river Ahr, right: derived maximum run-off based only on a digital surface model (DSM, darker blue is higher run-off volume) Figure 2 left: aerial image of Ahrbrück, manually derived maximum water level of flood event as overlayed outline, simulated water-level for estimated rain-fall of 125 mm/m² over catchment as blue pixelmask, right: 3D view of DSM, same area including buildings, colors denoting flood-risk danger from dark-blue (water level 10 cm or higher at rainfall of 5 mm/m² over catchment) over middle blue (25 mm/m²), light blue (125 mm/m²), green (500 mm/m²) to brown (2500 mm/m²), light blue profile "wall": lower section profile for 150 mm/m², top section profile for 1500 mm/m².

Use of remote sensing for assessing water quality in open-surface water systems in Cyprus

Varvaris Ioannis[1], Christiana Papoutsa[1,2], Marios Tzouvaras[1], Felix Bachofer[3], Albert Ansmann[4], Johannes Bühl[4], Kyriacos Themistocleous[1,2], Kyriacos Neocleous[1,2], Chris Danezis[1,2], Nicholas Kyriakides[1,2], Georgios Komodromos[5], Charalampos Kontoes[6], Silas Michaelides[1], Diofantos Hadjimitsis[1,2]

[1] Eratosthenes Centre of Excellence, Limassol, Cyprus

[2] Department of Civil Engineering and Geomatics, Faculty of Engineering and Technology, Cyprus University of Technology, Limassol, Cyprus

[3] Earth Observation Center, German Aerospace Center (DLR), Wessling, Germany

[4] Leibniz Institute for Tropospheric Research, Leipzig, Germany

[5] Department of Electronic Communications, Ministry of Transport, Communications and Works, Nicosia, Cyprus

[6] National Observatory of Athens, Athens, Greece

Keywords (5): Water quality, water bodies, agriculture, fertilizers, remote sensing

The challenge

The total agricultural area of Cyprus is about 15% of the total land area (> 75% as arable farming), setting as a national concern the contamination of groundwater and surface water by the applied agricultural chemicals, which are indispensable in modern agriculture. Agricultural runoff is one of the major sources of nonpoint source pollution. Moreover, a share of the nitrate-N and P enriched water percolates and recharges subjacent aquifers by following natural flow pathways and, finally, discharges in open-surface water systems. Consequently, increased nitrate and phosphorus concentrations are observed in water bodies, which are believed to originate from agricultural lands due to the significant losses of N and P from cropping systems. In Cyprus, a substantial challenge for water resource management is reducing the pollutant load to reservoirs from agricultural areas. Therefore, water quality monitoring could benefit significantly from information derived from Earth observation (EO) satellites.

Methodology

For the water quality analysis, Sentinel-2A images were downloaded from COPERNICUS/S2_SR dataset through the Google Earth Engine (GEE) within R (https://earthengine.google.com/). The study area is the surface water systems of Cyprus, including lakes, rivers, and reservoirs (e.g., dams). Cyprus is situated in the north-eastern end of the East Mediterranean basin with an area of 9251 km^2, and winter rainfall is the primary source for replenishing water resources. For the current study, a period from 1-January to 1-November 2020 has been chosen. Chlorophyll-a (Chl-a), total nitrogen (TN), and ammonia nitrogen (NH_3-N) concentrations were estimated utilizing different band combinations of remote sensing analyses on Sentinel-2 images, which have been developed and validated for other case studies[1, 2]. The bands that have been used were the B2-blue, B3-green, B4-red, B5-red edge-1, B8-near-infrared, B8A-Red edge 4, and the band for masking the clouds (i.e., the QA60 bitmask for opaque and cirrus clouds). The satellite images were clipped to include only Cyprus's water bodies and projected in the GCS WGS84 World Geodetic System. The relationships between the band combination and the concentration of TN, NH_3-N, and the Chl a are presented below:

$$TN = 0.114(B_2 * B_8) + 0.843 \qquad [1]$$

$$NH_3 - N = 0.474(B_3 / B_2) + 0.276 \qquad [2]$$

$$Chl - a = (1 / B_4) - (1 / B_5)B_{8A} \qquad [3]$$

The analysis was carried out in R software.

Results

Figure 1 illustrates the simulated Chl-a, TN, and NH_3-N concentrations for the open-surface water systems in Cyprus, as these have been estimated utilizing Eq. 1-3 and EO data. The estimated TN concentrations indicate a similar behavior during all the examined months, and the simulated values varied from 0.84 to 0.85 mg L^{-1}. Regarding the NH_3-N, the highest concentrations were observed during April, for which the estimated value was 1.91 mg L^{-1}, while the most frequent value throughout the entire studied period was approximately 0.75 mg L^{-1}. Moreover, the highest variability for Chl-a was observed during April varying from 2.47 to 77.50 mg m^{-3}.

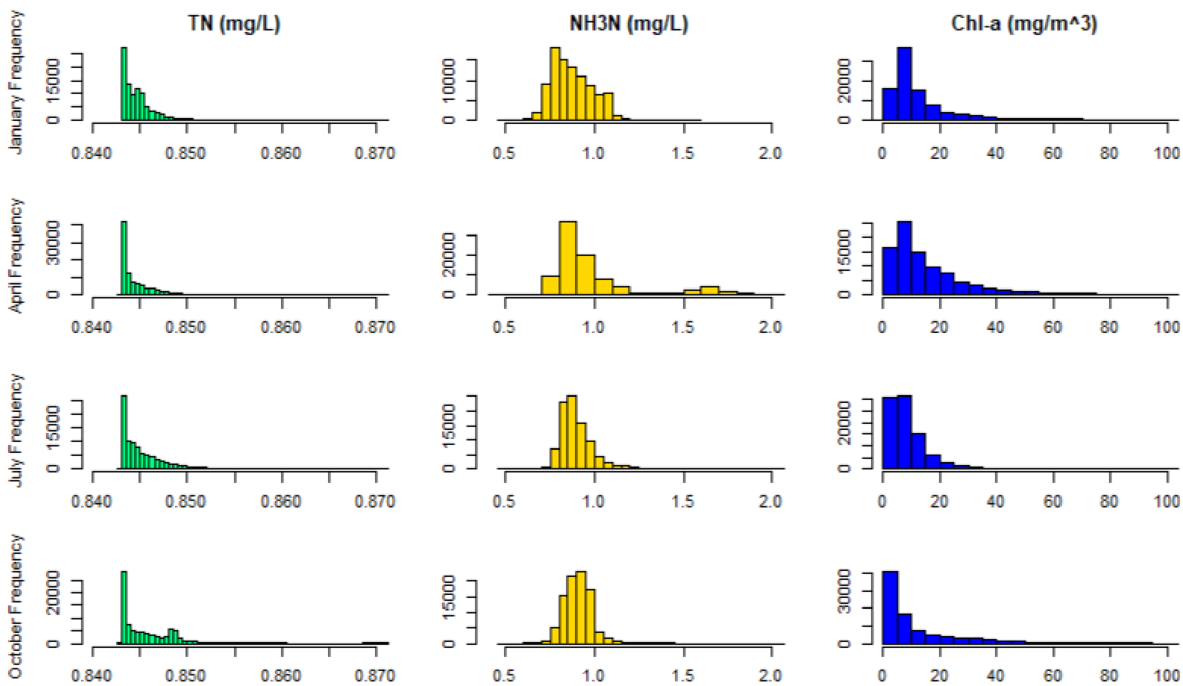

1 Buma W.G., Lee S.-I. (2020) Evaluation of Sentinel-2 and Landsat 8 Images for Estimating Chlorophyll-a Concentrations in Lake Chad, Africa. Remote Sensing 12. DOI: 10.3390/rs12152437.
2 Dong G., Hu Z., Liu X., Fu Y., Zhang W. (2020) Spatio-Temporal Variation of Total Nitrogen and Ammonia Nitrogen in the Water Source of the Middle Route of the South-To-North Water Diversion Project. Water 12. DOI: 10.3390/w12092615.

Figure 1. Histogram illustrating the frequency of the pixels of the estimated concentrations of Chlorophyll-a, total nitrogen, and ammonia nitrogen for January, April, July, and October 2020 for the open-surface systems in Cyprus utilizing EO data.

High spatial variability was generally identified across the entire island for all the water quality parameters. The lowest values were observed close to the inland water systems (close to the Troodos complex). In contrast, the highest values were depicted in the reservoirs close to the coastline (Akrotiri, Kition, and Kokkinochoria), which are mainly used for irrigation purposes.

Additional information on agricultural management practices is essential to understand the results and sufficiently correlate the spatio-temporal dynamics of the three studied water quality parameters with potential nonpoint pollution sources.

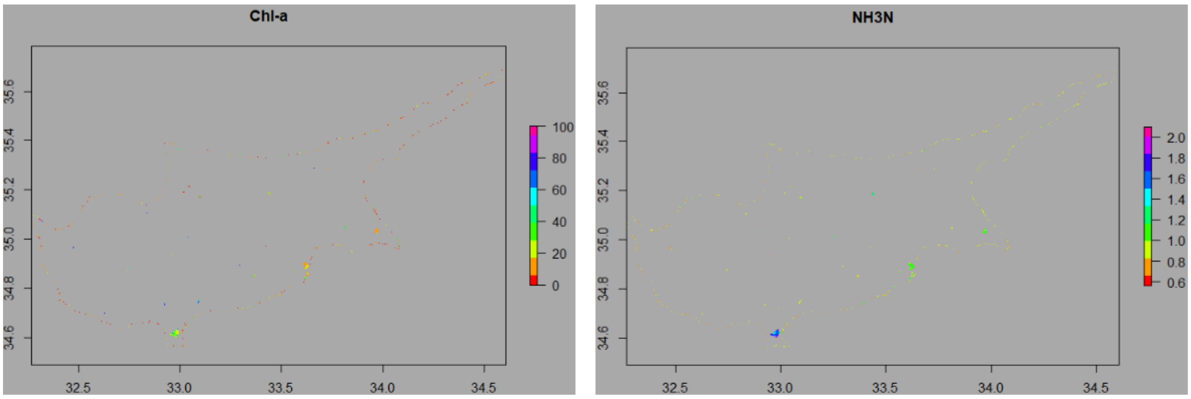

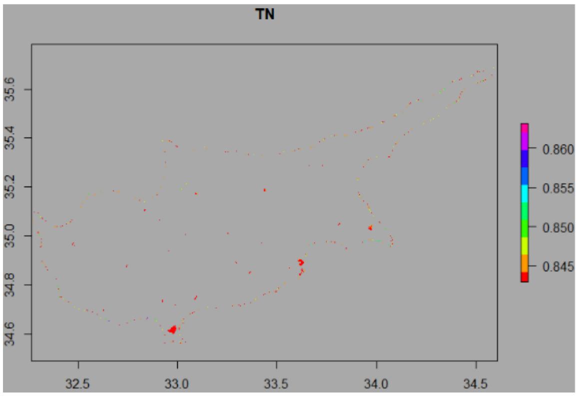

Figure 2. Maps presenting the estimated concentrations of Chlorophyll-a, total nitrogen, and ammonia nitrogen for April 2020 for the open-surface systems in Cyprus utilizing EO data.

Outlook

Monitoring water quality by constantly collecting water samples with sufficient spatio-temporal variability is a time-consuming and costly process. In contrast, water quality monitoring utilizing EO services can effectively provide all the necessary information for calibrating and validating hydrogeological models, which will potentially be the tools for establishing more efficient regulations regarding the use of surface-applied agrochemicals in Cyprus. Therefore, EO services will be the source of the objective functions for assisting the development of better water resource management tools and locally differentiated regulations, which will consider the spatial variability of the attenuation and soil filtering capacity for nutrients across Cyprus. However, before an operational monitoring system can be installed, the provided EO data and the used spectral functions need to be validated utilizing ground measurements to determine their applicability for local conditions and, if necessary, to be further adjusted.

Acknowledgements

The authors acknowledge the 'EXCELSIOR': ERATOSTHENES: EXcellence Research Centre for Earth Surveillance and Space-Based Monitoring of the Environment H2020 Widespread Teaming project (www.excelsior2020.eu). The 'EXCELSIOR' project has received funding from the European Union's Horizon 2020 research and innovation programme under Grant Agreement No 857510, from the Government of the Republic of Cyprus through the Directorate General for the European Programmes, Coordination and Development and the Cyprus University of Technology.

Remotely-Sensed early warning signals of critical transitions of forest ecosystems"

Filippos Eliades[1,2], Diofantos Hadjimitsis[1,2], Chris Danezis[1,2] and Felix Bachofer[3]

[1]Department of Civil Engineering and Geomatics, Cyprus University of Technology, Limassol, Cyprus
[2]ERATOSTHENES Centre of Excellence, Limassol, Cyprus

[3]German Aerospace Center / Deutsches Zentrum für Luft- und Raumfahrt (DLR)—Earth Observation Center (EOC), Wessling, Germany

Keywords: tree mortality, early warning signal, land degradation, desertification, remote sensing

The Challenge

Land degradation and desertification have severe negative effects on land-use, water resources, soil stability, agriculture and biodiversity. Drylands cover 33.8% of northern Mediterranean countries: foremost Spain and Cyprus with more than 65%. The European Environment Agency (EEA) indicated that 8% of the territory of the European Union (mostly in Bulgaria, Cyprus, Greece, Italy, Romania, Spain and Portugal) experience a 'very high' or 'high' sensitivity to desertification. For the island of Cyprus, 9.68% of the land area was found to be susceptible to land degradation (Kepner, 2006).

Sensitive ecosystems such as lakes, wetlands and forests may experience irreversible changes, called 'regime shifts' or 'critical transitions', with extreme changes of dynamic environmental variables. In case a certain threshold / tipping point in the resilience capability of an ecosystem is exceeded, the state of the ecosystem might become irretrievable (Alibakhshi, Groen, Rautiainen and Naimi, 2017). Early warning signals can be derived from statistical metrics that have been proposed to identify impeding regime shifts. Yet, regular monitoring of key ecosystem variables is limited by the lack of appropriate in-situ measurements and data and therefore the identification of these transitions is ambiguous. Correlating the available data with the available Earth Observation (EO) data, can enable the assessment of ecosystem resilience against global change.

The proposed study presents a holistic view on remotely-sensed, meteorological (drought) data and metrics-based indicators to identify critical transitions in a forest ecosystem. Mediterranean forests experience regime shifts frequently. The potential of using detailed EO-based time-series for monitoring Normalized Difference Vegetation Index (NDVI), Normalized Difference Water Index (NDWI) and Land Surface Temperature (LST), in combination with statistical metrics can provide a comprehensive analysis to determine and characterise the timing of regime shifts and specifically of tree mortality of Cyprus forests in Akamas, Machairas and Stavrovouni. The analysis of these three study areas that faced tree mortality in three different periods allows us to analyse and understand under which conditions critical transitions appear.

Statistical metrics of climate variables, as well as EO-based time-series can describe the conditions leading to tree mortality in forest ecosystems. Eventually, a detailed EO-based time-series monitoring and analysis of statistical metrics could propose a new composite indicator set that may serve as early warning signal indicating the risk of increased tree mortality, which might further lead to land degradation or even desertification.

Methodology

1. Data collection

The research focused on study areas under the risk of tree mortality. Remotely-sensed indicators such as NDVI, NDWI and LST were derived processing data from Landsat 5 and Landsat 8, as well as Sentinel 2 in the cloud-based Google Earth Engine (GEE). The LST correlates with air temperature (Richter et al., 2021) and thereby contributes an important climate change parameter (Alibakhshi, Groen, Rautiainen and Naimi, 2017). Having the NDVI, the LST has been calculated with the proportion of vegetation Pv and the emissivity ε. At the same time, the drought indices Palmer Drought Severity Index (PDSI), Standardized Precipitation Index (SPI) and Standardized Precipitation Evapotranspiration Index (SPEI) were used as well as statistical indicators of autocorrelation, skewness and standard deviation/variance. The Cyprus Department of Meteorology provided the daily data of temperature, precipitation and relative humidity for the period 1990-2020 in order to process these drought indicators.

2. Data pre-processing

The software tools used for processing the remote sensing vegetation indicators were Google Earth Engine and ArcGIS Pro. The pre-processing included cloud masking and image improvement for further index analyses.

3. <u>Analysis of EO-based time-series and statistical indicators to identify potential climate change effects on tree mortality</u>

Preliminary results show the response of precipitation through the Standardized Precipitation Index (SPI) to extreme droughts. Additionally, the Standardized Precipitation Evapotranspiration Index (SPEI) is an extension of the widely used Standardized Precipitation Index (SPI). The SPEI is designed to consider both precipitation (P) and potential evapotranspiration (PET) in determining a drought. Thus, unlike the SPI, the SPEI captures the main impact of increased temperatures on water demand. The SPI and SPEI indicators response range between 0 and -1.0 in abnormally dry conditions, in moderately dry conditions between -1.0 and -1.5, in severely dry conditions between -1.5 and -2.0, and in extremely dry conditions below -2.0. In all study areas, within the year of tree mortality both the SPI and SPEI indicators contained a major peak.

To fully understand the potential effects of climate change on the resilience of forest ecosystems, the PDSI, SPI and SPEI were analysed from 1990 to 2018 for Akamas Forest, 1990-2020 for Machairas Forest and 1990-2020 for Stavrovouni Forest. The PDSI generally spans from +10 (wet) to -10 (dry).

<u>4. Predictions and evaluation</u>

Detailed EO-based time-series monitoring and analysis of statistical metrics could propose a new composite indicator set that may serve as early warning signal indicating the risk of increased tree mortality, which in the end might further lead to land degradation or even desertification.

The three metric-based indicators that depict an upcoming critical transition in any dynamic system such as a forest ecosystem are autocorrelation, skewness and standard deviation / variance. The estimation trends of these indicators are implemented through Kendall's Tau. Prior to a critical transition transgressing the ecosystem's resilience, autocorrelation and standard deviation / variance always depict an increasing trend.

Generally, the new composite indicator must predict the upcoming tree mortality by providing the best possible trend, meaning Kendall's Tau ≈1 in autocorrelation, skewness and standard deviation / variance.

<u>Metric-based indicators</u>

Autocorrelation

Autocorrelation is the most suitable way to predict the tipping point. For instance, a lag k=1 autocorrelation depicts the correlation between values that are one time period apart. Generally, a lag k autocorrelation is the correlation between values that are k time periods apart. Various studies applied time lags of one-time step or lag k=1 autocorrelation to depict the critical transitions. An increase in autocorrelation at lag k=1 indicates that the state of the system has become increasingly similar between consecutive observations. An increasing signal of autocorrelation similarities between consecutive observations is the most suitable way to predict the tipping point.

Skewness

Skewness refers to a distortion or asymmetry that deviates from the symmetrical bell curve, or normal distribution, in a data set. If the curve is shifted to the left or to the right, it is said to be skewed. Simply put, skewness is the measure of how much the probability distribution of a random variable deviates from the normal distribution. Prior to a critical transition of an ecosystem due to perturbations, an increase of skewness and decrease of "normalcy" of data series can be observed.

Standard deviation / variance

A standard deviation (σ) is a measure of how dispersed the data is in relation to the mean. Low standard deviation means that the data are clustered around the mean, and high standard deviation means that the data are more spread out away from mean.

Variance is the average of squared deviation from the mean, while standard deviation is the square root of this number. Both measures reflect variability in a distribution, but their units vary. Standard deviation is expressed in the same units as the original values (e.g., meters or minutes).

Increasing standard deviation indicates flickering and critical slowing down before a critical transition.

Results

The results from the presented study show a considerable correlation on how parameters of climatic stressors such as, lack of precipitation and extremely high temperature constitute the major drivers leading to a critical transition of an ecosystem.

In 2008, Machairas Forest experienced tree mortality under an extreme drought. The result of the abrupt transition could be observed with the NDVI, which agrees with the response of the PDSI, SPI and SPEI indicators. In the same year (2008), Stavrovouni Forest also experienced tree mortality as a result of an extreme drought. Similarly, an abrupt transition could be identified from the NDVI that agrees with the response of the PDSI, SPI and SPEI indicators. In 2016, Akamas Forest suffered from tree mortality induced by an extreme drought. Likewise, an abrupt transition was observed from the NDVI response of the aforementioned indicators.

Comparing EO-based time-series indicators, such as NDVI, NDWI and LST in semi-arid regions, especially in Mediterranean forests, to climatic conditions and other hydrological parameters can improve the mortality prediction at fine spatial scales. Finally, analysis of the remotely-sensed vegetation indices along with the metric-based analyses can potentially provide early warning signals for tree mortality. The monitoring of semi-arid regions that are struggling to cope with climatic changes and are experiencing changes in the state of vegetation may contribute to a better understanding of current processes. This will support the development of adaptation and mitigation strategies.

Outlook for the future

Further research will include:

Inclusion of additional vegetation indices that are adapted to Mediterranean forests

Analysis of geomorphological parameters such as aspect, elevation, geology and slope to include local conditions in the analyses

Analysis and comparison between vegetation indices, metric-based indicators, precipitation and temperature

Development of an innovative remotely-sensed indicator for predicting tree mortality under extreme droughts.

Acknowledgements

The authors acknowledge the 'EXCELSIOR': ERATOSTHENES: EXcellence Research Centre for Earth Surveillance and Space-Based Monitoring of the Environment H2020 Widespread Teaming project (www.excelsior2020.eu). The 'EXCELSIOR' project has received funding from the European Union's Horizon 2020 research and innovation programme under Grant Agreement No 857510, from the Government of the Republic of Cyprus through the Directorate General for the European Programmes, Coordination and Development and the Cyprus University of Technology.

Poster(s)

Detecting ships in the Cyprus region using Sentinel-1 SAR data: A comparison of results using Sentinel Application Platform (SNAP) and Arc GIS Pro - deep learning

Eleftheria Kalogirou[1], Diofantos G. Hadjimitsis[12], George Melillos[12]

[1] Department of Civil Engineering and Geomatics, Cyprus University of Technology, Limassol, Cyprus

[2] ERATOSTHENES Centre of Excellence, Limassol, Cyprus

Keywords (5): Maritime safety, SNAP, Arc GIS Pro, Detect ships Using Deep Learning, Cyprus

The challenge

Maritime surveillance is critical to threat prevention, national security and maintaining security. Marine traffic involves the navigation of millions of vessels worldwide. Satellite missions such as Sentinel-1 have made collecting systematic data for vessel tracking possible. Using the Copernicus Open Access Hub service, free available Sentinel 1 SAR satellite, data was retrieved in fully automated and near 'real-time' operation. The present study aims at locating vessels in the Cyprus Region using the software Sentinel Application Platform (SNAP) and Arc GIS Pro - Deep Learning. By comparing the results obtained from the abovementioned software, the study concluded that both software can be used to detect vessels and yield satisfactory results.

Methodology

The study's methodological approach is vessel detection (marine surveillance) in the study's area of interest (AoI), which is part of Cyprus' Exclusive Economic Zone (EEZ, which corresponds to 200 nautical miles over which a nation has certain sovereign rights). Vessel detection can be described as a task detecting small objects, because of the characteristic of a large aspect ratio of a vessel. Generally, marine surveillance can be completed using different methodologies. A first option consists of cooperative systems in which vessels themselves report their identities and positions. The three most common options are Automatic Identification System (AIS), Long Range Identification and Tracking (LRIT) and Vessel Monitoring System (VMS). While the first one is, in fact, available continuously and globally, the two others are not. Another option is the non-cooperative system that does not require cooperation on the vessel's side. These systems most commonly use cameras and radars on various platforms (ships, aeroplanes, satellites, etc.). Vessel detection with Sentinel-1 falls into the non-cooperative category. It detects vessels not carrying AIS or other tracking systems on board, such as smaller fishing ships or ships illegally present in the surveyed area (illegal fishing, piracy, etc.).

In addition, the SAR is not dependent on sunlight and is independent of weather conditions, allowing frequent monitoring. The Copernicus Open Access Hub provides access to Sentinel satellite data by providing Sentinel-1 data for processing. The first vessel tracking methodology used SNAP - Sentinel Application Platform software, a standard architecture for all Sentinel satellite toolboxes. The vessels are then located through the second methodology using the ArcGIS pro software following the Detect Objects Using Deep Learning process, where it is available in the Image Analyst toolbox and you use it to analyse the collected data. Object detection works by executing an in-depth instructional learning model utilizing its available techniques in an input mosaic. The complete workflow includes steps after editing using additional tools. The last step of the methodology compares the results obtained using the Sentinel Application Platform (SNAP) and Arc GIS Pro.

Results

Our research evaluated the results of SNAP and ArcGIS Pro software. The preliminary results of the two software during the vessel detection process, showed that a large number of objects were detected. Priority was given to matching target impressions to improve results accuracy and data relevance. The results of the two software are very satisfactory and their combination is suitable for fast mapping. The sum of the results is significantly enhanced and the results show that the different techniques and methods provide a thorough detection analysis, as a result, they can be used in surveillance and maritime safety missions.

Outlook for the future

The availability of repeated observations allows vessel detections: most of these detections are vessels of interest, and some are of no interest for maritime surveillance purposes. In the future, observations are planned shortly to study different periods and different study areas to evaluate the satellites' sensitivity and perform time series analysis.

Flood Risk Assessment in catchment areas in Cyprus using Earth Observation

Iosifina Kountouri[1,2], Christodoulos Mettas [1,2], Christiana Papoutsa[1,2], Argyro Nisantzi[1,2], Chris Danezis[1,2], Kyriacos Themistocleous[1,2], Silas Michaelides[1,2], Evagoras Evagorou[1,2], Haris Kontoes [3], Diofantos Hadjimitsis[1,2]

[1] Department of Civil Engineering and Geomatics, Cyprus University of Technology, Limassol, Cyprus

[2] ERATOSTHENES Centre of Excellence, Limassol, Cyprus

[3] National Observatory of Athens, Beyond Centre of Excellence, Athens, Cyprus

Keywords: Earth observation, floods, risk assessment, GIS

Abstract

In the recently years climate change and anthropogenic pressure have rapidly increased frequency in occurrence and the severity of flood phenomena globally. In many countries, this causes increasing damage and threats to life, property and cultural heritage. Floods are considered to be one of the most devastating natural disasters worldwide. A flood can be determined as a mass of water that produces runoff on land that is not normally covered by water. This includes floods from rivers, mountainous torrents, ephemeral Mediterranean currents and floods from the sea in coastal areas, can exclude floods from systems sewerage. Ecosystems and floods are closely related; any changes in the ecosystem, such as urbanization across the catchment's area, may trigger off a sequence of flood occurrence causes. Floods can destroy homes, roads, tear out trees, cause mudslides and take many human lives. Floods management is an important issue of concern among around the world. However, earth observation techniques such as satellite remote sensing can contribute toward a more efficient flood risk mapping according to European Directive 2007/60/EC on the assessment and management of flood risks. Flood disaster management cycle has three main phases viz. flood preparedness (before flood occurs), flood response (during a flood) and the last phase called flood mitigation (after flood has occurred). Flood preparedness involves identification of chronically flood prone areas, identification of areas that are liable to be affected by a flood and planning of optimum evacuation plans. Flood response involves the immediate action taken once the flood disaster has occurred in terms of the identification of the region affected, spatial extent of inundation, flood damage statistics, flood progression and recession which can help in carrying out the relief and rescue operations on ground. Flood mitigation phase starts after the flood has occurred by identification of the changes in the river course due to flooding, status of flood control works, river bank erosion, drainage congestion, flood hazard and risk vulnerability assessment. Several authors have analysed and reviewed flood monitoring and risk assessment flood around the world. In the past few year, airborne and spaceborne remote sensing technologies along with geographical information systems have been widely used for flood monitoring and flood risk analyses. The aims of this PhD Thesis under the EXCELSIOR H2020 Teaming Project is: to develop predictive models that will be used by the local authorities as guideline maps for 2 (Style: Footer) a future sustainable urban planning; to establish an integrated service for local authorities (e.g. preparedness, response, risk reduction, mitigation). A multidisciplinary-integrated approach will be used and presented by blending earth observation, GIS, hydraulic engineering, surveying engineering, crowdsourcing for the present and the past regime of a selected catchment area in Cyprus. At this stage, the authors present a literature review of the existing remote sensing techniques for risk assessment in catchment areas.

Cultural and Natural Heritage

Organizers:

Heritage SIG Chairs

Jolanda Patruno, Exploitation Platforms Support Engineer c/o ESA-ESRIN and EARSeL co-Chair on Cultural and Natural Heritage and Mario Hernandez, EARSeL co-Chair on Cultural and Natural Heritage and Vice-President International Society of Digital Earth.

Summary:

Natural Heritage sites comprises a large variety of worldwide areas (national parks, biosphere reserves, World Heritage sites, etc. Natural Heritage refers to the whole set of elements of biodiversity, flora and fauna, ecosystems and geological structures. Natural Heritage sites are part of our natural resources. Natural World Heritage sites provide crucial habitats to many iconic species, as well as protect rare ecological processes and stunning landscapes. Cultural Heritage sites fall into the category of tangible culture (such as buildings, monuments, landscapes, historic cities, archaeological areas, cultural landscapes, and many other forms). Cultural heritage gives people a sense of unity and belonging within a group and allows them to better understand previous generations and the history of where they come from. Cultural heritage implies a shared bond and our belonging to a community. However, both Natural and Cultural heritage sites are not only exclusive protected areas where no humans live. On the contrary, Natural and Cultural heritage sites do host important populations of people, these sites provide jobs and most of them are extremely important for their contribution to the national economy (e.g. tourism, etc.).

The Special Session Earth Observation and Remote Sensing are emerging technologies that slowly, through a series of successful worldwide showcases are showing to be extremely beneficial in the support of Natural and Cultural heritage sites, for example in the monitoring, preserving, managing, disseminating and promoting. There are many threats to these heritage sites (e.g. climate change, anthropogenic activities, etc.). In all these themes EO is assisting through applications assessing land cover changes, land use changes, interferometry to assess the movement of buildings, etc. The Special Session aims to bring together both EO and Heritage experts to present and discuss how EO is currently being used for the benefit of Natural and Cultural heritage. Presentations will be followed by round table discussions in order to make the point on how EO is currently supporting these heritage sites. For this Special Session, we consider EO not only as using satellite sensors but in the overall general concept of non-invasive sensors, including satellite sensors, laser scanning, rapid prototyping, red-green-blue-depth (RGB-D) sensors, high dynamic range imaging, spherical and infrared imaging, mobile mapping systems, unmanned aircraft systems (UAS), etc.

Topics:

- Overall applications of EO for Natural and Cultural heritage
- EO assisting Natural and Cultural heritage to assess and reduce the threats form climate change
- Uses of multiple resolutions to document, monitor and model Natural and Cultural heritage sites
- Photogrammetry in support of natural and cultural heritage sites
- Lessons learnt from applying EO to natural and cultural heritage sites
- Support to archaeology e.g. LiDAR to increase identification of sites
- Space archaeology and crowd sourcing
- Land use/ and cover mapping in the Global South
- Educational activities related with EO and GIS for cultural and natural heritage sites
- Heritage authorities using EO technologies

Scientific Committee:

- Mario Hernandez, Vice-President International Society of Digital Earth
- Jolanda Patruno, Exploitation Platforms Support Engineer c/o ESA-ESRIN
- Athos Agapiou, Cyprus University of Technology
- Alain De Wulf, Ghent University
- Anca Claudia Prodan, Institute Heritage Studies

An experimental study for the detection of surface ceramics through Unmanned Aerial Vehicles (UAV)

Argyro Argyrou[1*], Vasiliki Lysandrou[1], Michalis Christoforou[1], Athos Agapiou[1]

[1]Earth Observation Cultural Heritage Research Lab, Department of Civil Engineering and Geomatics,

Faculty of Engineering and Technology, Cyprus University of Technology, Lemesos 3036, Cyprus

Keywords: Remote Sensing Archaeology, Machine Learning (ML), Potsherds, Classification, Unmanned Aerial Vehicles (UAV)

The challenge

One of the most popular techniques for detecting archaeological sites and characterization of archaeological landscapes is the archaeological pedestrian survey, with fieldwalking being the most common type of survey (Orengo H.A., Garcia-Molsosa A. 2019). Further important findings, together with those published by Agapiou et al. (2021), followed the work of Orengo and Garcia-Molsosa (2019), show that low-altitude remote sensing sensors (e.g., Unmanned Aerial Vehicles, UAVs) can provide significant outcomes. This study is designed, under the newly established research project "Innovative survey techniques for detection of surface and sub-surface archaeological remains", in short ENSURE, along with the scientific objectives of the PhD of the first author oriented on the same topic.

The overall objective of the study is to present the methodology of a simulation study towards the semiautomatic detection of surface ceramics through low altitude multispectral and RGB cameras. Surface ceramics detection will be carried out through machine learning (ML) methods and image postprocessing techniques. The results show the potential of this technique, under appropriate field circumstances, to produce accurate distribution maps of surface ceramics.

Methodology

The aim of our pilot study is to investigate whether a semi-automated methodology for recording potsherds could be developed and to answer research questions for a more efficient approach in terms of time and accuracy compared to traditional fieldwalking archaeological surveys. In this study, we have implemented an artificial intelligence image processing methods over o plot approximately 20m x 20m (Area 1) in an area of interest near the village of Alambra, in Lefkosia District of the Republic of Cyprus.

The workflow followed includes a drone-based image acquisition. In spring 2022, a campaign over Area

1 was performed, using the DJI P4 Multispectral system with the following spectral bands: Blue (B): 450 nm ± 16 nm; Green (G): 560 nm ± 16 nm; Red (R): 650 nm ± 16 nm; Red edge (RE): 730 nm ± 16 nm and Nearinfrared (NIR): 840 nm ± 26 nm. Flight height was set to approximately 20m above ground level (AGL), providing orthophotos with a spatial resolution of a few centimetres, and sufficient to clearly identify ceramics on Area 1.

As a second step, was the ground truth data collection (simulating thus the traditional pedestrian survey). We divided Area 1, in a 5×5 m grid and the field-walkers identified and counted 300 ceramics. The largest width of the identified surface ceramic fragments ranges from 3 cm to 6 cm (Figure 1), while the colour of their surface also varies, depending on firing, from reddish orange to brown.

Next process included standard photogrammetric processing to combine all these photographs into a single orthophoto-mosaic. Finally, two steps included computational processing (ML techniques) and geospatial analyses (GIS software) to identify and isolate ceramic fragments.

Results

Various ML algorithms such as the Support Vector Machine (SVM) and the Random Forest (RF) classifiers have been implemented and compared along with the results from foot surveys. This is also demonstrated through numerous articles highlighting decision-making and the analysis of scientific models using ML techniques with minimal human interaction. Utilizing workflow of Orengo and Garcia-Molsosa (2019), in our study, the overall accuracy and relative accuracy were estimated. The results were compared with the archaeological surface-survey records showing that semi-automatic detections methods using lowaltitude remote sensing sensors can be used as a first proxy indicator for the detection of surface archaeological ceramics.

These results and accuracy can vary, depending on variety of factors like, the type of soil, the conditions of the plot, the period of flight, the visibility and quantity of the material culture but also the number and experience of the inspectors.

Outlook for the future

The aim of this study was to investigate the potential of low-altitude remote sensing sensors that use highresolution UAV multispectral sensors to detect fragmented ceramics at archaeological sites. The overall findings, show that low-altitude remote sensing sensors can be innovative in the field of archaeological field research. Future archaeological projects may rely on such methodologies to be cost-effective, especially in cases where there is an urgent need to record rapidly disappearing archaeological sites or even when the research schedule is limited. In addition, it is especially important both before the flight operations with the UAV sensors, and during the image analysis for ceramic detection to make critical preparations such as spectral analysis of the camera, spatial analysis, etc.

In the future further improvements are expected, while more sophisticated remote sensing algorithms will be tested to cover even larger areas with a higher success rate.

 

Figure1. Example of unwashed surface potsherds and washed surface potsherds (Photos: A. Argyrou, Earth Observation Cultural Heritage Research Lab©).

Automated mapping of cultural heritage in Norway from airborne laser scanning data using Faster R-CNN

Øivind Due Trier[1], Jarle Hamar Reksten[1], Kristian Løseth[2]

1 Norwegian Computing Center, Section for Earth Observation, Norway

2 The Directorate for Cultural Heritage, Norway

Keywords: Airborne laser scanning, deep learning, grave mounds, deer hunting systems, charcoal kilns

The challenge

The existing cultural heritage mapping in Norway is incomplete. Some selected areas are mapped well, while many areas only contain chance discoveries, often with bad positional accuracy. The goal of this research was to develop automated tools for improving the cultural heritage mapping, thus enabling detailed mapping of large areas within realistic budgets and time frames.

Most of Norway will soon be covered by airborne laser scanning (ALS) data. The Directorate for Cultural Heritage in Norway wants to use this opportunity to obtain a more complete and accurate mapping of cultural heritage in the landscape. The highest priority is to map Iron Age grave mounds and ancient deer hunting systems, as these are automatically protected by Norwegian law due to their age. There is risk of the monuments being unintentionally destroyed due to lack of knowledge of their existence. It is also desirable to map charcoal kilns, as these occur frequently in some parts of Norway.

Methodology

ALS point cloud datasets were downloaded from http://hoydedata.no, which provides free access to all ALS data in Norway.

A recent development in deep neural networks for object detection in natural images is the regionproposing convolutional neural network (R-CNN), which may also be used for cultural heritage detection in local relief model (LRM) visualizations of ALS data.

The Python code library "simple faster R-CNN" was downloaded from https://github.com/chenyuntc/simple-faster-rcnn-pytorch. For each detected object, the R-CNN predicts a bounding box, a class label and a score value in the range 0.0 – 1.0. Pre-training of the neural network was done by importing parameters learned from the VGG16 deep neural network on the ImageNet dataset of photographs with labelled objects such as cars, dogs, etc.

A few modifications had to be done:

1. The list of class labels was changed to match the class labels used in the image annotations.
2. Additional training was done on annotated LRM images containing cultural heritage objects.
3. The downloaded code crashed if there were no detected objects within an image. Thus, if-tests had to be added.

When these changes were made, the Python code predicted the locations and sizes of grave mounds, pitfall traps and charcoal kilns (Figure 1a-c) in LRM images of size 600×600 pixels (150m × 150m). A score value between 0.0 and 1.0 was given for each predicted object. Objects with a score value below 0.7 were discarded by the automatic method.

Results

On 737 test images (16.6 km2) not seen during training, 87% of the true cultural heritage objects were correctly identified, while 24% of the predicted cultural heritage locations were false. However, all test images were small (150 m × 150 m) and contained at least one cultural heritage object, meaning that the false positive rate may be higher for an entire landscape. In Larvik municipality, Vestfold and Telemark County, on a 67 km2 area not seen during training, the R-CNN correctly identified 38% of the true grave mounds, thus missing 62%, and with 89% false positives.

The method was then used on Øvre Eiker municipality (937 km2), an area with few recorded charcoal kilns; thus, no ground truth existed. This is the normal situation for the practical use of the method, to discover previously unknown cultural heritage locations. 1130 charcoal kilns were predicted by the method (Figure 1d). All of these were checked manually by visual inspection of the LRM visualizations of the ALS data. In this way, 51% were confirmed as being charcoal kilns, while another 11% appeared to be possible charcoal kilns. By including confirmed and possible charcoal kilns, the producer's accuracy was 62%, thus the false positive rate was 38%. During the visual inspection, 66 charcoal kiln locations missing automatic prediction were identified. By counting only the visually confirmed charcoal kiln locations, the true positive rate was 90%, thus the false negative rate was 10%.

Outlook for the future

The current version of the method has two major challenges that makes it difficult to use as a standard method for cultural heritage mapping in Norway. Firstly, the detection results must be manually verified by an experienced archaeologist, although this may, in many cases be done by visual inspection of the LRM, meaning that only a fraction of the automatic detection results need field verification. Secondly, a workflow is missing for bulk uploading of verified detection results into the national cultural heritage database (Askeladden). Despite these limitations, an experienced archaeologist may save a substantial amount of time by using the method compared to a purely manual workflow. For areas with no previous archaeological mapping, the method may give a quick overview, provided the type of landscape is well represented in the training data for the method. The availability of free lidar data in all of Norway made it possible to train the method on a large variety of landscapes.

Our method is based on transfer learning, but in a setting that may not be optimal. We used a deep neural network that is pre-trained on natural scene images, followed by training on lidar visualisations with labelled cultural heritage remains. As the two types of image are quite different, there is a potential for improvement by pre-training the deep neural network on a large image set that is more similar to the lidar visualisations that we used.

In conclusion, we have demonstrated that Faster R-CNN is well suited for semi-automatic detection of cultural heritage objects such as charcoal kilns, grave mounds and pitfall traps in high resolution airborne lidar data. However, it is desirable to reduce the false positive rate in order to limit the amount of visual inspection needed when the method is applied to large areas for detailed archaeological mapping.

Note: This extended abstract is based on a recently published paper: Ø. D. Trier, J. H. Reksten, and K.
Løseth, 2021. Automated mapping of cultural heritage in Norway from airborne lidar data using faster RCNN. International Journal of Applied Earth Observations and Geoinformation, vol. 95, article no. 102241.
https://doi.org/10.1016/j.jag.2020.102241.

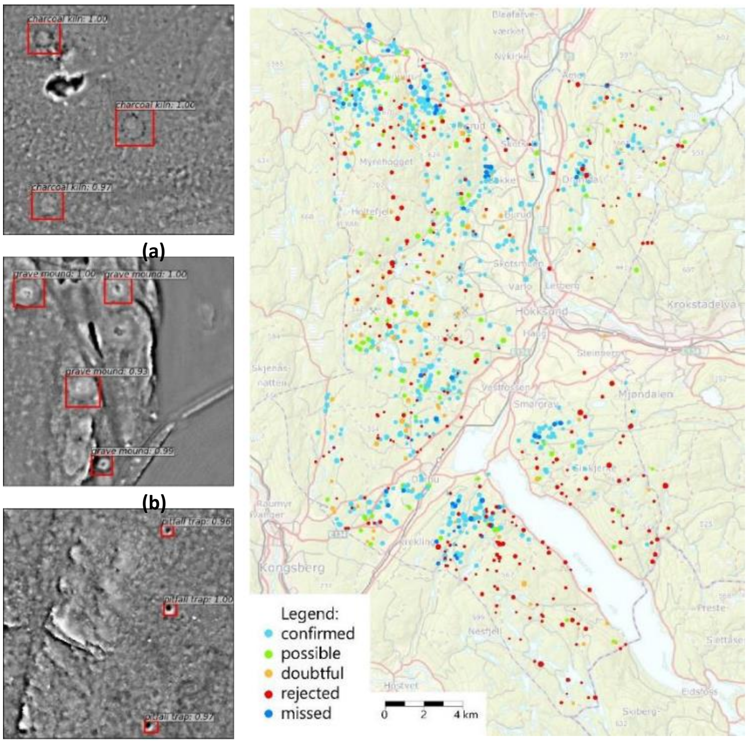

(c) (d)

Figure 1 (a) Predicted charcoal kiln locations. (b) Predicted grave mound locations. (c) Predicted pitfall trap locations. (d) Predicted charcoal kiln locations in Øvre Eiker municipality, Viken County. 'Missed' means missed by automatic method but manually detected and confirmed. Topographic map from https://hoydedata.no, the Norwegian Mapping Authority (Kartverket).

Optimal Selection of Physiologically Distinct Periods To Detect Invasive Plant Robinia Pseudoacacia In Natura 2000 Sites Of The Danubian Lowland, Slovakia

Tomáš Rusňák[1], Andrej Halabuk[1], Juraj Lieskovský[1],

[1]Institute of Landscape Ecology, Slovak Academy of Sciences, Slovakia

Keywords: Robinia pseudocacia, Black locust, Invasive plant, Sentinel-2, Natura 2000, Random Forest

The challenge

Recognition of invasive species and their distribution is key for managing and protecting native ecosystems. Robinia pseudoacacia is one of the Europe's most widely distributed invasive tree species, affecting certain ecosystem services. In this study, we explore a multitemporal classification approach to distinguish optimal selection of physiologically distinct periods to detect Robinia pseudoacacia in Natura 2000 sites of the Danubian Lowland, Slovakia. We utilized dense Sentinel-2 reflectance products from 2019 to 2021.

Methodology

We applied a pixel-based compositing approach for Sentinel-2 imagery for creating cloud-free monthly temporal composite product based on maximum NDVI. This method prioritizes the observation with the highest NDVI value within a given period, assuming the best quality observation of the given pixel follows the highest value of NDVI. We used the satellite images recorded between February and November 2019-2021 to prevent any quality concerns that might have occurred outside of this time period. We used Sentinel-2 spectral bands B2, B3, B4, B8 at native 10 m resolution and bands B5, B6, B7, B8A, B11 and B12 at native 20 m resolution. Three Sentinel-2 tiles have been used to fully cover the extent of the study area. For classification we used The Random Forest Classifier. For the reference, we collected the field samples of the tree stands affected and also unaffected by Robinia pseudacacia. The field campaign was conducted during the early spring period (April), allowing easy recognition of the Robinia pseudacacia stands since they did not have fully developed leaves compared to surrounding native vegetation in full leaf at that stage. We used independent validation datasets that were skipped from the training.

Results

Classification models using monthly maximum NDVI composites performed well across years, achieving overall accuracy 73.4 to 85.87 percent (Figure 1.). Distinction was evident across all seasons, being the highest in the beginning of vegetation season, which might be determined by the Robinia pseudoacacia, e.g. later onset of greenness and specific flowering. April and May composites yield the best results, followed by July and June. The spatial detail of detectable stands was surprisingly high. Figure 2. provides the distribution of Robinia pseudoacacia proportion within 1 km buffer zones of the Natura 2000 sites. Analysis of feature importance for classification models revealed the high importance of red edge spectral bands (e.g. Sentinel-2 bands 5 and 6) and SWIR spectral bands (e.g., Sentinel-2 bands 11 and 12). This was consistent across whole study period, which implies a spectral distinction between Robinia pseudoacacia canopies and native vegetation mainly in the red edge and SWIR spectral range. Notably, spectral bands B8 and B8A were ranked low in importance, though comparison of spectral profiles of Robinia pseudoacacia canopies with those of native vegetation revealed consistent differences in the whole NIR spectral range, including bands B8 and B8A.

Outlook for the future

We demonstrated that using the Sentinell-2 products for classification of Robinia pseudoacacia stands in is possible. This confirms the assumption about the distinctive spectral response of invasive vegetation. More detailed research on specific spectral characteristics of Robinia pseudoacacia canopies is open for further research, mainly with the prospects of the recent and upcoming spaceborne spectral imaging missions such as PRISMA, EnMAP, or CHIME. Even though Robinia pseudoacacia are supposed to be widely distributed in Central

Europe, landscape analysis revealed that the spatial trends can be seen at a regional level. This could be because of historical management (e.g., planting) or environmental constraints. Further research into spatial factors behind Robinia pseudoacacia distribution at a regional scale is needed. Finally, the detailed maps of Robinia pseudoacacia distribution may be used to support both the spatial assessment of ecosystem services and the mitigation of potential negative effects on biodiversity in agricultural landscapes.

Acknowledgments

This research was supported by the Integrated Infrastructure Operational Programme funded by the ERDF, project ITMS2014+ 313011W580, “Scientific support of climate change adaptation in agriculture and mitigation of soil degradation” (80%) and by the Slovak Research and Development Agency (APVV), project No. APVV-17-0377 “Assessment of recent changes and trends in agricultural landscape of Slovakia”.

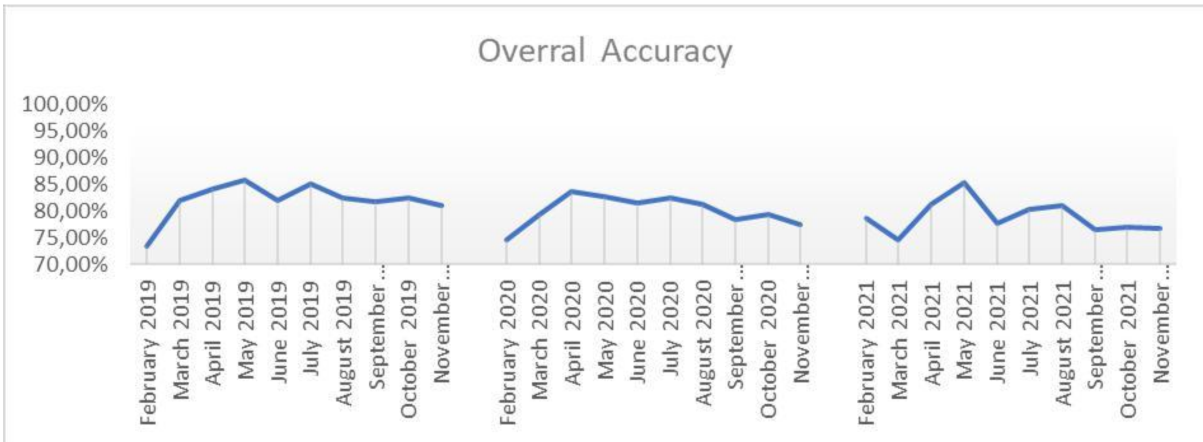

Figure 1. Overall accuracy of monthly composites.

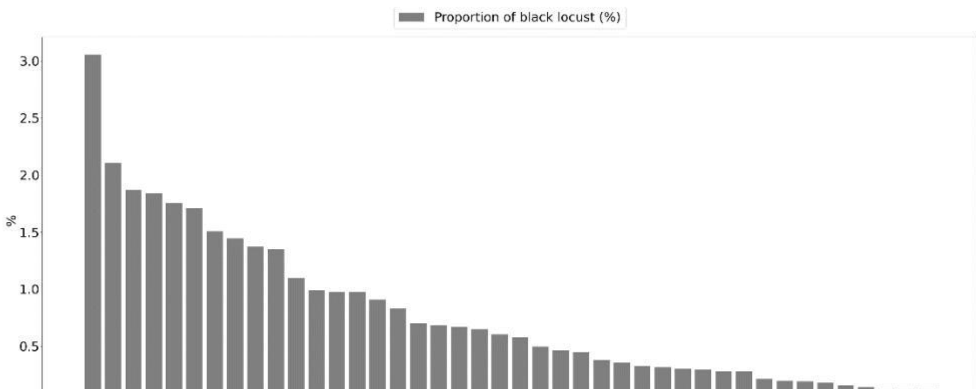

Figure 2. Proportion of Robinia pseudoacacia stands within 1 km buffer zone of the Natura2000 sites (SKUEV represent name of the Nature2000 sites (absences of black locust in Natura2000 sites, e.g., 0% proportions were omitted for better visualizations; they represent 24 cases)).

The Use of Digital Geomedia for Management of UNESCO Sites – Current State of Knowledge and Future Potential

Lisa Dannwolf[1], Emmanuel Eze[1,2], Maike Petersen[1], Nicolás Zanetta-Colombo[1,2], Alexander Siegmund[1,2]

[1]Department of Geography – Research Group for Earth Observation (rgeo), Heidelberg University of Education, Germany

[2]Heidelberg Center for the Environment (HCE) & Institute of Geography, Heidelberg University, Germany

Keywords: Capacity Building, Training Concept, Remote Sensing, World Heritage, Biosphere Reserves

The challenge

UNESCO sites such as World Heritage, Biosphere Reserves, and Geoparks need to be especially protected due to their universal value. In the context of monitoring, modelling, management, and visualization of spatial structures and changes in the vicinity of the UNESCO sites, the use of digital geomedia such as remote sensing, geographic information systems (GIS) and mobile geotools holds a great potential. Especially remote-sensing methods offer manifold options for UNESCO sites, in order to monitor and evaluate past and model future developments to ensure their protection and sustainable development. The use of digital geomedia requires technical and methodological knowledge and skills by the user, but the level of expertise among UNESCO-site stakeholders is currently unknown. To develop adequate and effective concepts to train this target group in the interpretation and use of digital geomedia, detailed information on the state of their knowledge needs to be generated.

Methodology

To design a learning concept in accordance with the actual situation and requirements of UNESCO-site stakeholders, a needs assessment was conducted based on an online survey. The questionnaire was sent out to UNESCO sites within Germany and around the world to collect information on previous experience with different types of geodata, the frequency of tasks involving digital geomedia, and possibly relevant use cases at their respective site. The questionnaire furthermore retrieves information on the demand for training courses on digital geomedia. By collecting the potential participants’ expectations beforehand, the capacity-development programme and related courses can be designed to exactly fit the needs, local hardware and software availability, as well as time and financial resources of UNESCO-site stakeholders. In collaboration with four young researchers from Costa Rica, Germany and Malawi and local partner institutions (e.g., National Commission for UNESCO) within the context of the ASA Program by Engagement Global, a capacity-development program will be designed. In addition to the quantitative results from the questionnaire they will include qualitative interviews with local UNESCO stakeholders in the preparation of the concept. Based on these results, two pilot courses will be designed and conducted in Costa

Rica and Malawi. To further improve these courses, they will be accompanied by pre-post evaluations which monitor the learning effect on the participants.

Results

The first set of responses to the needs-assessment survey within Germany (n=66) included stakeholders from Biosphere Reserves, Heritage Sites, and Geoparks. The preliminary results indicate that UNESCO-site stakeholder have some basic knowledge of remote sensing, GIS and mobile geotools and know their potential and advantages. However, in many cases using this type of data is restricted to basic applications. The potential use cases for digital geomedia, however, are manifold. Especially monitoring land-use and land-cover changes, forest degradation, and visualisation of the UNESCO sites are of interest to the respondents. Limiting factors for the use of remote-sensing data in their work are time and financial 2 (Style: Footer) resources, lack of theoretical knowledge, but especially difficulties in data acquisition. The majority of respondents states that they have the need for training in the use of digital geomedia and most would prefer the course to cover specific use cases over general information. For the duration, one to a maximum of four days would be preferred and most respondents would choose face-to-face or blendedlearning courses over online offers.

Outlook for the future

The needs assessment, the pilot courses, and the accompanying evaluations will provide valuable insights into the potential to train UNESCO-site stakeholders in the use of digital geomedia. The courses can be adjusted to fit different levels of prior knowledge (e.g., basic or advanced level) and different professional backgrounds. By developing a training concept, the agency of UNESCO sites can be improved greatly. On one level, stakeholders will be informed about the potentials of digital geomedia and how to interpret and utilize resulting products. On another level, they will be enabled to conduct monitoring, spatial analysis, and visualisation by themselves instead of depending on external partners for such services. This can greatly support protective measures, disaster risk preparedness, and local capacity building in the future.

U-Net: A Deep Convolutional EncoderDecoder Architecture to Discover Ancient Agricultural Terraces using LiDAR and Orthophoto

Arti Tiwari [1] , Micha Silver[2], Aviv Lee Cohen-Zada[3], Arnon Karnieli [4]

[1,2,3,4] Ben-Gurion University Of The Negev, The Remote Sensing Laboratory, Jacob Blaustein Institutes For Desert Research, Israel

Keywords: U-Net, Object-based image analysis (OBIA), Terraces, LiDAR, Orthophoto

The challenge

Since the 7th century, the traditional agricultural terraces (typically less than 1 m) have been deserted. Currently, terraces can be seen as a height of a few centimeters above the ground or a buried surface above the linear vegetation pattern in the wadi surface. There is a need to discover these geoarchaeological features to identify appropriate agricultural land resources resulting in increased crop yield production in a hyper-arid environment. The main aim of the study is to develop a deep convolutional neural network (DCNNs) system for the automatic identification of terraces. OBIA was used to extract features and combined with LiDAR-derived models to know their spatial pattern distribution. The study was performed in Avadat area, Israel. The model achieved Mean IoU (MIoU) for testing datasets were 53.

Methodology

The methods involve number of steps that includes LiDAR derivatives, object-based image analysis (OBIA) and a modified U-Net architecture. A geomorphological dataset was required for improving the model performance in terms of learning exact locations of terraces. Slope model (SM), profile curvature model (PCM), and flow direction model (FDM) were produced using LiDAR. Object-based method was used to extract features in the research area using eCognition developer. The study uses an encoder-decoderbased deep convolutional neural U-net architecture (Figure 1). The encoder section is used for feature extraction with the help of convolutional layers followed by max-pooling layers to get reduced feature maps. The decoder segments involve upsampling in sequence with convolutional layers to generate a predicted mask corresponding to image objects.

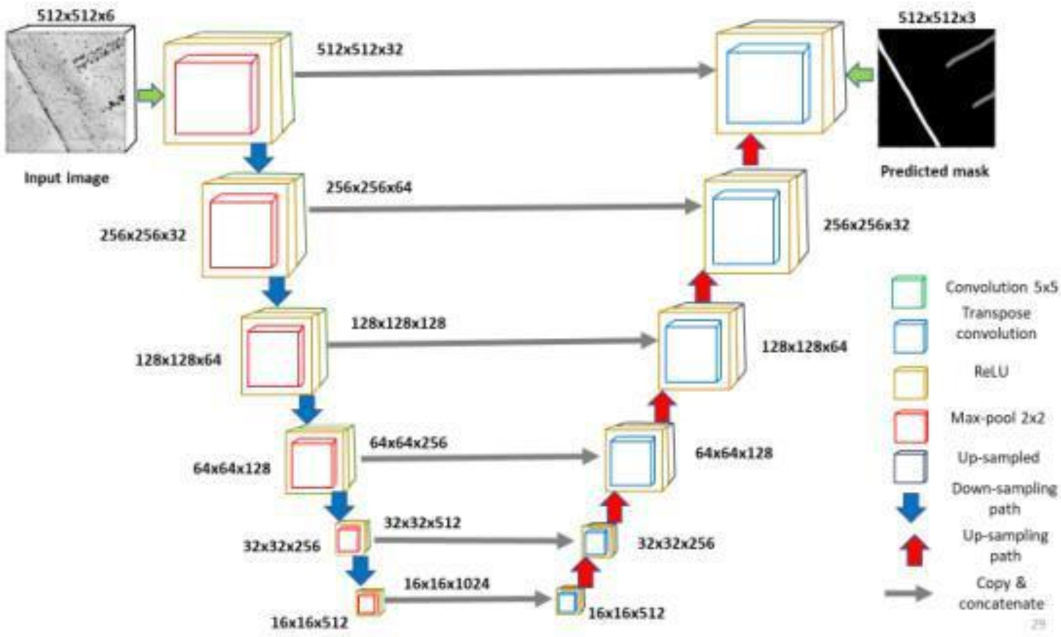

Figure 1: A U-net model architecture was used in this research. The image size and convolutional filters are denoted at each step.

Results

The LiDAR models are shown in figure 2.

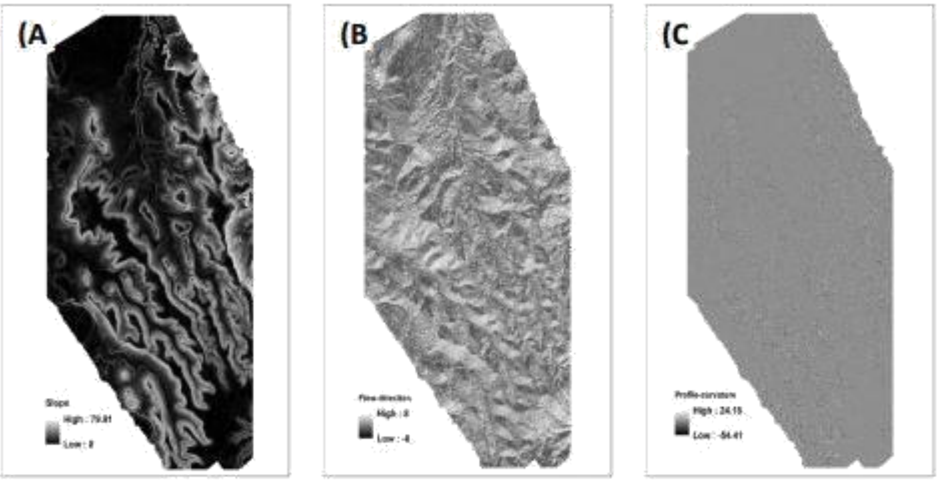

Figure 2: LiDAR models: (A) Slope (SM); (B) Flow-direction model (FDM); (C) Profile-curvature model (PCM)

The OBIA results are given below:

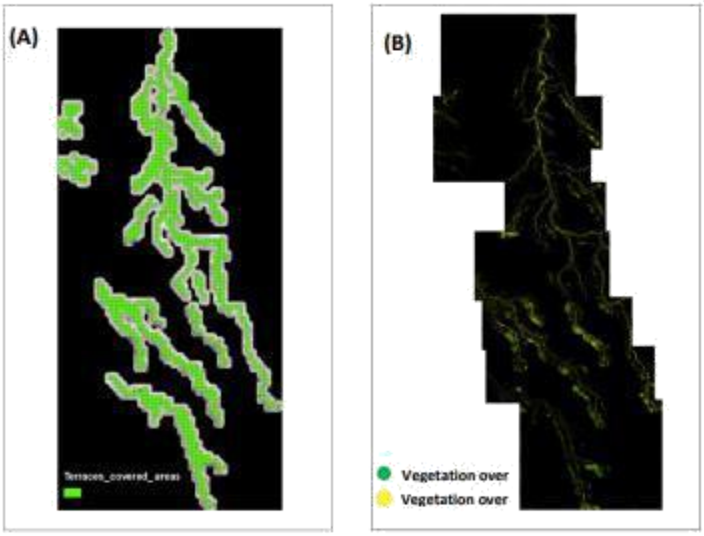

Figure 3: (A) Classification Level-I of terraces covered areas; (B) Classification Level-II of two major classes (vegetation over plane and vegetation over slope).

Modified U-net model performance

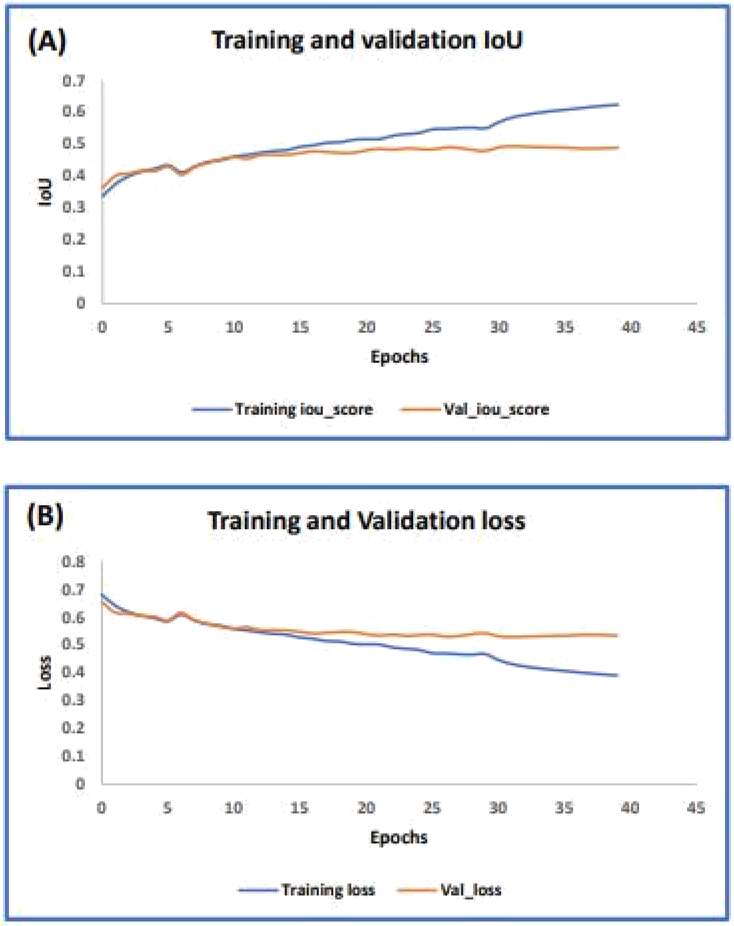

Figure 4(A) Training and validation IoU curve and (B) Training and validation loss curve

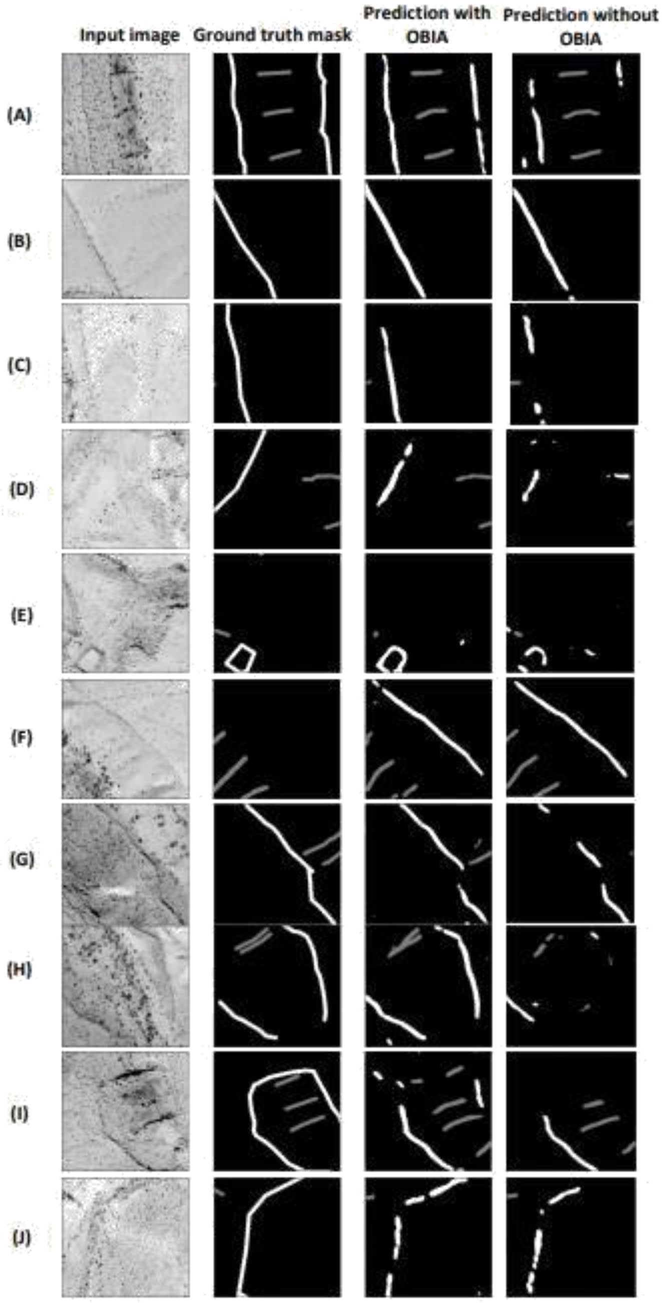

Figure 5: Testing image input samples (A-J), generated ground truth mask with help of GPS markings in the field and semantic segmentation (prediction with OBIA and without OBIA) of the corresponding using modified U-net model.

Poster(s)

Documentation and monitoring of the rehabilitation of the historic World War II US Air Force Base in Greenland

Karel Pavelka[1], Jaroslav Šedina[1], Eva Matoušková[1], Karel Pavelka, jr.[1], Martin Kýhos [1]

[1] Czech Technical University in Prague (CTU FCE), Faculty of Civil Engineering, Department of Geomatics, Czech Republic, Thakurova 7, Prague 6, 166 29

Keywords (5): Bluei East II., monitoring, drone, Greenland, photogrammetry, military air base

The challenge

The CTU FCE has been focused for a long time on historical monument and landscape documentation using digital photogrammetry, laser scanning and geophysical methods. In 2014, cooperation focused on Arctic research was established between German and Czech universities. The last expedition to Greenland was realized in 2019. We focused on the abandoned US base Bluei East II. In the Ikateq Canal, approximately 60km north-east from the Kulusuk on the east Greenland coast. The former US air bases in Greenland were constructed during WW2; some from them were rebuilt as Danish /Greenland's internationals airports, but most were abandoned, which is also the case with the air base Bluei East II. After leaving the area at the end of WW2, the US handed over the base to Denmark. It is just a coincidence that after a long period of negotiations, the liquidation of the remnants of the base began in September 2019, just after our expedition and measurements.

Methodology

There were several expedition goals such as research focused glaciology, warming monitoring, biology, and geography. Our part (CTU FCE) was focused on glacier movement and the documentation of an abandoned US air base using aerial drone photogrammetry. Our aim was to document this base, create detailed maps using drone photogrammetry and to use terrestrial measurements and documentation of interesting objects. This measurement was carried out in September 2019. During our two-day measurement, the winged eBee drone was used for the documentation of the abandoned US base and nearby neighbourhood. Two flights were carried out, both approximately for 35 minutes at an altitude of 130 m. The abandoned US base is not only a runway, but also a broad area with warehouses and hangars. Data processing was performed using an Agisoft Metashape software and Pix4D. We did not find historical aerial data in the archives. That's why we ordered satellite data. Although they do not show the old and original state of the base, they are used to compare the results of aerial photogrammetry using a drone in 2019 with data from WordView3 (GSD pan 33cm). The data are of good quality and aim to compare the results of our research and multispectral analysis of the area with high-resolution satellite data. We further analyse the situation after rehabilitation of the territory from satellite data from 2020 and 2021 using data GeoEye1 (GSD Pan 45cm) satellite. It can be stated that the rehabilitation of the area is slow (Fig.1-2).

Results

Our results were a precise orthophoto map (GSD 5 cm) created from acquired photographs and produced a digital surface model; both were used as a basic map document for botanical research, which should answer the question of whether the area was contaminated with the remnants of oil products from the thousands of barrels stored there. An unknown number of rusting barrels originally filled with fuel and lubricants are still present at the location. Estimates of the number of barrels vary - from tens of thousands to 200 thousand. Due to the remote area, no one cared much, and only recently has there been a reversal of possible contamination and impact on the fragile ecological conditions of the entire Arctic. Besides, our aim was to calculate the affected area and to estimate more precisely the number of present barrels using a digital surface model and classification of infrared photos taken from drone and from satellite data, which succeeded. Another result was the monitoring of the rehabilitation of the area by satellite data and comparison with drone data. It is interesting that several vehicles and construction that remained were still in relatively good condition. We documented the selected ones by describing and creating a 3D model using close-range photogrammetry. However, no significant contamination was noted on the first on-site survey; volatile petroleum products were long gone, so only heavy lubricants could possibly contaminate the soil, but this has not been proven.

Outlook for the future

There is little information on the web and searching the archive takes a long time. We focused on the Danish archive of historical aerial photographs, and we failed here, as we did not find till now historical relevant data in cooperation with the Danish side in this area. We can therefore say that our documentation shows the latest state before its liquidation commencement. However, our research did not end with the acquisition of an orthophoto and a brief documentation of the objects. We also tried to find historical information on the web and by querying the Air Force Historical Research Agency.

(a) (b)

Figure 1 (a) Digital orthophoto created from drone using infrared camera Canon IXUS powershot, (b) Beginning of area rehabilitation in 2019

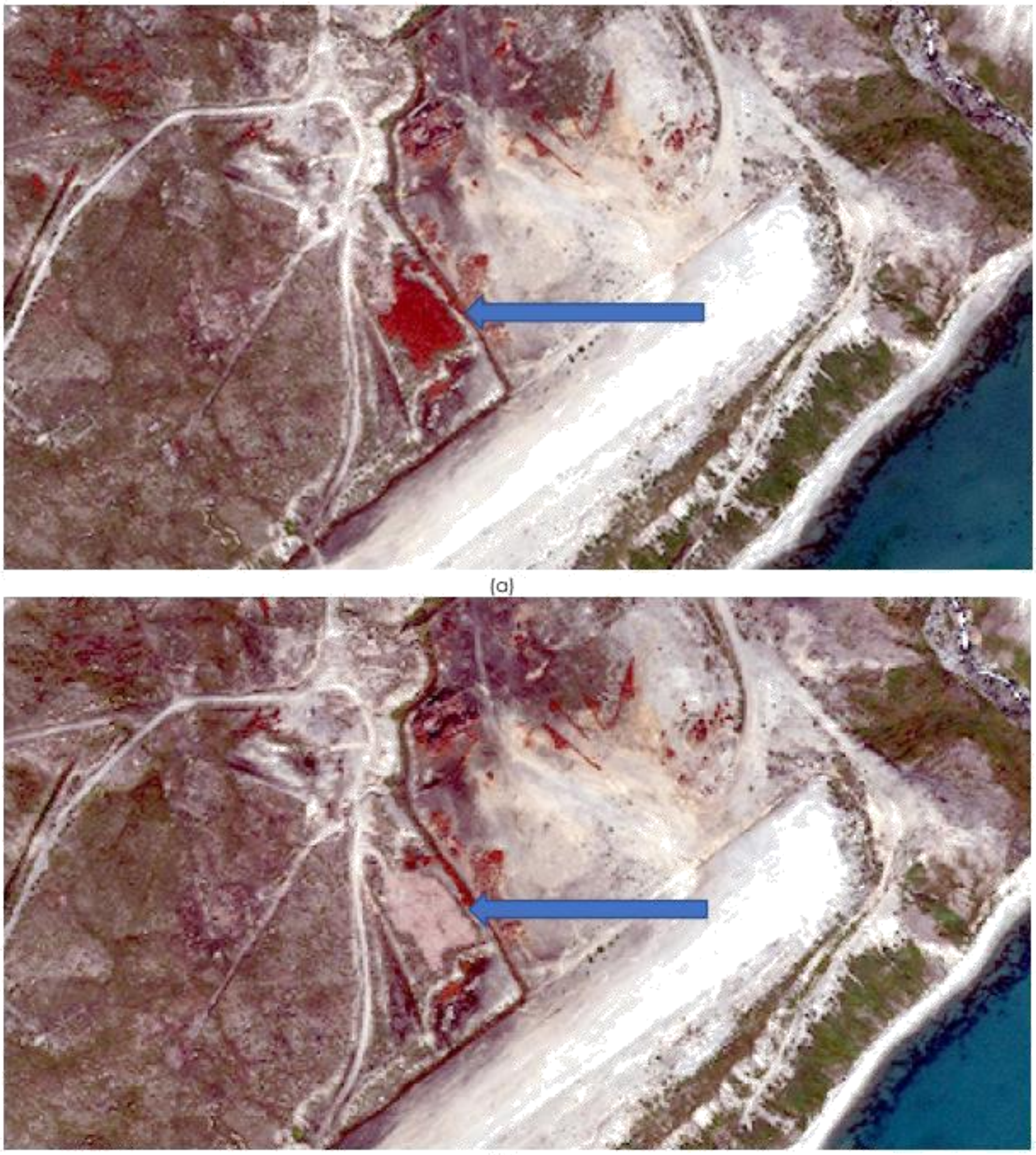

(a)

(b)

Figure 2 Overview on satellite data from (a) GE1 satellite (8/2020) and (b) GE1 (8/2021); a big barrel depot is removed and cleaned

6th EARSeL Workshop on Developing Countries "Earth Observation and the Global South"

Organizers:

Developing Countries SIG Chairs

Monika Kuffer, University of Twente, ITC, Enschede, The Netherlands (SIG Chairs Developing Countries) and Stefanos Georganos Division of Geoinformatics, KTH, Stockholm.

Summary:

Rapid transformation processes occur in the Global South, impacting natural habitats, rural, peri-urban and urban areas. In particular, low- and middle-income countries (LMICs) have accelerated economic growth combined with rapid conversion of natural habitats. The newly emerging human settlements exhibit varying degrees of inequalities in terms of access to basic infrastructure and essential services. Moreover, local environmental conditions can have severe impacts on living conditions and health outcomes. To adequately monitor these transformation processes, timely and spatially disaggregated data are essential but often not available. Earth Observation (EO) data can provide immense opportunities for monitoring these transformations, but several challenges, pertaining to their use, need to be tackled. First, EO data need to be provided with sufficient spatial and temporal granularity. Second, the development of innovative, transferable and scalable mapping approaches both with respect to the methods and data are imperative. Third, FAIR (Findability, Accessibility, Interoperability, and Reusability) data standards are important to support easy access and exchange of data and methods. The thematic workshop will allow researchers to exchange on state-of-the-art EO methods to analyse transformation processes in the Global South (e.g., environmental risk, hazards, urbanisation, demographic and socio-economic conditions, conservation, agriculture), while enabling their integration for evidence-based policy making (e.g., SDGs). As technologies, available data, and computing power rapidly evolve, new opportunities are emerging to co-create and integrate data (e.g., citizen science). We must ensure that these approaches are inclusive, result in benefits to all stakeholders, and that we have mitigated unintended consequences for the most vulnerable populations.

Topics:

- Urban or rural poverty modelling (e.g., deprived urban areas, slums)
- Natural hazards, vulnerabilities, resilience and climate change in the Global South
- Socioconomic, demographic and health mapping in the Global South
- Urbanization in the Global South: Urban growth, urban land consumption rates and temporal dynamics
- Agricultural monitoring and applications in the Global South
- Natural resource management and monitoring in the Global South
- Urban morphology and infrastructure in the Global South
- Land use/ and cover mapping in the Global South
- Urban environment (climate, air, water and land) and their dynamics at various scales in the Global South
- Sustainable Development Goals and Earth Observation

Scientific Committee:

- Monika Kuffer, University of Twente
- Stefanos Georganos, KTH
- Jon Wang, University of Twente
- Caroline Gevaert, University of Twente
- Eleonore Wolff, Free University of Brussels
- Sabine Vanhuysse, Free University of Brussels
- Angela Abascal, University of Navarra
- Nicholus Mboga, Free University of Brussels
- Tais Grippa, Free University of Brussels
- Claudio Persello, University of Twente
- Jasper de Vliet, VU Amsterdam
- Catherine Linard, University of Namur
- Yifang Ban, KTH
- Oscar Brousse, University College London
- Frank Canters, Free University of Brussels
- Michael Wurm, German Aerospace Center
- Mariana Belgiu, University of Twente
- Matthias Demuzere, Ruhr University of Bochum
- Joana Barros, Birkbeck - University of London
- Andrea Nascetti, KTH
- Ron Mahabir, George Mason University
- Elnaz Neinavaz, University of Twente
- Aguilar Bolivar, University of Twente
- Mila Koeva, University of Twente
- Divyani Kohli, University of Twente
- Christian Geiss, German Aerospace Center

WSDC_DUA1: Deprived Urban Areas I

Chair(s): Dr. Stefanos Goerganos and Monika Kuffer

Deprived Area Mapping using Deep and Machine Learning on Sentinel-2 Imagery

Ryan Engstrom[1], Amir Jafari[2], Arathi Nair[2], Abdulaziz Gebril[2], Mina Hanna[2], Mojahid Osman[2], Jake Lieberfarb[2], Bradely Reardon[2], Maxwell Owusu[2], Dana Thomson[3], Monika Kuffer[3]

[1]George Washington University, Department Of Geography And Data Science, Usa
[2]George Washington University, Usa
[3]University Of Twente, Netherlands

Keywords: Deprived Areas, Deep Learning, Machine Learning, Medium Resolution

The challenge

The number of people living in deprived urban areas within low and middle income countries is large and predicted to continue to grow. Mapping these areas over time and space in a consistent manner is important for monitoring the sustainable development goals (SDGS). In order to improve the consistency and accuracy of mapping these areas between cities the integrated deprived area mapping system (ideamaps) project was initiated. one aspect of this work is to determine the ability to utilize satellite imagery to make a cost effective and globally applicable maps. In order to do this, we examine the ability to use sentinel-2, 10 meter spatial resolution imagery to map deprived areas using a combination of deep learning, contextual features, and machine learning in three cities, Lagos Nigeria, Nairobi Kenya, and Accra Ghana. the ability to map deprived areas using these data would allow for a repeatable and cost effective method for mapping deprived areas globally.

Methodology

Cloud free Sentinel-2 scenes for each city were created using Google Earth Engine using the Sentinel Hub S2 cloudless machine learning algorithm to detect and mask the clouds/cloud shadows reflected on earth's surface. For each city a range of dates were examined to produce the most visually cloud free image possible, that were up to date, and had a relatively short time frames. The dates chosen were December 20, 2021 to January 23, 2022 for Lagos, November 14, 2021 to December 23, 2021 for Accra, and January 3, 2022 to January 14, 2022 for Nairobi.

Once imagery were extracted multiple machine learning and deep learning methods were explored using training and validation data consisting of three classes, non-built, built-up, and deprived area provided by the IDEAMAPS project that were collected in-situ and from Open Street Map data. The first step was to calculate contextual features. These can be defined as representing the statistical quantification of different levels of image features, such as low level edge patterns, pixel groups, gaps, which forms high level image textures, and the raw spectral signatures calculated over groups of pixels or neighbourhoods. Once calculated these were used as inputs to machine learning models including random forests, gradient boosting, and MLP. Additionally, Multi Layer Perceptron and Convolutional Neural Network models were derived from the imagery.

Results

Relatively clear images Sentinel 2 images were able to be created from Google Earth Engine even though cloud cover in cities such as Lagos had make this difficult in the past. This is very encouraging for working in countries near the equator and for using these data on a global scale. Preliminary results for Lagos indicate that using just the Sentinel 2 derived contextual features in a Gradient Boosted model, an F1 macro score of 0.84 can be achieved, with 0.73 F1-class score for deprived areas when the two classes are considered. Preliminary results using an Autoencoder and Deep Learning indicates the class imbalance (very few deprived areas relative to the other classes) impacted the results. Using a variety of methods to increase the training sites, and reducing the classes to just built-up and deprived, the best models produce a macro average F1 score of 0.74 for Lagos, Nigeria. Overall, these preliminary results indicate Sentinel 2 data do provide significant information about deprived areas and maybe when combined with other geospatial data sets, may be able to provide accurate maps of deprived areas.

Outlook for the future

This work has highlighted the capability of using free and open source remotely sensed data to map deprived areas. While these results are preliminary there are a few areas that we are currently working on. One of the ways we are looking to improve results is deriving additional training and validation data, in particular for the deprived area class (Figure 1). To do this we are trying to find as many training sites as possible and examining shifting, rotating, and rolling through adjacent parts of the imagery that are part of the current training data sites to create more training data. Much of the training data was collected in-situ and was designed to represent a 100m grid cell being deprived. What is visible in the imagery is that, for most cases, areas around the 100m cell being labelled as deprived are also deprived. Using these techniques we can increase the number of 100m grid cells labelled as deprived. Additionally, we are working on automated ways to extract information from open street map that can augment these data and improve the class imbalance that is impacting model performance. The next steps are to test the models in the other cities of Accra and Nairobi and see both if training data collected there can improve the models and/or the ability of the models to transfer between cities.

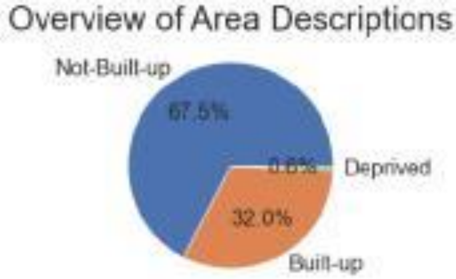

Figure 1 Overview of the training data area descriptions and class imbalance in the three classes of the training/validation data of non-built up, built-up, and deprived.

The diversity of deprived areas: applications of unsupervised machine learning and open geodata to São Paulo, Brazil

Lorraine Oliveira[1], Monika Kuffer[2], Nina Schwarz[3], Julio Pedrassoli[4]

[1] University of Twente, Department of Urban and Regional Planning and Geo-Information Management (PGM), The Netherlands

[2]University of Twente, The Netherlands

[3] University of Twente, The Netherlands

[4] Federal University of Bahia, Brazil

Keywords (4): deprived areas, urban remote sensing, open data, unsupervised machine learning

The challenge

Most fast-growing cities of Low- to Middle-Income Countries (LMICs) are facing an unprecedented growth of deprived areas, marked by poor housing, services and environmental quality. These areas require consistent and updated information about their physical and living conditions. Yet, there are data and methodological challenges. When available, census data has large temporal gaps; it is resource-intensive and often aggregates information, masking spatial differences. Meanwhile, most remote sensing (RS) studies focus on spatial commonalities of deprived areas, overlooking their local heterogeneity. In addition, they often use supervised classification models, which are resource-intensive, and rarely address city-wide analysis. To address these challenges, this research explores the potential of unsupervised machine learning (ML) models to capture intra-urban diversity of deprived areas at city-wide scale, using solely open geodata, resulting in a typology of deprived areas.

Methodology

The city of São Paulo, Brazil, was used as case study and a spatially disaggregated approach was adopted to account for the spatial heterogeneity within deprived areas. In the first step, literature guided the development of a pool of Geographic Information System (GIS)- and Remote Sensing (RS)-based features to derive morphological and environmental characteristics of the study area. In the second step, an geodatabase was built from open data, and spatial features were extracted with specific metrics and integrated as model input. The third step developed a k-means clustering model with robustness and optimization experiments. A feature importance tool was coupled to the model to stress the relevance of the features for each resulting cluster type. The last step validated the model and the resulting clusters of deprived areas with visual inspection and expert evaluation, analysing the relationships between the clusters and the spatial features used. A model only with census-derived features and the official land use layer were used as a reference to assess the results.

Results

The model produced four distinct clusters that characterize the deprived areas in the city, that show morphological and environmental variations. The first cluster, named “Infant settlements in open spaces”, is characterised by low accessibility to services and infrastructures, very sparse occupation and the presence of vegetation. The second, “Unordered and poorly consolidated settlements”, is marked by steep terrain, lack of infrastructure and relatively low population densities. The third, “Less deprived settlements connected to non-residential areas”, is identified mainly by a more regular layout and mixed land uses. And the fourth, “Densely urbanized and mature settlements with irregular layout”, is highly influenced by built-up density and complex (slum-like) morphology. The qualitative validation of the model evinces that the unsupervised ML model successfully captures the intra-urban diversity of deprived settlements in São Paulo, stressing higher precariousness for the second identified cluster. The qualitative assessment demonstrates that the proposed approach can be an alternative to current characterization studies using solely open data. The cluster types are profiled and can be comprehensively used for decision-making processes.

Outlook for the future

Within deprivation and slum studies, an unsupervised ML approach was not yet exploited in literature. While the present study profile local deprivation nuances, posing the great potential of unsupervised models and open data to characterize deprived areas, there are still limitations. For future recommendations, the utmost suggestions are (1) upscaling the model to regional/national level, even encouraging to replicate the workflow to cities in other global contexts exploring its transferability; (2) full automation of the workflow. It would be valuable not only to automate the model in an API environment, but also the feature extraction process, instead of relying on geospatial tools, that often require larger computational capacity. Developing a fully automated process can facilitate model’s scalability and ensure its applicability to the municipalities without requiring advanced programming skills by the local experts.

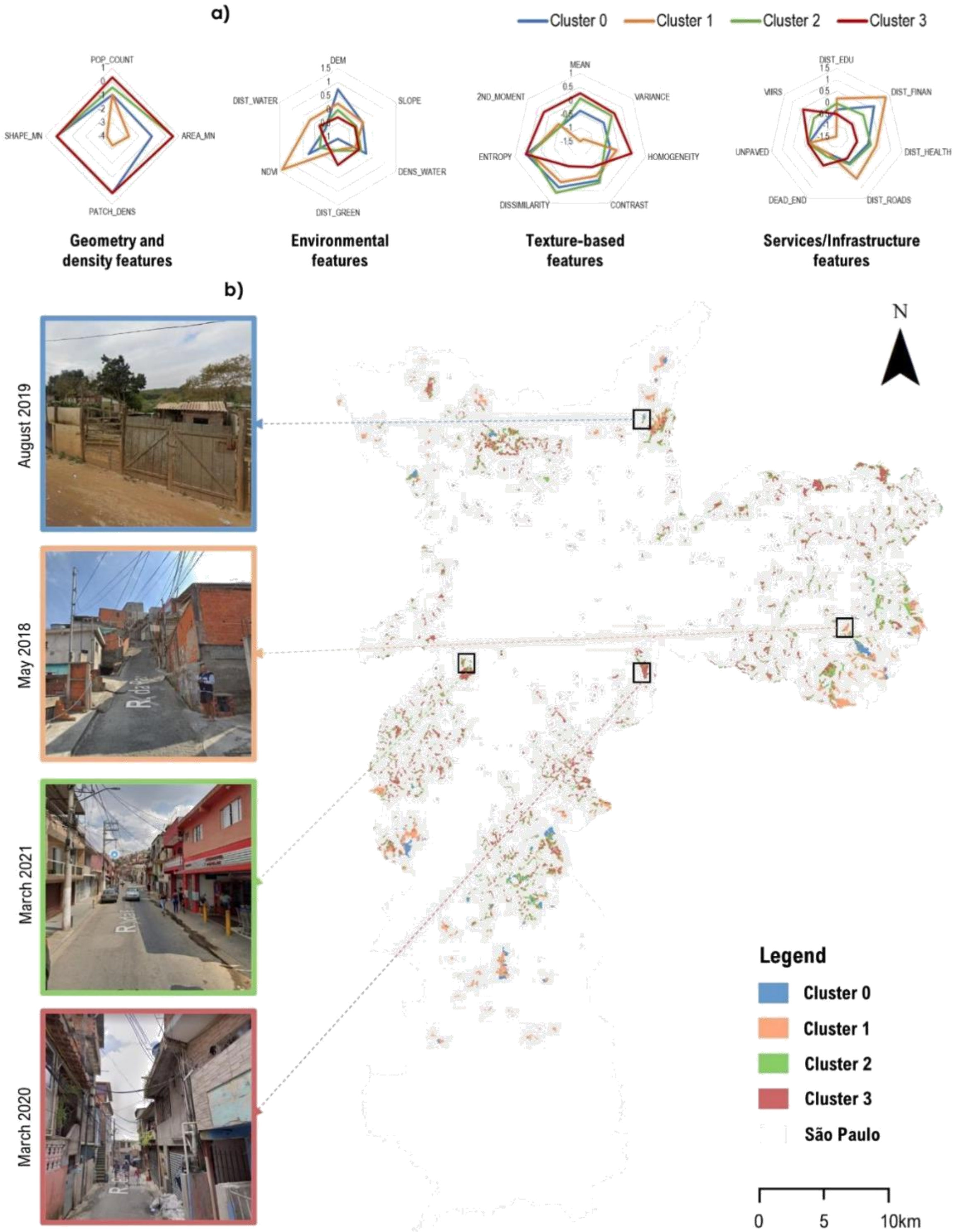

Figure (a) Spider graphs profiling the emerged clusters according to the mean values of each feature and (b) Clustering map with examples of deprived areas in each cluster type, including their capturing date (Street View images).

Predicting Perceived Urban Deprivation Using Deep Learning

Taïs Grippa[1], Angela Abascal[12] , Sabine Vanhuysse[1] , Eleonore Wolff[1]

[1] Department of Geosciences, Environment & Society, Université libre De Bruxelles (ULB), avenue Franklin Roosevelt, 50, 1050 Bruxelles, Belgium

[2] Navarra Center for International Development, University of Navarra, 31009 Pamplona, Spain

Keywords: Urban deprivation ; Human perception ; Sub-Saharan African city ; Deep learning ; Transfer learning

The challenge

More and more research is made on slums and the mapping of deprivation. However, most of research has focused on mapping slums neighbourhoods versus the rest of the city. Only few concentrate their efforts on analysing the intra-slum variation and relating these differences to levels of deprivation. In this research we use a morphological urban deprivation score created from citizens' local knowledge and assess how deep learning (DL) approach can be used to predict citizens perceived deprivation score (CPDC). Using a voting system, Worldview3 image chips were assigned with a score which has been used as ground truth for supervised training (regression task). The advantage of a DL approach versus old-fashioned machine learning approaches is that it relies solely on image patches and does not require feature engineering. However, the entire dataset is made of 1998 patches only, which can be considered as a challenging data-scarce context when dealing with deep learning.

Methodology

To generate the CPDC, citizens from several local communities were invited to vote for the best place to live in a pairwise comparison of 1ha WorldView3 image chips. More than 1 million votes were used to rank patches and generate a deprivation score using the TrueSkill algorithm. It is this score, based on human perception, which we try to predict using DL models. We conducted experiments using two Convolutional Neural Network (CNN) approaches. The first rely on a VGG-like model trained from scratch on our dataset. This custom VGG9 includes 7 convolutions and 2 fully-connected layers. The second approach is based on transfer learning and uses a DenseNet121 model pretrained on ImageNet and fine-tuned on our dataset. The earth observation data consist of WV3 images whose initial input size of 333x333 pixels (patches of 1ha) was resampled to 224x224 to match the patch size of the DenseNet121 model pretrained on ImageNet. Moderate data augmentation has been used to avoid overfitting with our small-sized dataset. We conducted experiments using RGB images and RGNir images. Considering the high variance in the results depending on the random state of the training/test split, we decide to use a k-fold cross-validation approach. Ten partitions (90% for training, 10% for independent validation) were generated and used to fit ten different models. We report both R^2 and RMSE metrics of the best model as well as mean and standard deviation of the 10-fold crossvalidation.

Results

As illustrated below, the performance achieved by the VGG9 model is relatively limited. This can be explained by the fact that the training dataset is limited and thus it is difficult for the model to learn properly. Other experiments conducted with 4 bands (VIS-NIR) did not lead to a significant improvement. With the VGG9 model, the use of RGNir overperformed RGB input with a mean R^2 of 0.52 on the validation set. The results obtained using the pretrained DenseNet121 are significantly higher, achieving a mean R^2 of 0.80 and a much smaller variance in the cross-validation process, for the experiment using RGB input. Quite surprisingly, the near-infrared information does not perform better with this model, while it is generally assumed that near-infrared band is important. This below par performance could be explained by the fact that the model is pretrained on an RGB dataset (ImageNet) and thus was not able to correctly adjust the weights of the discarded blue band to the new near-infrared band, at least with the limited number of epochs used for fine-tuning. Another explanation could be that the vegetation, for which the near-infrared band is reputed to be important, is not an important feature to predict the deprivation perception score. Training Validation Best R^2 R^2 (mean) R^2 (std) Best R^2 R^2 (mean) R^2 (std) VGG9_RGB 0.505 0.503 0.046 0.601 0.487 0.101 VGG9_RGNir 0.519 0.532 0.066 0.716 0.520 0.101 DenseNet121_RGB 0.912 0.903 0.016 0.841 0.801 0.021 DenseNet121_RGNir 0.908 0.886 0.038 0.822 0.789 0.021

Outlook for the future

Here, the model is trained from a visual perception of deprivation and cannot be considered as the actual deprivation. In the near future, some micro-survey data will be available for few numbers of images patches in Nairobi and will allow assessing how good is the correlation between the perceived and the actual deprivation. In case of high correlation, that would mean that we can predict actual deprivation with very high confidence using such kind of DL approach. It would be interesting to investigate the transferability of the DL model fine-tuned on Nairobi to predict deprivation score on a new, unseen city. However, there is a high probability that it would not be straightforwardly transferred, the urban appearance of slums changes according to the context, and will require to implement domain adaptation strategies. Also, further research could explore the contribution of other pretrained model and conduct a specific benchmarking for this kind of task.

Figure Predicted deprivation score over the whole deprived urban areas of Nairobi.

Mapping Slums Using Satellite Imagery: A Comparison of Image Processing Techniques

Agatha Mattos[1], Gavin McArdle[1], Michela Bertolotto[1]

[1] University College Dublin, School of Computer Science, Ireland

Keywords (5): Sustainable Development Goals, Slums, Deprived Areas, Machine Learning, Remote Sensing

The challenge

The United Nations Habitat estimates that over one billion people live in slums around the world; however, these estimates are mostly from census surveys, which are expensive to collect and not conducted frequently enough to keep up with the pace of change in many deprived communities. An alternative is combining information from infrequent official household interviews with estimates from sources of information that can be collected remotely, cheaply and at scale. Recently, researchers have looked at methods employing satellite imagery and processing it using machine learning algorithms, but presently there is no consensus on the most appropriate imagery and processing that should be used for this task. Results obtained to date are not comparable since they analysed different locations, employed imagery from various sensors, used distinct proportions of training data to train models (train/test split ratio) and evaluated results using different metrics. This study fills this gap in the literature by comparing the three most used image processing techniques to map slums for three global locations.

Methodology

The three locations examined in this study are Mumbai in India and El Daein and Geneina in Sudan. These locations were selected due to the availability of labelled data. The data used to map slums are Sentinel-2A satellite imagery with 10-metre resolution and ground-truth data with the same resolution, provided by Gram-Hansen et al. (2019). The techniques evaluated are 1) multispectral data classification using random forests, 2) feature extraction using grey-level co-occurrence matrix (GLCM) and posterior classification using random forests and 3) classification using a fine-tuned residual neural network (ResNet18) pre-trained with the ImageNet dataset. In the first technique, the classification is performed at pixel-level, while in the other two tiles of 10x10 pixels are used to train the model. A binary classification was used, and a 50% threshold was applied for majority classification. The same tiles were given to train each of the classifiers. For the deep learning technique (ResNet18), only three bands of the imagery were used (blue, green, and red); for GLCM, the same three bands were used, plus the Near Infrared (NIR) band, and for the multispectral classification all bands were used. Four different train/test split proportions were investigated: 20, 40, 60 and 80% of the slum tiles. The classifiers were trained with the same amount of slum/non-slum data, which meant that the non-slum class was undersampled for all locations. For each location and train/test split, the experiments were repeated three times using different random seed numbers to select the tiles that would be used to train the model. The classifiers were compared using intersection over union (IoU), a common metric in computer vision tasks. Experiments were run in Python, and the code and data are available.

Results

For all locations, the performance of the different machine learning techniques was consistent. Multispectral data paired with a random forest classifier (RF) performed better (mean IoU for all locations was on average 57% +/- 3), followed by GLCM paired with a RF classifier (45% +/- 2) and neural network (30% +/- 2). All techniques presented a higher IoU for the non-slum class, the average for all locations was 65% +/- 8, and the IoU for the slum class was 23% +/- 10. The increase of training data from 20% to 80% led to an increase in the IoU for the slum non-class for all classifiers and to a decrease in the IoU for the slum class. That increase was less prominent for Mumbai, only 1%, followed by El Daein, 4%, and Geneina, which saw an increase in the IoU for the non-slum class of 6%. Given that training models with more data consume more computing resources, these numbers suggest that training with fewer data may be a good option when computing capacity is limited or when obtaining better results for the slum class is preferable. However, the lower IoU for the slum class compared to the non-slum class suggests that strategies other than undersampling the non-slum class could be investigated to deal with the imbalanced dataset. Finally, classification at the pixel-level seems to work better when there is not much data to train deep learning models or/and when working with medium-resolution satellite imagery.

Outlook for the future

This experiment shows that medium-resolution satellite imagery has patterns that can be learned using machine learning techniques to distinguish deprived areas (slums) from non-deprived areas. Looking to the future, it would be desirable to investigate strategies to improve the results for the slum class, such as adopting more sophisticated sampling for the slum and non-slum classes, for instance, cluster centroids or nearest-neighbour-based methods. Moreover, it would be desirable to expand this study to analyse the generalisability of the developed models.

WSDC_DUA2: Deprived Urban Areas 2

Chair(s): Dr. Stefanos Goerganos and Angela Abascal

Urban morphology for mapping deprived urban areas across cities in sub-Saharan Africa

Sabine Vanhuysse[1], Jiong Wang[2], Priscilla Kabiru[3], Monika Kuffer[2], Stefanos Georganos[4], Angela Abascal[5,1], Eléonore Wolff[1]

[1] Université libre de Bruxelles (ULB), Department of Geosciences, Environment and Society, Belgium

[2] University of Twente, Faculty of Geo-Information Science and Earth Observation (ITC), The Netherlands

[3] Foresight Planners Limited, Kenya

[4] KTH Royal Institute of Technology, Division of Geoinformatics, Sweden

[5] University of Navarra, Navarra Center for International Development, Spain

Keywords: Slums, Sub-Saharan Africa, Building footprints, Transferability, Scalability Morphological deprivation

The challenge

It is estimated that more than half of city dwellers in sub-Saharan Africa (SSA) currently live in deprived urban areas (DUAs), often called slums. While the first target of SDG 11 is 'to ensure access for all to adequate, safe and affordable housing and basic services and upgrade slums', there is a huge gap in timely spatial data to support evidence-based policies and monitor progress towards that objective. One of the major challenges of slum mapping (or DUA mapping) at city scale lies in developing methods that rely on free or low-cost data and can be applied to a wide variety of cities with limited adaptations and labelling efforts. Due to the high degree of morphological variability of DUAs across cities, one possible option for attaining this objective is to implement workflows involving unsupervised methods. We propose such an approach, and leverage the potential of a recently released open layer of building footprints to map the physical dimension of urban deprivation.

Methodology

Focusing on three SSA cities, namely Ouagadougou (Burkina Faso), Nairobi and Kisumu (Kenya), we computed a set of morphology metrics from the recently released Google Open Buildings dataset containing more than half a billion building footprints across most of Africa. These metrics not only characterise each individual building in terms of shape, size, orientation etc., but they also account for their neighbouring buildings and surroundings (e.g., distance between buildings, spatial arrangements etc.). We derived features by computing statistics and aggregating them in grid cells of 100m x 100m to conform to a growing trend towards the production of gridded spatial datasets at this resolution. Next, we performed dimensionality reduction with principal component analysis, based on a threshold of cumulative percentage of variance explained. We used a probabilistic clustering algorithm (namely Gaussian mixture), and used cluster membership to compute and map the morphological deprivation probability of each city (Figure 1). The output of this unsupervised process can subsequently be refined and serve to train a supervised machine learning model using free or low-cost imagery (e.g., Sentinel-2, PlanetScope), for producing morphological deprivation maps at different dates for which building footprints are not available. The process is mostly automated and requires reduced manual intervention. To evaluate the morphological deprivation probability derived from Gaussian mixture clustering, we delineated DUAs in Ouagadougou, Nairobi and Kisumu through visual interpretation of very-high resolution WorldView-3 imagery (30cm). Delineating DUAs is a difficult task that involves a certain degree of subjectivity, especially when it comes to areas that include a mix of different types of dwellings, display some regularity in the street patterns, and have fuzzy boundaries. Therefore, to reduce subjectivity, we included ancillary data (i.e., delineations obtained from local sources) and field knowledge in the process.

Results

The agreement between cluster-derived probability and manual delineation was particularly good in Ouagadougou. This good performance can be ascribed to the consistency in morphological differences between DUAs and the other types of residential areas. In Kisumu, we managed to capture DUAs, but some planned neighbourhoods were also included in the DUA cluster. Nairobi is the most challenging case study due to the variety of DUA types, the presence of small slum pockets, and the fuzzy boundaries between some DUAs and planned neighbourhoods. Nevertheless, the probability map reflects quite well the patterns of deprivation. For further refinement, we estimate that for one city, creating labels for the supervised classification of satellite imagery based on the morphological deprivation probability map could be completed in less than one hour.

Outlook for the future

In further research, we intend to apply our method to a wider variety of SSA cities. We also propose to classify Sentinel-2 (and possibly PlanetScope) imagery acquired at different dates using labelled samples derived from the cluster-based morphological deprivation probability maps, to study the dynamics of DUAs. Since our ambition is to progress towards a generic solution for mapping DUAs, we will strive to limit the labelling effort as much as possible. We do not know if the Open Buildings layer will be updated, but there are several initiatives that aim at mapping building footprints at continental scale and providing them as open data, and we are confident that their output will improve over time in DUAs. In the unlikely case that no progress is made in that direction, we think that research in slum mapping at city scale would benefit from CNN-based extraction of building footprints from very-high resolution imagery, the cost of such imagery remaining the main hurdle to date.

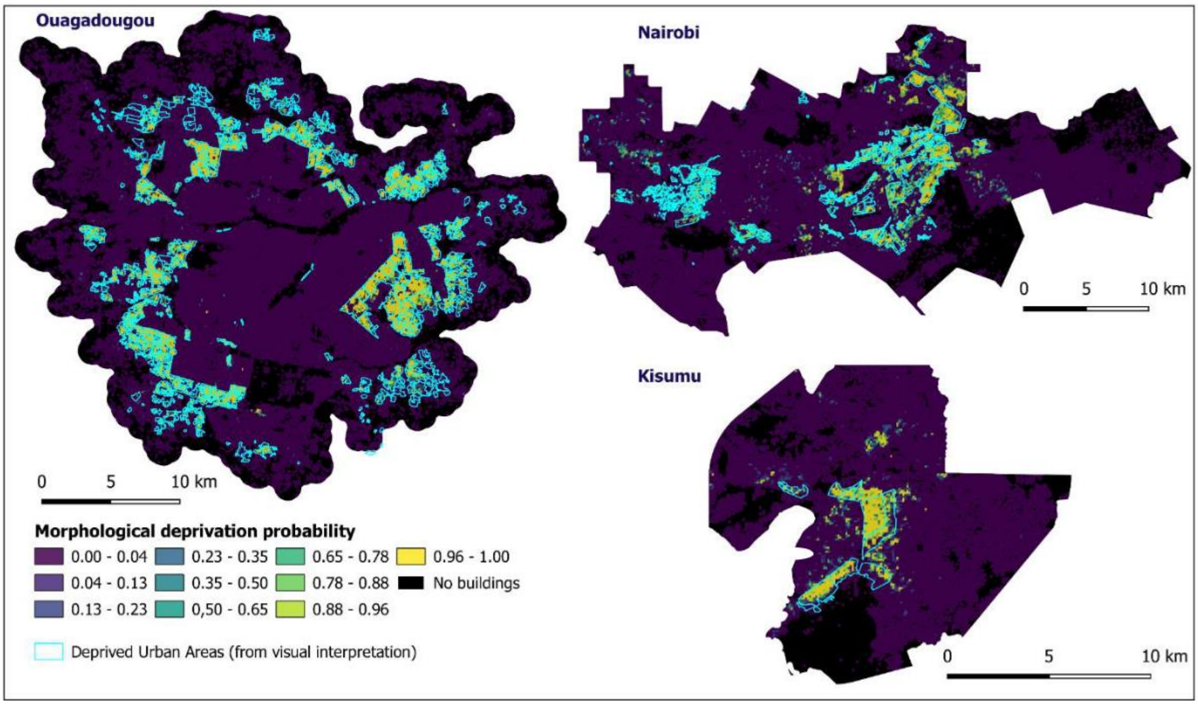

Figure For three sub-Saharan African cities, comparison of (i) morphological deprivation probability patterns (Gaussian mixture clustering of morphology metrics from Google Open Buildings) and (ii) delineation from visual interpretation. Resolution: 100m x 100m.

Requirements to Model Slums in Cities of the Global South

John Friesen[1], Julius Beuer[1]

[1]Technische Universität Darmstadt, Chair of Fluid Systems, Germany

Keywords (5): slums, modelling, model requirements, slum models

The challenge

Around 1 billion people worldwide live in slums. This form of settlement is characterized by its poor access to infrastructure. It is estimated that this number of slum dwellers is expected to increase further in the coming years. For urban planners, this raises the question of how best to anticipate the growth of slums and especially the amount of population in these settlements. One way to do this is through simulation models. In recent years, different model concepts have been introduced. Agent-based models, cellular automata or equation-based models. While some of these models were only conceptual, others are calibrated and validated on example cities. Although some works started to formulate requirements, slum simulation models should fulfill, the questions of minimal spatial or temporal resolutions remain unanswered. Based on information from Earth Observation (EO), we present approaches to systematically answer these questions below.

Methodology

To determine the requirements for slum models, we propose a three-step procedure.

First it is necessary to specify the purpose of the planned model: planning infrastructure, develop emergency scenarios, etc.

In the second step, we determine the nature of slum development in recent years based on earth observation data combined with population estimates to quantify the dynamics of the urban development in recent years. Therefore, we developed metrics to quantitatively distinguish processes of densification from processes of dispersal by analyzing temporally and spatially resolved data on slum areas. The findings of this analysis provide an initial indication of whether inter- or intra-urban migration processes or natural population growth are more likely to lead to the formation of new slums, or whether the population in existing slums is increasing. The analysis of EO-data gives an indication of the necessary temporal resolution of a model. However, the question arises as to the purpose of a potential model, e.g. modeling population for utility infrastructure planning requires lower temporal resolution than modeling natural disasters.

In a third step, based on the slum data the minimum spatial resolution of a potential model can be determined. One starting point is the so-called inaccessibility, which describes the longest possible shortest path from the center of a slum (Fig. 1) to its edge and thus provides an indication of the minimum resolution of a simulation model.

Results

The two cities of Rio de Janeiro, Brazil and Dhaka, Bangladesh can be used to explain the approach.

The question we want to answer with a possible model is the emergence and temporal development of slums in order to provide sustainable infrastructures for the supply of the population.

In a second step, we used publicly available earth observation data and data from WorldPop to quantify the processes of change in the two cities in recent years. While the population in Rio de Janeiro's favelas tends to grow, the emergence of new slums can be observed in Dhaka.

Based on the Earth Observation Data, we also estimated the inaccessibility of the slums in the different cities. We see, that due to the small slum patches in Dhaka, a simulation model would require a much higher temporal as well as spatial resolution to model urban growth processes.

Outlook for the future

George Box once said that "All models are wrong, but some are useful". Based on the analysis of existing empirical data, the considerations presented here are intended to represent a further step toward a methodological development of models with which we can describe processes of slum formation and growth in cities of the Global South. Fundamental to the considerations made here is the approach of empirically justifying the model assumptions used in each case. A further step is a systematic analysis of current models with regard to the approach presented here and the development of suggestions as to which type of modeling is best suited for which problem.

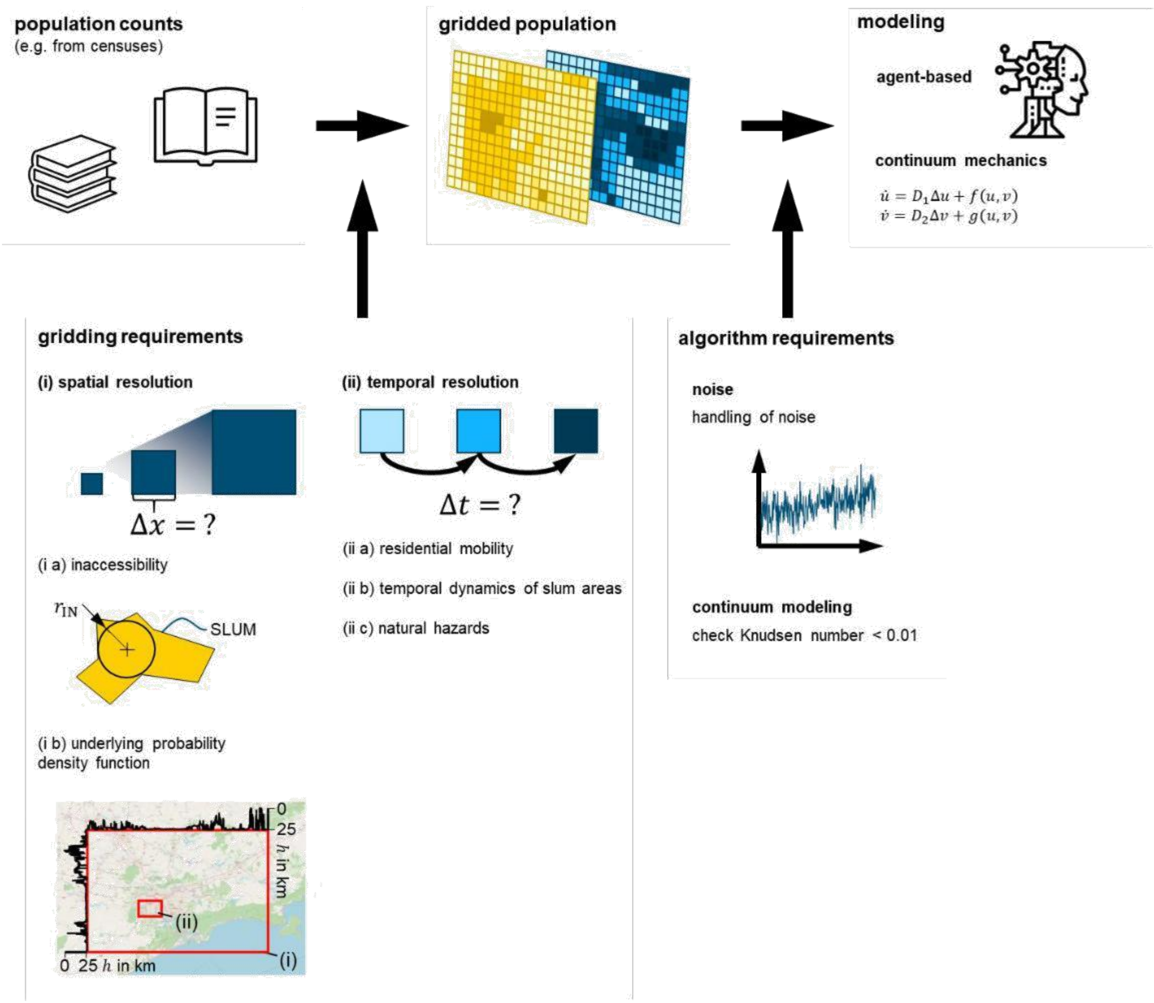

Figure Framework to determine requirements for the modelling of slums

The varying similarity in the morphology of the urban divide

Jiong Wang[1], Sabine Vanhuysse[2], Stefanos Georganos[3,2], Monika Kuffer[1], Angela Abascal[4,1]

[1] University of Twente, Faculty of Geo-Information Science and Earth Observation (ITC), The Netherlands

[2] Université libre de Bruxelles (ULB), Department of Geosciences, Environment and Society, Belgium

[3] KTH Royal Institute of Technology, Division of Geoinformatics, Sweden

[4] University of Navarra, Navarra Center for International Development, Spain

Keywords: Slums, Sub-Saharan Africa, Geographic information, Building morphology

The challenge

Over 25% of the global urban population live in slums with deprivation of basic living conditions. Although it has been decades of effort exploring the potential of geospatial data for consistent mapping and characterizing of slums, one fundamental question remains unanswered: How much can we tell about the divergent living conditions of human settlements from their physical forms? There is only a handful of studies that either investigated only very basic physical characteristics, such as size and distribution of slums, or focused only on sample slum areas across several cities. We believe that building a thorough understanding of the urban divide in terms of the physical forms in cities must simultaneously: satisfy (1) large scale comparisons of *within-slum* morphology across cities, given (2) the characterization of the overall morphological context of each of the cities, while using (3) consistent and preferably interpretable morphological metrics. These criteria mark the major challenges of both techniques and the scale of this study.

Methodology

We take the challenges by measuring many detailed, interpretable and consistent urban morphological metrics regarding the configuration of building footprint in several major sub-Saharan African cities. Such a substantial amount of computation leads to a morphological comparison of deprivation across cities while not ignoring the urban divide within the context of each city. Hence, we have a chance to see the varying morphological characteristics of slums across cities, while such morphological manifestation can potentially be hidden or brought out by the local morphological context in each city. All technical components, including algorithms and computation, are implemented in open geospatial tools and computing environments. The data are derived from multisource very high resolution remote sensing imagery, and provided by the Google AI Open Buildings datasets (https://sites.research.google/open-buildings/). More specifically, we compute nearly a hundred of morphological indices in terms of building footprint configuration, and test if unsupervised clustering algorithms can automatically bring morphologically varying deprived areas out of their local urban contexts.

Results

Our preliminary finding shows that there is shared urban morphology across these sub-Saharan African cities, while such morphology can or cannot stand out from the local urban morphological context. Figure 1 presents a sample of several large cities, we have been experimenting with, where many deprived areas are with varying urban morphology in terms of building footprint configuration. However, once put in the local urban morphological context, due to the contrasting morphological divide, these deprived areas are more or less highlighted (in dark yellow and red tone) as distinctively different types of building forms.

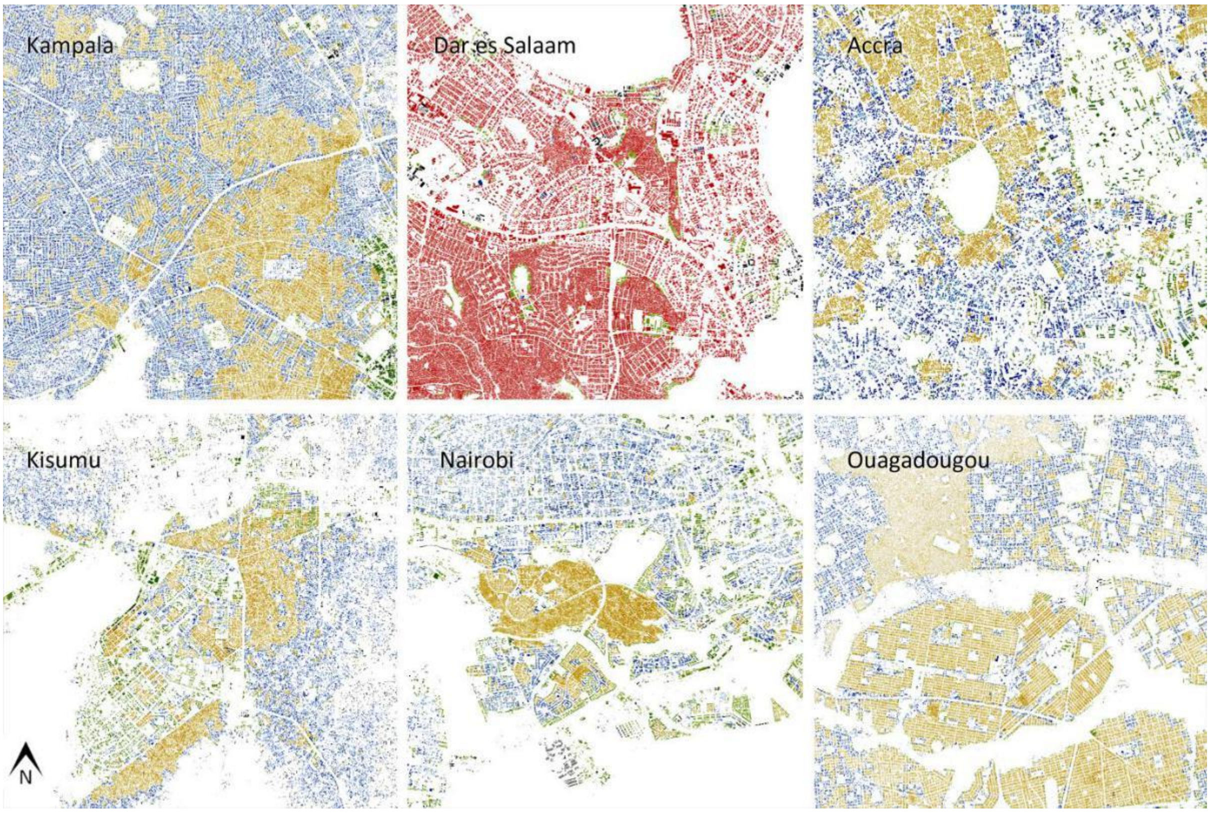

Figure 1 Sample areas from large African cities showing varying urban morphology of deprived areas across cities, yet similarly stand out from local urban morphological context as highlighted by dark yellow and red.

Outlook for the future

Given the preliminary finding, it is worth continuing such type of research by further exploring

(1) consistent morphological characters at a level as detailed as buildings, as well as other urban elements, such as streets and open spaces, and (2) measurements of the separability that characterize physical manifestation of urban divide and deprivation.

IDeaMapSudan: Mapping Urban Deprivation in Khartoum combining EO and Geospatial Data

Monika Kuffer[1] , Nuha Eltinay[2] , Maysoon Badi[2] , Wafa Sakhi[2] , Inas M.M. Ali[3] , Asgad Gummah[4] , Julia Kumi[4] , Ibrahim Kushieb[4] , Mosub Abdallah[6] , Taha Elzaki[5] , Mustafa Hamza[6] , Fatima Ahmed5 , Marwa Ali[6] , Jon Wang[1] , Caroline Margaux Gevaert[1] , Charlotte Flasse[7] , Andre Da Silva Mano[1] , Serkan Girgin[1] , Francis Cheruiyot Onyambu[8] , Dana Thomson[1] , Caroline Kabaria[8]

[1]Faculty ITC, University of Twente, The Netherlands

[2]Sudan Urban Development Think Tank Organization, Sudan

[3]Independent consultant, Sudan,

[4]Ministry of Social Development, Sudan

[5]Ministry of Transport, Sudan

[6]Ministry of Physical Planning-Khartoum State, Sudan

[7]Université Libre de Bruxelles, Belgium

[8]African Population & Health Research Center, Kenya

Keywords (5): urban deprivation, poverty, displacement, Khartoum, information system

The challenge

Khartoum (Sudan) is one of the fast-growing urban centres in Africa, with an annual growth rate of 2.5% (population) and 2.2% (built-up area), according to the urban centre database. Presently, Khartoum has over 8 million inhabitants. Its rapid growth is driven by displacements (IDPs) and climate change, besides natural growth. With the lack of sustainable planning strategies, the city is characterized by the stark contrast between planned areas and informal developments. However, data that can contribute to the development of planning strategies are not available. In response, IDeaMapSudan was launched in 2020, training local experts (NGOs and Government) and building a spatial information system on urban deprivation, which is co-designed with local experts. The spatial information is built on the IDEAMAPS Domains of Deprivation Framework (Abascal et al., 2022). We present the design and first results of IDeaMapSudan that combines Earth Observation (EO), local data and open Geospatial data.

Methodology

IDeaMapSudan is co-developing together with local experts and international EO and Geospatial experts, to bridge local data gaps. It combines local data that are scattered in different organizations and are largely inaccessible with EO and Geospatial data. Major steps towards the development of IDeaMapSudan are (1) the analysis of information gaps and information needs, (2) a review of available datasets, (3) the training of EO and Geospatial skills of local experts, (4) the design of IDeaMapSudan, (5) the modelling of EO and Geo-spatial data that allow mapping deprivation in Khartoum and (6) local dissemination of IDEMAPSUDAN. IDeaMapSudan combines EO and Geospatial within a 100 by 100 m gridded deprivation modelling framework. This gridded framework compiles relevant indicators within six deprivation domains which have been defined based on the IDEAMAPS framework within two large expert workshops in Khartoum. IDeaMapSudan is built on open and freely available EO data and opensource solutions, to support the long-term sustainability of the system. Ultimately, IDeaMapSudan will support routine updates of Geo-spatial data, access to relevant community-based Geospatial information, local data sharing and communication in support of urban planning and decision-making processes.

Results

IDeAMapSudan is built within the cloud-based data infrastructure of the Geospatial Computing Platform (CRIB at ITC) that allows combining a massive amount of deprivation indicators. IDeAMapSudan is built on the principles of sustainability, openness and FAIR data principles. The individual deprivation indicators have been harmonized and put into a gridded model at a 100 by 100 m cell size. Within our defined urban extent of Khartoum, which combines the contiguous built-up and administrative urban extents, individual deprivation indicators are available, as well as combined domain indices. Various environmental dimensions are supported by EO data (e.g., vegetation densities, air pollution, heat exposure). EO data play an essential role in a data-poor environment to compensate for missing ground-based measurements (e.g., air pollution). Furthermore, EO-based indicators (e.g., built-up densities, vegetation cover, open spaces) offer proxies of socio-economic conditions. Thus the first prototype of IDeAMapSudan supports displaying deprivation indicators (e.g., air pollution extracted from Sentinel-5P) and combined deprivation domain indices (e.g., environmental contamination)(Figure 1).

Results

Displayed in Figure 1 show service and infrastructure, environmental contamination and social hazards deprivation domain indices, ranging from 0 (least deprived) to 1 (most deprived) areas. Central areas in Khartoum show high contamination index values that also include many informal areas. In contrast, service and infrastructure and social hazards show high deprivation values in the outskirts, which are dominated by (former) IDP camps. Outlook for the future IDeAMapSudan aims to fill local data gaps, supports urban policy formulation and is addressing several of the SDGs (e.g., SDGs 1 and 11). The next steps will be the construction of overall deprivation models, local validation and dissemination. Further training activities will focus on a larger group of staff of different ministries, NGOs, community-based organizations (CBOs) and local academics to effectively use IDeAMapSudan and its model outputs.

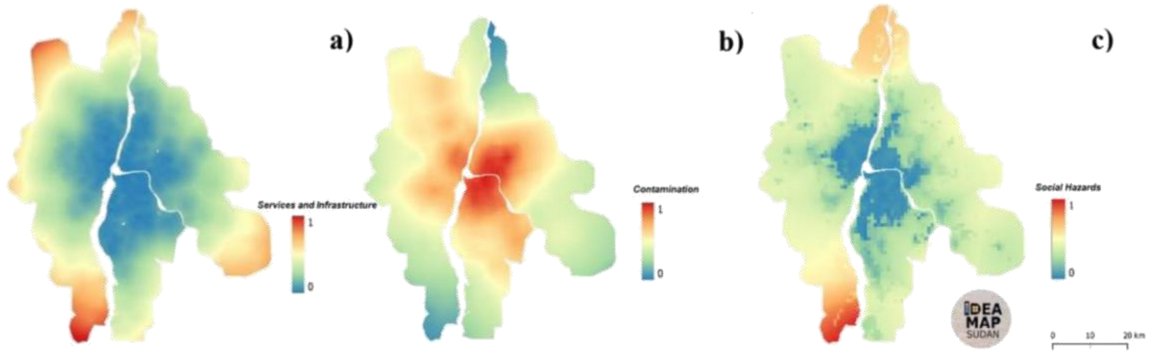

Figure1 Khartoum State Deprivation Maps (a) public services, (b)environmental contamination and (c)social hazards (by the authors).

Leveraging community-generated data in research: The KnowYourCity Campaign data set by Slum Dwellers International

Dana R. Thomson[1] , Hazem Mahmoud[2], Forrest R. Stevens[3], Robert Chen[4], Argyro Kavvada[5], Andrea Gaughan[3]

[1]University of Twente, Faculty of Geo-Information Science & Earth Observation, Netherlands

[2]University of Texas at San Antonio, Department of Geological Sciences, USA

[3] University of Louisville, Department of Geography and Geosciences, USA

[4] Columbia University, Center for International Earth Science Information Network, USA

[5] National Aeronautics and Space Administration, Earth Sciences Division, USA

Keywords (5): slum, informal settlement, deprived area, open data, citizen science

The challenge

90% of population growth in the next 25 years will be in African and Asian cities, and most people will be added in deprived "slum" areas. Due to informality, dynamism, and insecurity, data on "slums" and their residents are incomplete and dispersed, at best. Many "slums" are simply missing from official (e.g., census, survey) and other widely used datasets (e.g., OSM). Satellite imagery is often used to fill this data gap with "slums" being identified as clusters of small disorganized buildings and other morphologies of informality. Who generates these data, however, matters because deprivation manifests in myriad of ways within and between cities. Whether training AI models, evaluating the accuracy of modelled data sets, identifying areas at risk of hazards, etcetera, data about "slums" by residents themselves reflect important contextual variations. We present the KnowYourCity (KYC) Campaign dataset by Slum Dwellers International (SDI) and demonstrate its use for research.

Methodology

SDI is a global network of community-based organizations (CBOs) founded by the urban poor more than 25 years ago to ensure that "slums" are integrated into cities, and that their residents enjoy basic human rights. A key activity among SDI-affiliated CBOs is to map their own settlement boundaries and collect key infrastructure and population data using mapping, survey, and community engagement methods. In 2016, SDI launched the KYC Campaign website (https://sdinet.org) where thousands of CBOs have since submitted standardized community profiles with: settlement boundaries; population counts; status (e.g., illegal); number of water taps, toilets, and other key infrastructure; common diseases; health care access; and commercial facilities. The website intends to strengthen the network among CBOs, provide visibility to systematic issues that affect the urban poor, engage city governments, and showcase the work of community-based data collectors, most of whom volunteer their time and expertise. While KYC settlement profiles are open, they are not cleaned, documented, and compiled into an easily downloadable format, making them challenging to use in research. We applied a web-scraping algorithm to gather settlement profiles from the KYC website (as of Dec 2021) into a single shapefile, and applied a data cleaning procedure to ensure boundaries only included built-up areas (e.g., not water bodies) and dropped records with unrealistic population counts. 2

Results

SDI has profiled more than 7700 "slum" settlements in 224 cities across Africa, Asia, and Latin America. We reviewed and cleaned settlement boundaries and population counts in 15 African and Asian cities which had at least a dozen profiled "slum" settlements. After cleaning, 12 cities had at least a dozen settlements remaining: Ghana: Accra (41). Kenya: Athiriver (12), Kisumu (25), Nairobi (63). Nigeria: Lagos (32), Port Harcourt (39). Philippines: Davao (24), Malabon (26). Sierra Leone: Freetown (21). South Africa: Cape Town (34). Tanzania: Dar Es Salaam (93). Uganda: Kampala (31). Data cleaning involved visual inspection of each settlement boundary over satellite imagery from the same year as data collection, and modifying some boundaries slightly to follow the edges of built-up areas. We further identified outliers in terms of population total and density, and assessed whether the reported population counts were plausible given approximate counts of buildings. Settlements without boundaries or non-plausible population values were excluded. We documented our data cleaning procedure along with SDI's data collection practices, and share the dataset on GitHub. We also provide guidance about how to attribute the dataset to SDI members, and recommend ways to engage with SDI directly regarding use of their data. We then demonstrate application of KYC data to assess the accuracy of publicly available modelled gridded population datasets in "slums".

Outlook for the future

Given gross inaccuracies about "slum" populations in existing official datasets, and problematic assumptions about what is a "slum" when mapped by non-residents, KYC data is a rich source of information for research. Residents of "slums" are uniquely positioned to collect the most accurate information about local population and conditions. However, unlike other open data initiative, KYC does not exist for the purpose of being a public good and thus needs to be treated thoughtfully. In addition to attributing SDI affiliates for their work, researchers should consider offering financial, training, or similar compensation in exchange for use of these data. Not doing so can be viewed as exploitive (i.e., paid researchers gaining funding and accolades with data they did not collect while the data collectors were unpaid and struggle to meet basic needs). Additionally, communicating research results/outputs to SDIaffiliates means local data collectors are seen and valued for their work.

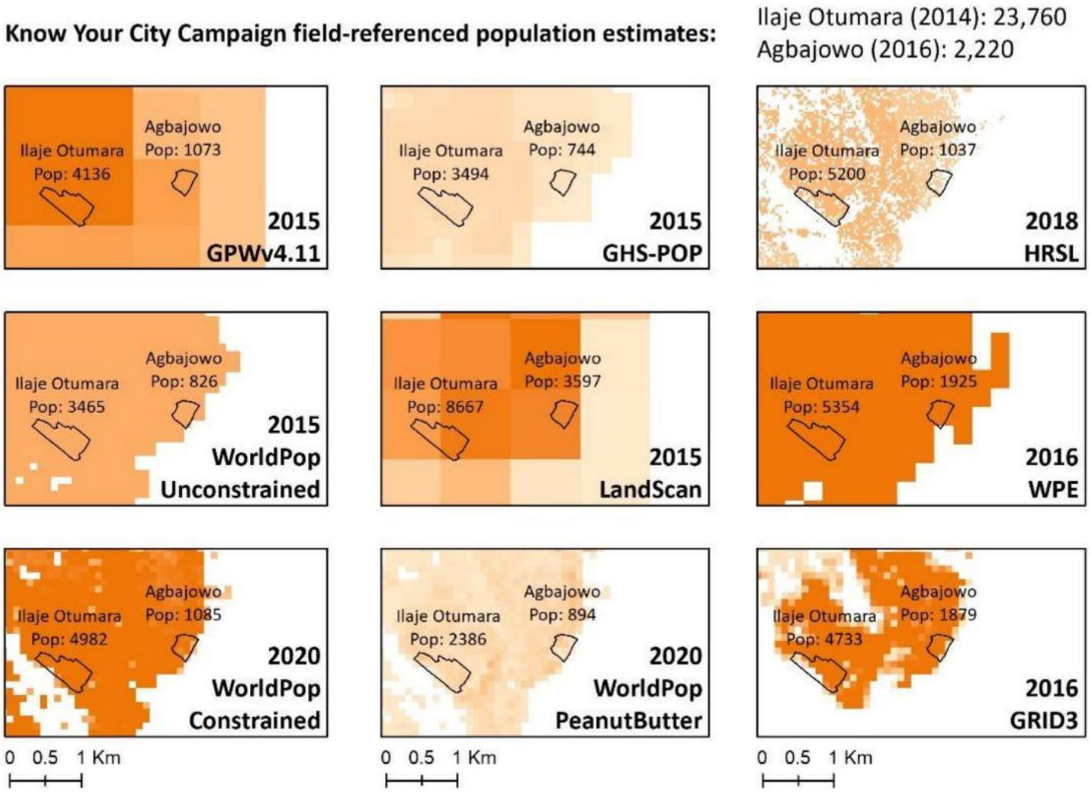

Figure Example application of KnowYourCity Campaign community-generated "slum" maps and field population counts used to evaluate the accuracy of various gridded population estimates

Finding biases in geospatial datasets in the global south – are we missing vulnerable populations?

Caroline M. Gevaert[1]

[1] University of Twente, Faculty ITC, Department of Earth Observation Science, the Netherlands

Keywords (5): machine learning, bias, ethics, building detection, humanitarian aid

The challenge

Unintended biases regarding gender and race have been observed in artificial intelligence algorithms used for image recognition, credit scoring, and criminal recidivism. It is logical that such biases are also present in algorithms utilized for disaster response or humanitarian aid – and yet there is very little knowledge on how this is manifested in practical applications. For example, what if AI algorithms delineating buildings actually perform worse in informal areas of a city than formal areas? And what if the results of this algorithm are used to distribute aid after a flooding event? We will actually be missing the people who need it most.

This submission investigates biases in global datasets of building outlines. It links the literature from ethical AI with applications in the geospatial domain. It is very relevant for Global South applications where the lack of local data often causes GIS experts to turn to global datasets – which may not always have been trained or validated with local data. For example, Figure 1 below compares local data of building outlines mapped through community mapping campaigns with building outlines generated by an AI algorithm.

Methodology

The work considers three large open datasets of building outlines: Open Street Map (a community-generated dataset), Google Open Buildings, and Microsoft's building footprints of Tanzania and Uganda. Different study areas are selected for both Tanzania and Uganda representing both formal and informal areas. Each tile is visually inspected to analyze the accuracy of the building outlines.

Next, the Aequitas Bias and Fairness Audit Toolkit is utilized to examine the three datasets for possible biases. More specifically, it compares the False Positive and False Negative rates for the building outlines for specific "sensitive groups" in the three datasets. In this case, the sensitive groups are the country and whether it comes from a formal or informal area. The relative difference between the False Positive and False Negative rates, also known as the False Positive Rate Disparity and False Negative Rate Disparity, indicates whether there is a significant difference between the accuracy metrics for the two groups. In this case, differences of maximum 20% are considered fair. If the difference between the two groups is larger, then we consider there to be a bias in the dataset.

Results

Preliminary results indicate that the False Positive Rate Disparity and False Negative Rate Disparity for neighbourhoods displaying informal settlement-like characteristics is much higher than that of more formal-appearing areas of cities in Tanzania and Uganda. There are no significant differences in the error rates for Tanzania versus Uganda, so there is no country-based bias in the datasets. The False Positive Rate is higher for the Microsoft dataset, whereas the False Negative Rate is higher for the Google Open Buildings dataset.

If this submission is accepted for the EARSeL event, the results will be finalized before the presentation and presented in a rigorous fashion.

Outlook for the future

Ethical concerns of the utilization of AI algorithms are growing in many domains, and we can expect to face similar concerns in the geospatial domain in the future. The emergence of regulatory frameworks such as the UNESCO Recommendations for Artificial Intelligence and the EU Artificial Intelligence Act support this. Especially when utilizing large-scale datasets for development, humanitarian, or disaster risk management applications, it is critical to understand where possible biases are and whether specific population groups are systematically underrepresented. This is particularly important when using datasets developed in the Global North for applications in the Global South.

In the geospatial domain, we must get a better understanding of what types of biases we face in the datasets, so we can also help develop better auditing mechanisms – and ultimately help end users understand potential weaknesses in the datasets they are using and avoid discriminating against certain cultural groups.

(a) (b)

Figure 1 Example of building outlines generated by community mapping campaigns (a) and an open dataset of AI-generated building outlines (b)

SkySat – Geometry and Effective Resolution

Karsten Jacobsen

Leibniz University Hannover, Germany

Keywords: SkySat, Geometry, Satellite orientation, Accuracy, Resolution, Economics

The challenge

Very high-resolution space imagery, with a ground sampling distance (GSD) up to 1m now competes with aerial imagery for mapping purposes. A cheaper possibility rose with the microsatellites SkySat, BlackSky and Nu-Sat. These less expensive satellites have some limited functions as lower direct sensor orientation accuracy and a small swath width. The swath width is partially compensated by the higher number of satellites. The usability of SkySat images was analyzed for a project to check the completeness of buildings in cadastral maps. SkySat-1 was launched in 2013 and -2 in 2014, both at 600km orbital altitude, SkySat 3 – 15 launched from 2016 to 2018 at 500km orbital altitude, which was reduced to 450km in 2020, and SkySat-16 – 21 were launched in 2020 for 400km altitude. The physical GSD for SkySat 3 – 15 today is 0.81m and for 16 – 21 0.72m. The Basic Panchromatic images for 3 – 15 come with 0.65m and the Collect orthoimages of the 3 CMOS sensors with 0.5m GSD. It has to be checked whether the reduced GSD is justified or not and whether the geometric potential is better than the required RMSE of at least 4m.

Methodology and Results

The methodology of analyzing and handling of space imagery is directly affected by the results, leading to a loop of the methodology and the results.

SkySat images are taken with 30 Hz, which can be used for videos but also for image sharpening. The effective resolution was checked using edge analysis. The differentiation of the average grey value response across the edge of a sudden change from dark to bright leads to the edge spread function. The width of this function at the turning tangent is the double normalized factor for the effective resolution. The nominal GSD multiplied by the factor for effective resolution gives the effective GSD. SkySat Basic Panchromatic and the multispectral Basic Analytic were analyzed using a sequence of images with different angles of incidence. For the Basic Panchromatic images, the effective resolution corresponds to the pixel size of the enhanced 5.2µm. The Basic Analytical supplied with a geometric pixel size of 6.5µm have a slightly larger effective pixel size of 7µm. In both cases this is independent of the angle of incidence, since the Basic images correspond to the original images.

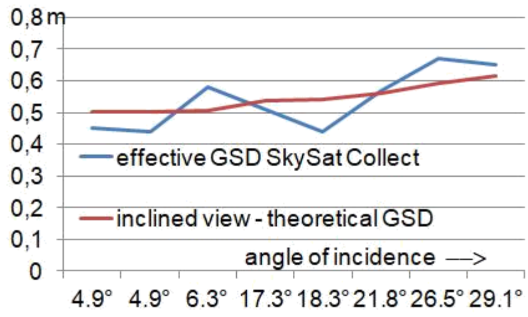

Figure 1: Effective GSD of SkySat Collect orthoimages as a function of angle of incidence and the average GSD of 0.5m at nadir

For SkySat Collect orthoimages, the nominal GSD does not depend on the angle of incidence. Nevertheless, the image quality depends on what is clear in Figure 1. Up to an angle of incidence of 20°, the effective resolution is in the range of +/-10% of 0.5m GSD, exceeding it for larger incidence.

Planet orients the Basic images in relation to available reference orthoimages and generates SkySat Collect orthoimages with 0.5m GSD from the orthoimages of the 3 CMOS arrays and a selectable number of images in the direction of flight, paying attention to misfits of neighbouring images.

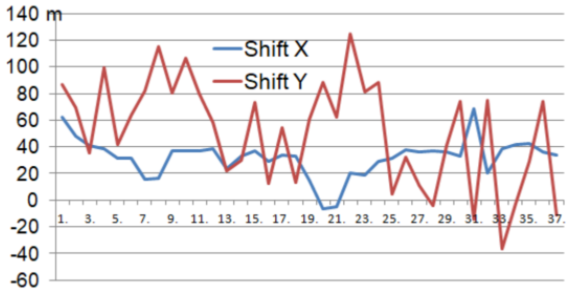

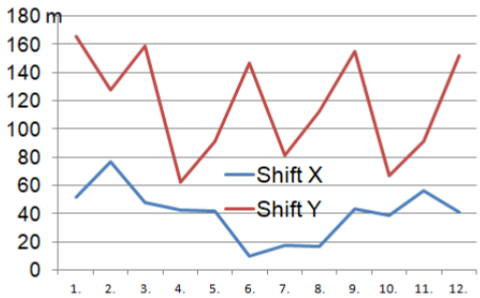

Figure 2: Shifts in RPC-orientations versus ground control left: for Basic Analytic right for Basic Panchromatic

For checking purposes, some Basic images were oriented using manually measured ground control points. The shifts determined by bias-corrected RPC-orientation can be seen in Figure2. The strong and rapid changes in flight direction are obvious. The images from the 3 CMOS sensors are not captured simultaneously and due to the changing orientation it is not possible to calibrate the relation of the 3 corresponding images from the CMOS arrays. Orientation by resection, also using 6 unknowns as the bias-corrected RPC-orientation, yielded similar results. The image residuals showed no systematic errors.

An examination of SkySat Collect orthoimages against an aerial orthoimage yielded satisfactory results well below the required RMSE of 4m when the used Basic images were recorded with an angle of incidence below 20°. The results could not been accepted for larger angles of incidence.

Outlook for the future

It has been shown that the completeness check of buildings in cadastral maps is possible with SkySat images if the images used were taken with an angle of incidence of less than 20°. Up to this limit, the effective resolution and the accuracy are satisfactory. The Basic images cover only 2074m x 875m in nadir view. An individual orientation of the Basic images is required. This is not economical when measuring manually, for this reason Planet has developed an automatic process. Also the handling of such small images is too time consuming and requires the use of SkySat Collect orthoimages. SkySat images are sold at a lower price per area covered than large format satellite imagery of the same resolution. The disadvantage of the swath width of SkySat Collect images of 5780m in nadir view is compensated by the higher number of SkySat satellites, making it an economical solution to use for the related project.

Garbage in/Garbage out: Understanding Cities Through a Geospatial Analysis of Waste Management Processes

Isaac Oluoch[1], Monika Kuffer[2], Michael Nagenborg[1], Kevin Pijpers[3], Dana R. Thomson[2], Stefanos Georganos[4], Angela Abascal[5], Sabine Vanhuysse[6], Nicera Wanjiru[7], Eric Rovoga[7]

[1]University of Twente, Department of Philosophy, Netherlands

[2]University of Twente, Department of Urban and Regional Planning and Geo-information Management, Netherlands

[3]University of Twente, Department of Psychology, Health and Technology, Netherlands

[4]Division of Geoinformatics, Royal Institute of Technology, Sweden

[5]School of Architecture, University of Navarra, Spain

[6]Department of Geosciences, Environment and Society, Université libre de Bruxelles (ULB), Belgium

[7]Community Mappers, Kenya

The challenge

We present a comparative geospatial analysis of waste management processes and their effect on citizen inclusion and participation in the cities of Nairobi and Rotterdam. The Nairobi study focuses on mapping deprived areas (i.e. ‘slums’) and locations of waste piles, by community members assisted with Earth Observation (EO) tools. And we show that while EO is used to assist communities, it can remain exclusionary to non-experts whose local knowledge is essential. The Rotterdam study analyzes the production of spaces of waste, and growing reliance on algorithmic interventions in public waste management. But we observe these increasingly data-driven waste management processes alienate citizens from policy involvement and technological understanding. Thus, in this paper we will: i) assess the role and impact of EO and AI on waste management in these two cities; ii) assess the dynamics that produce accumulations of waste and reveal those accountable for it.

Methodology

While waste management is a well known problem in low- and middle-income countries, high-income countries face their own challenges, especially regarding citizen inclusion. For Nairobi, we focus on the synergistic potential of community-driven research for advocacy to also improve EO modeling initiatives (e.g., to use local data to train city scale mapping algorithms). Using their own smartphones, community members mapped point locations of all waste piles present in Mathare, Majengo, Kariobangi and Kibera in August 2021, which they visualized and presented to the Nairobi County Government in attempts to improve the formal waste collection system. Funding and survey/mapping training was provided by members of the IDEAMAPS and SLUMAP research projects.. In Rotterdam, we provide an organizational ethnography of waste mapping practices comparing former citizen participation processes to produce official maps of waste accumulation in the city versus new image recognition technologies to map the presence and flows of waste in the city. We compare and contrast these 'community-first' versus 'technology-first' approaches, and discuss the dynamics in both cities in the acquisition and use of spatial data for waste management.

Results

The Nairobi study produced three important initial findings. Firstly, studying the morphology of waste in four deprived neighborhoods revealed the concentration of large waste piles along drainage systems and at larger roads[3]. Second, the data became a valuable bridge to initiate dialogue between community members and municipal authorities involved in waste management of these neighborhoods, and was rendered more valid in the eyes of authorities by the collaboration with external research teams. Thirdly, the data became a point of reference for holding these authorities (along with private waste collectors) accountable for managing the waste by geospatially representing how underserviced they are. In Rotterdam, we observe the ambiguous effects of using geovisualization and algorithmic technologies in place of community-based data collection. Whereby the smart city technologies used to collect data and more transparent visualizations of waste increased the political legitimacy of waste maps, the amount of waste has not decreased in part due to community disengagement and disempowerment. While image recognition technologies were intended to create 'operational convergence' (e.g., combining the cleaning of waste *and* policing of polluters in a singular workflow), the study of Rotterdam reveals that waste is not so much 'managed', as instead algorithms become active agents in networks of city cleaners, trash bins, and cameras in urban spaces.

Outlook for the future

Urban waste poses enormous environmental and health challenges in many deprived communities of Nairobi, and the lack of reliable geospatial information exaggerates the issue

3 For details on the community-based data collection: https://www.youtube.com/watch?v=dlvZ0UTw2Ho

as it furthers ignorance of the conditions these communities face. Such information in the hands of communities can be a useful negotiating tool, to aid developing innovative community-based interventions.

Similarly, waste is one of the biggest problems citizens of Rotterdam face, with waste management ranking highly on the list of political agendas. This has meant a push for data-driven and algorithmic solutions, but whether these ambitions can meet (and resolve) citizen concerns, is something we must pay attention to.

While contextually the Nairobi study and Rotterdam study are quite different, both studies point towards the awareness that using geospatial technologies to resolve the challenges of urban waste, requires a renegotiation of the relationship between researchers, municipalities and citizens.

Figure 1. Combining Earth-Observation Mapping with Community-Based Data Collection (Source: SLUMAP, 2022).

WSDC_SDGs: Developing Countries: SDGs urban sustainability, demographic and health modelling

Chair(s): Dr. Dana Renee Thomson and Sabine Vanhuysse

Vector-borne disease risk mapping in sub-Saharan African cities: challenges and opportunities

Catherine Linard[1], Camille Morlighem[1]

[1]University of Namur, Department of Geography, Belgium

Keywords (5): urban malaria; sub-Saharan Africa; DHS; random forest modelling; risk maps

The challenge

Sub-Saharan Africa is facing a rapid and uncontrolled urbanization process, with significant impacts on the health and well-being of urban dwellers. To mitigate such impacts, and advance towards SDG 11 “Make cities and human settlements inclusive, safe, resilient and sustainable”, (i) more spatially-detailed and quantitative data are necessary to identify the most vulnerable and (ii) such information must be accessible and useful to policymakers. Taking *Plasmodium falciparum* (*Pf*) malaria – a vector-borne disease impacted by these rapid environmental changes – as an example, this presentation will synthetize and discuss the opportunities offered by EO to better identify intra-urban high-risk areas and the remaining challenges for an effective use of risk maps by decision-makers. A better identification of infectious disease high-risk areas can help decision-makers to better target interventions to the most in need, which is especially important in resource-limited countries.

Methodology

EO now offers a large panel of data that have the potential to greatly improve and refine intra-urban malaria risk maps by combining environmental factors expected to create suitable habitats for the vector and socio-economic data expected to influence the vulnerability of people to the hazard. Intra-urban malaria risk was here predicted across four African cities (Dakar, Dar es Salaam, Kampala and Ouagadougou) using random forest models based on satellite-derived environmental (including climatic), land cover, land use and socioeconomic factors. As dependent variable, we used the *Pf* Parasite Rate standardized to the 2 to 10 age range ($Pf\mathrm{PR}_{2\text{-}10}$), an indicator routinely collected by standardized surveys such as the Demographic and Health Surveys (DHS). For ethical reasons, these surveys impose a random spatial displacement of data point coordinates within a 2 km radius, which may hinder their use at the intra-urban scale. In this research, we tested the ability of two spatial optimization methods to overcome the effect of DHS point displacement. Methods consist at (i) enriching the dataset by duplicating data points in surrounding locations or (ii) refining the dataset by randomly selecting duplicated data points. The predictive performance of different models based on various EO datasets and using different spatial optimization methods were compared for the four cities.

Results

Results show that a combination of factors derived from different remote sensors provided the best results, and more specifically models including climatic, land cover and land use predictors. Predictive maps suggest that malaria risk either follows an increasing trend from the city centre to the peri-urban areas or develops as urban hotspots when specific climatic conditions or LCLU classes are found (e.g. high land surface temperature, dense informal settlements). The figure shows examples of predicted maps obtained for Dar es Salaam and Kampala. Our results also show that spatial optimization methods allow to mitigate to some extent the inaccuracies induced by the DHS cluster displacements.

Beyond these risk modelling results, our work highlights the complexity of urban malaria and the quantity and quality issues associated with survey-based malaria data that limit their representativeness and comparability. Building on our results, we propose a list of recommendations to revise the DHS sampling strategy to make it an even more valuable tool to study and map intra-urban malaria risk.

Outlook for the future

Our research highlights the remaining challenges associated with urban malaria mapping and bottlenecks that need to be tackled for a more efficient use of EO for disease risk mapping in the Global South. First, our models require the processing of multi-source and large datasets, which is resource-demanding and therefore limit their potential for wide application. Second, while huge improvements have been made over the last decades in terms of remote sensing data acquisition and processing, the quantity and quality of epidemiological data are not yet sufficient to take full advantage of these improvements. Third, continued efforts must be done to bridge the gap between fundamental research results and local impact. Here, particular attention was given to the open access of data and methods, and to the automation of processes in order to facilitate their transferability and generalization. This is however not yet sufficient for an effective use of disease risk maps for better targeting health interventions. Future work should focus on improving collaboration and knowledge transfer between researchers and stakeholders.

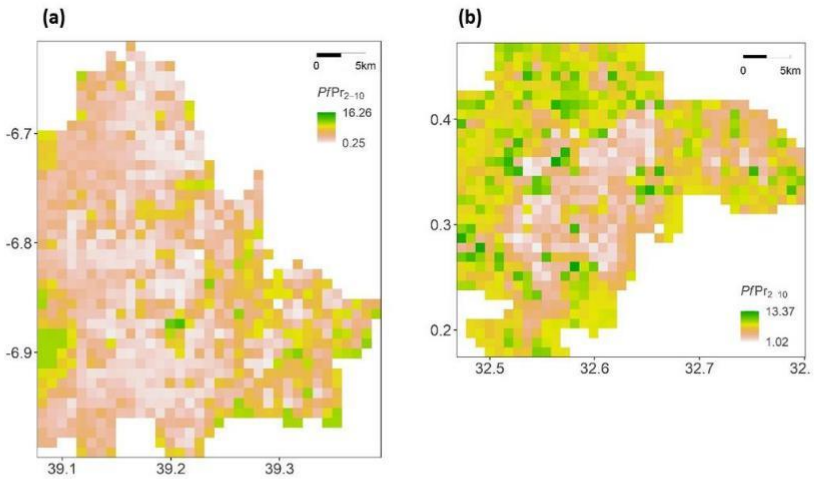

Figure Predicted *Pf*PR$_{2-10}$ at 1km resolution for (a) Dar es Salaam (Tanzania) and (b) Kampala (Uganda)

Making urban slum population visible: An Earth-Observation based approach

Jorge Klinnert[1], Angela Abascal[1*], Stefanos Georganos[2], Sabine Vanhuysse[3], Monika Kuffer[4], Eleonore Wolff[3]

[1]University of Navarra, Navarra centre for international development, Spain (jjorgeklinn@alumni.unav.es, maabascal@unav.es)
[2]Division of Geoinformatics, KTH Royal Institute of Technology, Sweden(stegeo@kth.se)
[3] Université libre de Bruxelles (ULB), Department of Geosciences, Environment & Society, Belgium (sabine.vanhuysse@ulb.be, eleonore.wolff@ulb.be)
[4]University of Twente, Faculty of Geo-information Science and Earth Observation, Netherlands (m.kuffer@utwente.nl)

Keywords (5): Population; Slums; Census; Earth-Observation; Machine Learning

The challenge

Sub-Saharan African cities' population has been growing rapidly since the 1960s-1970s wave of independence, reaching an average growth of 4.1% per annum since then. The capital cities have the highest population densities, and in general, the highest population growth rates. For instance, Nairobi, the capital city of Kenya, exhibits an annual growth rate of 3.8% and is home to 4,3 million people (Kenya Bureau of Statistics). As a consequence, many urban residents end up living in unplanned areas, referred to as slums, under deprived conditions. One of the observed phenomena, that concern most urban residents in such areas, is **extreme household crowding**. To date, according to official sources, 56 % of the urban population of Kenya is living in slums, reaching up to 75 % in the case of Nairobi. This proportion of the population resides in only 6 % of the total area of the city. These areas are characterised by sub-standard provision of services, lack of open space, and **high building density**. Therefore, deprivation is compounded by both high urban density and high household crowding. Our hypothesis is that bottom-up Earth Observation (EO) methods can be leveraged to improve slum population estimations provided by censuses and existing open gridded population datasets.

Methodology

It has been demonstrated that top-down approaches to distributing spatial patterns of population vastly underestimate the slum population. To address this issue, we build statistical models between the in-situ surveys within the slum areas and EO-based features, e.g., land cover and building footprints geospatial layers. Such a bottom-up approach is typically more accurate in cases where top-down models based on census data might be unreliable – which is the case for urban slums.

To develop the bottom-up slum population models, we use commonly employed statistical and machine learning approaches. We rely on the assumption that households living in similar physical housing conditions have similar demographic characteristics, and therefore, in similar urban morphologies, we estimate the same population density. We use household survey data collected by slum dwellers themselves in five of the major Nairobi slums. The survey consists of two data collection steps: a plot observation in which the number of households is counted, and individual household surveys. The population estimate is more complete, as many households could not be reached. Residents do not have stable jobs and their hours of rest are unpredictable. The geo-data surveys is collected through a mobile application designed for this research.

After collection, the data is cleaned, and gaps are filled. The data is used to calibrate and validate our model considering state-of-the-art spatial aggregation methods. Finally, we compare the predicted population distribution with the most recent census data, whereas censuses are known to underestimate slum population densities; with open gridded population datasets (e.g., World Pop and GSL-Pop); and with self-report slum estimates from local sources (e.g., Slum Dwellers International NGO). Resulting in an assessment of the statistical accuracy of open population data sources in slums.

Results

Slum population density is predicted across all urban slums within the city of Nairobi. We evaluate the results both by visual inspection but also by validating our predictions against a set of surveys left out of the training stage. For the validation locations, we extract performance indicators such as Root Mean Square Error, Mean Absolute Error. The comparison with updated censuses, existing gridded datasets and local sources highlights the need to produce reliable population datasets to have a more reliable and complete understanding of the urban population (including slums).

Outlook for the future

To reduce urban poverty, including upgrading, planning and service provision, it is necessary to improve statistics on the total population within cities. For this purpose, the extent, nature, and location of slums are needed. Making the population of urban slums visible will help design suitable urban policies, such as the provision of local services. Our work will provide insights as to how urban population models should tackle slum areas, as there is currently a lack of ad hoc approaches. The knowledge gained will contribute to a better understanding of the evolution of sub-Saharan African cities, enhancing evidence-based policy making and sustainable urban growth.

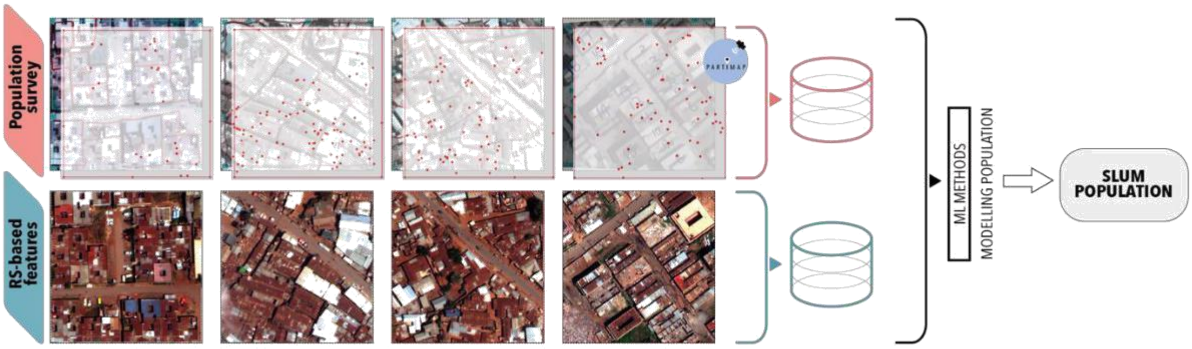

Spatial and temporal urban population distribution mapping in Sub-Saharan African cities using Earth Observation and deep learning

Stefanos Georganos[1], Sebastian Hafner[1], Theodomir Mugiraneza[2], Yifang Ban[1]

[1] Division of Geoinformatics, KTH Royal Institute of Technology, Sweden

[2] University of Rwanda, Centre for GIS and Remote Sensing, Rwanda

Keywords (5): Deep Learning, Population Mapping, Earth Observation, Urban Sustainability

The challenge

Spatially detailed population distribution information are vital indicators to enhance evidence-based policy making and promote sustainable development initiatives. Typically, fine-grained population distribution maps are produced by disaggregating census data. However, in many countries of the Global South and particularly in Sub-Saharan Africa (SSA), census information is spatially and temporally restricted (i.e., dates between two censuses for the same area can exceed the usual decadal period or available population data are found ta very coarse spatial resolution). As shown in Figure 1, in many SSA countries census information is heavily outdated. Indeed, in some cases a larger than 15 years gap is observed since a census took place. Even when census information is measured at regular decadal intervals, intermittent population estimates (such as at 5 years) are necessary as SSA faces very high and often uncontrollable degrees of urbanization. As such, it is imperative to be able to retrieve both spatially and temporally accurate population estimates to facilitate the sustainable future of these regions.

Methodology

To achieve our objectives, we propose an end-to-end framework relying on publicly available Earth Observation data (Sentinel-2 imagery) and deep learning (DL). As a proof of concept, we apply our idea in various SSA cities, such as Dar Es Salaam (Tanzania,) Dakar (Senegal), Nairobi (Kenya) and Kigali (Rwanda). We first develop a DL-based model that takes as input

Sentinel-2 imagery, coupled with the population estimates. Afterwards, we predict and validate temporally and spatially. For the former, we predict in intermittent census dates, in the cities where such information is available (i.e., Kigali), allowing us to assess if DL-EO models can capture the increasing/decreasing trend of population change in short temporal scales. For the latter (spatial transferability), we train our models in a single city, and attempt to transfer it and predict population in other urban areas where no local training data are used. To enhance the potential of this experiment we assess the potential of building footprint data as an additional input with EO information. The general DL architecture is based on ResNet-18. It contains 17 convolutional layers with 3x3 kernels, followed by an average pooling layer. The network is partitioned into four blocks, each consisting of four convolutional layers. Starting with 64, the number of filters is doubled at the first layer of each consecutive block, while the size of the feature map is halved. The network involves residual connections that are used to mitigate the vanishing gradient problem during the training stage.

Results

We use a spatial resolution of 100 meters and aggregate our predictions at the census level to retrieve performance indicators (Mean Absolute Error, Coefficient of Determination and Root Mean Squared Error). Upon the positive results of the validation experiments, we will apply our method in each year and city from 2014 to 2022 and assess the population growth in a detailed fashion, both temporally and spatially. We will compare our results with existing global population products such as WorldPop and GHSPOP and discuss the benefits and limitations of our proposed method.

Outlook for the future

The outcomes of this work are pertinent to the next generation of population products, as they require minimal use of detailed spatial layers of land-use and land-cover information that is typically required for such experiments. On the contrary, it demonstrates an efficient and highly accurate solution relying on publicly available satellite data that require little postprocessing efforts. Moreover, the proposed framework can be easily enriched by upcoming sources of information to further increase its predictive accuracy such as building footprint and 3D information datasets.

Such approaches will help researchers and stakeholders shift from sometimes unrealistic national-level population projections that are used to interpolate between census-dates and provide spatially and temporally reliable estimates for regions of interest such as a specific city. We hope that this will work will pave the road for essentially a “near-real time” satellite-based population estimation framework, addressing the needs of the citizens of the countries of the Global South and meaningfully contribute to the monitoring of the Sustainable Development Goals and evidence-based decision making.

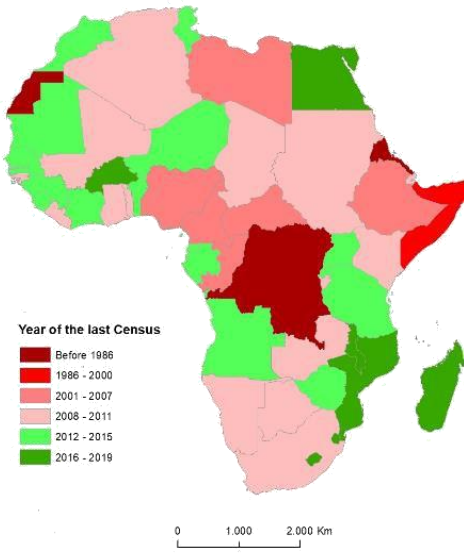

Figure 1. Number of years since the last census in Africa using 2019 as the reference date. Source: United Nation Statistical Division.

Fusing earth observation and socioeconomic data to increase the transferability of large-scale urban land use classification

Job F. Rosier[1], Hannes Taubenböck[2,3], Peter H. Verburg[1], and Jasper van Vliet[1]

[1] Institute for Environmental Studies, Vrije Universiteit Amsterdam, De Boelelaan 1105, Amsterdam, the Netherlands

[2] German Aerospace Center (DLR), German Remote Sensing Data Center (DFD), Oberpfaffenhofen, 82234, Wessling, Germany

[3] Institute for Geography and Geology, Julius-Maximilians-Universität Würzburg, Würzburg 97074, Germany

Keywords (5): Deep learning, Model transferability, Remote sensing, Point-of-interest, Road networks

The challenge

A major bottleneck in large scale urban land use mapping in data scarce regions is the availability of ground truth data. To partly overcome the need for training data, we focus our analysis on the transferability of a deep learning approach. Additionally, using very high resolution imagery is resource intensive, which limits their capacity to be used in large scale urban land use mapping. Therefore, we use a combination of open-source satellite imagery and socio-economic data, constituting of points-of-interest and spatial metrics from road networks to classify urban land-use at a national scale. By dividing the Netherlands into four regions we investigated whether the combination of satellite and socioeconomic data increases the transferability of our deep learning approach. The Netherlands was chosen for this study, as ground truth for the entire country was readily available, while the results of this study will be used to map large scale urban land use in a following study.

Methodology

Firstly, we investigated whether combining Sentinel-1 and -2 data with spatial statistics derived from road networks, and POI data will improve the classification accuracy of urban land-use compared to only using Sentinel-1 and -2 data by training a wide contextual residual neural network (WCRN) on data from the entire country of the Netherlands. Secondly, we investigated whether adding road network, and POI statistics will improve the classification in a new, unseen region in two different settings. We divided the Netherlands in four parts and, firstly, trained on three regions and tested on the region left out. Secondly, we trained on one region and tested on the three regions left out. All results were compared to the classification accuracy using a Random Forest (RF), which served as a benchmark. The average F1 score and overall accuracy were used as evaluation metrics. The land-use dataset was created by sampling the most recent publicly available land-use dataset of the Netherlands. Sample size was set to 200x200 m and only samples which were covered by at least 50% of one land-use category were included in the dataset. POI and road network data from Open Street Map was used and Sentine-1 and -2 data was downloaded from the Google Earth Engine.

Results

We found that the combination of Sentinel-1, Sentinel-2, POI, and road network statistics yields a higher accuracy than Sentinel data alone, POI combined with road network statistics, or the Sentinel data in combination with either POI or road network data for the whole of the Netherlands. The increase in accuracy after adding socioeconomic data is larger when training on three regions and testing on one region left out as compared to the classification result for the entire Netherlands. Specifically, the increase in OA ranges from 3 to 5 p.p. in the transferability experiments, while it was maximum 3 p.p. in the classification of the complete country. When the classification model was trained on one region and applied on another region, the increase in accuracy due to the addition of POI and RN data varied much more than when the model was trained on three regions. The increase in OA was between 0 and 7 p.p., and the increase in F1 score between 0 and 9 p.p. (Figure 1). The results of the RF model results were consistently lower than the results from the WCRN model for all regions in the 3vs1 as in the 1v1 transferability test. The difference the in average F1 score between the RF model and the WCRN model is comparable for the results of the whole Netherlands and the 3vs1 region test (7 and 8 p.p.), but converges more for the 1v1 region tests (5 p.p.).

Outlook for the future

Using satellite images when applying a trained model to a new region assumes that there are physical similarities between the same urban land-use categories located in different regions.

Even within the Netherlands, the differences between regions caused a reduction in classification accuracy. When our approach would be applied to a larger area, the algorithm would have to depend more on socioeconomic data to classify urban land-use correctly. Yet, even with socioeconomic data dissimilarities can reduce the classification accuracy and only a training dataset consisting of a diverse set of samples contains enough information to be transferred to a new region. Next, we aim to classify urban land use in the global south, where morphological differences between regions are expected to be greater than in the Netherlands. Therefore, depending on the regions, a more active domain adaptation strategy might be required.

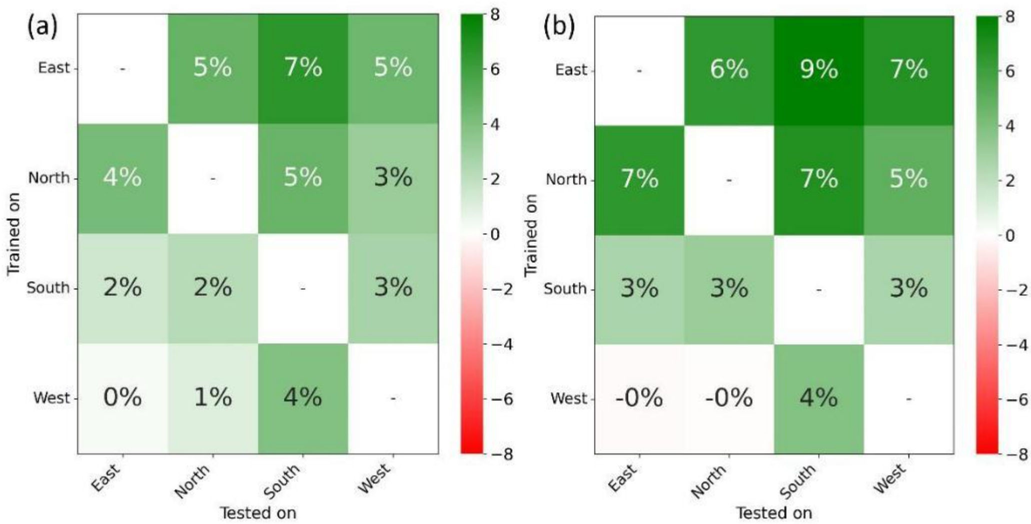

Figure Difference in overall accuracy between using satellite data vs the combination of Sentinel, POI, and RN data per region (A). Difference in F1 score between using satellite data vs the combination of Sentinel, POI, and RN data per region (B).

Assessing the Utility of Open-Source Geo-Spatial Data for AI-Driven Estimation of Fire Spread Risk in Informal Settlements

Dagmara Panas[1*], Sohan Seth[1*], Gary Watmough[3*], David Rush[4*] [1]University Of Edinburgh, School Of Informatics, Uk,

[2]University Of Edinburgh, School Of Geosciences, Uk,

[3] University Of Edinburgh, School Of Engineering, Uk
* This Work Was Supported by Wellcome Trust

Keywords (5): open-source, remote sensing, AI, fire, resilience, informal settlements

The challenge

Populations housed in informal settlements are rapidly growing, and due to their informal nature, they are typically lacking in basic safety features. For example, dense layouts and unsupervised building practices result in increased vulnerability to fire spread. Developing an open-source, data-driven AI model of assessing the risk of fire spread at any location within informal settlements using remote sensing and geospatial data could aid risk mitigation and contribute to Sustainable Development Targets 11.1 and 11.5 We present an analysis of suitability of publicly available data for this purpose. Specifically, we assessed the coverage and volume of geo-mapped fire events, required as target for training the AI model; and the quality of building footprint data, from Google Open Buildings (abbrev. OB), that is crucial for deriving relevant risk factors such as density of dwellings.

Methodology

To understand the quality of fire event data we have performed basic exploratory analysis, examining the completeness, coverage, and resolution in both spatial and temporal domains of two existing datasets from Cape Town, South Africa from 2020. We also visualised the distributions of event sizes to verify whether these comprised a representative sample. To understand the quality of publicly available building footprint data we have performed both an exploratory analysis, and a comparative analysis against an independently obtained ground truth dataset (obtained from VHR aerial photography and LIDAR via manually-corrected automatic detection) in the region of interest. The comparative analysis can be further subdivided in two parts: first, we computed the values of several previously identified aggregate settlement risk metrics (e.g. average distance to nearest neighbour) and computed correlation and goodness-of-fit statistics between OB and the ground truth dataset (across the 291 known settlements in the region of interest); second, we performed a left-intersecting spatial join (joining data wherever an OB footprint overlaps with a ground truth footprint), followed by a comparison of distributions of individual footprint characteristics across all the settlements, and an assessment of observed overlaps between individual footprints. We have focussed specifically on OB as the most comprehensive and mature product (e.g., recently released Microsoft footprints do not cover South Africa where we have ground truth data).

Results

The first dataset, a tabular dataset provided by the city of Cape Town, is heavily biased towards single dwellings, which would be a serious obstacle in extrapolating fire spread risks. The second dataset, a geomapped spatial dataset co-curated by the city of Cape Town and University of Edinburgh, presents excellent spatial precision and size distribution, but consists of only 46 events, which limits its use. 2 (Style: Footer) While the footprint data provided freely by Google represents an unprecedented opportunity for humanitarian efforts, it is not sufficient in and of itself to support fire spread risk modelling. The spatial coverage is excellent, nominally the entirety of sub-Saharan Africa. However, the temporal coverage is limited to a single point in time. As such, it would therefore not be suitable for modelling, unless backdated versions in regions of interest were available. Furthermore, a comparison against reference data indicated that the quality of detections within informal settlements would most likely be insufficient for accurate representation of layout characteristics informative of fire risk assessment (Jaccard Index of 0.722). At individual dwelling level, it appears that Open Buildings are skewed towards small and scattered, sometimes overlapping structures. At settlement level, average inter-building distance and landscape density tend to be under-estimated, while edge density, patch density and fractal dimension tend to be over-estimated (see Figure).

Outlook for the future

A previous feasibility study (L. Gibson et al., 2019, in Fire Safety Journal) has demonstrated the utility of remote sensing in geo-mapping of fire events when the approximate location and time are known. While both socioeconomic factors and satellite imagery availability can prevent capturing every single fire event and their respective burn scars, we believe in large part the lack of data is due to the lack of necessary systems and tools to use the data in a meaningful way. We hypothesise that the quality gap of footprint data for our specific purpose is due to the broad applicability of the data product, and in particular the fact that it had been developed to work well across both rural and urban settings, and with limited labelled data compared to the diversity of architecture throughout sub-Saharan Africa. An algorithm specifically targeted towards informal settlement footprints is achievable. We propose that with a larger set of geo-mapped fire events, and more accurate footprint dataset, fire spread risk modelling is feasible, as suggested by previous analysis of the relationship between fire severity and settlement footprint characteristics and weather conditions (L. Gibson et al., 2022, in Computers, Environment and Urban Systems).

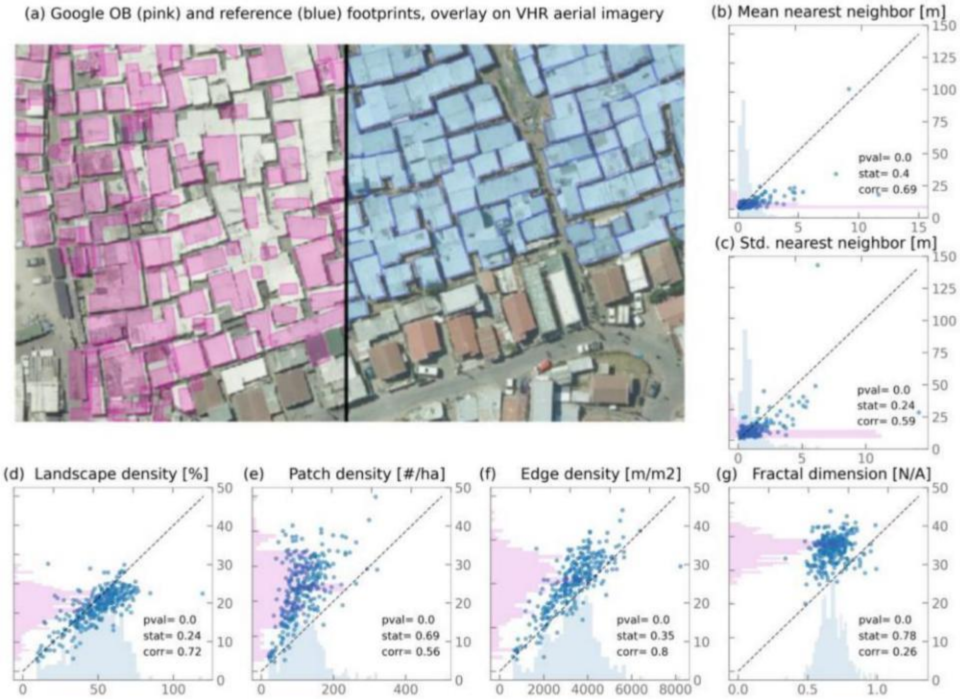

Figure Comparison of Google OB and ground-truth footprints. Note that for panels b-g the x/y axes show risk metric values, the secondary x/y axes (right/top) show histogram counts.

Mapping Access to Electricity and Urban Night Lights: Leveraging the Massive Repository of Astronaut Photography of the Earth

Monika Kuffer[1] , Tobias Storch[2], Alejandro Sánchez De Miguel[3], Franz Hölker[4], Eleanor Stokes[5]

[1] Faculty of Geo-Information Science and Earth Observation (ITC), University of Twente, The Netherlands

[2]Earth Observation Center (EOC), German Aerospace Center (DLR), 82234 Weßling, Germany
[3] Universidad Complutense de Madrid, Spain

[4] Leibniz Institute of Freshwater Ecology and Inland Fisheries (IGB), 12587 Berlin, Germany
[5] Universities Space Research Association, USA

Keywords (5): Nighttime lights, light pollution, access to electricity, urban night lights, International Space Station (ISS)

The challenge

Nighttime light (NTL) images from the International Space Station (ISS) have been used by very few researchers without exploring their full potential. Potential application fields have a large range, including the monitoring of energy consumption, light pollution, urban extent, socio-economic and population modelling, and electrification. The low spatial resolution of satellite-based observations, e.g., 750m for Suomi-NPP VIIRS-DNB has restricted researchers from exploring the full potential of NTL images for withinurban scales. In addition to the coarse spatial resolution, NPP was designed primarily for meteorological, and the recent shift to LED lights is not well captured because VIIRS-DNB is blind to blue wavelengths. Since the 1990s, NASA astronauts and later also ESA, JAXA, ROSCOSMOS and CSA-ASC, have been acquiring NTL images with DSLR cameras. However, images are not systematically calibrated, georeferenced and accessible.

Methodology

Urban monitoring with nighttime remote sensing is very different from daytime remote sensing. Commonly built-up areas have traces of NTL; however, many informal areas in the Global South are not (well) connected to the electricity grid (Figure 1b). In ISS images, NTLs are often linear features along the main transport axes (Figure 1a). Acquired ISS NTL images come with various geometric distortions and require georeferencing (high order transformation) and radiometric correction for quantitative, temporal and comparative applications. The Citizen Science program Cities at Night tagged, located and georeferenced them to make NTL images accessible. Leveraging this repository of ISS NTL, we show the potential of ISS to support diverse EO application fields. For several application fields, we explore the required spatial resolution (defined by the focal length of the DSLR camera and the position of the ISS). For example, for monitoring the energy transition and the reduction of light pollution (e.g., for European cities), high spatial resolution is required to identify individual pollution sources. High spatial resolution nightlights are also needed for mapping access to the electricity grid (e.g., in African cities), to map the heterogenous intra urban patterns of NTL. We also explore whether high radiometric resolution and RGB images allow determining sources of lighting (e.g., the shift to LED lights), comparing images of different years for the same city.

Results

Related to lighting sources, since the LED lights have started to replace the old discharge lights, the radiometry values that VIIRS-DNB provides (DMSP-OLS did not have any radiometric calibration) can be misleading as they largely exclude light emitted in the blue spectrum. Therefore, VIIRS-DNB images might indicate a light reduction, which is not the case when compared to ISS images. Related to electrification, high spatial resolution (e.g., ISS images acquired with a focal length of 400 mm) is required to detect small neighbourhoods not connected with the electricity grid, while the presence or absence of street lights can be concluded with a focal length of 180 mm (slightly lower spatial resolution). Such information is essential for infrastructure development and the upgrading of informal settlements or planning to connect services (e.g., health, education) to the electricity grid. Related to light pollution, very highresolution images allow the mapping of sources of light pollution and the modelling of dark corridors to support applications in the field of biodiversity. For example, the massive reduction of insects is related to the increase in light pollution in urban, suburban and peri-urban areas.

Outlook for the future

For the development of a high-resolution NTL satellite-based sensor system, characteristics are not well understood and are challenging to define. Generally, there is limited scientific knowledge across application fields of suitable sensor requirements. The repository of ISS NTL images, which is extremely rich but very under-utilised by researchers, is an optimal testbed to develop applications and an understanding of requirements. Such requirements include defining spatial, spectral, radiometric and temporal base requirements for the application fields. We are presently exploring, collecting and expanding different applications and documenting their requirements toward defining sensor requirements for a high-resolution nighttime light mission.

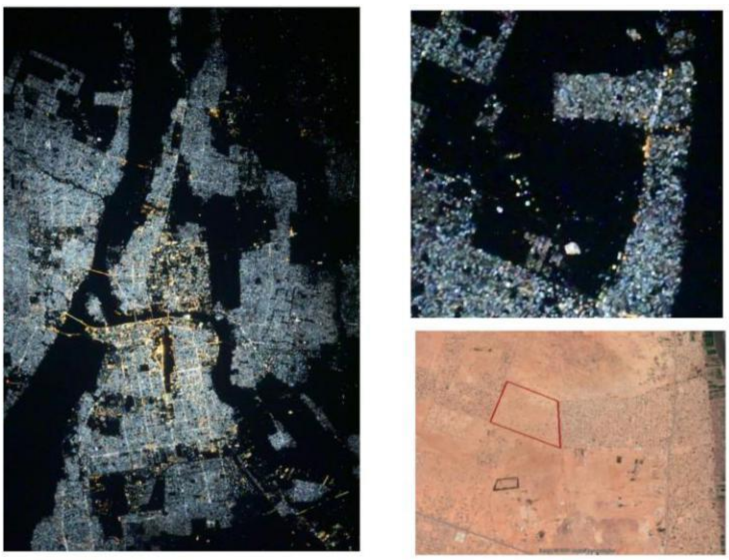

Figure (a) Khartoum, Sudan ISS NTL, 2021 and (b) zoom into an informal area without NTL and (c) red polygon showing an informal area (without NTL) on a Google Earth image.

WSDC_EC: Environmental and Climatic Applications

Chair(s): Dr. Jiong Wang and Prof. Catherine Linard

Characterising the Changes in Land Use and Land Cover amid Changing Climatic Conditions using Remote Sensing Techniques in the Muringato Basin, Kenya

Simon Wachira Muthee [1] , Bartholomew Thiong'o Kuria[1], Charles Ndegwa Mundia[1],

[1]Dedan Kimathi University of Technology, Institute of Geomatics, GIS and Remote Sensing, Kenya

Keywords: Land Use and Land Cover (LULC) Characterisation, Remote sensing, Time Series Analysis

The challenge

Hydrological Basins and sub-basins provide natural occurring sources of water. However, their existence is at risk due to environmental changes (Ciobotaru et al., 2018). Thus there is a need to monitor, manage and conserve them for sustainable utilisation. The degradation over the years of the Muringato basin located in Nyeri County, Kenya has been greatly influenced by anthropogenic factors, key among them being unsustainable deforestation, increased quarrying activities, conversion of wetlands into agricultural land and unchecked abstraction of water from the existing rivers within the catchment (Muringato WRUA, 2014). Increase in population and changing climatic patterns have also been observed. This research therefore aimed at characterising the changes in LULC amid changing climatic conditions from 1990 to 2020. From the results LULC trends were established and mapped, evidence in changing climatic conditions provided and they could advice in conservation policies.

Methodology

LULC analysis was undertaken to establish the climatic conditions changes that had occurred within the Muringato basin. This was achieved through a time series analysis of Landsat 4, 5, 7 and 8 satellite Imagery acquired between 1990 and 2020 (Liu et al., 2009). The research epoch was significant, since climatic projections showed rising temperatures by 2.5 °C, long dry seasons and high intensity rainfall that would be less predictable (ReliefWeb, 2018). The imagery was pre-processed and a LULC classification performed using the Support Vector Machine Classifier. This classifier was preferred since it works well with both even and uneven structured data (Rudrapal et al., 2015). USGS classification classes were used: forest, range, agricultural, barren and built up land. The training and validation of the classification results utilised data collected using handheld GPS receivers for the year 2020 and from Google Earth historical Imagery for the earlier epochs. In addition, monthly climatic data: rainfall, temperature (max and min), wind speed, solar radiation and relative humidity was obtained with 4000 km spatial resolution from TerraClimate (Abatzoglou et al., 2018). The data was resampled to 30 m and rasterised. A correlation analysis between LULC and the climatic data was then performed to establish their relationship. The population density change in the basin was done using data from Kenya National Bureau of Statistics at a 10 years temporal resolution (KNBS, 2019).

Results

There was a 21.4%, 0.5% and 2.3% decrease in forest, agricultural and barren lands respectively, and increases of 21.8% and 2.4% in range and built up lands respectively (Figure 1). The average climatic changes in the basin observed were: a rise of 1.36°C and 0.94°C in max and min temperature respectively, increased precipitation by 337.86 mm, a minimal change in wind speed of 0.01 m/s, reduced solar radiation by 10.44 W/m2 and 2.41 reduction in relative humidity. An average population density change of 266 persons per kilometre was noted from 1989 to 2019. Reduction in forest land was as a results of conversion into range and built up lands (Temgoua et al., 2018). As population increased more land is cleared for settlement and in search of arable land (MacHiwal et al., 2011). Such reduction in forest land can negatively affect the water balance and play a role in changing the climatic cycle in the area (Mutayoba et al., 2018). The fluctuations in the agricultural and barren is due to changes and dependency in the climatic patterns. During the wet and cool seasons more land is used for agricultural purposes while in the dry and hot years, the land is converted into barren land (Temgoua et al., 2018). The unpredictable climatic patterns and its changes over the years has a great effect on the status of LULC in the area (Bonan, 1997).

Outlook for the future

A 21.4% loss in forest land can cause rise in temperatures by 2°C, and a likely reduction in precipitation by 12% of the average received, thus less water availability. Moreover, with reduced forest land, the ability of the basin to recycle its precipitation is affected (Eltahir & Bras, 1996). Surface run off velocities increase and peak discharge time of stream reduces, more occurrences of flooding and increased erosion (Bahremand et al., 2006). Most of the agricultural activities in the area are rain dependent and less rainfall results to the LULC transiting to barren land. Due to increasing population the built up land is increasing and is highly negatively correlated to forest land. Therefore, understanding the LULC dynamics amid changing climatic conditions can act as a catalyst in sensitising the community on the need for sustainable resources utilisation.

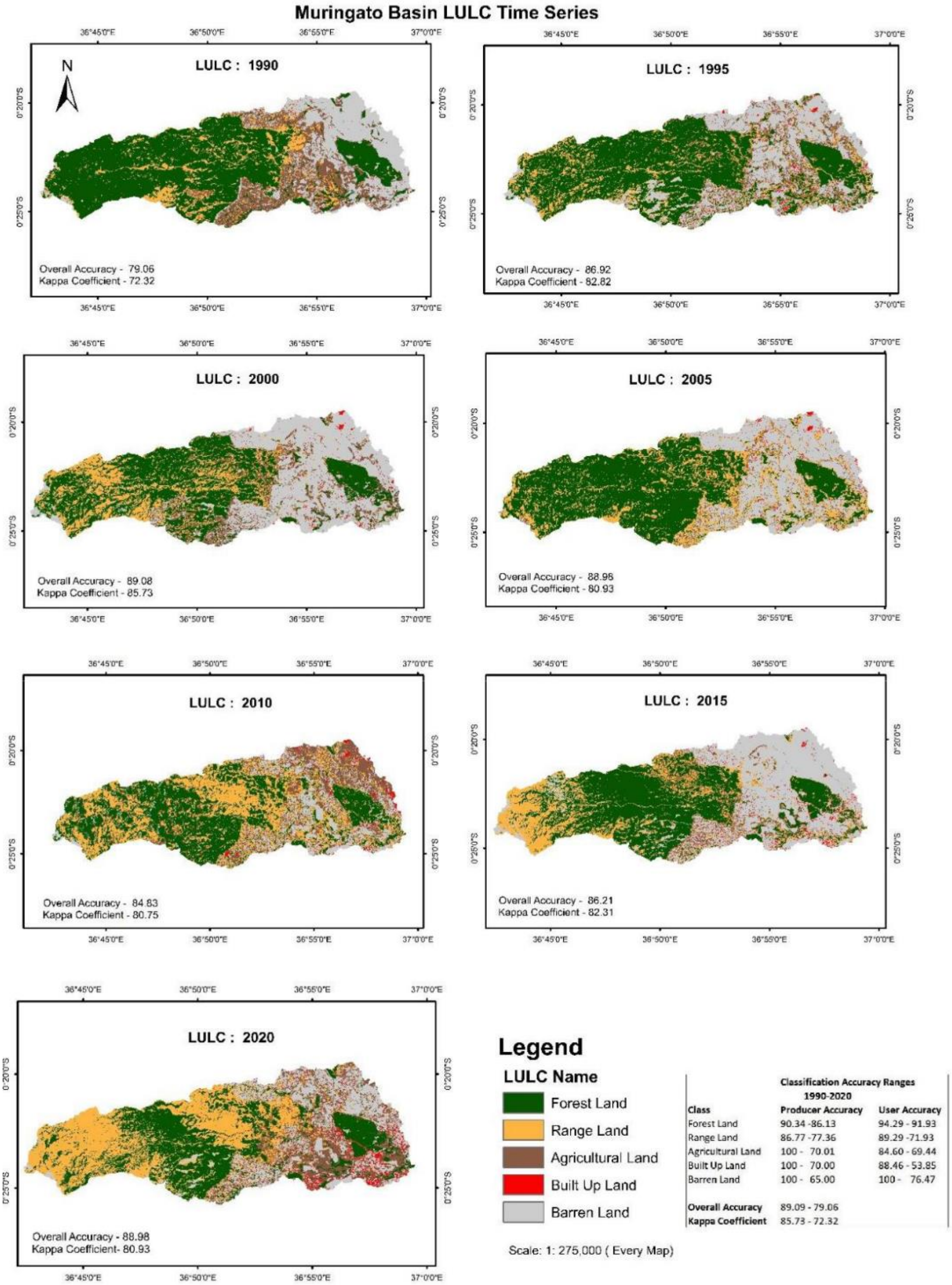

Figure 1: Muringato Basin LULC Time Series from 1990 to 2020

Evaluation of the Dempster-Shafer Theory for Oil Palm Plantations Mapping: Application to Sumatra (Indonesia)

Carl Bethuel[1], Damien Arvor[1], Thomas Corpetti[1], Jérémie Gignoux[2], Samuel Corgne[1]

[1]Umr Letg 6554 Cnrs, University Of Rennes 2, Place Du Recteur H. Le Moal, Rennes, 35043, France
[2] PSE– Paris School Of Economics, Paris, France

Keywords (5): oil palm monitoring, remote sensing, Indonesia, land cover change, data fusion

The challenge

Oil palm plantations (OPP) are one of the most important crops in the world's food supply. Indonesia, leading global producer of crude palm oil, has seen its forest areas impacted in recent decades with an evolution of the OPP from 4 million hectares in 2006 to 15 million hectares nowadays. Palm oil is mainly produce by two types of agricultural systems:

- Industrial farms (60% of OPP)
- Independent smallholders (40% of OPP)

OPP expansion have huge environmental impacts (deforestation, biodiversity loss…) and their fine scale mapping represents an important challenge for the scientific community. In this work, we combined three existing OPP maps with the Dempster-Shafer Theory (DST) in order to produce an improved map that allows to identify both OPP with high level of confidence and regions with high uncertainties (which represent an important spatial information for further studies and for the end-users).

Methodology

The method is based on the evaluation of three OPP maps in Indonesia produced with various data and methods and show high accuracies (table.1).

Table.1: Datasets summary

Maps	Years studied	Data used	Spatial scale	Methods	Results
Descals, 2021 (DE)	2019	Sentinel-1 Sentinel-2	10 m	Deep learning model	OA = 94.02%
Danylo, 2021 (DA)	2017	Sentinel-1 Landsat	30 m	Unsupervised classification	OA = 84.83%
Xu, 2020 (XU)	2016	MODIS ALOS-PALSAR	100 m	Random forest classifier	F1-score = 0.86

The maps assessment is made with a reference dataset create from an OPP annual map produced by visual interpretation of SPOT-6 and Landsat images. We use the 2019 map to get our samples (since the 2016 OPP still exist in 2019 but the reverse is not always true). Only two classes (OPP and Other Land Use – OLU) are use on Sumatra Island (area of 473,481 km²), the most impacted region by the OPP.

We perform a stratified sampling of 10000 points representing the real area of each land cover class (2160 points for OPP and 7840 points for OLU) that we intersect with the three maps to get an error matrix and the Kappa score (κ).

We then combine the three maps with the DST, which is widely used for uncertainty modeling. To this end, a universe (i.e. all possible hypotheses) is set (eq.1).

$$= \{ \quad , \quad , \cup \quad , \emptyset \} \text{ (eq.1)}$$

Here OPP and OLU are both the basic hypothesis, OPP u OLU is the union of these latter and represents the uncertainty and Ø is the empty set. The error matrix of each map is use to assign the basic belief for each hypothesis and a decision is taken based on the maximum of pignistic probability for each hypothesis.

Results

First results focus on the rating of the three maps and the DST result with our reference data (table.2).

Table.2: Statistical validation

Map	Error Matrix			Kappa
DE		OLU	OPP	0.70
	OLU	7710	140	
	OPP	760	1390	
DA		OLU	OPP	0.59
	OLU	7746	94	
	OPP	1063	1097	
Xu		OLU	OPP	0.38
	OLU	7577	262	
	OPP	1427	733	
DST		OLU	OPP	0.71
	OLU	7710	128	
	OPP	753	1406	

We note among the baseline maps gaps on the κ which are 0.70, 0.59 and 0.38 for the DE, DA and XU maps respectively. These discrepancies are due to the different data and methods used, e.g. supervised or unsupervised classifiers applied on high to moderate resolution data. Using maps with different κ values is not a problem because the belief assignment was made with these values and the error matrix. So, deep learning method develop by Descals gets the highest κ value which induces a greater weight in the decision-making process. Besides, the results between DE map and DST map are close for this reason. Using different maps informs us on the interest high spatial resolution over temporal resolution.

On Figure.1, we observe for the DE, DA and XU maps, OPP reflects 45%, 36% and 12% of the total area respectively. The DST results are show with the pignistic probability and we note that 46% of the area is covered by OPP. The pignistic map for the OPP hypothesis bring the information on the confidence level of the DST classification. The DST approach slightly improves the map accuracy but its major contribution stands in the spatial monitoring of confidence and uncertainty levels.

Outlook for the future

This work offers an evaluation of OPP mapping in Indonesia (Sumatra) performed with multisource satellite images. In this regard, we can highlight 1) the potential of radar and optical synergy and 2) the major contribution of high spatial resolution (< 30 meters) over temporal resolution to achieve for consistent results.

Furthermore, the Dempster-Shafer data fusion rule offers interesting opportunities for the scientific community and stakeholders as it identifies areas with high confidence and uncertainty. Specific work can be thus be focused on these areas characterized by high level of uncertainty.

Future work will investigate the potential of the radar and optical synergy for the discrimination of the OPP class and sub-classes, i.e. smallholders and industrial OPP in order to better understand of oil palm expansion in Indonesia.

Figure.1 Oil palm plantations maps comparison

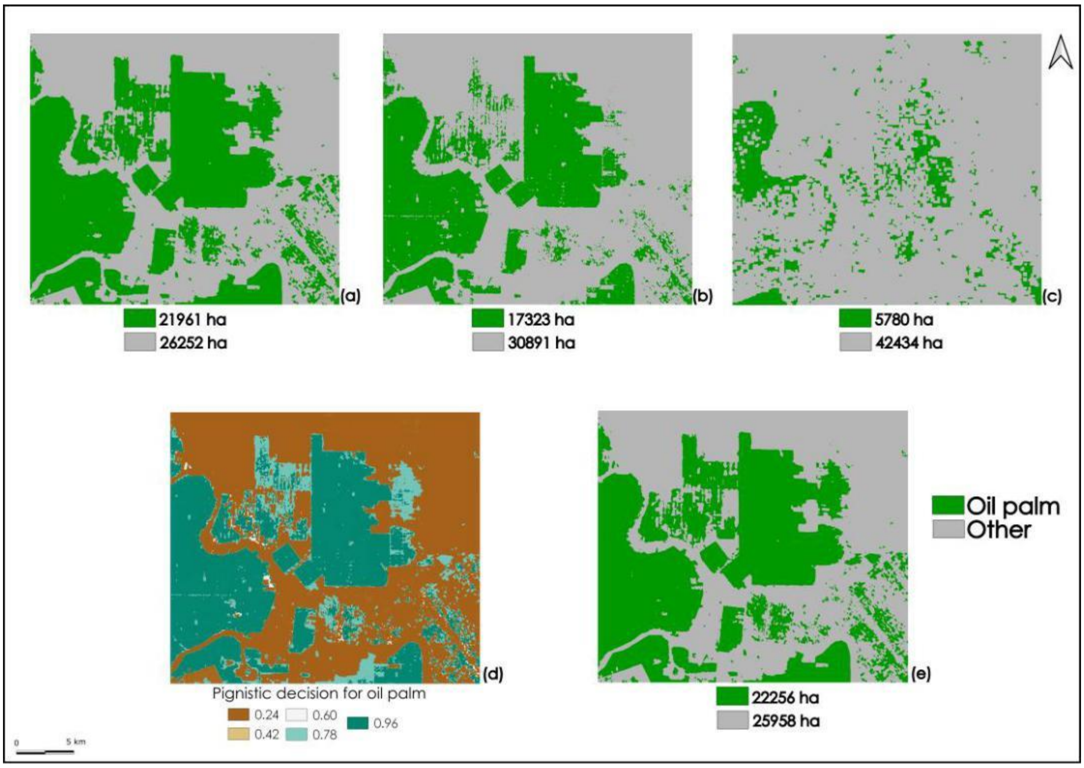

(a) Descals classification (b) Danylo classification (c) Xu classification (d) Pignistic map for OPP hypothesis (e) DST classification

Classification Features and Object-based Mapping for Heterogenous Tropical Highlands Using a Synergetic Multi-Sensor Approach Based on Sentinel-1, Sentinel-2, and GEDI Data - A Case Study of the Muringato Sub-catchment, Kenya

Marcus Goebel[1], Kuria Thiong'o[2], Andreas Rienow[1]

[1] Institute of Geography, Ruhr University of Bochum, Universitätsstraße 150, 44780 Bochum, Germany

[2] Institute of Geomatics, GIS and Remote Sensing, Dedan Kimathi University of Technology, Private Bag Dedan Kimathi, Nyeri, Kenya

Keywords (5): Data Fusion, Sentinel-1, Sentinel-2, GEDI, Object-Based Classification, Tropical Highlands

The challenge

Tropical highlands remain a challenging target for remote sensing due to their complex structure of high landscape heterogeneity and frequent cloud cover, causing a shortage of high-quality and reliable comprehensive data. This also applies to the Muringato sub-catchment in Nyeri County, Kenya, where poor land-use practices and unfavourable changes in landcover are known to be key factors putting pressure on the region's environmental resources. Existing land use and land cover (LULC) products of global or continental scale like ESA WorldCover fail to depict the regional characteristics of heterogenous regions like tropical highlands. To enable a sustainable development of resources by local stakeholders and decisionmakers, accurate data on the land's surface must therefore be generated using adapted strategies. The study's main objectives are examining possible classification features that can be derived from (near) global datasets and developing a strategy that meets the particularly heterogeneous structure of tropical highlands in Kenya.

Methodology

To analyse suitable classification features we have pre-processed Sentinel-1-MSI and Sentinel-2-SAR data covering two years (2020 and 2021) for bi-annual evaluation using Google Earth Engine. This includes advanced cloud masking for optical data and additional border noise reduction, radiometric terrain normalization and speckle-filtering for SAR to create comprehensive and comparable datasets. In addition, experimental ISS-borne Global Ecosystem Dynamics Investigation (GEDI) data has been taken into account. The resulting synergetic image stacks were analysed using visually interpreted reference data containing a total of 2,800 sample polygons targeting objects of varying size to find meaningful classification features that can be used to describe major environmental changes like deforestation, human land-use intensification, or loss of waterbodies. Findings have been incorporated into an adapted sequential and object-based classification scheme in which masks over several thematic levels are created by thresholding the most significant features. Fuzzy objects are classified using an k-Nearest-Neighbour approach. The strategy also includes a multi-scale image-object-homogeneity re-evaluation and local extrema analysis to be able to target regions such as larger national parks and very heterogeneous rural areas with adapted parameters considering the target object's sizes.

Results

Comparing different classification features to our reference data we found that a combination of the Sentinel-2-Water-Index (SWI) with SAR is suitable for masking waterbodies in the area that are less well captured by other common indices. Different types of vegetation (e.g., trees, shrubs) can be assessed by combining optical bands of Sentinel-2-MSI while SAR-data is only suitable as a potential exclusion criterion in extreme cases. GEDI data is a useful supplement that correlates strongly with the visual data and is helpful in excluding certain agricultural areas that otherwise would be classified as forest. The detection of built-up and their separation from bare ground is challenging as the targets are often small and scattered across the rural areas. The distinction between homogeneous and heterogeneous areas in combination with a local extrema analysis leads to satisfactory results, whereby the newer Enhanced Normalized Difference Impervious Surfaces Index (ENDISI) is performing better than other indices. Due to the small size of targets, SAR-backscatter patterns are comparatively ambiguous except for larger settlements. Comparing our LULC to 556 random validation points (partly from ground control and, where not accessible, from high-resolution orthoimages), we achieve an accuracy of ~88% with a kappa coefficient of 0.85 at a particularly dry scene, outperforming existing products in the region. Confusion occurs mainly in the transitions of vegetation classes and in particularly dry open soil.

Outlook for the future

As part of the project “CITGI4Muringato – Participatory Approach to Environmental Conservation of the Muringato Catchment Area for Sustainable Management and Enhanced Ecosystem Health[4]”, findings from this study will be incorporated into a regional environmental monitoring strategy, including a Water and Energy Budget-based Distributed Hydrological Model (WEB-DHM) that uses LULC information as an input. Furthermore, additional research on the classification scheme is pending. A time series component utilizing SAR-backscatter sequential change detection could be used to gather information in two rainy seasons that span almost half of the year in the region. Since the scheme allows the integration of additional data sources, we are planning an investigation of experimental ISS-based Spaceborne Thermal Radiometer Experiment on Space Station (ECOSTRESS) thermal data, which could later be substituted by the upcoming Copernicus Land Surface Temperature Monitoring (LSTM) programme for permanent monitoring.

4 CITGI4Muringato is funded by the Federal Ministry of Education and Research (BMBF) following a resolution of the Parliament of the Federal Republic of Germany (funding code 01DG20022).

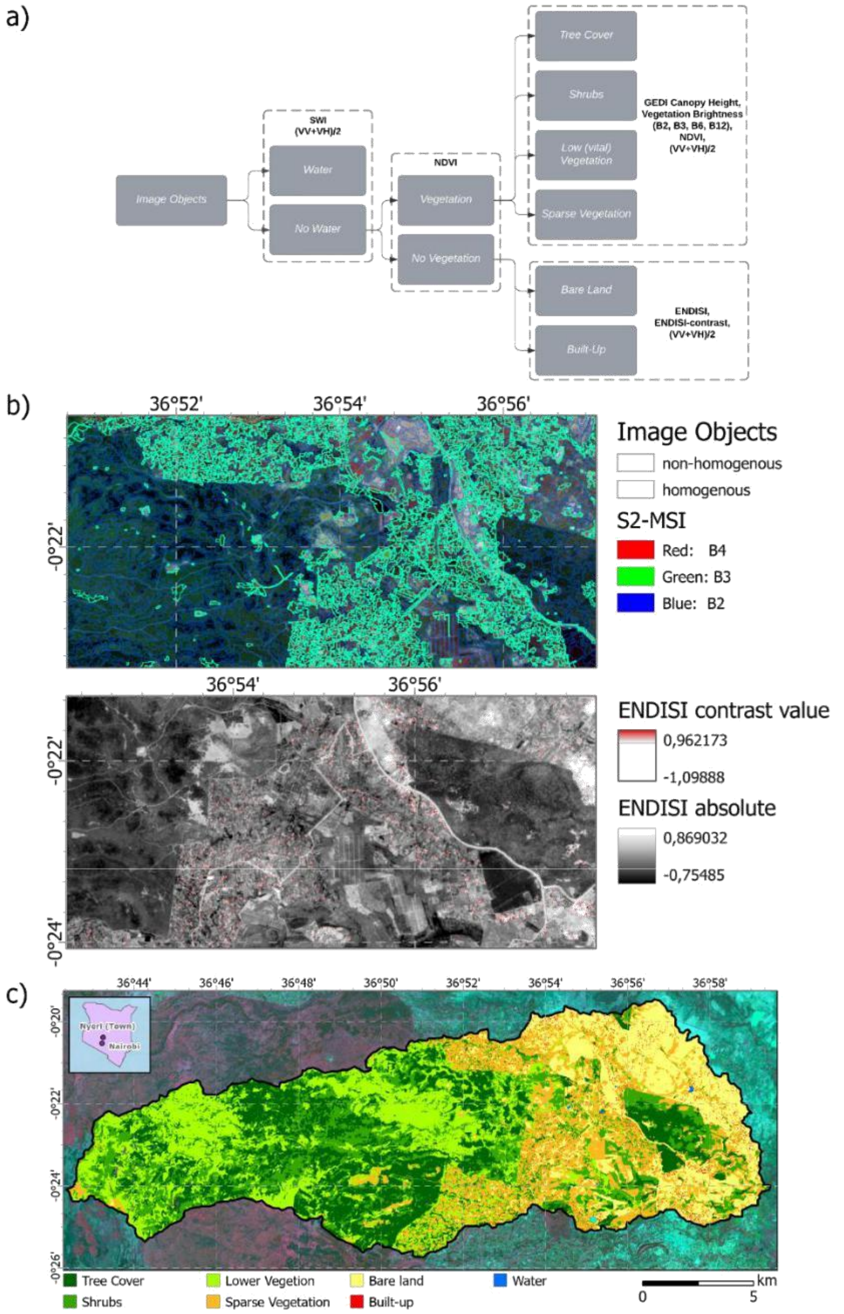

(a) Sequential classification scheme(b) multi-scale image-object-homogeneity re-evaluation and local extrema analysis (c) classification results for the Muringato study area, second half year 2021

A Universal Data Processing Method for Global Production of Water-quality Indicators in Support of SDG 6.3.2

Nima Pahlevan[1,2], Akash Ashapure[1,2], Asen Radov[2,3], Navid Golpayegani[2]

[1] Science Systems and Applications Inc., U.S.

[2] NASA Goddard Space Flight Center, U.S.

[3] University of Maryland, U.S.

Keywords (5): Water quality, machine learning, NRT processing, Landsat-8/9, Sentinel-2

The challenge

Water is essential for life on Earth. Over-exploitation of water resources through global population growth and impacts of climate change cause water scarcity and increases the demand for clean water. The shortage of healthy water raises concerns for food production and demands practical strategies for maintaining and tracking the health status of water supplies, such as lakes, reservoirs, and lakes. As the extreme weather events (e.g., extended monsoon seasons or longer intense droughts and heatwaves) become a new norm on a global scale, it is important for the countries to establish a reliable and sustainable strategy to monitor their progress toward achieving the Sustainable Development Goals (SDG) 6, i.e., access to clean water and sanitation for all, by 2030. Of all SDG 6 indicators, SDG 6.3.2 (proportion of bodies of water with good ambient water quality) and SDG 6.6.1 (change in the extent of water-related ecosystems over time Indicator) explicitly mandate participating countries to report the quality of surface waters, including lakes, rivers, reservoirs, wetlands, and estuaries. To surmount difficulties and complexities in the field- and laboratory-based reporting of water quality, the use of modern technologies, including Earth Observation (EO) and novel algorithms, seems inevitable.

Methodology

Our Satellite-based analysis Tool for Rapid Evaluation of Aquatic EnvironMents (STREAM) offers an innovative solution to facilitate the effective use of NASA and the European Space Agency (ESA) satellite observations (i.e., Landsat-8/9 and Sentinel-2) for water quality management. STREAM will enable near-real-time (NRT) detection of anomalous water-quality conditions for robust and timely decision-making. It will obtain and analyze the latest satellite data, notify water resource managers of potential water-quality issues in their regions of interest, and enable visualizations and basic analyses of satellite products. This system will bring NASA-ESA satellite observations to water-quality decision-making frameworks with end-users' ability to access satellite products.

Currently, this system is composed of a backend and a frontend. The backend (i.e., processing workflow) harnesses NASA's SeaWiFS Data Analysis System (SeaDAS) for accounting for atmospheric interferences (i.e., atmospheric correction) and our in-house machine-learning model for estimating chlorophyll-a (Chla), Total Suspended Solids (TSS), and the absorption by Coloured Dissolved Organic Matter (a_{CDOM}). Our ML models are a class of neural networks termed Mixture Density Networks (MDNs) adept at handling the non-unique nature of the inverse problem. The performance of our in-water MDNs was gauged against the best-performing algorithms in the field (see Table 1). Further, we have lately extended MDNs to address the atmospheric correction problem (termed ACI here) using a large synthetic dataset. This model will ultimately replace SeaDAS for an overall improvement in the quality of products.

Table 1. Retrieval algorithms assessed in this study

<table>
<tr><th>WQ indicator</th><th colspan="7">Algorithm</th></tr>
<tr><td>Chla</td><td rowspan="3">MDN</td><td>GI-2B* (Gilerson et al. 2010)</td><td>Gons (Gons et al. 2002)</td><td>GU-2B* (Gurlin et al. 2011)</td><td>Blend (Smith et al. 2018)</td><td>Moses-2B* (Moses et al. 2012b)</td><td>OC3 (O'Reilly and Werdell 2019)</td></tr>
<tr><td>TSS</td><td>SOLID (Balasubramanian et al. 2020)</td><td>Novoa (Novoa et al. 2017)</td><td>Nechad (Nechad et al. 2010)</td><td>Petus Petus et al. 2010)</td><td colspan="2">Miller & McKee (Miller and McKee 2004)</td></tr>
<tr><td>cdom(440)</td><td>Ficek (Ficek et al. 2011)</td><td>QAA-CDOM (Zhu and Yu 2012)</td><td colspan="4">Mannino (Mannino et al. 2008)</td></tr>
</table>

For the frontend, we harness various tools and capabilities that have already been developed in-house for NASA’s Level-1 and Atmosphere Archive and Distribution System (LAADS). The frontend will allow end-users to visualize water quality maps (i.e., Chla and TSS), identify pixel values, and view time-series plots for a given pixel or for a group of pixels (e.g., lake or its sub-basin). The system will further enable end-users to download time-series data and geolocated water quality maps.

Results

The performance of our MDNs evaluated against best-performing state-of-the-art models for Sentinel-2/MSI-like spectra are illustrated in Fig. 1. The improvements range from 40% to > 100% for all the three water constituents.

Fig. 1. Scatterplots showing the performances of MDN and best-performing state-of-the-art models for Rrs spectra resampled to Sentinel-2/MSI relative response functions. These analyses correspond to a 50-50% data split for which actual sample numbers are shown on the y-axes. Contour lines are presented to illustrate data distributions better. Red dots and the annotated values refer to invalid (negative) estimates. More details are provided in

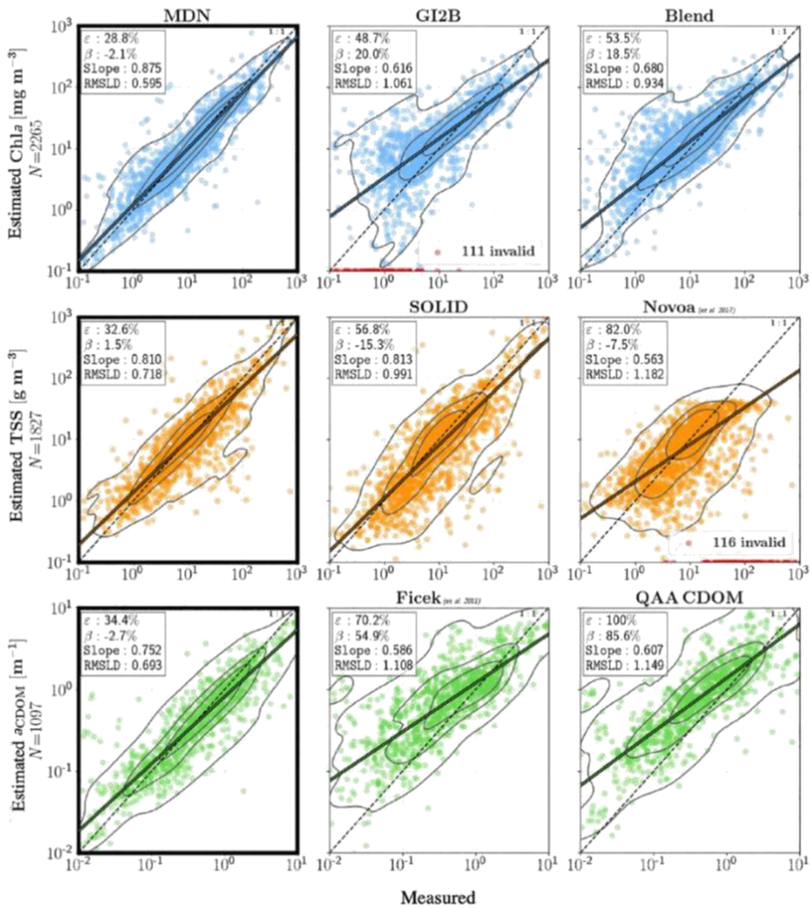

A preliminary performance of our atmospheric correction (ACI; top row) implemented for Landsat-8 is provided in Fig. 2. Using satellite matchups from five selected AERONET-OC sites, the efficiency of our model is compared to SeaDAS (i.e., L2gen) and ACOLITE.

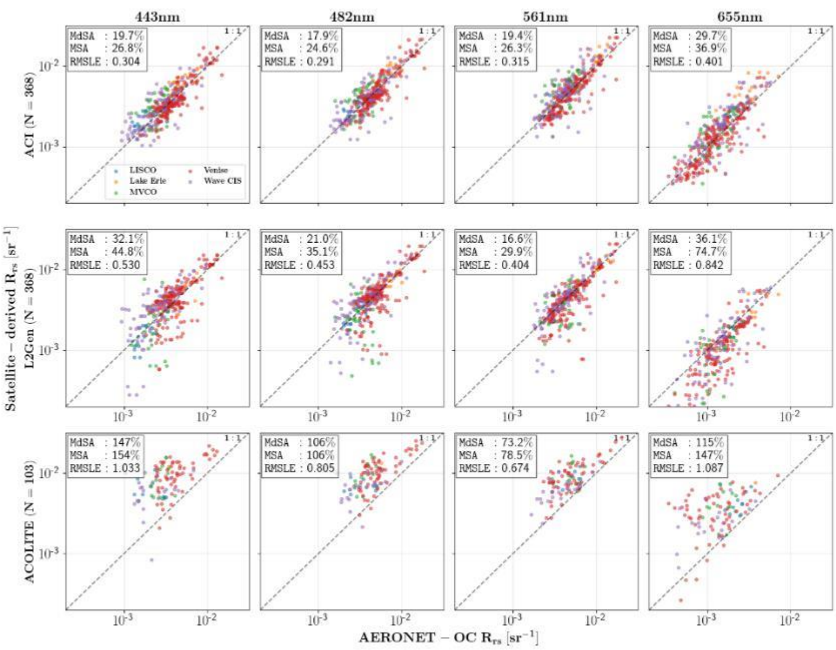

Fig. 2. Performance assessment of our atmospheric correction method (ACI) using AERONET-OC matchups. The performance of two other widely used atmospheric correction methods for the same matchups are presented. MdSA stands for the Median symmetric accuracy and MSA is Mean Symmetric Accuracy.

Fig. 3 shows the interface of STREAM which is currently being evaluated by water authorities of Peru and Uruguay for water-quality monitoring.

Fig. 3. Current web interface of STREAM. Shown is time-series plot of Chla products for El Pañe reservoir in southern Peru. This reservoir provides drinking water to the city of Arequipa.

Outlook for the future

We presented our latest research and development results that target major enhancements in our workflow towards generating globally consistent water-quality products for seamless reporting and progression assessments of SDGs 6.3.2 and 6.6.1. Our models/algorithms will replace the existing algorithms (e.g., SeaDAS used in STREAM backend) to allow for creating high-quality water-quality products for all.

Assessing The Effectiveness of Participatory GIS Tool For Environmental Conservation of The Muringato Catchment Area

W]isdom Kipkemboi [1], Bartholomew T. Kuria[1], David N. Kuria[1],

[1]Dedan Kimathi University of Technology, Institute of Geomatics, GIS and Remote Sensing, Kenya

Keywords: Participatory GIS tool evaluation, Stakeholders' engagement, Environmental conservation

The challenge

Economic sectors heavily rely on healthy ecosystems which demands for more holistic approaches to conserve and manage the natural environment. The same is true for environmental conservation, where adverse anthropogenic activities coupled with population pressure on the environment have necessitated the need for holistic approaches. The development of participatory GIS (PGIS) tools that are easy to use by various members of the community has been proposed as one of the environmental management tools in involving the members of the community in the mapping of their resources. The majority of PGIS tools are found in the fields of ecology, biodiversity and nature conservation, mainly due to the long history of the locals' involvement in these fields. However, there exists a gap in the evaluation of the uptake and usage of such applications. This study therefore sought to evaluate the effectiveness of a PGIS tool developed for participatory conservation of the Muringato catchment (Central Kenya).

Methodology

Community training and knowledge transfer sessions with the local community through the Muringato water resource users' association (WRUA) were undertaken to inform them of the developed PGIS tool for reporting of environmental disturbance incidences within the Muringato catchment. The PGIS tool was developed using Android studio and PHP scripting used for server configuration to enable the tool to publish data to PostgreSQL database hosted within a local server. To mobilize the community, formal invitations to training and fieldworks were sent out to the Muringato WRUA. This was followed up by phone call follow-ups to clarify and effectively plan for the sessions. Training manuals were also developed as part of the materials preparation planning. This ensured that the planned training sessions would be effective. To further enhance the planning and ensuring understanding by the local community, the training manual was translated to the local community dialect. This was to ensure that the trained members would effectively train other WRUA members and the local community at large. The manual detailed the prerequisites they should have and a thorough step by step process of how to access the PGIS tool, install it and use it to report the environmental disturbance incidences. With successful knowledge transfer of the PGIS tool and fieldwork sessions, an evaluation session was conducted after four (4) months to assess the effectiveness of the PGIS tool in monitoring the environment.

Results

A total of eighteen (18) WRUA members were trained who were to be trainer of trainers. This was based on target sampling of the local community who were members of the Muringato WRUA. The training sessions were conducted in the upper, middle and lower zones of the catchment. The members were taken through an indoor training session followed by field work sessions where the trainees were sent to the field to report on the environmental incidences that they found. An evaluation session was done after four months and it was attended by the WRUA members from all the zones. 64% of the attendees had attended the initial training out of which 33% of them had trained other members. Of the ones who had trained other members, some of them couldn't number the persons they had trained while others had trained as few as one member. 88% of those who had attended the initial training, successfully accessed and installed the PGIS tool and 78% of them reported on various environmental incidences. Additionally, from the members who used the tool, they all with a rating of 7 and above out of 10 recommended the application to be used for incidences reporting within the catchment. The challenges they encountered included; difficulty in identifying members to train, accessing the points of incidences while some forgot to use the application. Some of their recommendation included; organizing continuous training sessions and increasing the numbers of the persons being trained per session.

Outlook for the future

Although, local communities have long been involved in decisions that affect their daily lives, the global rise of PGIS approaches is much more of a recent occurrence. This rise could be attributed to factors such as the spread and penetration of location-enabled mobile devices where the locals are sources of location-based information and the advancement in technology which has led to a whole new generation of user generated content. With these advancements, more PGIS tools could be developed to aid policy planning and decision making by the top management of issues that affect the community.

Moreover, Earth Observation (EO) is the integration of in situ ground surveys with satellite imagery data concerning the Earth Surface. With the Muringato local community already trained and empowered to use the PGIS tool to report on various environmental incidences, these datasets could be integrated with satellite imagery data for auto-generation of land use land cover of the catchment based on the current reported incidences data. This will enable

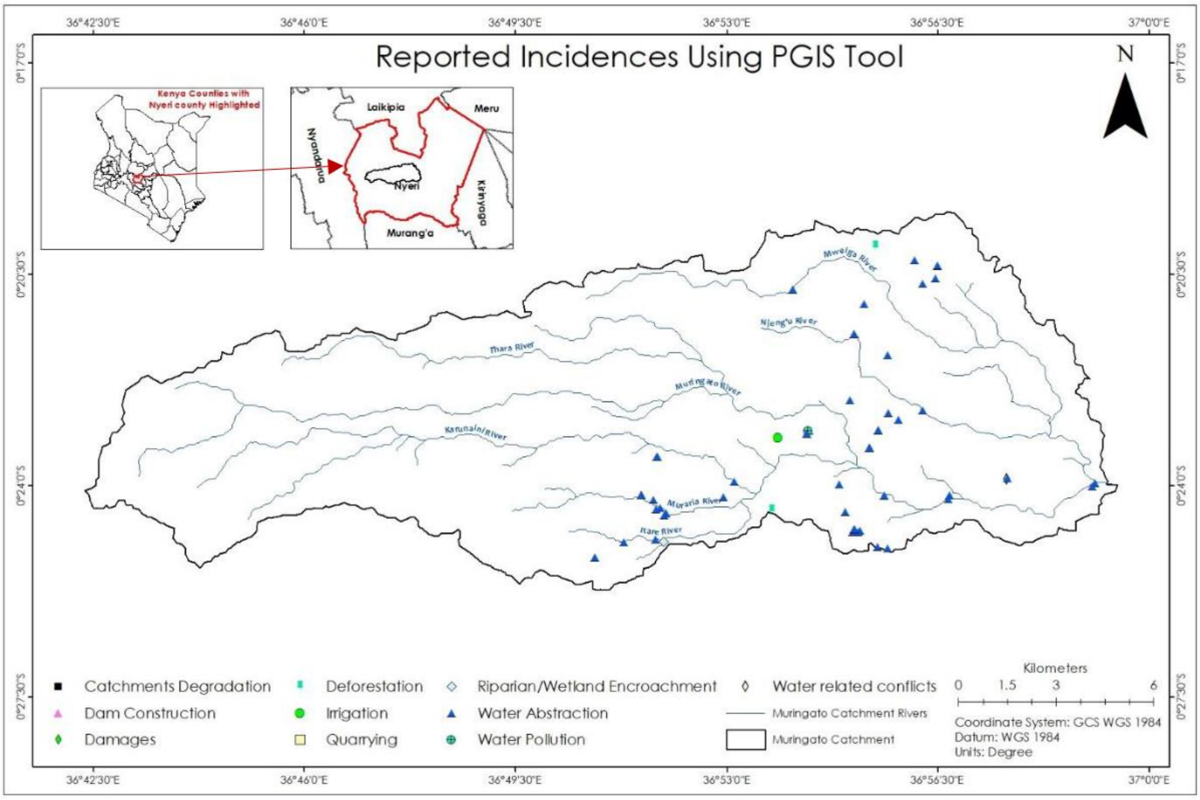

continuous trend analysis of the environmental changes of the catchment and thus further empower monitoring of the Muringato catchment.

Figure 1: The map shows some of the Crowd mapped incidences that were collected during and after the community training within the Muringato local catchment.

Conference Sessions

S_CC: Climate Change and Desertification

Chair(s): Dr. Felix Bachofer

Four decades of geophysical land, ocean and atmosphere products over Europe to answer climate-related questions - the TIMELINE project

Stefanie Holzwarth[1], Sarah Asam [1], Martin Bachmann[1], Martin Böttcher[2], Andreas Dietz [1], Christina Eisfelder[1], Andreas Hirner[1], Matthias Hofmann[1], Grit Kirches[2], Detmar Krause[1], Julian Meyer-Arnek[1], Simon Plank[1], Thomas Popp[1], Sophie Reinermann[1], Philipp Reiners [1], Sebastian Rößler[1], Thomas Rupert[1], Alexander Scherbachenko[1], Meinhard Wolfmüller[1]

[1] German Remote Sensing Data Center (DFD), German Aerospace Center (DLR), 82234 Wessling, Germany
[2] Brockmann Consult GmbH, 21029 Hamburg, Germany

Keywords (5): AVHRR; time series; processing automation; Europe; TIMELINE

The challenge

Since the early 1980s, the German Remote Sensing Data Center (DFD) of the German Aerospace Center (DLR) has been acquiring and processing data of Advanced Very High Resolution Radiometer (AVHRR) providing daily surface reflectance data sets with a spatial resolution of ca. 1.1 km. This unique multi-decadal time series allows to investigate long-term impacts of climate change on our environment. The project TIMELINE (TIMe Series Processing of Medium Resolution Earth Observation Data assessing Long-Term Dynamics In our Natural Environment) is aiming at the generation of a homogeneous time series from the sensors AVHRR/1, AVHRR/2 and AVHRR/3 for Europe. The challenges to produce a consistent and harmonized 40-year-long time series based on the AVHRR series of instruments operated on 14 different platforms are enormous. The effort is necessary to develop consistent, reproducible, reliable and generic variables enabling the detection of geoscientific phenomena and trends.

Methodology

The two major challenges to ensure the consistency of reflectance and thermal information are the corrections for satellite orbit drift and channel calibration drift of the different AVHRR instruments. The processing follows a sophisticated sequence of individual steps, including calibration, spectral band adjustment and radiometric harmonization, chip matching and orthorectification, cloud masking, atmospheric and BRDF correction. Daytime normalization models account for changes of the observation time due to the satellite orbit shift. In addition, data defects caused by malfunctions of the instrument are marked with per-pixel quality flags in each product. The scene-based L2 products are aggregated to L3 daily, 10-days, and monthly composites in order to reduce the influence of noise, outliers, and data gaps on the time series. The TIMELINE products are validated against different well-known EO based products (e.g., from MODIS) and for some products also against in-situ data.

The product suite consists of atmospherically corrected surface reflectance, NDVI, snow cover, fire hotspots and burnt area maps, land surface temperature (LST), sea surface temperature (SST), and different cloud properties (e.g., cloud top temperature). The long time-series and very high temporal resolution of the data set enables the derivation of related statistical parameters such as mean, variability, anomalies, and the derivation of trends and phenologies. For example, the TIMELINE NDVI time-series is used to investigate changes in the summer NDVI over Europe over a period of almost 40 years.

Results

The products produced within the TIMELINE project enable the long-term change detection as well as the identification of geo-physical phenomena and trends in Europe. The derivation of related statistical parameters such as monthly or decadal means and variances serves as input to investigate long-term impacts of climate change on our environment. Different trend analyses have already been carried out on the basis of the level 3 TIMELINE products:

- Temporal shift of spring green-up over Germany
- Change of summer NDVI in Europe
- Long-term dynamics of SST over the North Sea and Baltic Sea
- Trend of the urban heat island effect of European cities
- Temporal distribution of active fires per month for different land cover and climatic zones
- Cloud cover anomaly over Europe

The preliminary results of the analyses are consistent with information from other sources, adding the benefit of often prolonging former analysis based on remote sensing data. For example, TIMELINE SST observations for the Baltic Sea are in line with the Copernicus Marine Service data for the period 1993-2020.

To exploit the multitude of possibilities to use and analyse the TIMELINE data, a wide range of geoscientific products generated within the project will be made available to the public via a free and open data policy.

Outlook for the future

The availability of a harmonized time series of daily AVHRR observation data over four decades with the increased resolution of 1 km and the special focus on Europe offers the possibility to investigate long term impacts of climate change on our environment. The possibilities for evaluating and upgrading the data set are far from being exhausted. We also see great potential to adapt the TIMELINE processing framework to further Earth Observation time series data and to continue with other sensors with higher spatial and spectral resolution (e.g., Sentinel-3).

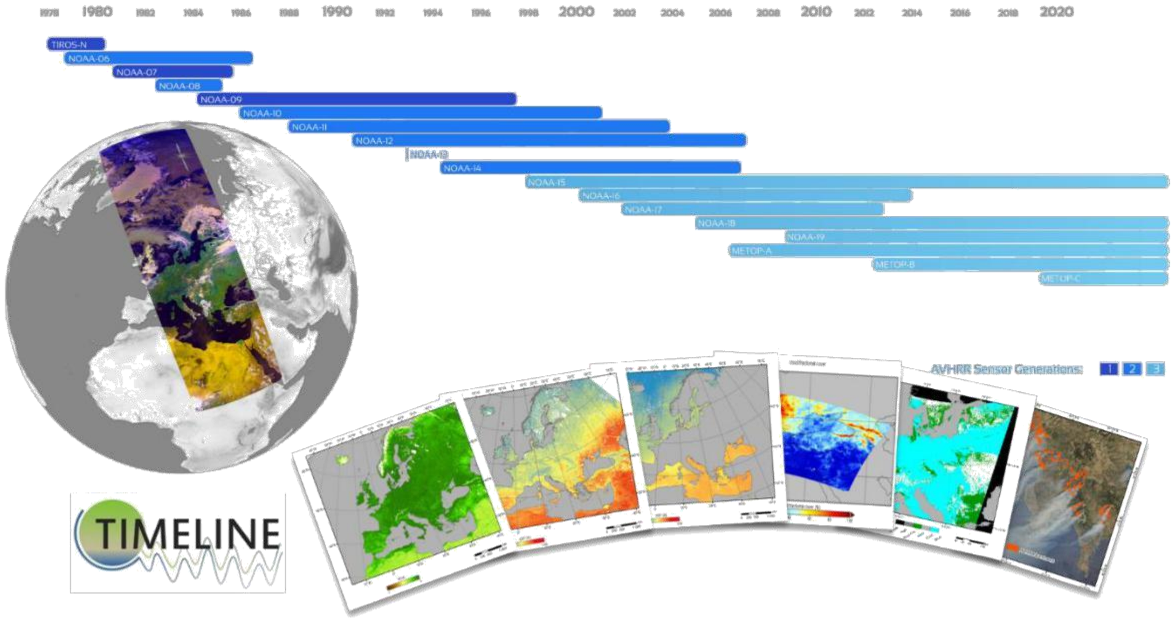

Figure TIMELINE at a glance (adapted from Dech, S., et al., Potential and Challenges of Harmonizing 40 Years of AVHRR Data: The TIMELINE Experience. Remote Sensing, 2021)

Monitoring drought events in Germany and Cyprus using more than 20 years of MODIS data

Ursula Gessner[1], Sophie Reinermann[2], Sarah Asam[1], Ioannis Varvaris[3], Eleni Loulli[3,4], Felix, Bachofer[1], Diofantos Hadjimitsis[3,4], Claudia Kuenzer[1,2]

[1] German Aerospace Center (DLR), Earth Observation Center (EOC), German Remote Sensing Data Center (DFD), Germany
[2] Department of Remote Sensing, Institute of Geography and Geology, University of Würzburg, 97074 Wuerzburg, Germany
[3] ERATOSTHENES Centre of Excellence, Limassol, Cyprus
[4] Department of Civil Engineering and Geomatics, Faculty of Engineering and Technology, Cyprus University of Technology, Limassol, Cyprus

Keywords (5): droughts, vegetation, anomalies, MODIS, time series

The challenge

In the recent past, climate extremes have impacted vegetation all over Europe. European regions have experienced droughts and heat waves, but also cold spells with associated impacts on agricultural yields, the productivity of natural vegetation, and on water resources. For example, in Central Europe, extreme droughts and heat waves occurred in 2003 and in 2018. In Cyprus, the years 2008 as well as 2016-2018 were characterized by strong and persisting droughts. Multi-annual time series of optical satellite data are a unique data basis for characterizing climate-related vegetation anomalies over large temporal and spatial scales. This study analyses more than 20 years of Moderate Resolution Spectroradiometer (MODIS) Enhanced Vegetation Index (EVI) data at a spatial resolution of 250 m for Cyprus and

Germany. The spatial and temporal development of cropland and grassland vegetation during drought years was quantified and compared to the average long-term conditions.

Methodology

Data basis for this study was the complete archive of 250 m resolution 16-day MODIS Terra EVI (MOD13Q1) time series covering the years 2000 until today. Climate-related effects on vegetation were analysed based on the deviations of MODIS 16-day EVI composites from their long-term (21-year, 2000–2020) averages. Data processing was conducted on the Google Earth Engine platform. In order to only consider MODIS observations of high quality, the MODIS "pixel reliability" layer was considered, and all pixels that did not show best quality (class 0) were excluded from further processing. The analysis of vegetation anomalies was restricted to vegetated areas by masking all pixels with negative EVI values and all pixels where the CORINE land cover (CLC) dataset of the year 2012 showed non-vegetated land cover classes (e.g., "urban" and "water"). With the aim to avoid confusion of climate-related effects with land cover/use change effects, all pixels of land cover/use changes as indicated in the CLC change products were masked. The 21-year median EVI was calculated for each MODIS 16-day composite. It was calculated separately for all vegetation, cropland, and grassland pixels (with >75% sub-pixel coverage of the respective class). Subsequently, we calculated the deviation of each individual 16-day composite of the time series from the respective 21-year median composite. These 16-day deviations were then averaged to monthly intervals to reduce outlier effects.

Results

The MODIS-based vegetation anomalies delineated for both countries depict strong drought effects on vegetation, e.g., in 2003 and 2018 in Germany (Figure 1, top). The results show that in Germany, the extreme drought and heat summer 2018 however did not affect the whole country but rather concentrated on eastern, northern and north-western Germany. Furthermore, the method is able to capture vegetation stress caused by more moderate rainfall deficits as observed in 2019 and 2020 in Germany. Also in Cyprus, the strong drought effects in 2008 are reflected in the results (Figure 1, bottom). As shown on the map, the area of Paphos Forest (central-western Cyprus), being the densest forest of the island, was the least affected by the drought during spring. Nevertheless, the heatwave that prevailed during the summer months affected the whole island which is visible in the MODIS-based negative vegetation anomalies for almost the whole island throughout June, July and August 2008. Next to heat and drought impacts, the MODIS time-series-based approach also depicts below-normal vegetation development in case of long-lasting winters with late phenological onsets such as in spring 2021 in Germany or in case of fire events such as in 2021 in Cyprus. Thus, for a correct interpretation of the factors influencing the observed anomalies, additional information on weather conditions and fire is essential.

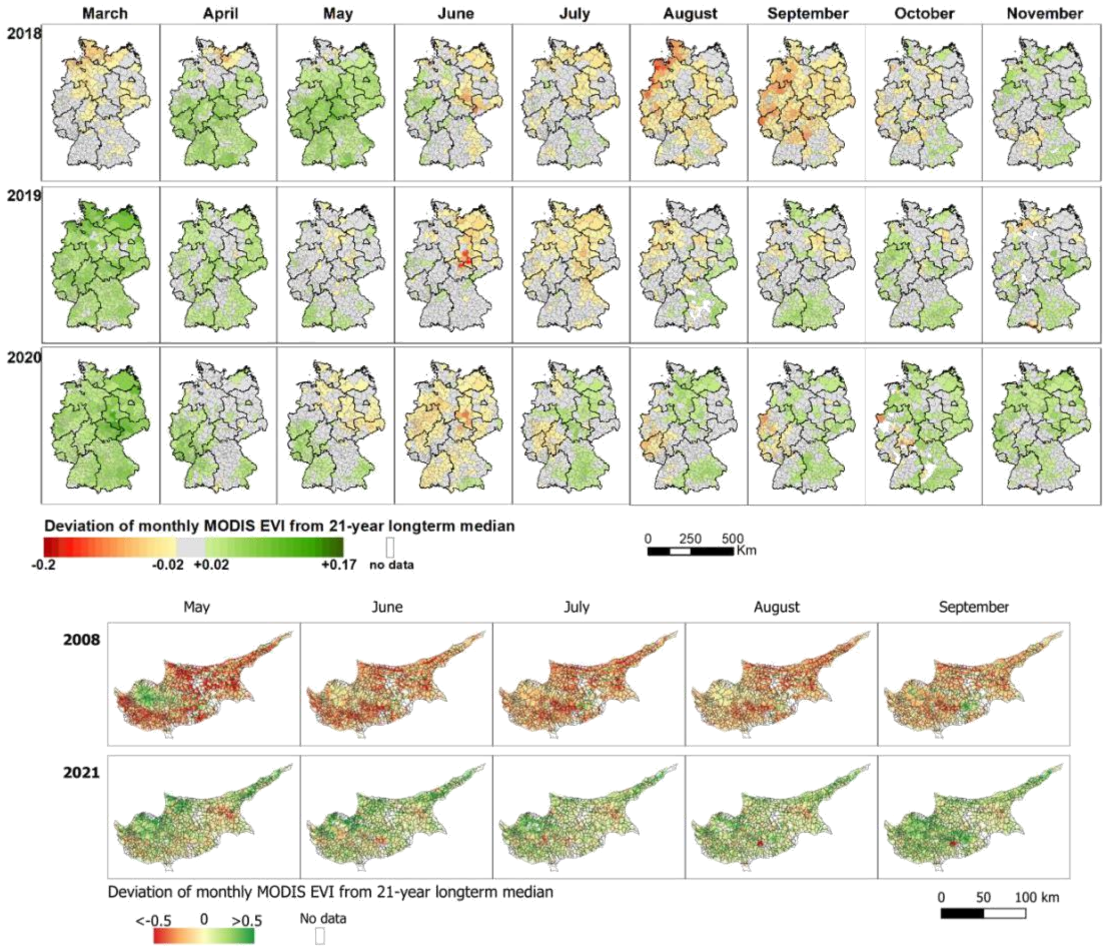

Figure 1 Vegetation anomalies for 2018-2020 for Germany (top) as well as for 2008 and 2021 for Cyprus (bottom) as detected from MODIS EVI time series (2000-2021).

Outlook for the future

The presented approach draws its strength from the long time series of vegetation conditions available from the MODIS mission, which acts as a normalizing reference for anomaly detection. To ensure the continuation of the presented approach to longer time-frames in future, the integration of freely available Sentinel-3 data has high potential. At the same time, agricultural applications, particularly in cropland systems, could benefit from a higher spatial-resolution (e.g., 10-30 m of Sentinel-2 and Landsat) that would allow field-scale and crop-type specific investigations.

Light pollution in selected Polish cities using VIIRS and census data

Aleksandra Łęczek[1]

Wojciech Łachowski[1]

[1] Institute of Urban and Regional Development, Poland

KEYWORDS (5): LIGHT POLLUTION, VIIRS, CENSUS DATA

The challenge

Excessive emission of artificial light is a problem that affects all major cities in Poland and in the world. It may disturb the functioning of the human circadian cycle and thus increase the risk of various medical ailments, including depression and cancer. A number of methods and tools are used to measure the phenomenon, e.g. sky quality meter (SQM) or the Bortle scale. Remote sensing data, in particular VIIRS provided by NOAA, is also widely used. However, there is no common method for assessing scale across the city and comparing the results between cities. The use of accurate population distribution data allows an additional assessment of the number of people exposed to excessive light pollution. The aim of the study is therefore to provide a method for assessing the scale of light pollution in selected Polish cities (Warsaw, Cracow, Lublin, Gdansk) with the use of VIIRS and census data.

Methodology

The first step necessary to carry out light pollution analysis was an estimate values of excessive electromagnetic radiation resulting from the emission of artificial light.

For the purposes of this research, we developed an eight-level one light pollution classification. Electromagnetic radiation threshold values at night (for each class) was prepared based on their ratio to the maximum values with an unpolluted sky and the results of previous papers For example, areas with radiation no more than 0,25 *10-9 W/cm2 * sr were assigned to the first pollution level. Such areas characterize black sky, resulting in no impact of light pollution on the human body. The classification included the following levels: 1) black sky, 2) rural sky, 3) rural/suburban transition sky, 4) suburban sky, 5) bright suburban sky, 6) urban sky, 7) city sky, 8) inner city sky.

In the next step, we have reclassified the light radiation values in the raster cells to the levels of light pollution. Performing this operation enabled the designation area and percentage in the total area of each of the analysed cities. In the last step, we have calculated the degree of people living in the area of each light pollution level using the census data.

Results

Lublin and Warsaw have the most illuminated downtown areas of all the analyzed cities. Additionally almost half of the area of these cities is covered by land 6 or higher level of light pollution. In Lublin, the largest part of the city is covered by 8 level, characteristic of the very center of large cities. In Warsaw, however, it is class 7, which proves the level illumination that could have a negative effect on human health. In all cities except Warsaw, there are areas with a lower level of light pollution - assigned to class 3 (Fig.).

Our research shows that over 65% of Lublin and Warsaw residents live in areas with high and very high levels of light pollution (class 7 and 8). In the case of Cracow and Gdansk, the percentage of people living in areas with such characteristics was less than 20%. The greatest amount of light radiation (on average during one night) per capita is emitted by Gdańsk

Outlook for the future

The excessive emission of artificial light still remains an imperceptible problem of cities. Results it with relatively low harmfulness in comparison to other types of pollution, e.g. air pollution or water pollution. However, due to the lighting technologies used street light smog will intensify and its negative the impact may increase. Research on spatial distribution and measurement of the discussed phenomenon may prove to be important in the management of the urban environment over time. The application of this method is universal and it can be applied to any city. In the future, the study could be expanded with additional data, related not only to the lives of humans but also animals, which are also affected by light pollution.

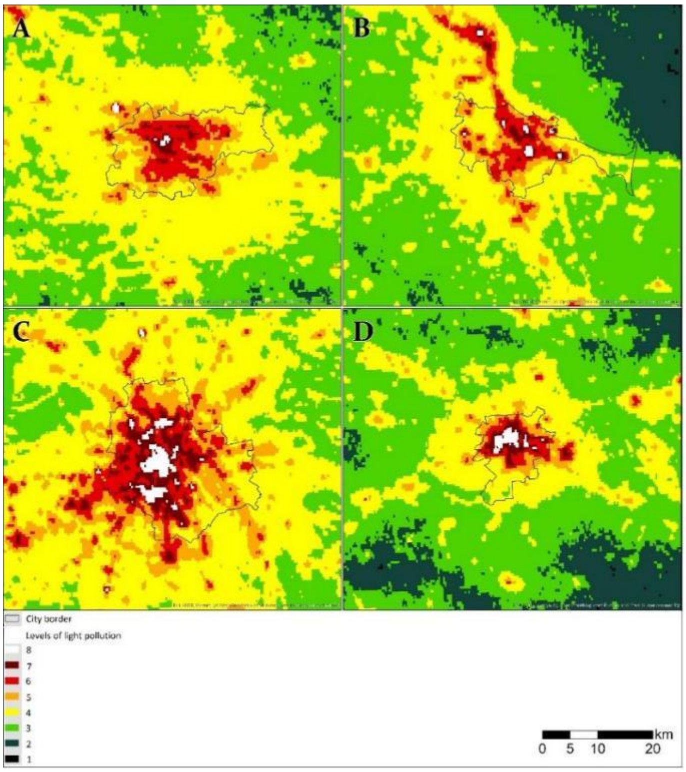

Figure. Classification of light pollution based on VIIRS data

Correlation of abrupt shifts in forest phenology with amplitude changes in Sentinel-1 SAR data and Land Surface Temperature from Landsat-8.

Christos Theocharidis [1,2], Chris Danezis [2,1], Ioannis Gitas [3], Diofantos Hadjimitsis [2,1]

[1] ERATOSTHENES Centre of Excellence, Cyprus
[2] Cyprus University of Technology, Department of Civil Engineering and Geomatics, Cyprus
[3] Aristotle University of Thessaloniki, School of Forestry and Natural Environment, Greece

Keywords: Sentinel-1, time-series, phenology, SAR, forestry

The challenge

Satellite image time-series methods have contributed notably to monitoring forest phenology and forest health since we can observe how climate change has affected these ecosystems and how this will change in the following years. Researchers report that heat stress and water scarcity expected in the Mediterranean will increase the frequency of forest mortality events and, thus, affect forest diversity (Behrens, Georgiev, and Carraro 2010). Inside all these predictions, the already affected Cyprus's natural resources are anticipated to further exacerbate climate change pressure due to the island's semi-arid climatic conditions (Zachariadis 2012). Recent climate simulations project a decrease in rainfall during autumn in all forested areas of Cyprus. That will lead to a gradual reduction of forest growth since autumn follows a continuous dry summer period where forests are under stress (Giannakopoulos et al., 2012).

Methodology

This study examines potential abrupt shifts in forest phenology influenced by LST, utilising Synthetic Aperture Radar (SAR) backscatter coefficient and Land Surface Temperature (LST) from Sentinel-1 and Landsat-8 datasets, respectively, within the period 2014-2021 for SAR and 2013-2021 for LST. Moreover, assessments and investigations were made on how the Sentinel-1 backscatter observations (VH, VV) are correlated with Landsat-8 LST. This study assessed two time-series decomposition methods, the classical seasonal decomposition by moving averages and the breaks for the additive season and trend (BFAST), to evaluate their monitoring performance and detect possible abrupt changes in forest seasonality where correlations between SAR and thermal data were made, lag plots and analysis of the residuals were conducted. The study area is the Paphos Forest, managed by the Department of Forest. That forest could be described as a representative Mediterranean forest; thus, it is vital to monitor it because Mediterranean forests are expected to experience the first climate change in Europe. More specifically, the study focuses on the Northeast, East and Southeast areas since all the SAR images are from descending orbit.

Results

Preliminary results showed a negative trend line with a negative slope of 5.02% for 2013-2021. The hottest months were June 2014 and July 2016, with average temperatures of 36,8 oC and 36,7 oC, respectively. The year 2019 was the coldest, having the lowest standard deviation compared to the other years. The most stable month in the LST fluctuations is October, with a negative slope of 4.58% and 1.76 oC standard deviation. In the SAR data, the VH polarisation time-series trend tends to be stable with a positive slope of 0.068%, while the VV polarisation time-series has a negative slope of 0.38%. In the LST time series, two abrupt changes (breaks) in the LST trend component were detected by the BFAST algorithm in December 2013 and August 2018. The first detected abrupt change, which was statistically significant, is considered justifiable since December is the coldest month compared to the other months in the LST time series, with a monthly average temperature of 8.4 oC. The second break was spotted in the hottest month of the time series, August 2018, which was the beginning of a significant drop in the trend line and temperature. Concerning the abrupt changes in the trend of SAR data, BFAST did not show a break in VH polarisation, while in the VV polarisation, only one break was detected in October 2015 (Figure 1). The VH-LST correlation presented a higher correlation than in VV-LST. The VH-LST correlation also showed seasonality in their lag plots, indicating a mid to high connection between VH and LST data. After that, the analysis of the residuals showed the correctness of the choice of the additive decomposition model where the residuals are randomly distributed around the 0; the Q-Q plots showed no heteroscedasticity, and the histograms had a normal distribution.

Outlook for the future

The following steps in this study will include investigations that will be made to identify the possible factors (human activities, extreme weather events, insect infestation, etc.) that led to the abrupt changes. In addition, time series with different vegetation indices suitable for monitoring forest phenology will be added and examined to make a more extensive analysis and identify possible sudden changes in forest phenology and, consequently, in forest health. Additional rainfall data will be considered to clarify the importance of moisture in forest health. After analysing all the data, an extensive search will be conducted to find the possible causes of the abrupt changes in forest phenology. A future step will be a comparison within the areas from descending and ascending orbit from SAR images to fully understand the possible abrupt shifts in forest phenology and, consequently, forest health, which affects us directly and indirectly as humans.

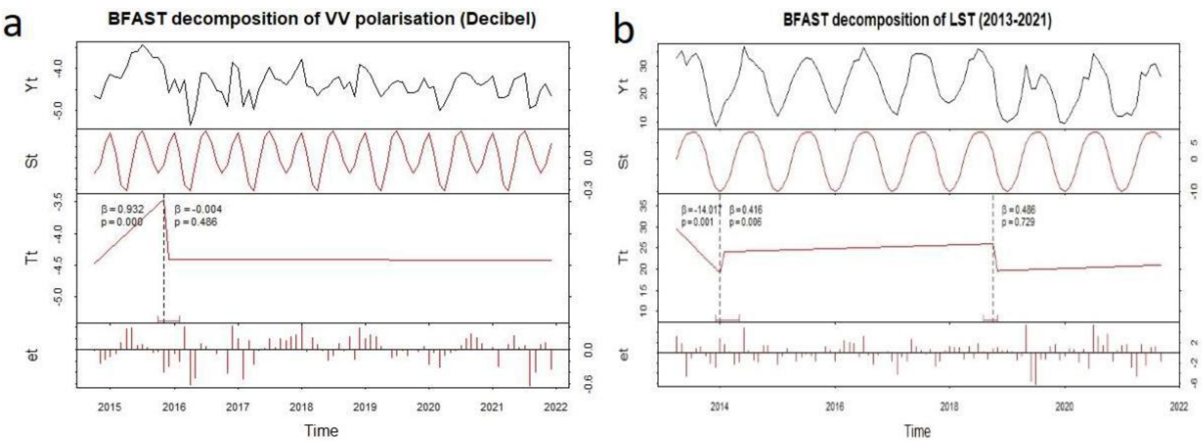

Figure 1. (a) The trend breakpoint for the Backscatter Coefficient-VV Polarisation 2014-2021 time series, (b) The trend breakpoint for LST 2013-2021 time series. The dot lines over the trendline show the breaks in the trend.

Acknowledgements

The authors acknowledge the 'EXCELSIOR': ERATOSTHENES: Excellence Research Centre for Earth Surveillance and Space-Based Monitoring of the Environment H2020 Widespread Teaming project (www.excelsior2020.eu). The 'EXCELSIOR' project has received funding from the European Union's Horizon 2020 research and innovation programme under Grant Agreement No 857510, from the Government of the Republic of Cyprus through the Directorate General for the European Programmes, Coordination and Development and the Cyprus University of Technology.

Poster(s)

Belgian experience in the Eagle LULUCF cross border mapping exercise

Benjamin Beaumont[1], Nathalie Stéphenne[2], Johannes Van Geertsom[3], Stefan Kleeschulte[4]

[1] Institut Scientifique de Service Public - ISSeP, Remote Sensing and Geodata Unit, Belgium
[2] Service Public de Wallonie - SPW, Geomatic Department, Belgium
[3] National Geographic Institute – NGI, Belgium
[4] Space4Environment, Luxembourg

Keywords: LULUCF, land use and land cover, climate change, Copernicus, Belgium

The challenge

Copernicus Corine Land Cover (CLC) is evolving towards a better harmonisation of the various Copernicus Land Monitoring Service (CLMS) products. Harmonisation means scales, resolutions, nomenclature but also integration of existing regional products. In Belgium, the three regions have LULC maps at higher resolution than the EU products. By consequence, the local authorities have limited interest in the EU products while some research centres and universities are using them.

National and regional Belgian actors are involved in the validation of CLC, CLC+ and High Resolution Layers (HRL) since the first version of CLC. Merging different datasets to provide an integrated cross-border map is interesting both for a national point of view and for cross border studies essential in climate crisis such as the flood events. In 2021, the enhancement of the CLC+ focused on Land Use, Land Use Change and Forestry (LULUCF) because the climate change mitigation is at the top of the EU policy agenda, and the LULUCF regulation requires countries to report on carbon stocks and emissions.

Methodology

The input data is often inconsistent, within countries and also across countries which impair the integration and comparison. The EAGLE concept provides a tool to increase comparability by providing 1) a framework for harmonisation and 2) a distinction between LC and LU. Harmonisation is achieved by translating national classes into EAGLE land cover components and land use attributes (Explanation of the EAGLE Data Model – what´s in, what´s out (copernicus.eu)).

Creating a LULUCF instance based on existing datasets is a new prospective in the CLMS history. To fit the LULUCF categories defined by the EC regulation, the EAGLE group proposed a translation between LULUCF categories and national data on a high level. The implementation at national level was left to the countries. Heterogeneity / inconsistencies remain of course within and across countries. A mix of LC and LU overcome the shortcomings of the datasets taken separately. LULC and LULUCF categories were proposed for an area including Belgium with challenges for classes such as greenhouses or wetlands. The Belgian actors and the Eagle group discussed the legend conversions. The exchange was necessary to integrate the national exercise in the EU interclasses nomenclature proposed.

Results

Several datasets are combined in this exercise. A detailed inventory of all datasets available for LU in the country was provided to EEA. However only the most largely used datasets covering the entire regions have been integrated in this cross border LULUCF mapping exercise. For Wallonia, two data sources are the LU "WAL_UTS__2018" and the LC "WAL_OCS__2018". For Flanders, the "landgebruik Vlaanderen 2016" and the Landbouwgebruikspercelen LV, 2018" are the data sources.

The processing chain integrates some LC and LU classes, such as the greenhouses in the WAL_OCS__2018. The maps are resampled to the 10m resolution and adjusted with the projection EPSG3035. Belgium provided a simplified LULUCF layer based on their three existing datasets. The figure illustrates the Belgian interclasses mapping at 10m spatial resolution with the results from Flanders and Wallonia merged.

Outlook for the future

Ingestion of existing datasets into European data collections, like CLC+, is an opportunity, because it makes use of the datasets defined by the regional authorities as fitting their needs, based on datasets which are regularly produced and validated by the MS. Ingestion of existing datasets would allow for terminating the need of having local and EU datasets in parallel. Because of the low use of the HRL datasets, the Belgian authorities are less and less ready to validate the EU datasets. Of course, integrating existing datasets has also limitations such as various scales, legend and specificities. This exercise illustrated the differences in member states datasets but proved also that it is possible to make a comprehensive regional dataset covering different countries from existing national sources. This paved the future with a continuous work to have a common nomenclature matrix.

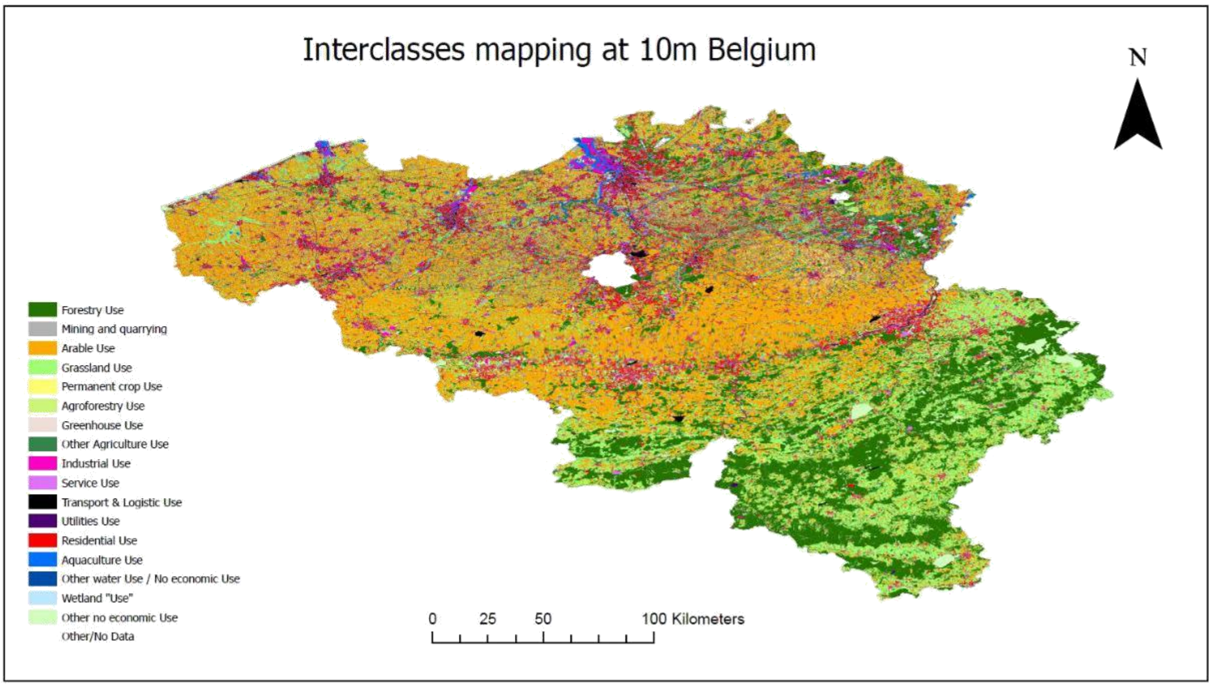

Figure Belgian interclasses mapping at 10m.

S_Agri1: Agroforestry, Forests, Agriculture and Food Security

Chair(s): Dr. Marios Tzouvaras

Detecting Large Scale Land Deals From Landsat Timeseries As Spatial Implications Of Export-Oriented Policies Along The Nacala Development Corridor, Mozambique

Ricardo Gellert Paris[1], Andreas Rienow[2],

[1] Ruhr University Bochum, Department of Geography, Germany
[2] Ruhr University Bochum, Department of Geography, Germany

Keywords: Land use changes, land grabbing, remote sensing , time series analysis, Africa

The challenge

Despite the steady increase in agricultural productivity and expansion of cropland, the world faces an increase in hunger combined with multiple crises – energy, environment and finance. The contemporary food regime shifts the production and distribution to a more globalized value chain impacting landscapes, access to resources, and the people's sovereignty in its frontiers. Additionally, development institutions operating in Africa are adopting development corridors' strategies to pursue the integration of multisectoral investments. Despite the efforts of organizations to monitor and track those land deals, there is a lack of spatial precision and territorial context to support the assessments of the impacted communities. The research focuses on the Nacala Corridor in Mozambique assessing the use of geospatial data as a tool to detect and model changes in the spatial configurations due to political changes favourable to massive land deals and exported oriented infrastructure.

Methodology

Firstly, information was collected from non-governmental reports regarding the infrastructure implemented in the region and the reported locations of land deals. The geographical accuracy of the reports varies a lot. The region was selected due to the location of the biggest development project of the country, connecting the district of Lichinga to the Nacala Port. Two LUC detection methods were implemented. Firstly, a 30 years' time-series analysis of LandSat imagery was implemented with the LandTrendr algorithm in GEE. It was considered abrupt disruptions on the time series by an increase of NDMI levels, considering that, for most of the reported cases, irrigated and capital-intensive crops were implemented. To decrease oscillation, the series was restricted to the dry season, from May to September. The second detection method applied was based on single MODIS images pre-processed and extracted from GEE with the mean EVI values calculated for each year during the dry season from the year 2000 to 2020. The images were stacked in a multidimensional image and an absolute pixel value change detection was done. Two standard deviation values were considered as a threshold and selected as a unique class of pixel changes. A kernel density map was done to highlight the hotspots where areas of detected changes have occurred and a timeseries analysis were conducted in sample locations.

The time series disturbances detection was compared with the area and dates that were reported by social organizations and with main political-economical facts, namely, the process of economic liberalization and implementation of infrastructure focused on external markets (port and railways).

Results

The results of the time series' occurrences at the district level presents four concentration of disturbances in land-use changes (Figure 1). During the first years after the implementation of the new constitution (1994). Around 2004 and 2006. Another concentration is during the first years of the year 2010 and the major concentration is during the years 2014 and 2016 when the infrastructure of the corridor was starting its operations. Indicating a possible relationship between exported-oriented policies and LUC modifications. The results, however, do not coincide with the reported years, which are concentrated between 2008 and 2010 and 2012 and 2014. This can be understood that the negotiation date of land deals antedates its modification. In this sense, it is possible to infer that land conflicts and displacement of population occurred before the actual implementation of LUC modifications, during the negotiation process, and that land deals were established before the release of the Corridor Masterplan or the opening of the railway to the Nacala Port. Sample areas were extracted from three hotspots (figure 2) and the EVI variation analysed (figure 3). The hotspot near the port showed a pattern of not expressive increase of EVI values; the hotspot in the south presents two different tendencies, one with little variation, probably from already productive areas, and a second presenting a steep increase between the years 2016-2018. Lastly, the hotspot located at the end of the railway line presents a unique pattern of steep increase in the years 2014-2016.

Outlook for the future

Due to the low accuracy regarding the size of the reported areas, specific methodologies would be applied with higher resolution that would enable border detections, enabling a better assessment not only regarding the location and date of land cover modification but the area. Also, a statistical model will be carried out for socio and geographical variables, therefore mapping the factors leading to land use modification and, therefore, possible conflicts. This will aggregate an increased land monitor capacity which currently is solely based on secondary sources. The research provides an increased set of information to support organizations in campaigning for land rights. The results are still to be shared and validated with local and international NGOs.

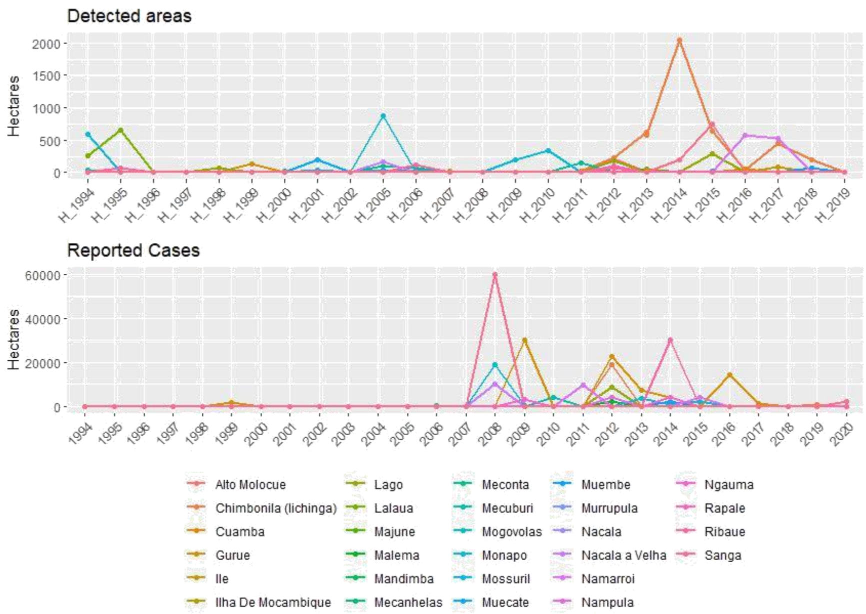

Figure1 Detection of land modifications and reported cases between 1994 and 2020

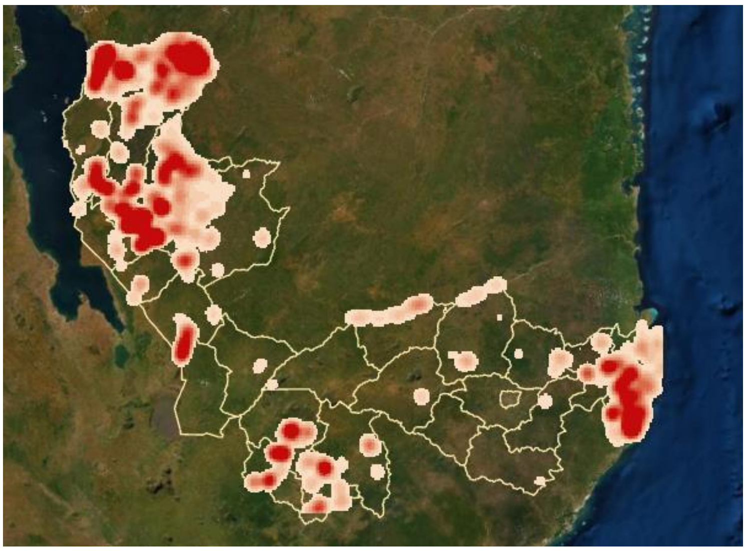

Figure2 Hotspots of land use/cover modification

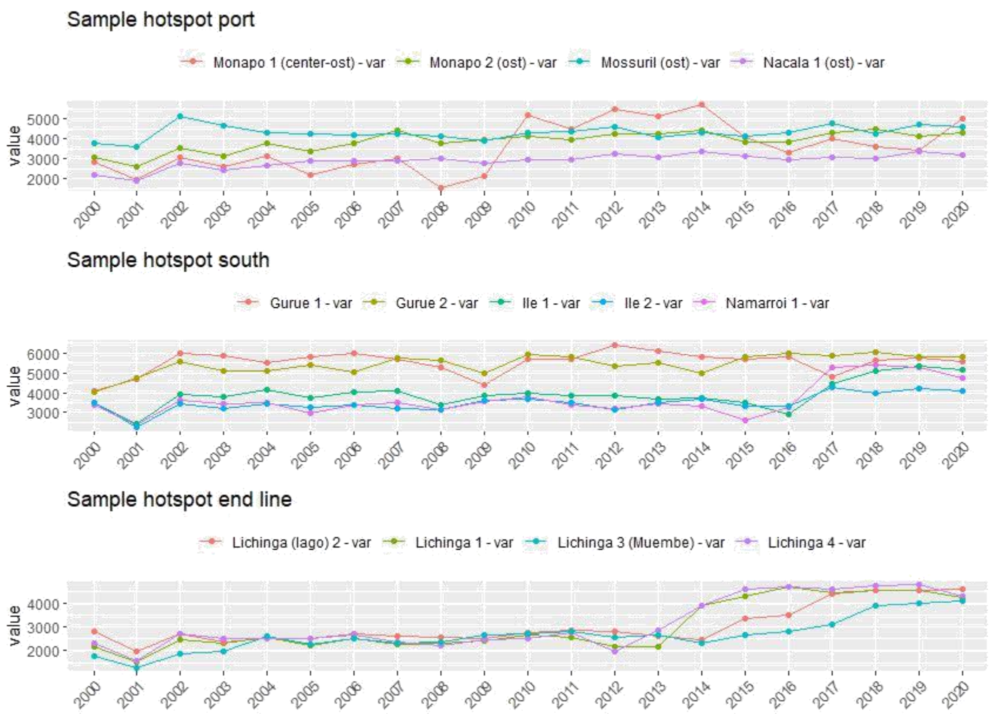

Figure3 EVI variation in sample areas

Mapping Forest Change Areas and Assessing Forest Disturbance Agents from Sentinel-2 Time Series

Janik Deutscher[1], Martin Puhm[1], Andreas Wimmer[1], Katja Öhmichen[2], Jens Wiesehahn[3]

1 Joanneum Research, Austria
2 Thünen Institute of Forest Ecosystems, Germany
3 Nordwestdeutsche Forstliche Versuchsanstalt, Germany

Keywords (5): forest disturbances, times series modelling, bark beetle infestation, storm damage

The challenge

Recent forest disturbances in Central and Eastern Europe show an unprecedented frequency and extent. Observed damages are mainly a result of windthrow events (e.g. Vaia, Friederike, Hartmut, Burglind, Yves) and of pest invasions. Recent drought conditions have fostered a dramatic increase in bark beetle activity in most of Central Europe. On a regional level, we also observe smaller scale invasions of e.g. gipsy moth or nun moth. As a result, there is a growing need to rapidly map, analyse and assess forest damage so that forest owners can initialize sanitary measures quickly. In addition, there is a demand for harmonized damage statistics to assess the economic damage incurred. In ongoing research projects, we are developing workflows to extract this information from Sentinel-2 time series. The challenge lies in quickly and accurately detecting forest damage and classifying the forest disturbance agents, which show spectral changes that vary considerably in both magnitude and time.

Methodology

The presented Sentinel-2 forest change detection workflow is based on two major components: a) a near real-time change detection workflow specifically tuned to forest areas, and b) an assessment of forest disturbance agents for the detected forest change areas.

The Sentinel-2 time series is pre-processed including atmospheric correction, terrain and BRDF correction, a coregsitration of all images, and a masking of clouds, cloud shadows and other artefacts with the Fmask algorithm. Time series modelling is based on a structural time series model. We use a Kalman filter to update the model with every new observation. Model updates are based on the differences (or innovations) between the model prediction (or filtered image) and the real image. These innovations are weighted by an additional observation quality file to further reduce the impact of remaining artefacts on the model update. We detect forest changes by calculating a cumulative sum of consecutive innovations and by applying empirical thresholds. The result is a near real-time map and an annual map of forest change areas >0.1ha.

Following the forest change detection, we classify all change areas by disturbance agent. Currently, classes “bark beetle”, “storm damage”, “gypsy moth”, “drought stress” and “clearcut” are considered. We perform a detailed separabilty analysis of these disturbance agents based on a reference dataset of more than 20.000 interpreted forest change areas in Germany and Austria.

Results

Results include an annual forest change map - with reference date end of August - and a near real-time forest change map. Both products have an MMU of 0.1ha and a spatial resolution of 10m. These products are now validated in several regions of Germany and Austria. First results from Niedersachsen in Germany show an overall accuracy of detected forest changes of 97.5% for the annual forest change map. Damaged forest areas show ~93% accuracy, while undamaged forest areas show >99% accuracy based on a stratified point based sampling. A classification of disturbance agents needs to analyse both the spectral magnitude and the temporal behaviour of the change event. First results from the separability analysis show that we can best detect windthrow areas in the SWIR and NIR band. Windthrow areas show an abrupt increase in reflectance. We can often separate two change stages: 1) the windthrow event itself, and 2) the subsequent clearing. Bark beetle infestation is mostly visible in the red band, the SWIR bands and the RE-bands. The observed reflectance changes relate to needle color changes and occur more slowly over the entire vegetation season with a peak in the late summer months. Gypsy moth invasion is characterized by a rapid high magnitude change in reflectance in late spring/early summer. The affected broadleaf stands recover quickly in

July/August. We will present examples for all disturbance types and discuss the implications for classifying forest disturbance agents.

Outlook for the future

Current, preliminary results show that an accurate detection of forest changes and an assessment of forest disturbance type is possible for change areas >0.1ha. A more detailed accuracy report covering seven Sentinel-2 tiles in Germany and two tiles in Austria is in progress and expected ready by fall 2022. It will cover both the annual and near real-time forest change products and the forest disturbance type layers. Once the best performing workflow is determined, we will set up an operational and uniform forest monitoring service for Germany and run it on a tailored EO cloud-processing infrastructure (CODE-DE). In the future, rapid Sentinel-2 information on forest damage and on disturbance type can be used to quickly respond to forest disturbance events, to report annual damage statistics and to assess the economic damage.

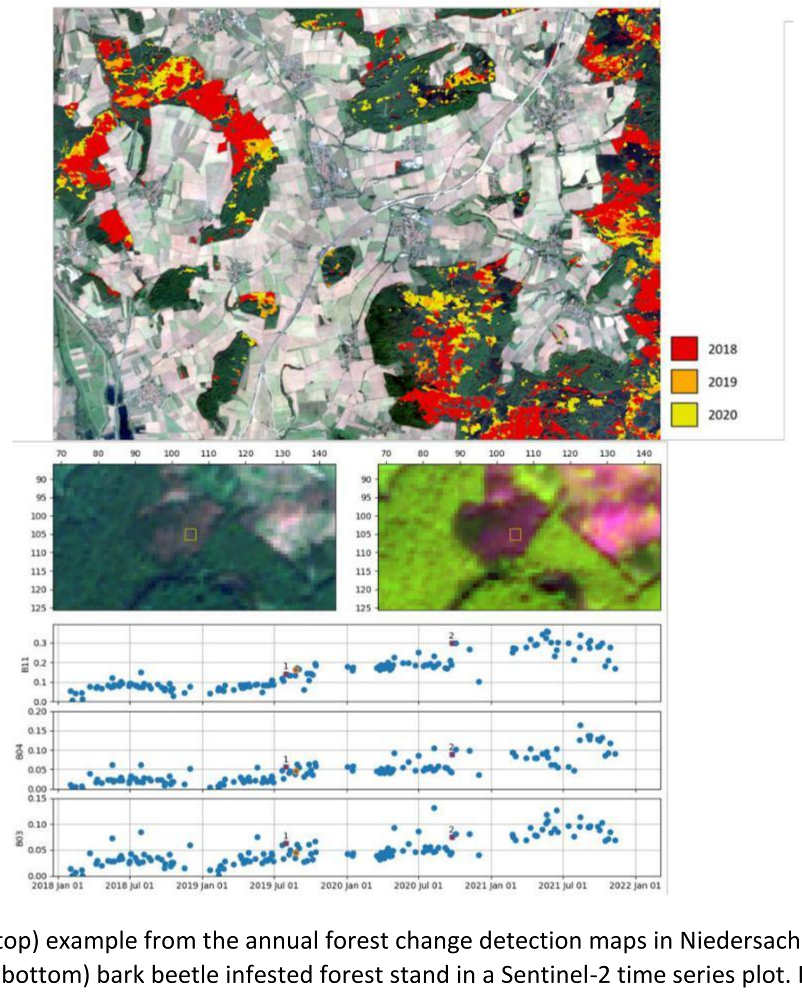

Figure 1 (top) example from the annual forest change detection maps in Niedersachsen, Germany (bottom) bark beetle infested forest stand in a Sentinel-2 time series plot. Image left is RGB, right is SWIR2/NIR1/RED. Point 1 marks the beginning of the infestation, point 2 marks the sanitary logging one year later.

Improved Handling of Artefacts in Sentinel-2 Time Series Modelling and in Detection of Vegetation Disturbances

Martin Puhm[1], Janik Deutscher[1], Andreas Wimmer[1]

[1] Joanneum Research, Austria

Keywords: time series analysis, NRT monitoring, signal artefact handling, observation quality, forestry

The challenge

When working with optical image time series, subtle changes in the spectral signal related to biotic and abiotic vegetation disturbances may be hidden between phenology, signal artefacts and noise, leading to high false alarm rates when trying to map small scale vegetation disturbances. Structural time series models in combination with the Kalman filter are powerful tools with respect to phenology adaptive signal tracking and noise reduction. This class of stochastic models enables an online decomposition of the input signal into trend and seasonal components, with the highest weight being placed on recent observations. However, the presence of a wide range of signal artefacts is problematic in this regard. After pre-processing, we still observe a large number of un-masked clouds with varying degrees of transparency, fog, haze, snow, and cloud shadows in pre-processed Sentinel-2 imagery. These artefacts cause signal deviations that are unrelated to vegetation changes on the ground. To improve the signal tracking ability of the Kalman filter, we designed a new workflow where observations influenced by artefacts are reliably down-weighted or discarded altogether.

Methodology

In order to better detect and handle signal artefacts in Sentinel-2 time series analysis, we propose a novel pre-processing workflow based on the tasseled cap transformation. For now, we tuned and tested this workflow for near real-time forest monitoring applications in Europe, Africa and Asia. The underlying principle is that we can use the properties of certain tasseled cap components to derive reliable information about the quality of an observation. We then use this quality indication to dynamically set the observation noise parameter for the Kalman filter on a per-pixel basis. During the dynamic model update step, observations (at single pixel level) with low quality receive a lesser weighting than observations of high quality. This significantly reduces the impact of artefacts during model state updates. The estimated model states (here trend and seasonals) now better represent the ground information, which better reflects the principle idea of vegetation monitoring. In addition to existing change detection methods, where affected areas are identified by comparing pre-change model forecasts with new observations, it is now also possible to include the effects of changes on the model states. This can improve the detection of subtle and slowly progressing disturbances.

Results

The result of the proposed workflow is a dynamic time series model with reduced noise levels from various artefacts. The reduced noise levels now allow us to map small magnitude vegetation changes that previously were of similar magnitude than the model noise and which we could therefore not detect accurately. The effect of the reduced noise levels is exemplified in the figure below, which shows the spectral behaviour of a Sentinel-2 pixel with beginning bark beetle infestation in summer 2019. The plot on the left shows the original time series after pre-processing, the plot on the right shows the weighted time series resulting from the improved workflow. Blue dots represent single observations; some dots are missing in the right hand plot, because the observation quality was considered too low. The middle section of the plot shows the deviations between model prediction and the unweighted (left) and weighted (right) observations. The yellow bars represent empirical thresholds for detecting forest changes. It is obvious that the model deviations are much reduced with the improved workflow. The original workflow (left) would detect a large number of potential vegetation changes that in fact are simply a result of remaining artefacts in the imagery. In addition, the trend and seasonal components (bottom) are more stable in the improved workflow. The new workflow also allows us to produce filtered artificial images of good quality for any DOY without including obvious artefacts.

Outlook for the future

The suggested improvements to reduce the impact of artefacts on dynamic time series modelling and near real-time change detection will allow us to detect more subtle vegetation changes from optical satellite image time series. Examples of applications that we are currently investigation include the detection of forest disturbances and the classification of their various disturbance agents. Currently, the proposed workflow is tuned to forestry applications, but the method has potential to also work for other LULUCF applications. In addition, the improved filtered and mostly artefact-free images could be used as input to various classification tasks. These filtered images have the advantage of being free from no data areas, which simplifies many classification tasks.

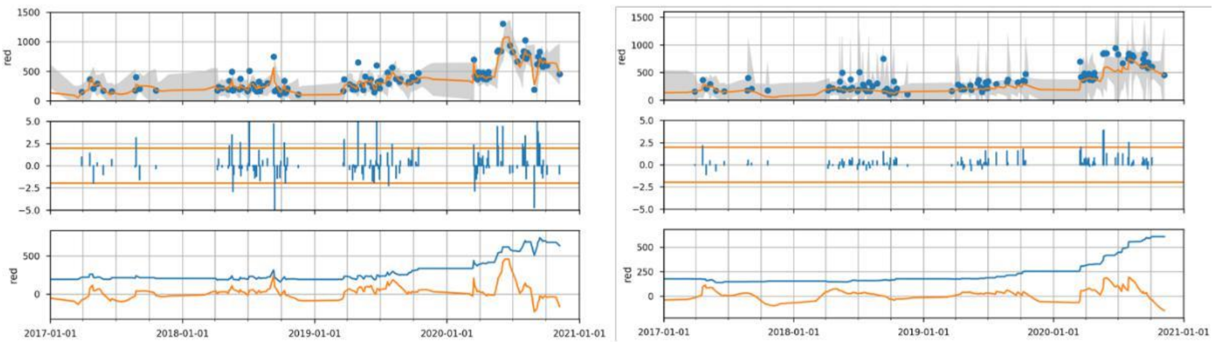

Figure 1 Sentinel-2 time series plots (red band) for a pixel affected by bark beetle infestation in 2019 and the following years. (left) normal pre-processed time series and structural time series model (top: yellow line);(right) time series and structural model with the proposed image quality weighting applied to reduce the effects of various artefacts on the model state updates

The use of Sen4CAP in an attempt to perform Common Agricultural Policy monitoring in Cyprus

Marios Tzouvaras[1,2], Dimitris Sykas[2], Christiana Papoutsa[1,2], Maria Prodromou[1,2], Elena Papageorgiou[3], Christiana Theodorou[3], Agathangelos Hadjichristofi[3], George Georgiou[4], Diofantos G. Hadjimitsis[1,2]

[1] Eratosthenes Centre of Excellence, Limassol, Cyprus
[2] Department of Civil Engineering and Geomatics, Faculty of Engineering and Technology, Cyprus University of Technology, Limassol, Cyprus
[3] Cyprus Agricultural Payments Organisation, Cyprus
[4] Novatex Solutions Ltd, Nicosia, Cyprus

Keywords: common agricultural policy, crop classification, remote sensing, Copernicus

The challenge

The 'Monitoring System' has been included in the EU Regulation (ER) 809/2014 by the Regulation's Amendment 746/2018, Article 40 (a) "Controls through Monitoring"[5]. It emphasises the use of Copernicus Sentinel data, or other data of equivalent value, by the competent authorities to establish a procedure for the systematic observation, tracing and evaluation of eligibility criteria, commitments and obligations related to the eligibility of the aid requested by farmers, and for the correct calculation of subsidies provided to them by the government. In this direction, CROSS project (ESA Contract No.: 4000131190/20/NL/SC) titled "Preparatory Activity for Monitoring & Identification of arable CRops in CypruS" was funded by the 3rd Call for Outline Proposals under the Plan for European Cooperating States (PECS) in Cyprus, to facilitate the adoption of Sen4CAP[6] by the national Common Agriculture Policy (CAP) monitoring and paying agency, the Cyprus Agricultural Payments Organisation (CAPO).

Methodology

The Sen4CAP software was used through CREODIAS, benefitting from direct access to the complete Copernicus Sentinel data repository and the dynamically scalable processing power of the CREODIAS cloud computing environment. Its performance on crop type classification was tested for year 2019, considering the specificities of the agricultural sector in Cyprus, i.e., soil conditions, parcel geometries, and parcel sizes. The farmers' declarations database, received by CAPO, was formatted appropriately, prior using it on Sen4CAP.

The farmer's declarations gathered by CAPO are classified into 345 crop types. Each type has its own crop variety, which leads to new additional codes, i.e., the crop type vineyard includes 40 crop variety codes. This detailed taxonomy is not optimal for satellite-based classification and does not provide added value in the monitoring objectives of CAP. For all the crop codes that CAPO uses, 51 groups were classified (Figure 1). Some crops were identified as separate crop groups while some others, which are not involved in Greening purposes and crop rotation, were grouped. Those crops have common characteristics such as a common

---

5 Article 40 of EU 746/2018: https://eur-lex.europa.eu/legal-content/EN/TXT/PDF/?uri=CELEX:32018R0746&from=en
6 Sen4CAP: http://esa-sen4cap.org/

phenological cycle, a similar cultivation method and also have the same sowing and harvesting periods. For example, in group 2 the durum wheat and non- durum wheat crops were grouped together because they have common characteristics when sowing, growing, and harvesting.

The Area of Interest (Figure 2), the farmers' declarations and a LookUp Table (LUT) file were uploaded, and the season under study, from 01/03/2019 until 01/09/2019, was defined. Two experiments were performed: a standard execution of the crop type classifier (1) including all crop codes; and (2) without grassland and fallow land related codes. The latter are classes with high variability and usually contain high rates of false declarations. The overall classification accuracy and the kappa coefficient were used to evaluate the experiments' results, calculated as:

$$\text{Overall classification accuracy} = \frac{\sum_{i=1}^{M} n_{ii}}{N} \quad [1]$$

$$K = \frac{P_{correct} - P_{chance}}{1 - P_{chance}} \quad [2]$$

Overall classification accuracy is defined as the fraction of the total corrected classified parcels on all categories (n_{ii}) divided by the total number of parcels (N). Kappa coefficient (K) is an indicator of how closely the parcels classified by the used classifier matched the data labelled as ground truth.

Results

The pilot application of Sen4CAP was carried out to test the usability and accuracy of Sen4CAP in the crop type classification. In the 2019 farmers' declarations provided by CAPO, 86 different crop types were found, summing up to 54,430 parcels. From these, 37 crop types were used for the classification. Barley, fallow land, wheat, potatoes, and olives were found to be the prevailing crop types in Cyprus, accounting for about 70% of the total number of parcels and roughly 80% of the total area. Using all the available crop types, the overall classification accuracy was 46.3% with a kappa coefficient of 0.29, whereas in the second experiment, the overall classification accuracy was 53.7% with a kappa coefficient of 0.32. Apart from the significant overall increase in these two metrics, after removing the fallow land and grass land classes, the classification accuracy increase was also substantial in each crop class. Indeed, the classification accuracy was significantly improved (more than 10% in most cases) in 26 classes, the accuracy was practically the same (less than 2% difference) in 8 classes, and there was a decrease in classification accuracy in only one class.

Due to the small parcel sizes and other specificities, and the spatial resolution of Sentinel-2 imagery, only 45% of the parcels were large enough to be classified using the Sen4CAP algorithm. Thus, at the moment, Sen4CAP can only be used to assist the CAP monitoring activities of CAPO in Cyprus.

Outlook for the future

Next steps of the current work will be to evaluate additional classification algorithms beside the random forest one that Sen4CAP uses, and add farmers' declarations from additional years, to understand the model generalization capabilities. As there is an emerging need from all CAP paying agencies in Europe to perform their CAP monitoring activities remotely, thus minimising or even eliminating their on-the-spot checks, ways to improve the accuracy of Sen4CAP and/ or other Earth Observation based solutions need to be further investigated. From the pilot application of Sen4CAP in Cyprus, certain steps were identified in the direction to adopt Sen4CAP as an operational tool. Some examples are the time series analysis of crops; the modification of the algorithm's threshold to extract information even in cases that 80%-90% of a pixel can be found in specific parcel; and the pan-sharpening/ spectral unmixing of the non-pure parcels that intersect with parcel boundaries. Finally, the inclusion of higher resolution satellite (e.g. Spot, WorldView, PlanetScope etc.) and UAV images to mitigate the small and elongated parcels issues, could further improve the crop classification accuracy of Sen4CAP.

Acknowledgements: The authors acknowledge the 'EXCELSIOR': ERATOSTHENES: EXcellence Research Centre for Earth Surveillance and Space-Based Monitoring of the Environment H2020 Widespread Teaming project (www.excelsior2020.eu). The 'EXCELSIOR' project has received funding from the European Union's Horizon 2020 research and innovation programme under Grant Agreement No 857510, from the Government of the Republic of Cyprus through the Directorate General for the European Programmes, Coordination and Development and the Cyprus University of Technology.

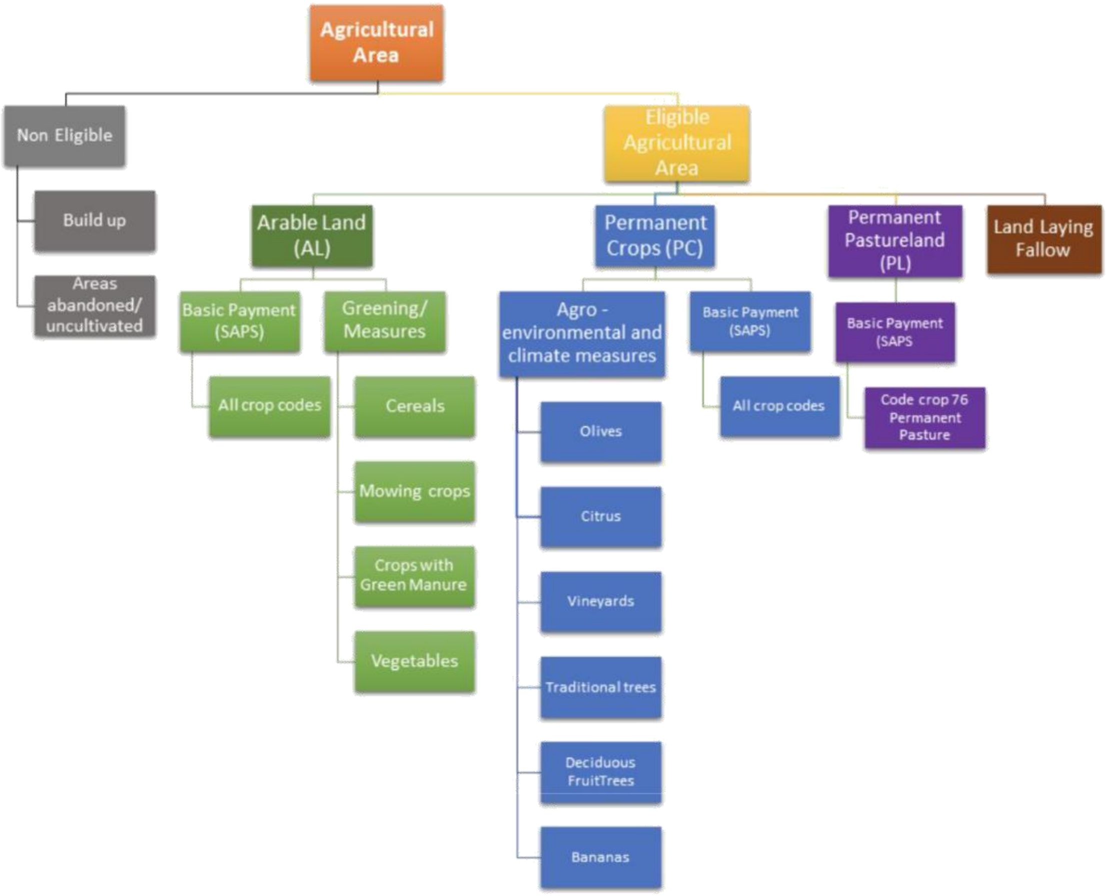

Figure 1. Crop type taxonomy

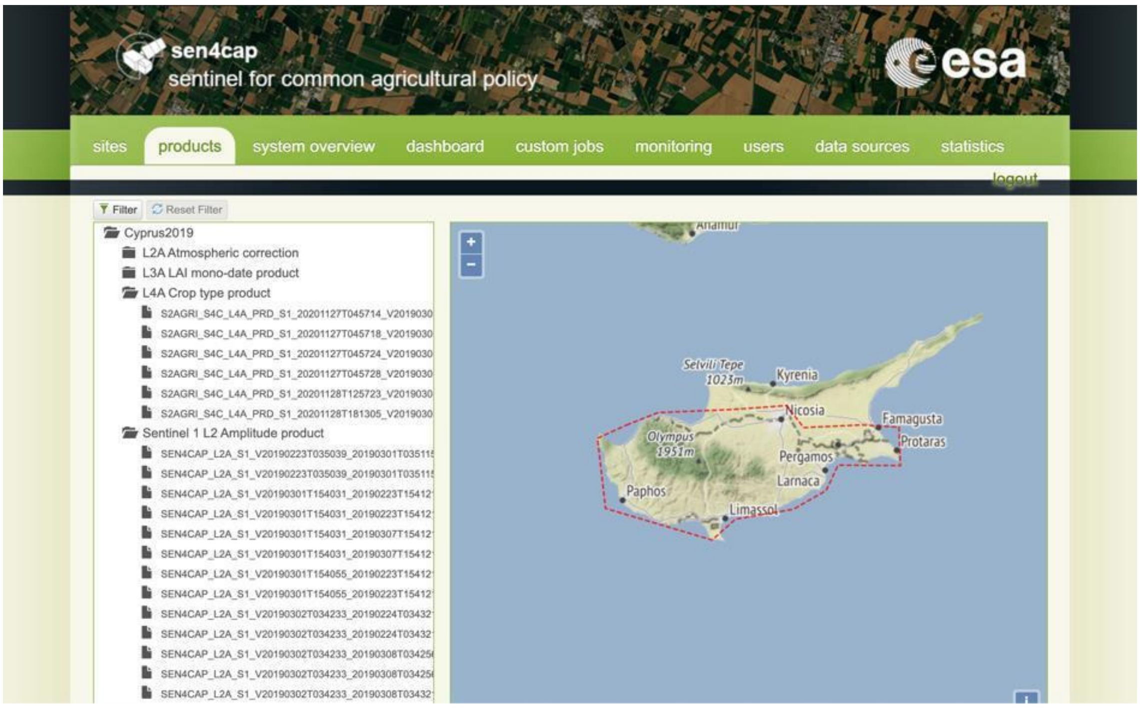

Figure 2. The Cypriot Area of Interest and products generated from Sen4CAP

S_Agri2: Agroforestry, Forests, Agriculture and Food Security

Chair(s): Dr. Marios Tzouvaras

Multi-annual monitoring of mowing dynamics in German grasslands with Sentinel-2 time series

Sophie Reinermann[1], Sarah Asam[2], Ursula Gessner[2], Claudia Kuenzer[1,2]

[1] Department of Remote Sensing, Institute of Geography and Geology, University of Würzburg, 97074 Wuerzburg, Germany

[2] German Aerospace Center (DLR), Earth Observation Center (EOC), German Remote Sensing Data Center (DFD), Germany

Keywords (5): Cutting, Sentinel, management, time series, detection

The challenge

Globally, grasslands cover about one third of the earth's surface, and in Germany, they make up for around one third of the agriculturally used area. They are mainly used for fodder production, however fulfil multiple ecosystem services, like provision of habitats for insects, spiders and birds, storage of carbon within below-ground biomass, water purification and erosion control. To what degree these ecosystem services are present is determined by site conditions and the management of the grasslands. In Germany, main management strategies include mowing (one to six times per year), grazing and fertilization. The management strategy and the use intensity (e.g. mowing frequency) vary strongly and their spatial distribution is not known in Germany. In order to enable the modelling of ecosystem service provision of grasslands, for example of yields or nutrient fluxes, information on the timing and frequency of mowing events are crucial. The exploitation of satellite data time series enables the analysis of grassland mowing dynamics.

Methodology

Time series of Sentinel-2 data were analysed to detect grassland mowing events for the years 2018, 2019, 2020 and 2021. The satellite data was masked with the Copernicus HRL (Grassland) of 2018 to extract pixels which are covered by grassland. Sentinel-2 data was pre-processed with the MAJA algorithm and pixel-based time series for the periods March to November were filtered, interpolated and smoothed. The Enhanced Vegetations Index (EVI) was calculated based on the pre-processed time series and mowing events were detected by using a rule-based thresholding approach. The approach was calibrated on grassland parcels in southern Germany which cover the full spectrum of management options. The mowing event detection was validated by comparing the derived dates to mowing information from farmers and mowing dates extracted from cameras. The amount of correctly detected mowing events and the F1-Score was calculated to evaluate the mowing event detection. Annual information on mowing dynamics, like the mowing frequency and the timing of the first mowing event, was investigated to highlight spatial patterns within Germany and differences within the four investigated years.

Results

For all four years, the detection approach resulted in plausible datasets at 10 m spatial resolution, as can be seen in the map of mowing frequencies (Figure 1). Even though the mowing detection is pixel-based, the resulting maps depict the field borders of single grassland sites. The validation with the reference dataset shows that the Sentinel-2-based thresholding approach detected around 65% of the mowing events successfully among the four years, when a time frame of 7 days between the detected date and the validation date was allowed. A detailed analysis of the time series of several sites shows that the detection approach is mainly limited by cloudy weather conditions as the mowing events are only visible for around 10 to 14 days within the satellite observations. There are differences within the mowing dynamics depictable among the four years. These patterns are not homogenous within Germany, but occur at smaller scales. For example, in 2018 the mowing frequency was changed and timing of the first mowing event was shifted towards an earlier date for large parts of Germany when compared to the other years. This might be the consequence of the extraordinarily warm and dry weather conditions in Central Europe in 2018.

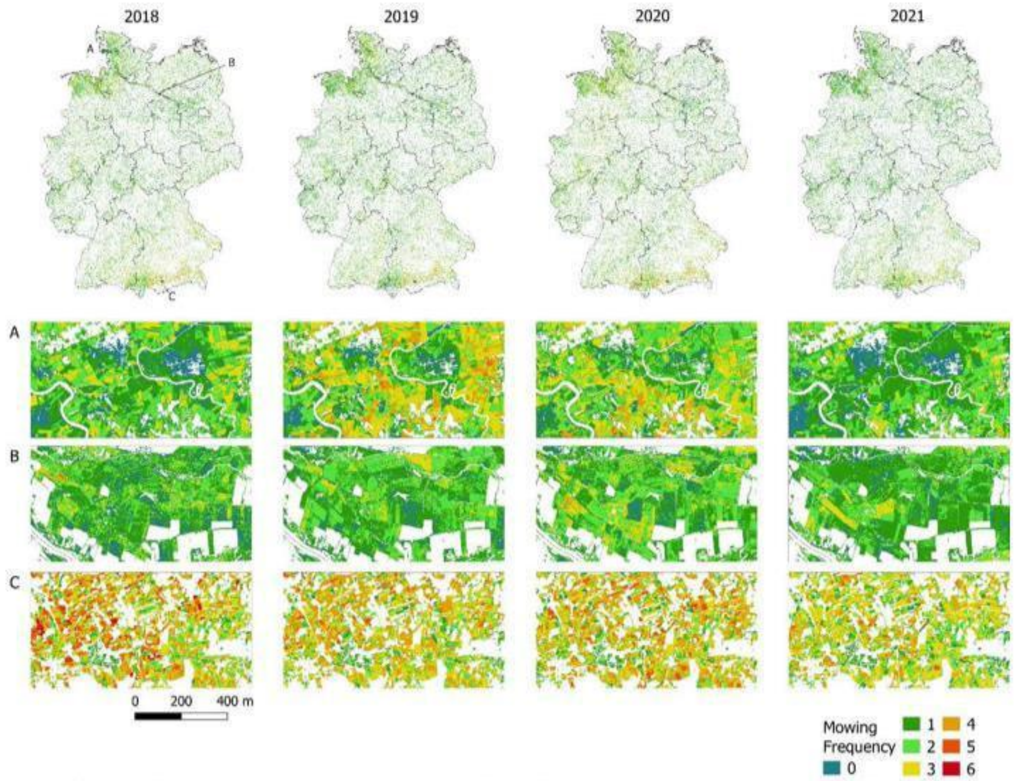

Figure 1 Grassland mowing frequency of four years detected by the Sentinel-2 time series-based thresholding approach for Germany and zooms (A-C) to three differently structured grassland landscapes.

Outlook for the future

The detection of grassland mowing events and the multi-annual analysis of mowing dynamics in Germany reveal general patterns of use intensity and small-scale fluctuations within the years. The detected dates of mowing events can serve as input for modelling grassland ecosystem services and consequently, support the development of sustainable management strategies. In addition, multi-temporal satellite based estimation of grassland biomass in combination with information on mowing events allows the estimation of annual grassland production. In this regard, information on the mowing regime might enable grassland yield estimation and quantification of annual fluctuations of yields, like potential shortages within a drought year.

Assessment of Growth and Mortality Rates in Canadian Boreal Forest using Landsat Time Series

Alexandre Morin-Bernard [1], Alexis Achim [1], Nicholas C. Coops [2]

[1] University Laval, Department of Wood and Forest Sciences, Canada
[2] University of British Columbia, Department of Forest Resources Management, Canada

Keywords (5): Landsat, Time series, Forest growth, Forest mortality, Tasseled cap transformation

The challenge

Forests are a key component of global efforts to mitigate climate change, because of their ability to sequester carbon during the lifetime of trees and afterwards through wood products. However, changes in growing conditions and increases in the occurrence of extreme climate events are likely to lead to a decreased productivity in some forest ecosystems. While tremendous progress has been achieved in detecting and monitoring severe disturbances using remote sensing, monitoring subtle changes in forest growth remains a challenge. Yet, these progressive changes could have major impacts on the future of forest carbon balance and wood supply. Recent findings have shown that using NDVI trends as a proxy of changes in forest productivity could be biased by the natural process of forest succession. The objective of this study was to identify more reliable satellite-derived vegetation indices for the monitoring forest growth and assess trends over the study area in the last decades.

Methodology

Study site was located in the eastern boreal forest of Canada. We used data from permanent sample plots located in black spruce (Picea mariana (Miller) BSP) stands to derive trends in net growth and mortality over periods ranging from 10 to 30 years between 1984 and 2019. We relied on Landsat data because of its temporal coverage and a spatial resolution appropriate for forest management purposes. Time series of annual, gap-free, best-available pixels surface reflectance composites were built over the study site during the investigated period. Annual values of several vegetation indices were calculated over a 3 x 3 pixel window enclosing the plots. The nonparametric Mann-Kendall test was used to detect significant monotonic trends in the vegetation indices values and the sen's slope was calculated. Relationships between detected trends and the growth and mortality rates derived from field measurements were investigated using ordinary least square and logistic regression.

Results

Results suggest that alternatives exist to greenness-based indices for the monitoring of forest growth and mortality rates that are more reliable and less influenced by successional stages. There were variable but statistically significant relationships between most vegetation indices and both growth and mortality rates derived from field measurements. Analysis of data using ordinary least square regression resulted in r-squared values ranging from 0.1 to 0.5 between Sen's slope of vegetation indices time series and annual net growth or mortality rates depending on the vegetation index and study site. Binary logistic regression models including the Tasseled Cap Wetness or NBR allowed to differentiate plots with high mortality rates from plots with low mortality rates with accuracy exceeding 70%. For some vegetation indices, presence of noise in the Landsat time series required to increase the minimum segment length in order to detect a significant trend. The best models were used to map the changes in growth rates over the study site in the last decades and identify areas of high mortality.

Outlook for the future

Results from this study will provide the required knowledge to pursue research efforts aiming to identify forest stands that are the most vulnerable to climate change and to identify forest structural and compositional attributes linked to a greater resistance and resilience to climate-related stressors. This knowledge will allow improving growth models and better assess the impacts of climate change on forest's carbon balance and wood supply projections. Growth and mortality maps generated in this study will also be used for upcoming field sampling efforts aiming to collect increment cores and discs on a wider range of stand structures and compositions to investigate the possibility to monitor growth and mortality on shorter timescales. As the temporal coverage of other satellite programs such as Sentinel increases, the data they provide will be integrated in the framework, allowing for a continuous monitoring of forest growth and mortality.

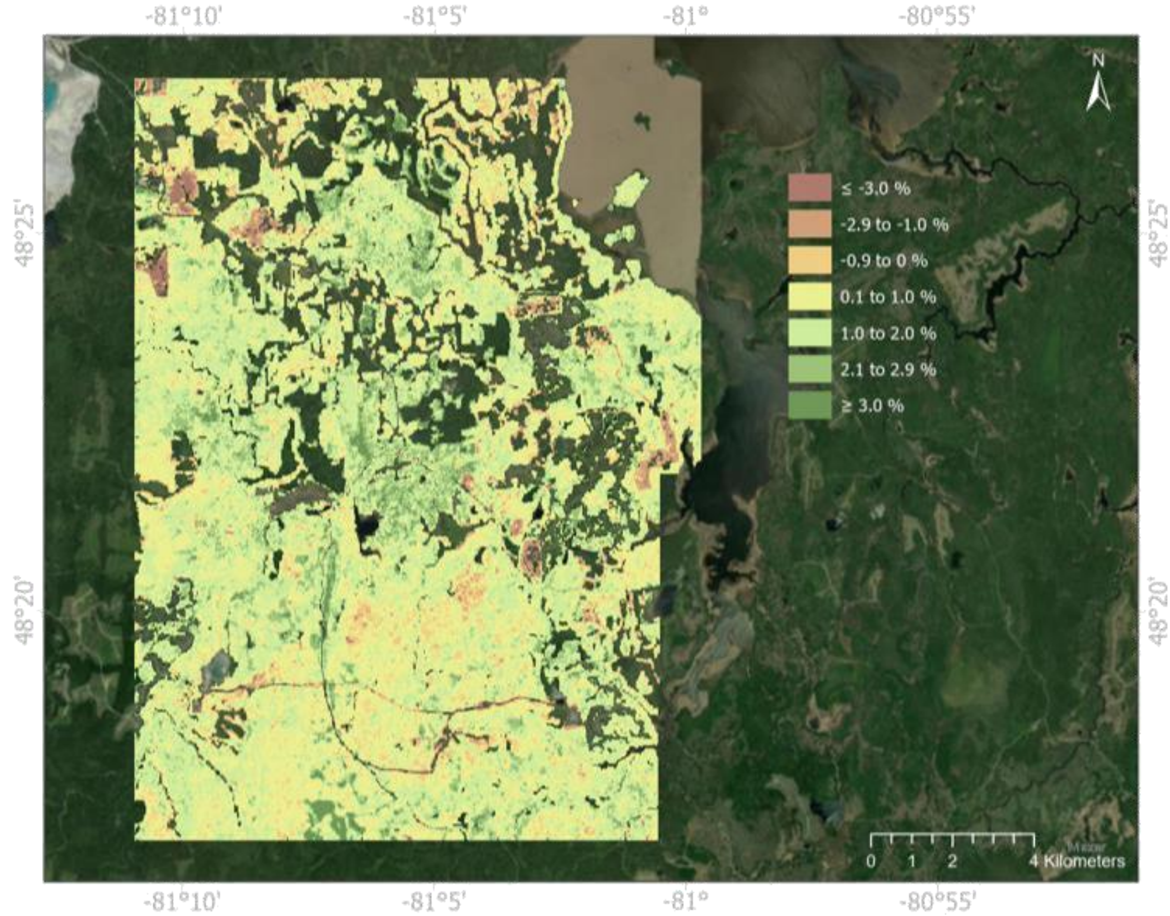

Figure 1 Estimated average annual change in living basal area for the 1984-2021 period in a section of the study site

Spectral Indices as a Tool to Assess the Moisture Status of Forest Habitats

Adam Młynarczyk[1], Monika Konatowska[2], Sławomir Królewicz[1], Paweł Rutkowski[2], Jan Piekarczyk[1], Wojciech Kowalewski[3]

[1] Adam Mickiewicz University in Poznań, Faculty of Geographic and Geological Sciences, Poland
[2] Poznań University of Life Sciences, Faculty of Forestry and Wood Technology, Poland
[3] Adam Mickiewicz University in Poznań, Faculty of *Mathematics and Computer Science, Poland*

Keywords (5): Spectral indices, forest habitats, NDVI, water, Sentinel-2

The challenge

Measurement of water content in forest habitats is considered essential not only in ecological research on forests, climate change, or forest management, but also in protection against floods, wildfires, and soil erosion. In the traditional forest habitat classification, two systems of habitat conditions analysis are found: single factor and multifactor methods. Both are laborious and therefore costly. Remote sensing methods provide a low-cost alternative. The aim of the presented study was to find the relationship between the spectral indices obtained from satellite images and the Forest Habitats Moisture Indexes used traditionally in the Polish forest habitats classification system and to enable their practical use in forest management and the protection of forest ecosystems.

Methodology

The research area is the Bory Tucholskie National Park (BTNP), considered by authors as a representative area for Polish forest conditions. Geometric data on the ranges of forest habitat units, available in the SHP format, together with the database in the following formats: .prj, .sbn, .sbx, .shx, were obtained from the website of the BTNP Geoportal (http://gis.pnbt.com.pl/). Due to the spatial resolution of satellite images (10-60 m), units with an area smaller than 1 ha were excluded from the analysis, which also corresponds to the methodology of identifying forest habitat conditions using the traditional terrestrial method. The search and download of Sentinel-2 (A, B) images of the European Space Agency were accomplished using the Polish data repository of the Copernicus program, managed by the Polish Institute of Meteorology and Water Management. The characteristics of the Multispectral Instrument sensor on S2A and S2B platforms are available on the ESA website. Data from the level of the product Level L2A were used for the analysis. For each Sentinel-2 data recording date, the average values from pixels DNs corresponding to a reflectance multiplication by 10,000, were calculated for forest habitat units (polygons) – for all spectral bands (except for band number 9, which is not present in the L2A product). Calculations were made in Microimages TNTmips v. 2021. After the selection and analysis of the formulas, 191 indicators were selected for the calculation.

Results

In the vector layer of the map of Park's habitats, 923 contours were distinguished, covering the area of forest habitats with seven degrees of Forest Habitats Moisture Indexes. Based on the level of the spectral curves (reflectance) in the near infrared range (channel 8A), three groups of habitats with different FHMI can be distinguished: (i) wet, with mainly deciduous trees, (ii) strongly moist, very moist and moist –covered with mixed forest and (iii) moist-mesic, mesic and dry, covered with pine forests. The driest habitats were distinguished by higher reflection in the visible range, especially in the red channel and in the range of short-wave infrared SWIR in channel 12. After analyzing 191 other indicators used in remote sensing, it was found that, NDVI is very useful to assess the degree of forest habitats moisture, but the data must be obtained during the full growing season, which in the conditions of Central Europe (and tested area) falls from June to August. The use of NDVI made it possible to distinguish and visualize on the map of the studied area 4 humidity groups of habitats (swampy, moist, mesic and dry), coinciding with the results obtained using traditional, ground-based measurements. The obtained results also indicate the possibility of using NDVI to assessing the fertility gradient of forest habitats. Within the studied area it has been shown that the fertility of habitats decreases with increase of distance from the water reservoir.

Outlook for the future

The presented results of the study could be implemented in forestry practice, which should significantly reduce the costs of identifying the diversity of forest habitats. The usefulness of the obtained results may, for example, refer to the determination of the boundaries of habitat units, which, based on the NDVI, are clearly visible, and their accuracy, related to the resolution of satellite images on which the study was conducted (10 × 10 m), is entirely sufficient for the needs of forestry practice. The results of the research can also be used to monitor the forest with regard to possible changes in the trophicity of habitats, which should help to protect forest ecosystems in the conditions of changing water resources, as a result of the impact of natural and anthropogenic factors.

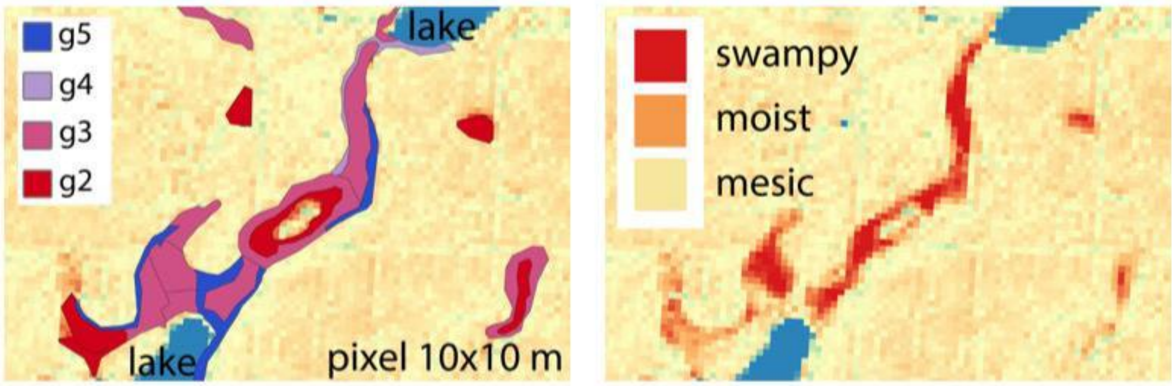

Figure 1. Comparison of the image of a fragment of the habitat map made with the traditional method of soil pits (left) with the image of the same area differentiated due to the NDVI values (right)

High-resolution Aerial RGB Imagery For Flowering Intensity Quantification: A Triennial Study In A High-density Apple Orchard

Chenglong Zhang[1,3], Lammert Kooistra[1], Joao Valente[2], Leifeng Guo[3], Wensheng Wang[3,4] (Style: Authors, presenting author underlined)

[1] Wageningen University & Research, Laboratory of Geo-Information Science and Remote Sensing, The Netherlands
[2] Wageningen University & Research, Information Technology Group, The Netherlands
[3] Chinese Academy of Agriculture Science, Agriculture Information Institute, China
[4] Ministry of Agriculture and Rural Affairs, Key Laboratory of Agricultural Big Data, China

Keywords (5): apple orchard, flower cluster, UAV, RGB, remote sensing

The challenge

Flower thinning has long been used in orchard management, especially in the practice of stone fruit production. This flower load control activity optimizes the sugar level, fruit size, fruit colour and even storage life of the fruits harvested in the autumn, therefore it guarantees the marketable competitiveness of the orchard. Yet, current technological progress still can not provide a precise flowering intensity estimation to guide this process. Whilst the research carried out in the machine vision community has achieved high accuracy in the flowering intensity estimation at picture level, there have been few investigations into the estimation at tree level. The main challenge of the flowering intensity estimation at tree level is the flower occlusion problem, which significantly affect the estimation performance based on image processing. Recent successful use of unmanned aerial vehicle (UAVs) in agriculture show potential in addressing these problems.

Methodology

An 'Elstar' apple orchard in Randwijk, the Netherlands, was taken as an example to develop the tree-level flowering intensity estimation approach based on RGB images derived from UAVs(Figure1,a). Aerial images and ground truth (GT) were collected for three consecutive years, and different UAV flying altitudes were conducted for comparison. GT consists of flower cluster number and floridity and was recorded for the fifth row in the orchard. UAV images derived from the oblique mission were first divided into two groups, East-view and West-view. Images from both groups captured row5 were filtered out using the image selection approach proposed in this study. Second, individual trees in row5 within the selected images were cropped based on an image crop algorithm developed. Afterwards the threshold segmentation method was applied in blue band for the segmentation of flower associated pixels. Based on the flower pixels segmented, three flowering index, percentage index (PGI),pixel index(PI) and area index(AI), were calculated for the estimation of flower cluster and floridity. Finally, the correlation between the flowering indices derived from UAV images and the ground truth recorded in-situ was calculated for the estimation of flowering intensity. In addition, the effects of the vertical and horizontal occlusion exists in UAV imagery was also investigated by comparing the estimation results derived from images captured at different distance to the target trees.

Results

Results showed that the proposed tree-level flowering intensity estimation method based on 2D RGB images derived UAVs is reliable. For the flower cluster estimation, the flowering index PGI showed a consistent correlation over the three years, 2018, 2019 and 2020, and performed better than the indices PI and AI(Figure1, b), with a R^2 of 0.7 and a RMSE of 40. Regarding the flower cluster estimation for individual year, index AI yielded the highest accuracy with a R^2 of 0.8 and a RMSE of 12, which performed better than the state-of-art in flower cluster estimation in orchards. A same pattern was observed for floridity estimation: PGI yielded a R^2 of 0.8 and a RMSE of 0.9 for the floridity estimation over three years, while AI is also the optimal index for the individual year estimation of floridity. To mimic the knowledge behind the floridity judgement derived by the expert, a comparable floridity judgement was also achieved, based on the UAV imagery derived flowering index. The investigation into the effects of vertical and horizontal occlusion towards flowering intensity estimation showed that vertical occlusion in UAV imagery has varying degrees of influence to the flower cluster estimation based on different flowering indices. Comparison between the flower cluster estimation derived from images with various horizontal level indicates that the highest estimation accuracy yielded from the circumstance when the camera position was right in front of the target tree.

Outlook for the future

The use of UAV in supporting orchard management is still in infancy. Though the flower occlusion problem limits the analysis based on 2D RGB images, results from this study provided the potential of tree-level flowering intensity estimation derived from 2D UAV imagery. Further research should be carried out to automate the proposed image selection approach and improve the flower segmentation performance by utilizing advanced computer vision technology, such as deep learning. In modern horticulture, high-density orchards challenge the ground vehicle dependent applications. By contrast, further studies regarding the role of UAV in orchard management would be worthwhile. In the context of precision agriculture, UAV-based applications would dominate multiple management activities in orchards because of its data collection efficiency and convenience.

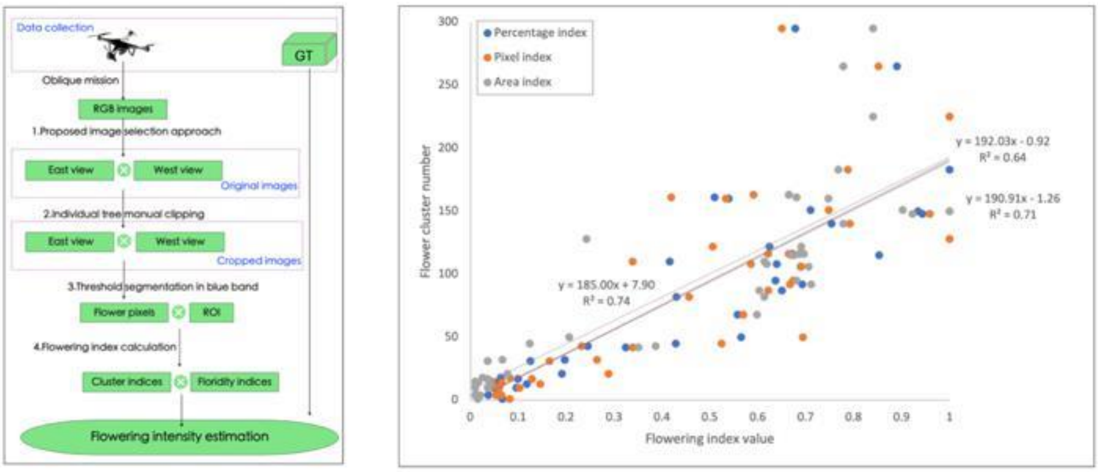

(a) (b)

Figure 1 (a) Workflow of the proposed flowering intensity estimation approach (b) Tree-level flower cluster estimation. Note: the data analysed for each of the three index covers the data collected in three years, 2018 2019 and 2020. GT: ground truth; ROI: region of interest

Poster(s)

Wood Decay Detection In Norway Spruce Trees With Multitemporal PlanetScope Data Analysis

Michele Dalponte[1], Yady Tatiana Solano-Correa[2], Hans Ole Ørka[3], Erik Næsset[3], Terje Gobakken[3]

[1] Research and Innovation Centre Fondazione Edmund Mach, Italy
[2] University of Cauca, Colombia.
[3] Faculty of Environmental Sciences and Natural Resource Management, Norwegian University of Life Sciences, Norway

Keywords (5): wood decay, multi-temporal, PlanetScope, individual tree crowns, classification

The challenge

Norway spruce trees Wood Decay (WD) due to fungal pathogens is among the most serious forest pathogens around Europe. It causes the decomposition of organic material on living trees. The wood of trees affected by WD is usable only as pulpwood or as an energy source, thus substantially reducing the tree's economic value. One of the biggest challenges for early detection of WD is the fact that there are almost no external visual signs of it. The detection of the infestation usually requires coring trees, a costly procedure when applied on a large scale. An alternative that could help to map extensive areas is the use of remotely sensed data. WD detection is complex: it does not usually affect the living tissues of the trees, but only its core, and thus the tree could be under no stress. This paper presents a study on the detection of WD in Norway spruce trees at individual tree crowns (ITCs) level that exploits lidar and PlanetScope (PS) multi-temporal satellite data.

Methodology

The study area is located in Etnedal (Norway). Field data were collected in winter 2019-2020 during the logging operation. Tree's species and WD presence at the stump were recorded. Norway spruce trees were split into 2 classes: "Healthy" (13'195 trees) and "WD" (3'015 trees).

PS images have 4 spectral bands (R, G, B, NIR) and 3m spatial resolution. PS images of May, June, July, August and September 2017, 2018 and 2019 were gathered over the study area: 53 images. Lidar data were collected on August 3 2019, with a Leica ALS70-HP laser scanner and a point density of 17.6pts/m^2. Up to 4 returns per pulse were recorded.

ITCs were delineated on the normalized lidar point cloud using the algorithm implemented in the function *itcLiDAR* of the R library *itcSegment*. The delineated ITCs were matched with the field-measured trees. PS images were aggregated into 13 groups corresponding to June, July, and August 2017, May, June, July, August and September 2018, and May, June, July, August and September 2019. Images of each group were averaged per band in order to obtain one composite multiband image per month (13 images). From each of the 13 PS monthly composite images, a series of vegetation indices (VIs) were extracted: CTVI, GEMI, GNDVI, MSAVI, MSAVI2, NDVI, NRVI, SAVI, TTVI and TVI. The weighted average of VIs pixels overlapping with each ITC was calculated in order to have one value per VI, month of the year and ITC. WD was classified using a weighted support vector machine classifier.

Results

Two subsets of ITCs were considered for evaluation, taking into account their size: (i) all, and (ii) only the ones with an area above 9 m^2 (the size of a PS pixel). The proportion of samples between the classes "Healthy", and "WD" changes considering the two subsets: in the first set we had 5'689 "Healthy" ITCs, and 1'654 "WD" ITCs, while in the second set we had 214 "Healthy" ITCs, and 70 "WD" ITCs. In the image below the results in terms of kappa accuracy obtained for the WD detection with all the possible combinations of features and time periods for all ITCs and only the ones with area >9 m^2 are shown. The accuracies are not very high, underlying the complexity of the problem, but are up to the state of the art results obtained with sensors providing higher spatial and spectral resolution. Thus, adding the multi-temporal variable, while working at coarser spatial and spectral resolutions, clearly helps to map WD. In addition to the ITC area, the time period of year appeared to be a factor with great influence on the results. Thus, the May, June and July images seem to outperform August and September when considering the ITCs with area >9 m^2. The difference in accuracy is smaller between the time periods when all ITCs were subject to analysis. By comparing all the uni-temporal results against the multi-temporal results it emerged that on average the multi-temporal datasets resulted in greater accuracy than the uni-temporal ones.

Outlook for the future

In this study, we explored the possibility to detect WD in Norway spruce trees at ITC level using multi-temporal satellite data acquired by PS constellation. From a management point of view, the possibility of having a WD presence map at ITC level, allows punctual, as well as more precise, interventions in the forest. In this way the spread of the fungi, and therefore the economic loss, could be minimized. The results from the present study could be useful to develop better and more precise management strategies for forests, especially in commercially managed ones. The accuracies obtained are not very high considering all the ITCs but they are promising when considering only the larger ITCs and considering the fact that coarse spatial and spectral resolution data is being used to perform the analysis. For future works, it would be interesting to explore an intermediate point of analysis. This means, considering very high spatial resolution sensors (<1m), with more spectral bands (>4).

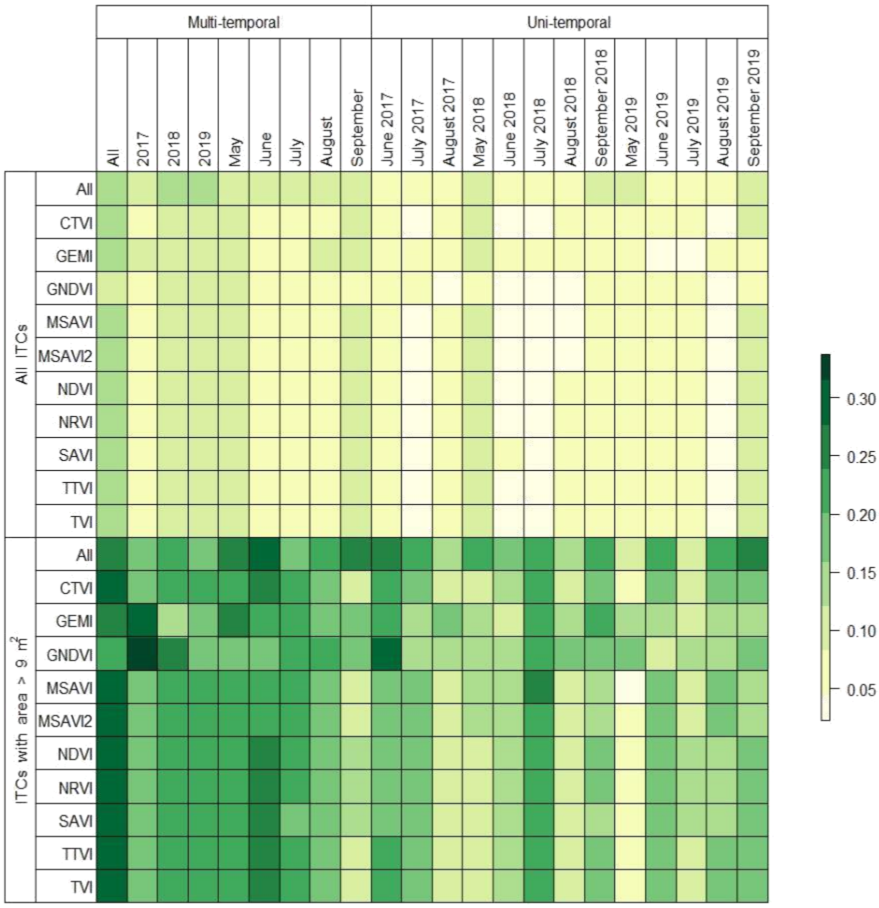

Figure 1 Kappa accuracy for each experiment for WD detection. The names on the top describe the timeperiod, while on the left there are the VIs names and the ITC subsets.

Assessing the consistency of forest biophysical parameters retrieved from Sentinel-2, Landsat-8 and GEDI in Central Germany

Birgitta Putzenlechner[1], Federico Filipponi[2], Philipp Koal[3], Iris Jeuffrard[4], Martin Kappas[1]

1 Georg-August-University Göttingen, Germany, birgitta.putzenlechner@uni-goettingen.de
2 Institute for Environmental Protection and Research (ISPRA), Rome, Italy
3 Forestry Research and Competence Center ThüringenForst, Gotha, Germany
4 National School of Geographic Sciences (ENSG), Champs-sur-Marne, France

Keywords (5): forest, GEDI, Landsat-8, Sentinel-2, vegetation parameters

The challenge

Accurate estimates of vegetation parameters are key for forest monitoring and Sentinel-2 (S2) and Landsat satellite missions currently stimulate the development of operational forest monitoring systems. With ESA's "Biophysical Processor", vegetation parameters can be retrieved (e.g., fractional vegetation cover (FCOVER), leaf area index (LAI), fraction of absorbed photosynthetic active radiation (FAPAR)). There are different versions of the algorithm, but they lack systematic inter-comparison and field validation, especially in forests. Currently, also Light Detection and Ranging (LiDAR) systems deliver promising datasets to obtain structural canopy parameters, such as the NASA's Global Ecosystem Dynamics Investigation (GEDI) mission. In this study it is hypothesized that GEDI data serves for evaluating the consistency of named optical remote sensing (RS) products. We present an initial assessment of the comparability of optical and LiDAR vegetation parameters needed for forest RS.

Methodology

The study was carried out in the Southern Harz region, Germany, in the period 2018-2022 (Fig. 1a). We acquired S2 Level 2A and L8 Collection 2 Level 2 data (corrected for atmospheric and topographic effects), considering quality information (e.g., for cloud masking). The “Biophysical Processor” of the ESA software SNAP was used to retrieve FAPAR, FCOVER and LAI. We applied the newly implemented version (2.0, since SNAP 8.0) for L8 and S2 imagery (either using S2 10 m or also S2 20 m bands). GEDI Level 2B data (v. 2) was collected for the period 2019-2021 and filtered according to quality information, resulting in vertical profile metrics as point data where we focus on canopy cover and PAI representative for the total canopy volume. As ground reference, in-situ data was collected during the vegetation period (AprSep) 2021-2022 in deciduous, coniferous and mixed stands. We acquired digital hemispherical photography (DHP) and used the CAN-EYE software to retrieve FAPAR, FCOVER and PAI. Data collection was scheduled closely around S2 and L8 overpasses. Retrieved products were intercompared, considering absolute values and temporal consistency and validated against in situ data. We compared S2 and L8 derived FCOVER and LAI to GEDI canopy cover and PAI at individual shot locations. Sampled sites had partly been covered by GEDI so that a limited comparison with in situ data could also be included.

Results

Preliminary results show negative change across all RS derived vegetation parameters, mostly in spruce stands which can be attributed to the consequences of recent drought. However, there is distinct disagreement between GEDI and parameters derived from optical RS for low GEDI canopy attributes, as shown for FCOVER in Fig. 1b (red circle). Here we suspect that recent disturbance areas have been undergone succession which cannot be properly detected with the optical products. We observe that the S2 biophysical parameters obtained from the 20 m version of the algorithm tend to show higher agreement with GEDI which we attribute to the additional information included in the S2 red edge and SWIR bands. Further, different definitions of quantities have to be considered: for example, GEDI canopy cover relates to percent of the ground covered by the vertical projection of all canopy material, whereas S2 and L9 FCOVER refer to green vegetation elements only. The comparison with in-situ data reveals mixed results, showing generally higher agreement for GEDI attributes. It is known from previous studies on S2 derived vegetation parameters that the retrieval needs further optimization for forests. While GEDI has been explicitly designed for forest monitoring, the S2 and L8 “Biophysical Processor” includes a generic algorithm for all kinds of vegetated land cover. Consequently, GEDI parameters show higher agreement with in-situ data, also considering geolocation uncertainty.

Outlook for the future

Our study showcases the current capabilities and consistency of different sensor systems to monitor vegetation parameters which are needed to monitor forest status in the context of rapid forest disturbance and the need for climate-adapted management. As for our study, the planned inclusion of high-resolution aerial LiDAR data will allow a better assessment of the actual capacities of GEDI. Further, the integration of a disturbance product for the delineation of disturbed pixels will increase the validity of the consistency assessment. As a longer perspective, the temporal and spatial availability of LiDAR data in forestry is likely to increase. In forest ecosystems where reference data is typically scarce, we suggest that retrieval algorithms for optical RS could benefit from LiDAR data.

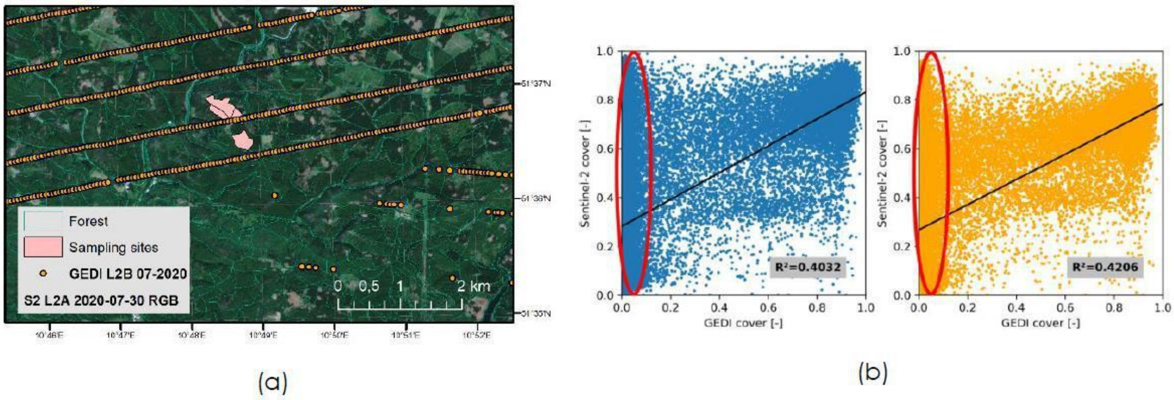

Figure 1 (a) Example of S2 image and GEDI tracks in July 2020; (b) Scatterplots between the GEDI canopy cover and the S2 FCOVER products (different versions of the S2 "Biophysical Processor": blue: 10 m, orange: 20 m).

Assessment of GEDI data for its use in deriving remote-sensing-based 3D forest information

Florian Lippl[1], Manuela Hirschmugl[1,2]

[1] University of Graz, Institute for Geography and Regional Sciences, Austria
[2] Joanneum Research, Institute DIGITAL, Graz, Austria

Keywords (5): GEDI, LiDAR, forest monitoring, 3D, forest structure

The challenge

Airborne Laser Scanning (ALS) data has become one of the main sources of information to derive 3dimensional attributes of forests such as forest height, volume, structure and for the modelling of related attributes like carbon content. However, ALS has its limitations due to high costs and lack of spatial coverage. We therefore investigate the use of space-borne laser scanning data from the Global Ecosystem Dynamic Investigation (GEDI) instrument, which is based on the International Space Station. The GEDI instrument provides point-wise 3D data between 51.6° N and 51.6° S, however with a much coarser resolution compared to ALS data. Comparisons of GEDI to classical ALS data have been done in the past, but mainly for "easy" settings, i.e. flat terrain and managed forests. We examine the GEDI data quality for near-natural forests in a mountainous environment.

Methodology

In order to evaluate GEDI data for complex environments, we compare it to existing ALS data of the Austrian National Park Kalkalpen. The mountainous and small-structured terrain together with near-natural forests may hamper the use of GEDI data. First, we analyse the quality of GEDI data by assessing (i) the accuracy of the GEDI-derived terrain height and (ii) the dependency of the accuracy of relative (forest) height metrics from slope inclination. Second, we evaluate the GEDI relative height (RH) metrics regarding their dependency from different forest parameters, such as canopy cover or height. Third, we assess existing vertical structural metrics (VSMs) from GEDI data and evaluate their correspondence to ALSderived VSMs. To do so, an ALS-based “pseudo foliage height diversity” (FHD) is calculated and used for comparison.

Results

The results show a strong influence of slope inclination on the GEDI derived terrain height accuracy with mean residuals ranging from 0.3m (+10.5/-9.3 m) for flat areas (slopes < 15°) up to 6.3m (+37.2/-33.1m) for steep slopes (> 35°). With regard to GEDI RH metrics, correlations are generally poor with the best results for RH100 with the ALS maximum height (R^2=0.44) and RH50 with the ALS mean height (R^2=0.49); both when including only GEDI plots with quality flag 1 and degrade flag 0. We found four major factors influencing the accuracy of the RH metrics: sensitivity of the GEDI beam, canopy cover, canopy height and terrain slope (Fig. 1a)). Most accurate results are obtained with a sensitivity of approximately 95% and a canopy cover of 50%-90%. Further, the RH100 is also affected by the canopy height itself with GEDI overestimating the height of small trees and underestimating the height of tall trees (Fig. 1a)) bottom left). Terrain slope also influences the RH values significantly (Fig. 1a) bottom right): when looking at flat areas only (slope < 15°), the R^2 between ALS maximum height and RH100 improves from 0.44 to 0.7.

Furthermore, GEDI waveforms as well as the FHD values are employed for the assessment of VSMs. The correlation between the ALS-based “pseudo FHD” and the GEDI FHD is poor (R^2=0.27). For some example plots, the waveforms are shown in Fig. 1b). The top row outlines two well-fitting examples, whereas the bottom row represents examples with very different behaviour. Comparisons with field assessments revealed a limited geo-location accuracy of the GEDI plots. We are currently testing to co-locate the waveforms to the ALS data for better fitting. Visual interpretations of the waveforms indicate that FHD values have some explanatory power to assess the number of layers, if the geo-position is fine.

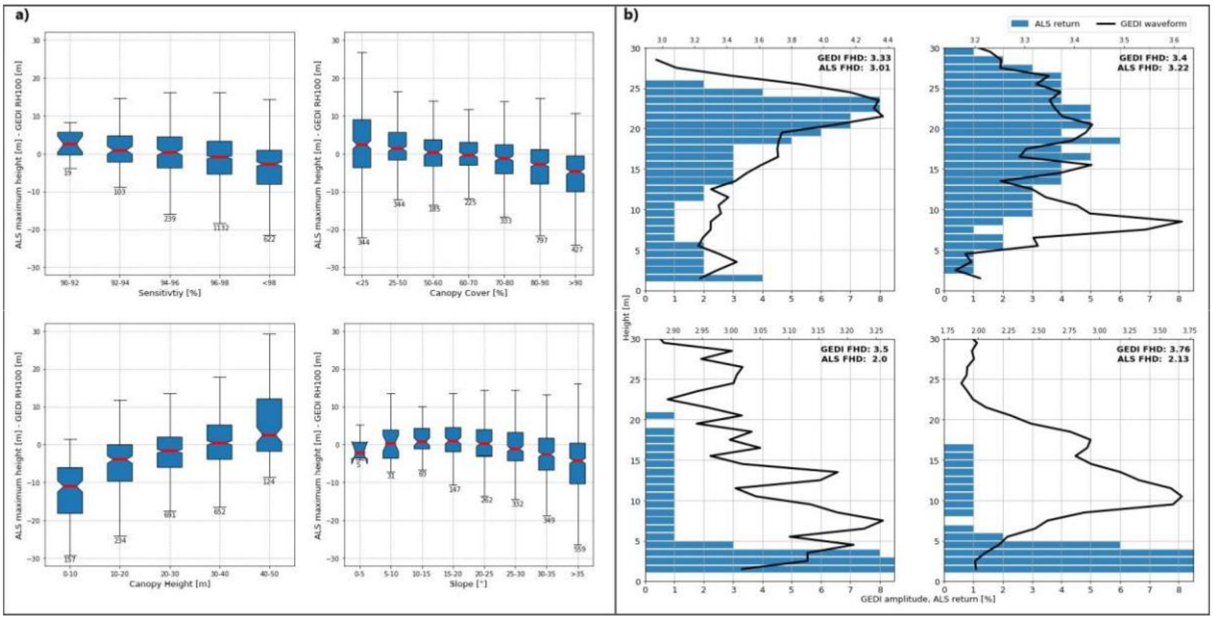

Figure 1 a) Influence of different parameters on RH100 accuracy - residuals; b) Comparison of ALS and GEDI vertical profiles and calculated FHD values

Outlook for the future

In summary, this study shows promising results that GEDI RH data are highly suitable for forest monitoring, especially in flat terrain (e.g., the Amazon basin). The applicability in mountainous areas has to be considered carefully. The sample plots illustrate first encouraging results to use GEDI data for vertical structure characterization. However, more work is still needed to fully understand the data and how to transfer it to meaningful indicators.

Future work will be threefold. First, after the thorough assessment of the usability of FHD values as indicator for number of layers or vertical structure, we want to improve the indicator by integrating the raw waveform data. Ideally, this information should also lead to an “index of naturalness” to measure and monitor the (degradation/restoration) status of forests over time. The second focus is on the combination of GEDI data with Copernicus Sentinel-1 and Sentinel-2 time series data to bring the point-wise information in a rollout. The third task is to apply the methods also to other ecosystems, e.g. to tropical forests in order to measure impacts on forests like agroforestry practices, selective logging or other forest disturbances.

Comparison of PRISMA and Sentinel-2 imagery for detection of agricultural areas

Francesco Pirotti[1], Mario Angelo Gomarasca[2], Enrico Borgogno Mondino[3]

[1] University of Padova, TESAF Department, Italy
[2] National Research Council (CNR-IREA), Italy
[3] University of Torino, Department of Agricultural, Forest and Food Sciences, Italy

Keywords: Precursore IperSpettrale della Missione Applicativa (PRISMA), Sentinel-2, Copernicus, Highperformance computing (HPC), Machine learning

The challenge

The Precursore IperSpettrale della Missione Applicativa (PRISMA) is a recent sensor with ~30 m ground sampling distance developed by the Italian Space Agency (ASI). It is able to capture a spectral range of 240 bands between wavelengths of 400 and 2500 nm and a spectral resolution below 12 nm. In this work we assess the accuracy of this sensor to determine agricultural areas as opposed to non-agricultural areas. We assess accuracy of computing percentage of agricultural area using a trained random forest classifier over a PRISMA image and over a Sentinel-2 image and discuss differences. Results are aggregated to agricultural areas as defined by the 2020 regional planning data - "PTRC 2020 - Diversità dello spazio agrario" see figure 1 (PTRC) that divides the Veneto region in parcels with an average100 ha (±81 ha SD). Each area has information on percentage of area covered by agricultural land-use (ALU). The same percentage was calculated using the classification results from PRISMA and Sentinel-2 and accuracy assessment is provided.

Methodology

PRISMA imagery was downloaded using ASI's portal, in binned L2D format and processed to VNIR, SWIR and PAN images using the "prismaread" package in R CRAN. VNIR and SWIR data cubes were merged together to a single hyperspectral data cube. Training and testing areas for the "agriculture" class were extracted by isolating polygons having ALU percentage above 98% and a surface area above 50 ha. These polygons where then buffered with a negative value of 30 m, thus shrinking the polygons. This was done to limit border effects of mixed pixels, as the borders of the parcels are often roads or water bodies. This totalled with 55 areas with 4874 ha of ALU. Non-agriculture (non-ALU) classes were defined by manually drawing polygons in urban, bare rocks and forest areas. Ensemble of machine learning methods from the "h2o" R CRAN package, that leverages distributed AI for High Performance Computing (HPC), were trained with a random pick of 30% of image pixels falling in the ALU/non-ALU areas; the other 70% were used for testing results and extracting accuracy metrics, i.e. precision, recall and F-score. This was done 10 times as per k-fold validation method were k=10. Final classified maps from PRISMA and Sentinel2 were then used to calculate a percentage of ALU in each of the PTRC areas and results reported with r-squared regression values to evaluate goodness of fit of the agriculture areas; PTRC vs. PRISMA and PTRC vs Sentinel-2.

Results

Results are shown in figure 1b, with relationship between true positive and false negative rates plotted as Receiver Operating Characteristic curves for both sensors over results in independent test data. It is worth keeping in mind that only two classes are considered, ALU and non-ALU. Confusion matrices are in table 1 below.

	Sentinel-2			PRISMA		
	AGR	**NOAGR**	**Error**	**AGR**	**NOAGR**	**Error**
AGR	38194	6753	0.15	12320	301	0.02
NOAGR	2495	19436	0.11	298	5403	0.05
Totals	40689	26189	0.14	12618	5704	0.03

Correlation between the predicted percentage of agriculture cover per parcel from PRISMA and Sentinel-2 with the “observed” official percentage from PTRC 2020 planning was practically identical for both sensors, r-squared of 0.532 and 0.531 respectively (difference is not significant).

Outlook for the future

Detecting automatically areas that are subject to agricultural practices can provide an important tool to planning at local and regional scales. Using data from latest sensors together with existing maps of agriculture cover, results show that it is feasible to scale and update information regarding the percentage of agricultural land-use. Important aspects for future development are to include an automatic cloud/cloud-shadow removal and a more classes to create a finer classification framework to avoid mixing similar classes, e.g. forest and agriculture areas. Multi-temporal aspects will also have to be considered, to leverage natural changes in production parcels that can add information to improve distinguishing agriculture from other green areas such as gardens, parks, football fields etc.

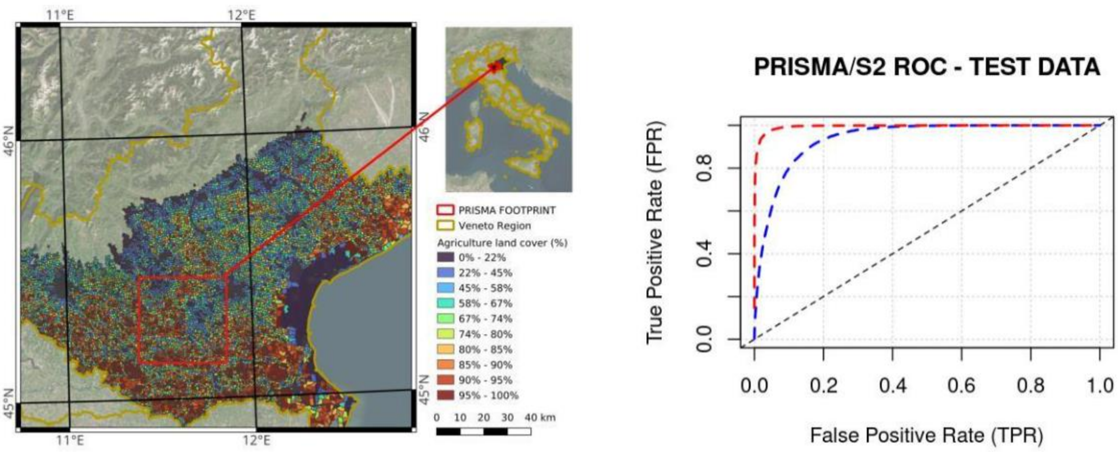

Figure 1 (a) study area (b) performance measure over binary classification on test data (red=PRISMA, blue=Sentinel-2)

Choosing Optimal Time For Estimating Yield of Winter Oilseed Rape And Winter Wheat

Jakub Tomasz Ceglarek[1], Agnieszka Glinko[2], Cezary Kaźmierowski[1], Remigiusz Łukowiak[3], Sławomir Królewicz[1], Jan Piekarczyk[1]

[1] Adam Mickiewicz University in Poznan, Poland;

[2] GISPRO S.A., Poland

[3] Poznan University of Life Sciences, Poland

Keywords (5): Crop yield prediction, optimal time, growing degree days, oilseed rape, wheat

The challenge

Early and accurate yield prediction helps in assessing the effectiveness of various agricultural practices and dividing fields into yield productivity zones. The challenge of selecting an optimal time for predicting yield stems from the differing start of vegetation season between years. Using data from Sentinel 1 and 2 satellites and yield measurements from three fields, across a couple of seasons, a yield of rapeseed and winter wheat was analysed. Due to varying conditions each year, the day of a year related to sowing, as well as the speed of growth change, accounting for that growing degree days was used to standardize timings and aggregate measurements from various seasons. Another challenge was to base the prediction on just freely, publicly available data, therefore satellite imagery was chosen, including Sentinel 1 and 2 platforms.

Methodology

Yield data were collected on three agricultural fields located in western Poland, distributed around 200 km from north to south, resulting in varying start and duration of vegetation season. Fields on which cultivation of winter oilseed rapes and winter wheat were studied. Productivity of the fields was monitored for multiple seasons, and estimated by crop cuts. On each field, 60 sampling locations were chosen and cutting and weighting of crops from 2 meter square patches was performed, used to report yield data. Sentinel 1 and cloud-free Sentinel 2 from each analysed year were obtained. After the necessary preprocessing of imagery, images were aggregated based on the accumulated growing degree days since sowing, therefore grouping data from different years. Based on reflectance in selected Sentinel 2 bands, a number of spectral indices, including NDVI, NDRE, TVI, and others were calculated. Likewise, Sentinel 1 data were pre-processed and polarized VV and VH values were obtained, due to frequent Sentinel 1 data acquisition, rolling average values from ten-day periods were used. All of the above-mentioned products, together with raw Sentinel 2 band reflectance were fed into prediction models. Three modeling algorithms were used and compared: cubist, partial least square regression, and random regression, separately for winter wheat and oilseed rapes. The whole procedure is summarized on Figure 1.

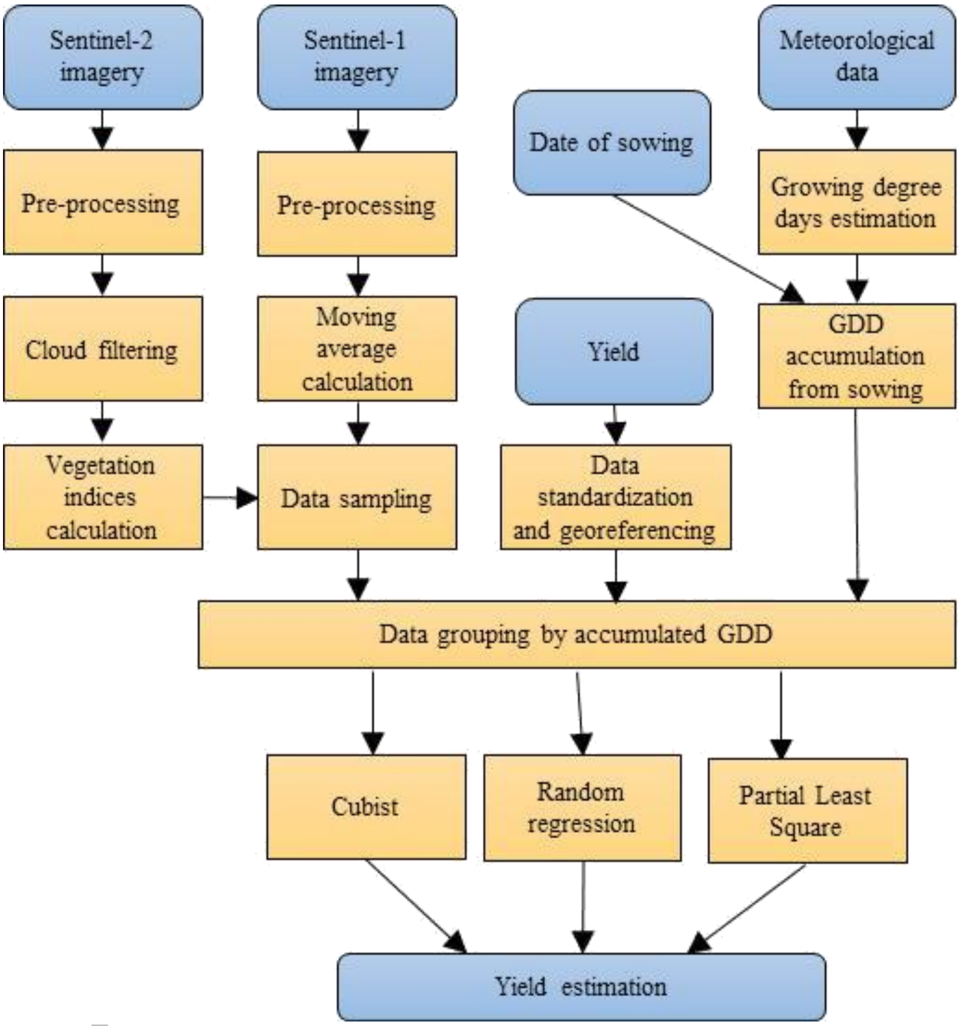

Figure 1 Flowchart showing the methodology applied for this study

Results

The obtained satellite imagery was aggregated in three growing degree day thresholds: every 50, 100, and 200 of accumulated GDD. The prediction of yield performed for winter wheat shows worse results than the modeling of winter oilseed rape. Aggregating data every 50 or 100 GDD produces models behaving similarly, whereas aggregating by 200 GDD is too wide of a window, resulting in poor prediction and significance of models. On best dates, the yield of winter oilseed rape can be estimated with a correlation between 0.6 and 0.7, depending on the used model (Figure 2). Prediction of the yield of winter wheat was less successful, being shy of 0.6 on the best dates. Between the selected modeling algorithms, in general, cubist behaved better than random forest and partial least square regression, barring a few exceptions. Interestingly, in all analyzed variations, the best or almost best prediction is based on satellite data recorded relatively early during the plant growth, associated with the emergence in oilseed rape and the emergence and tillering in wheat. In the case of oilseed rape, aggregated by either 50 or 100 GDD, another period of high yield prediction accuracy occurs around 600 accumulated GDD, connected with the rosette phenological phase. No such second peak was observed for winter wheat. The importance of predictors was higher for data from Sentinel 2 than Sentinel 1, and vegetation indexes were better predictors than band reflectance.

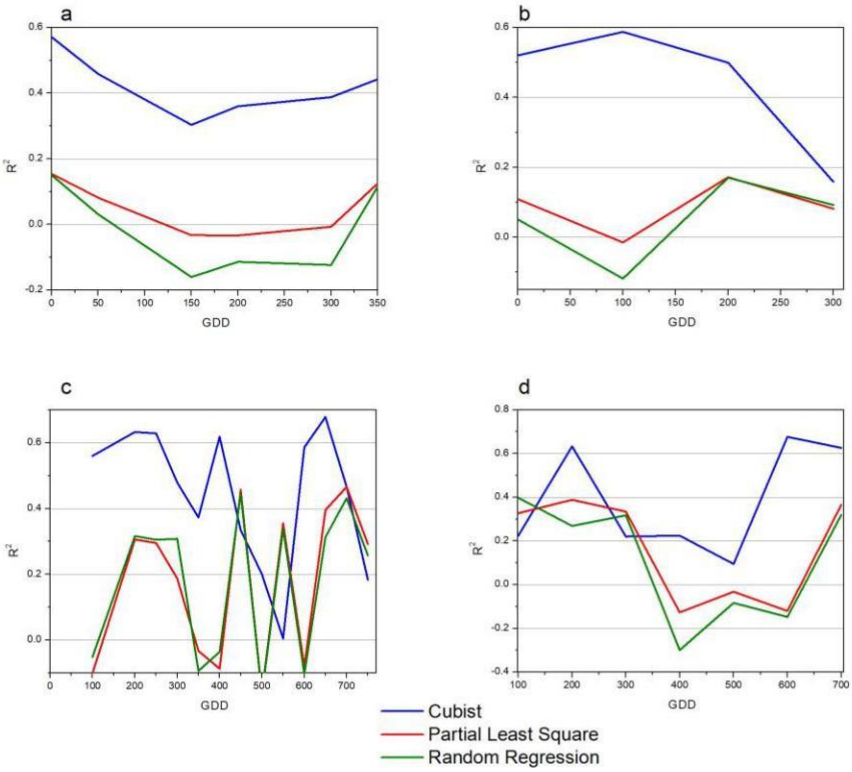

Figure 2 Performance of models predicting yield as a function of accumulated growing degree days (GDD), aggregated every: a) winter wheat 50 GDD, b) winter wheat 100 GDD, c) winter oilseed rape 50 GDD, d) winter oilseed rape 100 GDD

Outlook for the future

The presented study focuses on selecting the optimal time during vegetation season to estimate the yield of winter wheat and oilseed rape. The approach used so far aggregates data to chosen GDD interval and treats it separately. In the next iteration, a procedure to use all the data obtained up to the selected time will be devised. In that way, not only the condition of vegetation on a particular date but also all prior conditions will be taken into account and used for prediction. In that way, the rate of growth, possible occurrences of plant stress, and other dynamic processes could be accounted for, improving the prediction. In order to generalize the results, additional fields located in different parts of Poland will be included. Due to the weaknesses of estimating yield by crop cutting and weighting, crop monitoring systems will be used in the future.

Grassland mowing frequency estimation in Google Earth Engine using Sentinel-2 imagery.

Davide Andreatta[1,2], Damiano Gianelle[2], Michele Scotton[1], Loris Vescovo[2], Michele Dalponte[2]

[1] University of Padova, Department of Agronomy, Food, Natural Resources, Animals and Environment, Italy
[2] Edmund Mach Foundation, Research and Innovation Centre, Italy

Keywords (5): management intensity, NDII, Common Agricultural Policy, remote sensing, Google Earth Engine.

The challenge

Grassland management intensity is a key grassland trait, since it affects not only production but also carbon storage, water quality, animal, and plant diversity. Updated and publicly available data about management intensity are therefore needed to understand its relationship with species distribution and to develop conservation and management measures, including European Common Agricultural Policy subsidies. Mowing frequency is used as a proxy of management intensity for cut-grassland and several remote-sensing mowing-detection algorithms have been proposed. Both active and passive sensors potential was explored, but despite the recent improvements in cloud masking of S2 images, there are still few newly developed algorithms which use this freely available, 10 m resolution imagery. We aim to develop a more accurate estimation model whose provided code can be run in Google Earth Engine, a platform providing continuously updated imagery and outstanding computational capacity.

Methodology

The 240 ha of temperate grassland used for algorithm development and testing are located in 4 sites in the southern Italian Alps. The grassland fields had management intensity from 0 to 4 mowing events (2020 growing season), altitude from 450 m a.s.l. to 1990 m a.s.l., and very fragmented and small parcels. The reference mowing frequency dataset was partly acquired through farmer interviews and partly through photo interpretation on RGB daily Planet imagery at 3 m spatial resolution and visual inspection of a break in the NDVI curve. The imagery used in this study is Level 2A Sentinel-2 (S2), with revisiting time from 2 to 5 days and spatial resolution of 10 m (visible and NIR) and of 20 m (SWIR and Red Edge). The proposed algorithm included: i) vegetation index time-series computing (EVI, GVMI, MTCI, NDII, NDVI, $RENDVI_{783.740}$) for each pixel for the whole growing season, ii) smoothing and resampling, iii) mowing detection, and iv) majority analysis. First, we compared the overall accuracy (OA) and the mean absolute error (MAE) of algorithms based on different vegetation indices and separately optimized on the whole reference dataset, then we tested if all the algorithm phases are beneficial, and we compared pixel and parcel resolution accuracy. Lastly, we estimated the generalization error performing a k-fold cross validation using sites as stratification layers.

Results

The Normalized Difference Infrared Index (NDII) was selected as the best performing index, resulting in MAE of 0.07 and OA of 93% OA on average at the four sites used for optimization at pixel level. NDII outperformed the more used Normalized Difference Vegetation Index (MAE=0.09), probably because the first saturates later as biomass increases. The model including all phases was the most accurate in all four sites, but smoothing and resampling phases lead to a loss of temporal accuracy, as reported by previous literature. The accuracies obtained at parcel level were slightly lower than those obtained at the pixel level. Since erroneously classified parcels are smaller than average, results suggest that the accuracy reduction was probably due to edge effect of mixed pixels. Differently from previously available algorithms, the analysis concept in our study builds on the pixel level because in most of grassland systems management parcels are not available a priori, as administrative boundaries often differ substantially from real field limits. The average MAE obtained on the validation dataset in k-fold cross validation (0.12) was almost double than the average MAE obtained on optimization dataset (0.07), but it is still very low. It indicates that just approximately one pixel out of ten was wrongly classified and suggests it is possible to reliably apply the algorithm to other areas after appropriate testing.

Outlook for the future

Overall, this study demonstrates the suitability of the proposed algorithm to monitor very fragmented grasslands in complex mountain ecosystems, but limitations and further improvements are present. The major limitation of the proposed algorithm is that it is specifically designed to detect grassland mowing frequency and not to predict mowing dates. Mowing dates are often useful, for example to assess late cutting, necessary to protect ground nesting birds in protected areas. A prior management type (i.e., grazing/mowing) detection algorithm could be beneficial for an accurate application of the proposed algorithm at a landscape level. The growing season is defined manually based on climate statistics of the area and could be improved by applying the same rules at a pixel level. The algorithm should be tested and probably adapted before use in areas with very different climate and phenology, for example in mediterranean grasslands and in more cloudy regions.

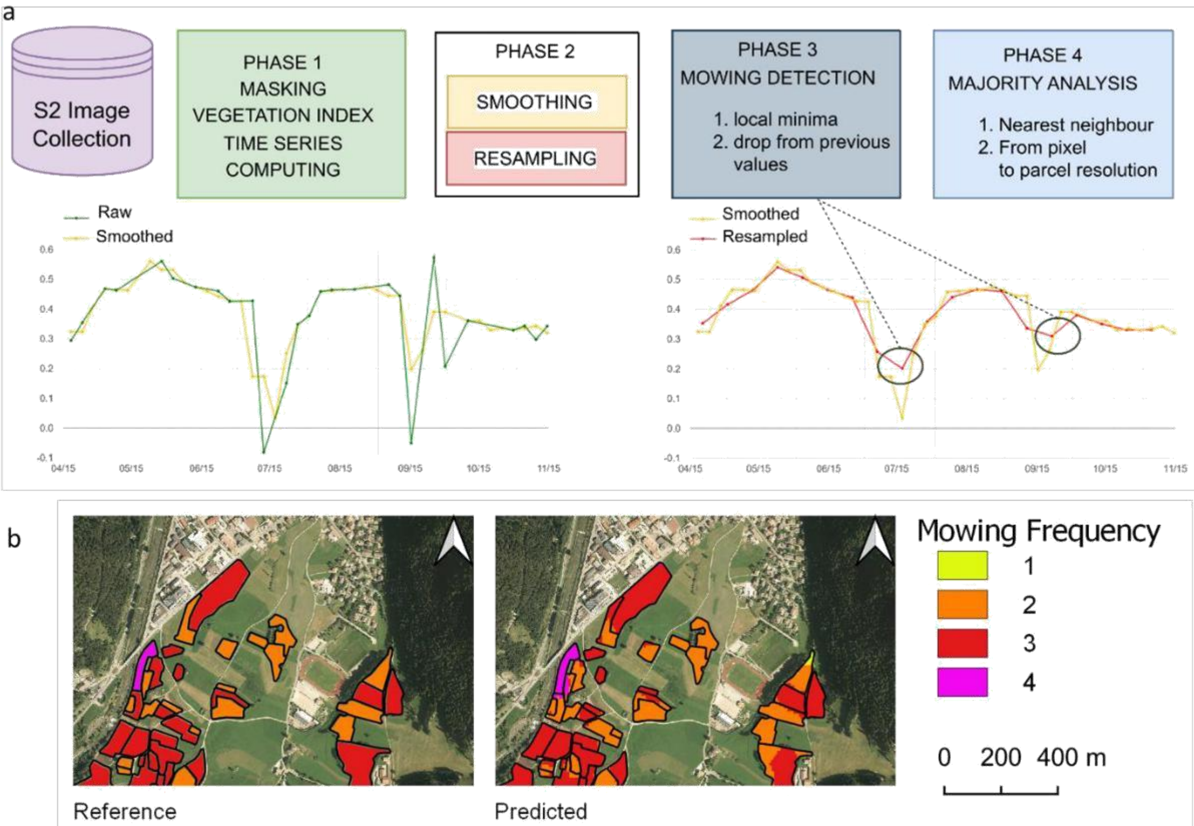

Figure (a) Architecture of the proposed algorithm. At the bottom of the panel raw and derived vegetation index time-series of a grassland pixel are presented. (b) Reference (left) and predicted (right) mowing frequency map at pixel level of the Predazzo site. Predicted values are obtained using best global optimization, and NDII as vegetation index

A web GIS mapping service for a better exploitation of the forest melliferous resources in South East Romania

ADRIAN LORENȚ[1,2], VLADIMIR GANCZ[1], MARIUS PETRILA[1],FLORIN CAPALB[1,2], BOGDAN APOSTOL[1], IONICA SOARE[3]

[1]NATIONAL INSTITUTE FOR RESEARCH AND DEVELOPMENT IN FORESTRY (INCDS), "MARIN DRĂCEA", ROMANIA
[2]"TRANSILVANIA" UNIVERSITY OF BRAŞOV, FACULTY OF SILVICULTURE AND FOREST ENGINEERING, BRAȘOV, ROMANIA

[3]"Dunărea de Jos" University of Galați, Faculty of Economics and Business Administration, Galați, Romania

Keywords: webGIS, pastoral beekeeping, melliferous resources, forestry

The challenge

Romania is one of the largest honey producers in Europe, ranking second as number of hives and eight as number of beekeepers. For the continuity of honey harvests over a season, the beekeepers move their hives around different areas, depending on the flowering of honey sources, from which the tree biomes with limes *(Tilia sp.),* black locust (*Robinia pseudaccacia*

L.) and willow (*Salix sp.*) have a significant contribution. The pastoral beekeeping is chaotically practiced due to lack of information about the geographical distribution and the melliferous potential of these forest biomes. To address this issue, we developed a web-GIS interactive map to support beekeepers, providing information regarding the location of honey tree biomes sources. We hereby present the results obtained by developing a web-GIS platform for two counties located in South-Eastern Romania (Tulcea and Brăila), renowned for their forest melliferous resources (i.e. within Tulcea county there is the largest limes massif from SE Europe).

Methodology

The main source of information were the forest management databases of forest administration units in GIS format, which contains a detailed description of the forest stands, both for the vegetation strata and the abiotic environment. The database was exploited to extract relevant melliferous information, i.e. the surface covered by limes, black locust and willow tree species within each stand and their average age. To simplify, the stands were grouped into 2 age classes: under and over 40 years for limes and under and over 10 years for black locust and willow (over these ages, the trees are more melliferous productive). Together with other relevant information like the mean altitude, the slope and terrain aspect of the parcel, additional informative layers were added (e.g. the natural protected areas limits, roads, watersheds). Labels and legends for each strata were set. In figure 1A is displayed a detail of this map. The next step was to upload the map into a WebGIS application (ArcGIS Online). Then, with a common web browser the application was opened and within specific tools (within *My Map* viewer) for each layer were set different parameters (labels, balloons, order of display etc.) and the background map. In figure 1B is displayed this viewer. Then a Web application was build based on an appropriate template from ArcGIS Online, the map was loaded, widgets from the template were selected and edited (figure 1C). Finally, the template was saved as a WebGIS application.

Results

The web map and the application are displaying, in conventional colors for each tree species, the percentage of each tree species within the stands, as five shading classes. The age classes are displayed using hatchings. If map is zoomed the labels showing tree species, the percentage and age are displayed. All other topographic elements are in the background map. A scale bar and the geographic coordinates (in decimal degree) are also displayed. Attributes table for each layer may be displayed, at request, using a button from bottom of the page.

There are several important functionalities embedded into the web map: clicking a map element a balloon will pop-up displaying more details (figure 1D); using specific widgets the user may measure distance, area and location on the map, may change the background map, add other strata, locate himself on the map etc. One of most useful functionalities (widget) is a geospatial analysis tool which allows to generate a pie chart with area and percentage, for each tree layer (e.g., limes) of the area selected by some different shapes. For example, it is known that the efficient collecting distance for a bee is maximum 1000 m. If a beekeeper wants to see an estimation of honey resources for a certain area, he will draw with this tool a circle of 500 m radius on the map, and a pie chart will show the areas by percentage of that specie (figure 1D).

Outlook for the future

The forest melliferous online map will help beekeepers to better plan their pastoral beekeeping by having a better knowledge of the melliferous resources of the two counties though a user-friendly web-GIS application which can be freely accessed via mobile or desktop devices. It will also better inform local regional authorities to improve policies through a better and more sustainable exploitation of the resources. The application can be improved by implementing and commissioning of an Electronic Exchange Market, in which the farmers demand for pollination services will meet the apiarian offer for entomophilous honey crops, and by providing the specific tools for realistic pollination contracts. The planning of beekeeping for cultivated honeycombs and the conclusion of pollination contracts will be able to be done in an efficient, transparent and easy way, the only condition being the access to the Internet.

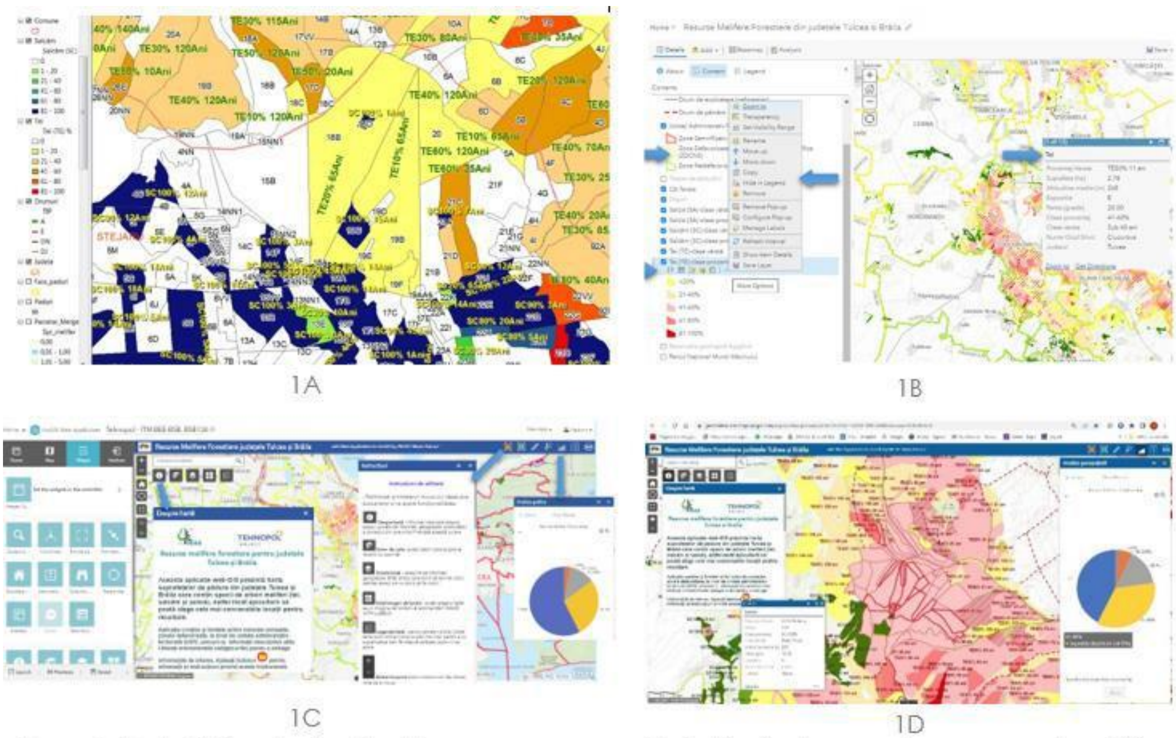

Figure 1 A- detail from the forest melliferous resources map; B - Setting the layers and map parameters within WebGIS environment; C – Editing the template: adding and editing widgets; D - Final result and some functionalities: explanations, pop-ap information balloon, geospatial analyse tool.

(https://geomatica-icas.maps.arcgis.com/apps/webappviewer/index.html?id=5d84b3f8b5b44feaaa2eac24dbdb8b2a)

Integration of terrestrial laser scanning (TLS) and airborne laser scanning (ALS) processed data for the assessment of Norway spruce dendrometric characteristics – a case study

Bogdan Apostol[1], Adrian Lorent[1,2], Şerban Chivulescu[1], Albert Ciceu[1,2], Marius Petrila[1], Florin Capalb[1,2], Cristiana Marcu[1], Ovidiu Badea[1,2]

[1]National Institute for Research and Development in Forestry (INCDS) "Marin Drăcea", Voluntari, Romania
[2]"Transilvania" University of Braşov, Faculty of Silviculture and Forest Engineering, Braşov, Romania

Keywords (5): TLS, ALS, dendrometric tree and stand characteristics

The challenge

Remote sensing technologies are increasingly used to assess the forest biophysical parameters over large areas. Among remote sensing-based data, the airborne LiDAR data (ALS) is considered to have a great potential for use, especially in the forestry field, even if the data acquisition is still expensive. In addition to ALS data, terrestrial laser scanning (TLS) systems present a bottom-up approach, also providing useful information for forest inventory. Thus, the combined use of ALS and TLS technology provides more information regarding both, vertical and horizontal forest structure than a separate use of each of them. In this context, the aim of the study is to assess the main dendrometric tree and stand characteristics by the use of integrated TLS and ALS processed datasets.

Methodology

The study is located in Southwestern Romania and analyses data collected from ten plots located in representative Norway spruce (*Picea abies*) stands. Each plot(P) consists of two circular sub-plots (SP) of 500 m^2. A computer-assisted field inventory system (Field Map) together with high an accuracy GNSS receiver, a Vertex inclinometer and a calliper were used to collect the reference ground data within each SP. The terrestrial laser scanning point clouds were collected using a Faro Focus 3D X130 HDR device. Airborne laser scanning data were collected using a LiDAR Riegl device. In order to minimize the occlusions effects, a multiple TLS stations approach was adopted for each SP. TLS point clouds were coregistered and tree position, dbh and height were extracted using specific methodology (*DendroCloud together with GIS analysis*). The ALS data were used to derived the normalized canopy height model for each SP. Based on a local filtering algorithm with a canopy-height based variable window size, it was possible to identify the position and the height of the trees from the upper canopy within each SP. The tree volume was calculated based on a specific national equation, considering the tree dbh extracted based on TLS and tree height extracted based on ALS datasets. The plot volume was calculated by summing al the trees volumes within each plot. Specific statistical analysis was performed based on three datasets (field measurements, TLS & ALS extracted data).

Results

By applying the field methodology, 767 trees were measured. Based on the analysis of TLS co-registered point clouds, there were identified 535 of the total number of trees measured in the field. By comparing the means of the trees' dbh for each plot, measured in the field and respectively, calculated based on the TLS processed data, there were obtained deviations in absolute values, ranging from 0.2 cm (P94) to 2.7 cm (P87)(Fig. 1(a)). In the case of using ALS data, 50% of the total number of field measured trees from the upper canopy were identified. By comparing the means of the trees' height for each plot, measured in the field and respectively, calculated based on the ALS data, there were obtained deviations in absolute values, ranging from 0.06m (P95) to 2.72m (P89)(Fig. 1(b)). Analysing the three datasets (field measurements, TLS and ALS extracted data), resulted 197 trees (from the upper canopy) whose dbh, height and volume were estimated based on the integration of TLS & ALS processed data. By comparing the heights extracted based on TLS and ALS data, respectively, with those measured in the field, we found mean deviations at plot level, much lower in the case of height estimates based on ALS data (0.04 - 2.6 m) than in the case of those based on TLS data (4.4 - 8.6 m). The linear regression between the total volume for each plot, calculated based on the field measurements, vs. the predicted volume based on the integration of TLS and ALS processed data, indicated a R^2 value of 0.96(Fig. 1(c)).

Outlook for the future

The method presented in this study is relatively fast and easy to use. However, it can be improved. Thus, by using specific equations (e.g., height curve) based on dendrometric characteristics determined by the integration of TLS and ALS processed data sets, both heights and dbhs of the undetected trees, could be estimated. An alternative for assessing the dendrometric characteristics of trees and stands based on integrated TLS and ALS data, is that which takes into account the spatial integration of the two TLS and ALS point clouds, followed by the estimation of the dendrometrics data. In this regard, the authors need to do further investigation. In addition, the results of the study based on the integration of the TLS and ALS processed datasets, could be upscaled to larger areas and used together with specific allometric equations, to address aspects related to above-ground biomass estimates and carbon sequestration.

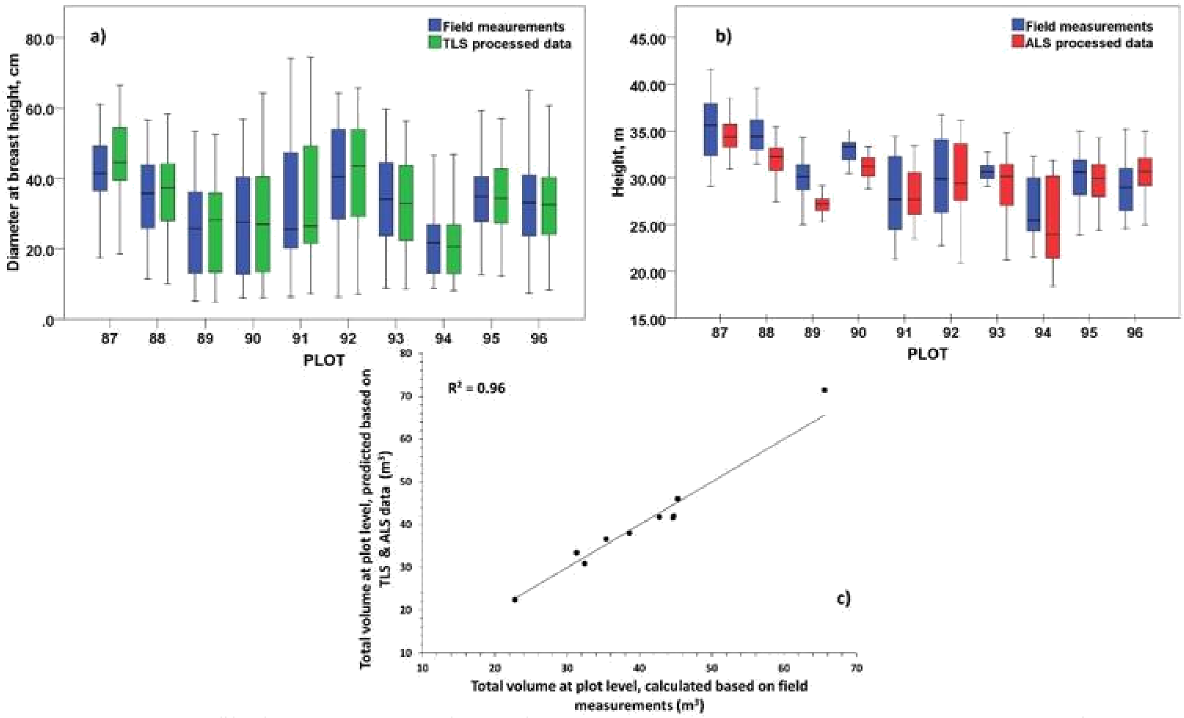

Figure 1 (a) Boxplot of dbh measured in the field and TLS processed based data, (b) Boxplot of height measured in the field and ALS processed based data, (c) Field measured based plot volume vs. predicted volume based on integrated TLS & ALS data

Integration of Canopy Height Models Derived from Airborne LiDAR Data and UAV Aerial Imagery by DTM-DSM Matching in the Forest Free Areas

Bogdan Apostol[1], Marius Petrila[1], Juan Garcia Duro[1], Adrian Lorent[1,2], Florin Capalb[1,2], Cristiana Macu[1], Sorina Farcaș[1]

[1]National Institute for Research and Development in Forestry (INCDS) “Marin Drăcea”, Voluntari, Romania
[2]“Transilvania” University of Brașov, Faculty of Silviculture and Forest Engineering, Brașov, Romania

Keywords (5): LiDAR, UAV, DTM, DSM, Canopy Height Models

The challenge

The research aimed to integrate Digital Terrain Model (DTM) resulted from airborne LiDAR data with Digital Surface Model (DSM) obtained from a UAV imagery to obtain a good quality canopy height model (CHM) in order to be used to determine biometric characteristics of trees. For the integration of DTM obtained by processing of LiDAR data with DSM obtained from the processing of UAV imagery it is necessary to ensure that they overlap with sufficient accuracy. For certain areas, namely, areas without forest vegetation (clearings, gaps, roads, logging areas) DTM obtained by processing of airborne LiDAR data and DSM obtained by data processing of UAV imagery have a high degree of coincidence. The method analyses the integration of airborne LiDAR and UAV derived CHMs by DTM-DSM matching by recalculating the derived CHM based on the statistic height difference between CHMs in the forest free areas.

Methodology

The research area is located in South-West of Romania, within the Experimental Base (B.E.) Caransebeș, administrated by the National Institute for Research-Development in Forestry (I.N.C.D.S.) "Marin Drăcea". From a geographical point of view, it is located at the sources of the river Sebeș, on the main valleys Cuntu and Valea Craiului.

The difference between DSM and DTM resulted from LiDAR data is currently used to obtain CHM in order to extract tree biometric data. This method aims to integrate DTM resulted from airborne LiDAR data with DSM obtained from a UAV imagery to obtain a good quality canopy height model (CHM) in order to be used to determine biometric characteristics of trees and forest stands.

The DSM obtained by processing UAV imagery and DTM obtained from LiDAR data correspond only in areas without forest vegetation. This fact was used to correct the CHM obtained from combining both types of data with the difference calculated to the CHM obtained only from LiDAR data in the forest free areas. The difference between the two CHMs was calculated considering the mean value of the raster pixels for those areas, the histogram presenting a high frequency of the values near “0” altitude corresponding to ground level.

Results

The raster files DTM (LiDAR) and DSM (LiDAR and UAV) containing altitude data were obtained through specific processing of point clouds. From the altitude difference between DSM (LiDAR and UAV) and DTM (LiDAR) were obtained two raster files with normalized values representing CHMs.

The analysis of the histogram of the first CHM (only LiDAR) showed a high frequency of the values in zone 0 ... 1 representing areas without forest vegetation (figure1(a)). On the second CHM model that combines both types of data (LiDAR and UAV) the histogram analysis showed a large number of values in the area -7 ... 1 representing areas without forest vegetation(figure1(b))..

To calculate the Z difference between the two data types, both CHM raster files were recalculated so that the values corresponding to the areas without forest vegetation were highlighted and the areas with forest vegetation were excluded from the calculation (assigning them the value "0"). After testing different algorithms, it was calculated an average difference of -2.71 m on the Z axis, resulted in areas without vegetation with a standard deviation of 0.79 m (the probable values are in the range given by the mean difference ± standard deviation, which is the altimetric difference between the two CHMs)(figure 1(c)).

The CHM obtained by integrating the processed LiDAR and UAV data was corrected with the mean value (including the standard deviation), and the recalculated raster MDC file was further used to determine dendrometric characteristics in trees and stands (figure 1(d)).

Outlook for the future

For the integration of DTM obtained from LiDAR data with DSM obtained from UAV imagery it is necessary to ensure that they overlap with sufficient accuracy. The differences that occur are both horizontally (X,Y) and vertically (Z) and can result from several error sources such as the projection system, positioning accuracy of the on-board aircraft GPS, the sloping perspective that appears at the edges of the areas covered with UAV images.

As the terrain does not undergo major changes over time, the DTMs obtained based on flights performed with airborne LiDAR technology do not require frequent updating. Data obtained by UAVs can provide very high spatial resolutions and are easier to achieve in short time intervals and with significantly lower costs, offering the possibility to track the growth of vegetation. The combination of these types of data offers the possibility of determining biometric characteristics, which can use the advantages of both types of data.

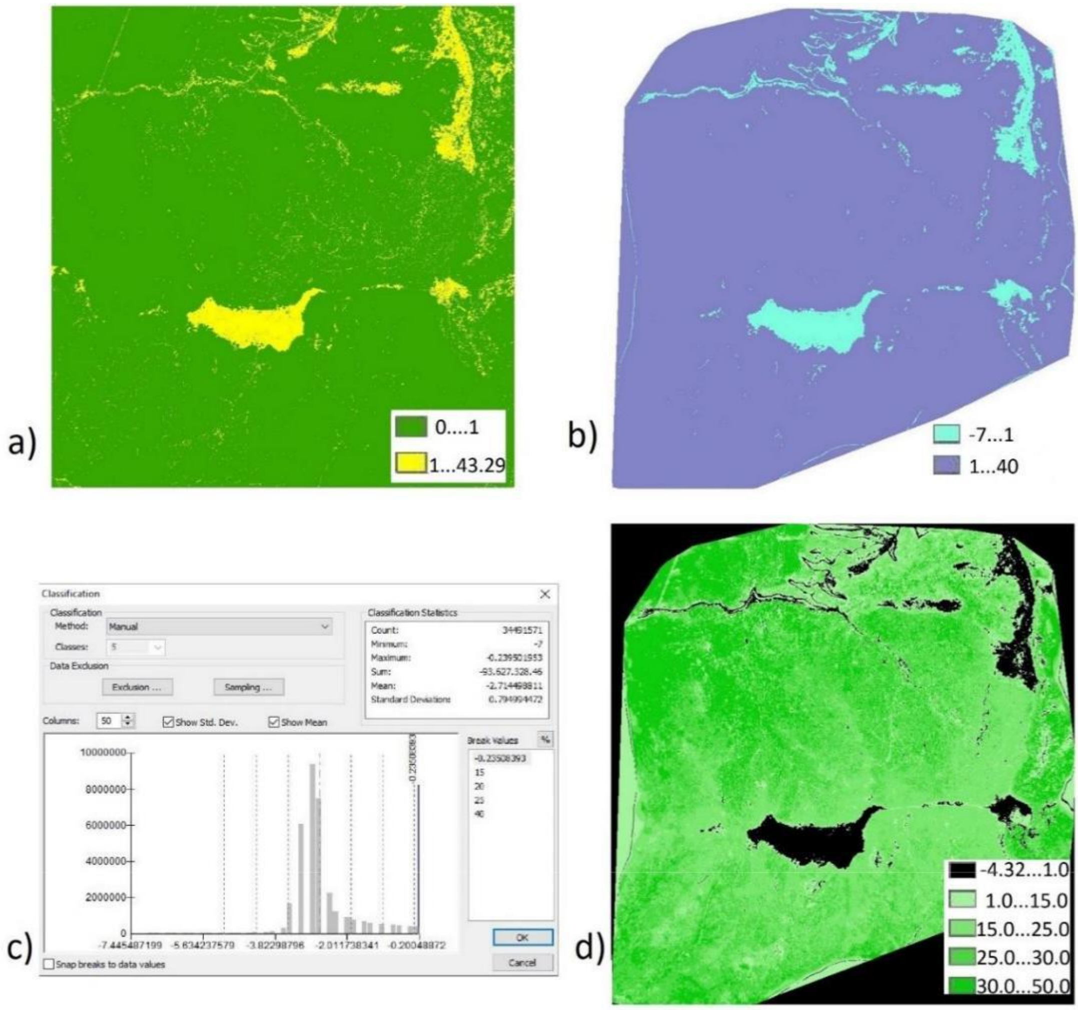

Figure 1 (a) Reclassified CHM, initially obtained by processing airborne LiDAR data (b) Reclassified CHM, obtained by integrating LiDAR and UAV data (c) Mean value of systematic difference and standard deviation on the Z axis for areas without forest vegetation. Value obtained as the altimetric difference between the two CHMs (LiDAR and LiDAR-UAV, respectively) (d) Recalculated CHM raster file obtained by integrating processed LiDAR and UAV data corrected with average value (including standard deviation)

Evaluation of Sentinel-2 vegetation indices to differentiate forest recovery phases in Czechia

Natalia Kobliuk [1], Daniel Paluba [1], Přemysl Štych [1]

[1] Charles University, Department of Applied Geoinformatics and Cartography, Czechia

Keywords: Sentinel-2, forest, recovery phases, vegetation indices, GEE.

The challenge

Forests in Czechia have been impacted by significant changes caused by many factors, e.g., wind or bark beetle calamities, and climate changes with drought episodes. Estimating the disturbance extent as soon as possible and monitoring the regeneration dynamics is an important task for forest management to assess the resilience of forests and to adequately guide post-disturbance management. Forest recovery phases play an important role in defining what kind of forest will be established, often driven by land management decisions. The main objective of this research is to test and evaluate the ability of optical vegetation indices Time Series (TS) to capture and differentiate stages of a forest's lifecycle. The main emphasis is the use of open-access Copernicus data Sentinel-2 (S2) processed in the freely available (for scientific purposes) cloud-based platform Google Earth Engine (GEE).

Methodology

Remote sensing methods and data make it possible to locate various changes better and faster in forest ecosystems. Optical Sentinel-2 Level-2A satellite data were processed using GEE. These data are available since March 2017, therefore localities that had been deforested at the beginning of 2017 were selected for field data collection and creation of short (max. 5 years) TS of multispectral vegetation indices. The mountains of Jeseníky and Vysočina were selected as areas of interest. The in-situ measurements were focused on the most important condition of the forest: e.g., tree species, the density of trees, height and age of trees and understory vegetation. Based on this information, different phases: Bare soil (I), Grassland (II), Transitional woodland (III) and Mature Forest (IV) were described and examined using satellite data. To define differences in spectral characteristics of stages of recovery, short-term TS of S2 data was created. This TS include NDVI, NDWI and Tasseled Cap Greenness (TCG) spectral indices for 2 groups of locations (deforested 4 years ago and 5 years ago). Also, TS for both groups was created for one phenology season. GEE was used to calculate the abovementioned indices from 45 locations in Jeseníky region of Czechia in a time range from 2017 till 2021. To eliminate the influence of cloudiness S2Cloudless cloud-masking methodology was applied. Mann – Whitney U Rank Test was used to evaluate similarity between pairs of data at significance level $\alpha = 0.05$. The Shapiro–Wilk test was used to check the normality of the data.

Results

Pairs of NDVI, NDWI and Tasseled Cap Greenness spectral indices values for different stages of recovery were examined. Among all 45 localities, only 1 was in the I stage of recovery (Bare Soil), so this stage was excluded from the analysis. TCG proved to be the least sensitive to differentiate stages of forest recovery. NDVI and NDMI indices show almost similar sensitivity to recovery phases with NDMI being slightly more effective. All indices showed high capability (>91%) on differentiation between phases III and IV and phases II and IV (>88%). The overall accuracy of NDMI index could be a result of the high impact of SWIR band on index values compared to NDVI and TCG. Conducted analyses also show that analysing forest recovery locations during only 1 phenology season provides less accurate results compared to longer TS analysis. However, differentiation between phases II and III in case of all indices showed low effectiveness for long-term TS (from 57 to 75% with NDMI being the most effective).

Outlook for the future

Received results showing that there are problematic phases which are hard to differentiate using TS of optical data. Thus, dividing forest regeneration into a greater number of phases and describing them more rigorously can solve this problem. Another limitation as well is optical data having certain shortcomings. Forest ecosystems are mostly located in mountainous areas, where it is difficult to obtain enough images on a regular basis due to clouds. In this case, Sentinel-1 C-band SAR satellite from the Copernicus program, whose signal can penetrate clouds and fog, being not dependent on the light of the Sun, thus enabling image acquisitions during the day and at night, should be very useful in monitoring forest changes. Radar imagery has potential use in monitoring forest ecosystems as complementary data to optical data. Exploration and evaluation of SAR backscatter and different SAR polarimetric indices in forest recovery monitoring will be done in the future.

NDVI		
	2	**3**
3	67	
4	89	84

NDVI		
	2	**3**
3	85	
4	96	94

NDVI		
	2	**3**
3	67	
4	90	100

NDMI		
	2	**3**
3	66	
4	88	84

NDMI		
	2	**3**
3	91	
4	91	90

NDMI		
	2	**3**
3	67	
4	99	100

TCG		
	2	**3**
3	48	
4	86	89

TCG		
	2	**3**
3	65	
4	88	94

TCG		
	2	**3**
3	58	
4	90	94

Figure 1 Intercomparison of NDVI, NDMI and TCG values for forest recovery locations from phase II (Grassland) to phase IV (Mature Forest). Columns from left to right represent the percentage of successful differentiation between pairs of locations in different recovery phases according to indices values: for all studied locations for phenology season 2021; for locations which were deforested 4 years ago (end of 2017 – beginning of 2018) and for locations which were deforested 5 years ago (end of 2016 – beginning of 2017) respectively.

S_DRR1: Disaster Risk Reduction

Chair(s): Dr. Kyriacos Themistocleous

Disaster capitalism and land grabbing revisited with volunteered geographic information and multi sensor earth observation: the case of Barbuda

Andreas Rienow[1], Torben Dedring[1], Marcus Goebel[1], Valerie Graw[1]

[1]Institute of Geography, Ruhr University of Bochum, Universitätsstraße 150, 44780 Bochum, Germany

Keywords (5): land grab, nighttime lights, volunteered geographic information, open street map, twitter

The challenge

Two months after the severe hurricanes Irma and Maria affected the island of Barbuda 2017, which was destroyed and evacuated, the construction of a new international airport had begun without prior approval from the Barbudan Council and without an environmental impact assessment. Since the government of Antigua and Barbuda subsided the costs of large-scale tourism projects called Peace, Love, and Happiness and Paradise Found, many Barbudans believe that the government located in Antigua is utilizing the crisis. Scientists have analyzed the effect of severe storms with respect to historical legacies and reconstruction politics, disaster capitalism, and manifestation of climate injustices and green gentrification However, no attempt has been made to quantify and allocate land use and land cover change (LULCC) of Barbuda before and after the 2017 Hurricane disasters. Hence, this was the main objective of this study.

Methodology

For the assessment of artificial LULCC and human activity on the ground, we mainly utilized two data sources: 1) remotely sensed satellite data and 2) in situ mapped volunteered geographic information. We processed Sentinel-1, Sentinel-2, NOAA VIIRS data, MODIS Terra, and RapidEye data, and obtained data from the Open Street Map (OSM) archive via the Ohsome API and Twitter via twarc2 API. The nighttime light (NTL) imagery enabled the assessment of dynamic human activity. Annual samples of S-2 were created based on simple median filter methods for 2016–2017 (before September 5, 2017) and 2019–2020. The object-based image analysis was conducted with a knn classifier to delineate three land cover classes: water, vegetation, soil/ artificial surfaces on a 10 m scale. MODIS Terra NDVI (MOD13Q1) 16-day composites at 250 m resolution were used to calculate the mean annual Vegetation Condition Index. To be able to visualize the potential hot spots of LULCC at a very high resolution (~5 m), we also acquired and analyzed 41 scenes of VIIRS Day Night Band (DNB) data. We enhanced the satellite-based samples with historic OSM feature data to accurately differentiate between vegetated and non-vegetated and artificial and non-artificial areas. The study wanted also to contribute to the discourse of land grabbing, neocolonialism, and disaster capitalism by enriching spatially explicit geoinformation with impressions of Barbudan LULCC from the Twitter community.

Results

We observed that human-induced LULCC is occurring on different sites on the island, with decreased activities in Codrington, but increased and ongoing activities leading to a LULCC in Coco Point and 2 Palmetto Point. With an accuracy of 97.1 %, we estimated a total increase of vegetated areas by 6.56 km2 and simultaneous increase in roads and buildings with a total length of 249.67 km and a total area of 1.43 km2 ; this includes the area of the under construction central international airport. The satellite classification measures an area of ~1.09 km2 , which is ten times the combined sum of all the buildings mapped with the OSM. This and the fact that the vegetation condition itself depict a steady decrease since 2017 show the severe human-induced LULCC since the hurricanes Irma and Maria hit Barbuda and led to its temporary evacuation. While some places show a decrease in human activity, such as Codrington and the Lighthouse Bay Resort, other places experienced increased human activities. They became new NTL radiance hotspots on the island. Since these hotspots are the sites of the Barbudan Ocean Club, the dispute along the human-induced LULCC in the aftermath of the 2017 Hurricanes will and needs to be continued. The study was conducted to quantify the LULCC in Barbuda in the context of the ongoing debate on neocolonialism and land grabbing.

Outlook for the future

It should be acknowledged that the Nobu Inn and the Palmetto Point site of the PLH are already under construction despite the international attention and applicable Barbudan land law. Hence, future work on geospatial analyses needs to focus on the connection between land rights and land development in Barbuda. While the Copernicus program does not provide data below 10 m spatial resolution, the base maps of the NICFI program could be an alternative; they are currently flawed by artifacts, geometric distortions, and atmospheric radiances. The OSM database needs to be updated so that the recently developed hotels and the international airport construction site can be found in the maps. Finally, landscape transformation needs to be analyzed with respect to the common wealth of the Barbudan citizens, and its impacts on the unique ecosystem of Barbuda.

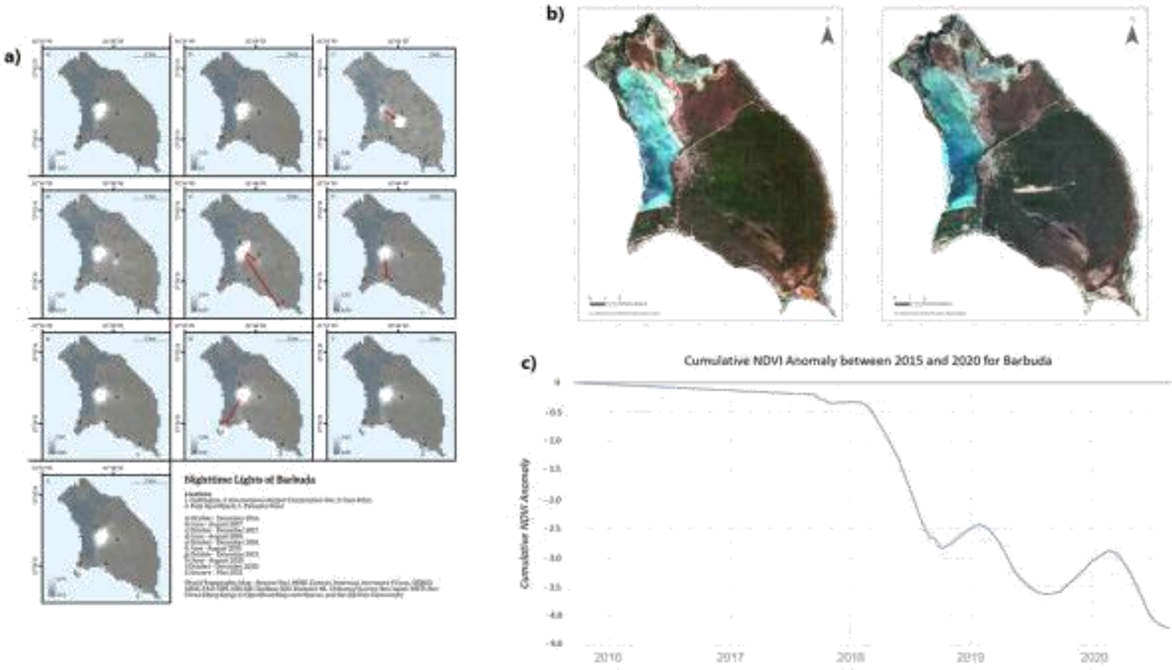

Figure (a) Development of NTL on Barbuda in 2015–2021. The red arrows depict NTL intensity clusters besides Codrington (central cluster). Note the temporary shift of the central cluster from Codrington to the international airport construction site in 2017 and back in 2018. (b) Sentinel-2 cloud free median mosaics 2016-17 (before September 5, 2017, left) and 2019-20 (right). (c) Cumulative NDVI anomalies 2015 and 2020

A multi-sensor approach towards a disaster risk reduction framework for tailings dam failures using the example of Brumadinho

Torben Dedring[1] , Valerie Graw[2], Kristina Thygesen[3], Andreas Rienow[4]

[1]Ruhr University of Bochum, Department of Geography, Germany

[2]Ruhr University of Bochum, Germany

[3]GRID-Arendal, Norway

[4] Ruhr University of Bochum, Germany

Keywords (5): Disaster management, Mining, Sentinel-1, MODIS, Modelling Tailings Dam Failures

The challenge

Over the last decades, the mining industry has reported a steady increase in the volume of extracted minerals and other materials due to the growing demand for consumer goods. However, the extraction of most minerals produces waste tailings, a conglomerate of crushed rock and fluids that are commonly stored behind earthen embankments, termed tailings storage facilities (TSFs). The failure of TDFs causes ecological damage and economic loss and can cause casualties. Hence, the monitoring of TSFs throughout all phases of the disaster management cycle is crucial to mitigate risk. Earth observation and geodata-driven modelling approaches can contribute to disaster risk reduction (DRR) by providing spatially and temporally relevant data to measure the characteristics of a tailings dam failure (TDF). This work takes a first step towards a framework for TDF-related DRR using three approaches for different phases of the disaster management cycle using the TDF in Brumadinho (Brazil) as a case example.

Methodology

Early warning systems or the identification of designated danger zones regarding TDFs can help to reduce the risk to surrounding communities. The empirical GIS-based Laharz model (created by Schilling et al. to estimate the spatial extent of the spill with the help of regressions to predict the cross-section and planimetric area under consideration of the released material volume) was considered to investigate its capabilities to predict affected areas in the course of a TDF to cover the disaster management cycle's phase of prevention and preparedness through the provision of spatial information which can be incorporated into land-use planning procedures (see figure a). The model makes use of several Application Programming Interfaces to gather relevant data such as elevation, infrastructural and population data. For the phase of emergency response, we exploited and compared different processing techniques for Sentinel-1 data to extract information for rapid mapping activities in the aftermath of the TDF. Regarding incoherent change detection algorithms, we calculated the log ratio of intensity and the intensity correlation normalised difference, while a normalised coherence difference and a multi-temporal approach were tested as an instance of coherent change detection algorithms. All algorithms were tested regarding their informative value using the Receiver Operating Characteristic curve. For long term monitoring of the vegetation cover after the TDF, the Standard Vegetation Index (SVI) was calculated in the Google Earth Engine based on 16-day Enhanced Vegetation Index data captured by the MODIS sensor. Even though the SVI is commonly used for drought monitoring, we tested its capabilities 2 for recovery monitoring in Brumadinho as it can provide information about the current vegetation condition compared to long term pre-TDF conditions. Unlike the normalized difference vegetation index, the SVI provides information on the deviation from the average condition of the vegetation. The approach makes use of 486 MODIS images captured between 2000 and 2021.

Results

Regarding the phase of prevention and preparedness, the deployed TDF model reached hit rates of over 80 per cent and critical success indices of approximately 60 per cent in Brumadinho. The built-in risk assessment delivered information about potentially affected people and infrastructure (see figure b). The Sentinel-1 based analysis conducted for the phase of emergency response has its strength in its low dependence on weather conditions and showed that incoherent methods delivered a better basis for rapid mapping activities in this case (see figure c), with an Area Under the Curve (AUC) of up to 0.849 under a logistic regression classifier and 0.833 under the intensity correlation normalised difference. The dense vegetation cover in this region caused low coherence values also in non-affected areas, which made the coherence-based methods less meaningful and resulted in AUCs less than 0.72 (normalised coherence difference) and 0.744 (multi-temporal coherence-based) respectively. The SVI analysis conducted as an approach for environmental recovery and reconstruction showed a severe drop in mean SVI values after the TDF (see figure d). After removing low-quality images from the collection, the calculated average z-scores show a persistent shortfall from pre-TDF conditions in the magnitude of several times the standard deviation. Thus, this remote sensing-based approach does not give any indication that the fauna in the affected area of the TDF has recovered yet.

Outlook for future

All mentioned approaches need to be tested on other TDFs to ensure their transferability. Furthermore, additional approaches have to be developed and tested to generate a comprehensive library of possible risk-mitigating approaches. Regarding the GIS-based model, more empirical research has to be done to refine the regression equations. Furthermore, up-to-date elevation models should be used instead of SRTM data, considering that mining changes the earth's topography rapidly. To improve the detection of affected regions during emergency response, a data fusion of different sensors is needed to merge the all-weather capabilities of radar sensors and high-resolution multispectral information from optical sensors. The MODIS-based SVI analysis exhibits problems regarding the resolution. Different systems, such as the Landsat or Sentinel-2 satellites should be tested. Furthermore, land-use changes have to be encountered, as the current approach assumes a recovery to pre-TDF conditions.

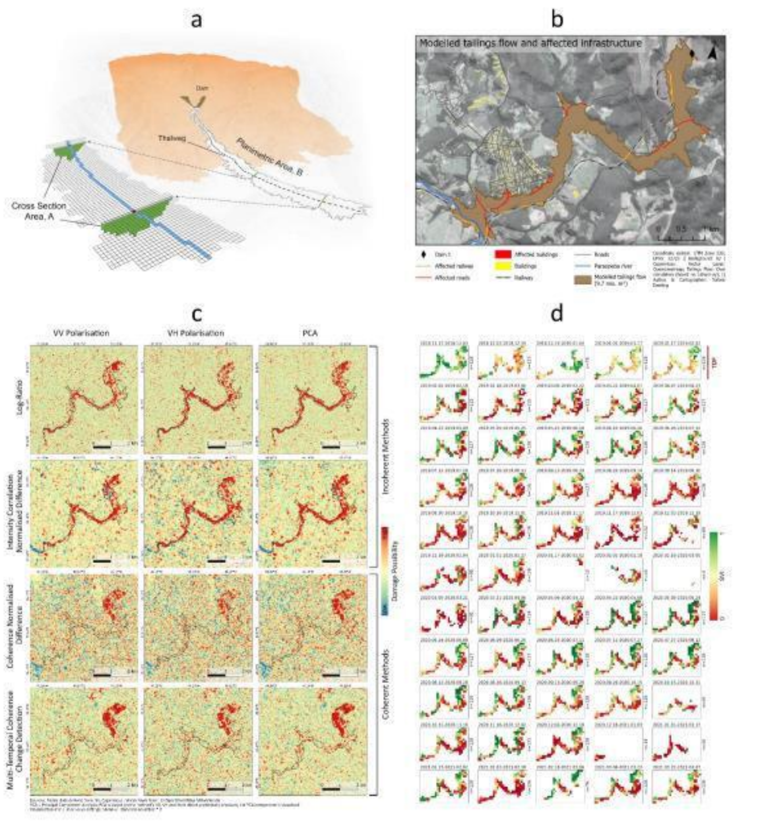

Figure (a) Schematic illustration of the cross-section area A and planimetric area B for the grid-wise modelling of a tailings flow (b) Modelling results of the TDF in Brumadinho, including the effected buildings and infrastructure (c) Results of Sentinel-1 mapping approaches for emergency response (d) Results of Standard Vegetation Index analysis shortly before and after the tailings dam failure

The Establishment of the CyCLOPS Integrated Strategic Research Infrastructure Unit for Geohazard Monitoring Activities: Considerations, Performance Assessment and Initial Results

Chris Danezis[1,2], Dimitris Kakoullis[1,2], Kyriaki Fotiou[1,2], Marina Pekri[1,2], Christopher Kotsakis[1,3], Miltiadis Chatzinikos[1,2], George Melillos[1,2]

[1] CYPRUS UNIVERSITY OF TECHNOLOGY, DEPARTMENT OF CIVIL ENGINEERING & GEOMATICS, PO BOX 50329, 3036, LIMASSOL, CYPRUS

[2] ERATOSTHENES CENTRE OF EXCELLENCE, LIMASSOL, CYPRUS

[3] ARISTOTLE UNIVERSITY OF THESSALONIKI, DEPARTMENT OF RURAL AND SURVEYING ENGINEERING, THESSALONIKI, GREECE

Keywords (5): *GNSS*; In*SAR*; *Corner Reflectors*; *earthquakes*; *landslides*; *Cyprus*

The challenge

CyCLOPS is a novel strategic research infrastructure unit established to monitor solid earth processes and geohazards, such as earthquakes and landslides via the integration of the two most prominent space-based Earth Observation deformation monitoring technologies; GNSS and InSAR. The objective of CyCLOPS is to augment the Cyprus geophysical and geodetic infrastructure and actively contribute to the growing demand for more precise positioning services aligned with important global frameworks and initiatives. One of the major challenges faced during the implementation of the project was the selection of sites for the establishment of the co-located sensor configuration to achieve maximum performance and deliver the most reliable deformation products. Concordantly, this paper aims to present an overview of the system architecture, the considerations followed and developed en route to its realization, and an initial performance assessment during the first months of its operation.

Methodology

CyCLOPS was designed and developed by the Cyprus University of Technology Department of Civil Engineering and Geomatics in collaboration with the German Aerospace Center (DLR) and supported by a wide range of national stakeholders. In this context, a network of Tier-1/2 permanent GNSS Continuously Operating Reference Stations (CORS) co-located with two permanent triangular trihedral Corner Reflectors (CRs) of 1.5 m inner length dimension, precise weather stations, and tiltmeters was established throughout the government-controlled areas of the Republic of Cyprus. Therefore, key parameters, such as monumentation specifications, equipment orientation and localization were seen, studied and dealt in accordance with the most stringent specifications set by international standards (i.e. UNAVCO, IGS and EPN) and scientific literature. A semi-automated multicriteria GIS-based site suitability methodology was developed to determine the most convenient CR locations using Analytical Hierarchy Process (AHP) analysis and a weighted overlay approach.

A campaign along with a 3D visibility analysis were then carried out to determine the final co-located GNSS and CR locations.

Results

To date, six (6) permanent sites have been established throughout the government-controlled areas of the Republic of Cyprus. Furthermore, a mobile segment of five (5) GNSS moveable stations was deployed in AOI, which have already suffered the impact of natural and anthropogenic hazards. An initial performance assessment of the permanent segment has been carried out, considering the requirements that a GNSS permanent station must meet for accuracy demanding applications, such as crustal motion i.e., stability, satellite visibility. The CRs were evaluated in terms of normalized Radar Cross Section (RCS). According to scientific literature, a GNSS CORS is considered stable if the horizontal and vertical coordinate changes do not exceed 10 mm and 15mm in 24 hours, respectively. Furthermore, the GNSS receiver should be able to track at least ten satellites above the elevation cut off angle of 0 degrees. Some preliminary results from GNSS station preprocessing are shown in Figure 4a. Regarding the CRs performance, an RCS of 34–38 dBm^2 in IW swath mode at C-band is the suitable range for a CR with an inner-length dimension of 1.5 m. Figure 4b illustrates the results of the normalized RCS for each CR, using thirty Sentinel-1 images (VV polarization) of ascending and descending orbit directions, respectively. The evaluation of the CRs resulted in suitable RCS values. Similarly to the CR results, the GNSS sites revealed sufficient daily horizontal stability and satellite availability.

Outlook for the future

The CyCLOPS unit is the first national strategic infrastructure to integrate dual CRs (one for each pass direction) with GNSS permanent stations and form the geodetic and geophysical backbone of the Republic of Cyprus. The next steps involve the exploitation of the integration of GNSS and SAR observations to form a seamless and reliable ground displacement monitoring system by fusing and referring deformation products from both techniques to a common datum. Furthermore, the unit will provide additional products, such as continuously updated displacement maps, hazard and risk maps, interactive earthquake and landslide GIS services, as well as a rapid crowdsourced-based damage assessment service. The aforementioned actions see to equally promote preparadeness, prevention and disaster recovery planning, increase resilience, and comply with global frameworks and initiatives, such as the UN SENDAI framework and the recommendations of UN-GGIM and its Subcommittee of Geodesy.

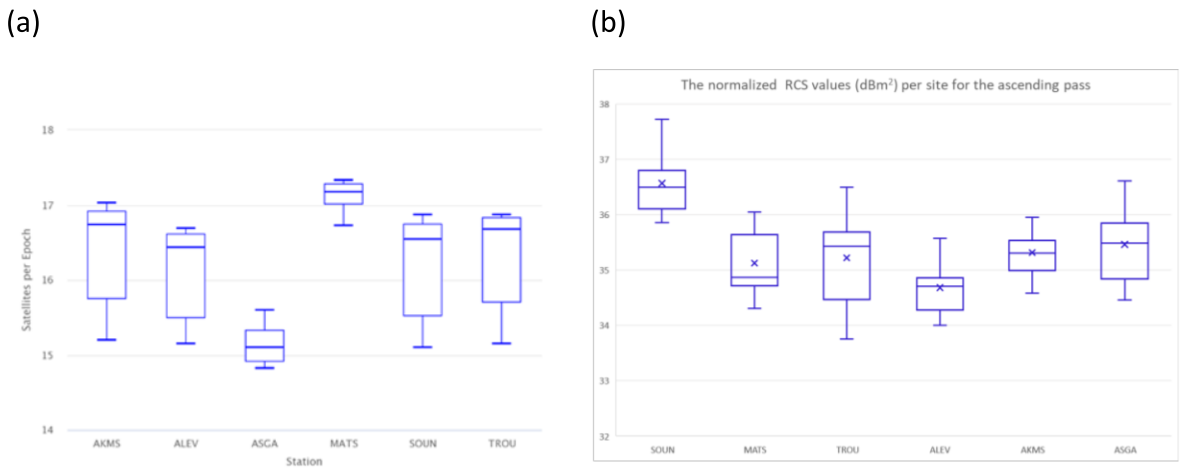

Figure 4: A snapshot from the initial performance assessment of the permanent segment. (a) The number of tracked satellites (GPS+GLONASS) per day and (b) the normalized RCS values derived from each CR oriented towards the Sentinel-1 ascending pass.

Acknowledgments:

The authors would like to acknowledge the 'CyCLOPS' (RIF/INFRASTRUCTURES/1216/0050) project (cyclops.cy), which is funded by the European Regional and Development Fund and the Republic of Cyprus through the Research & Innovation Foundation in the framework of the RESTART 2016 – 2020 programme.

The authors would like to acknowledge the 'EXCELSIOR' H2020 Teaming project (www.excelsior2020.eu). This paper is under the auspices of the activities of the 'ERATOSTHENES: Excellence Research Centre for Earth Surveillance and Space-Based Monitoring of the Environment'—'EXCELSIOR' project that has received funding from the European Union's Horizon 2020 research and innovation programme under Grant Agreement No. 857510 and from the Government of the Republic of Cyprus through the Directorate General for the European Programmes, Coordination, and Development.

A Review of Current GNSS Interference Detection and Localisation Techniques Towards the Development of Resilient GNSS Strategic Infrastructure

Nikolas Christoforou[1,2], Chris Danezis,[1,2],

[1]Cyprus University of Technology, Department of Civil Engineering and Geomatics, Cyprus

[2] Eratosthenes Centre of Excellence, Limassol Cyprus

Keywords: GNSS, Interference, Localisation, Geohazard, AoA, TDoA

The challenge

Global Navigation Satellite System (GNSS) technologies and applications are major building blocks of today's industrial revolution. A plethora of applications have already been developed covering essential domains of human life. This extends to science applications such as Geohazard monitoring systems that are heavily dependent on unobstructed reception of GNSS data to accurately monitor the effects of geohazards, such as earthquakes and landslides. Strategic infrastructure units are continuously incorporated in civil protection strategies and operation plans and constitute indispensable means for not only monitoring the hazards themselves but serve as critical damage assessment tools. The advent of jamming devices has recently increased intentional interference events. Interference detection techniques have been developed for the detection of jamming and in conjunction with localization techniques that derive the accurate location of the interfering source enable early warning and resolution of interference problems.

Methodology

The severe effects of interference on the GNSS signal integrity have alarmed the scientific community that has exerted significant efforts to comprehend, analyse and derive various methods for early interference detection. Through an extensive review of the existing literature the various detection techniques applied on different stages of the GNSS receiver have been comprehended. Through the review of the various techniques, it is evident that one cannot generally use the same detection method to deal with all types of interferences, as most techniques work relatively well on a fraction of cases. That said, the speed of interference identification is critical, especially in the critical domain of the Geohazard and Earth Observation domains. In addition to the early detection of interference it is equally important to be able to accurately geolocate the interfering source to be able to take any necessary actions to cease interference. According to the existing bibliography the most common approach is to incorporate a network of independent stations and by applying certain techniques such as the Angle of Arrival (AoA) where the orientation of a wavefront can be inferred from the time-difference, or phase difference measurements at two or more spatially displaced antennas or the Time Delay of Arrival where the interference source location can also be estimated from differences of signal propagation times that are measured at spatially displaced receivers.

Results

Existing infrastructure for monitoring natural Hazards in Cyprus and the Eastern Mediterranean as well as infrastructure from other local stakeholders are readily available and in use for a number of applications. The study aims to present the current interference detection and localisation techniques. These techniques will be chosen appropriately taking into consideration existing equipment apparatus as well as the topology and characteristics of the existing Geohazard and other monitoring stations. By incorporating additional equipment as needed the aim is to develop the first Cypriot GNSS Interference Early Warning System based on a network of stations that will enable continuous monitoring of the GNSS signals for interference detection and localisation. The study will evaluate critical parameters such as required equipment for the set-up of the network, the theoretical speed of interference detection that can be achieved and the theoretical localisation accuracy taking into consideration the preferred localisation technique. Finally, the results obtained can be validated by comparison with results from existing studies.

Outlook for the future

Following up the completion of the theoretical study and simulation of the preferred set-up, the study will be extended on a workbench environment where actual equipment and interference devices could be utilised to take real time readings and results. These results will be correlated to the simulated results and useful conclusions can be derived as far as concern the compatibility of proposed equipment and techniques as well as the validity and usefulness of the results. Further to that, the set-up can be incorporated on existing monitoring stations and operated for a dry-run period that will enable t define the availability and integrity of the system. Finally with the system fully operational and tested an effort will be made to secure approval from the respective National Authorities to contact an experiment by incorporating a low power jammer in real conditions to perform a real-time detection and geolocation, in the framework of the CyCLOPS research infrastructure unit.

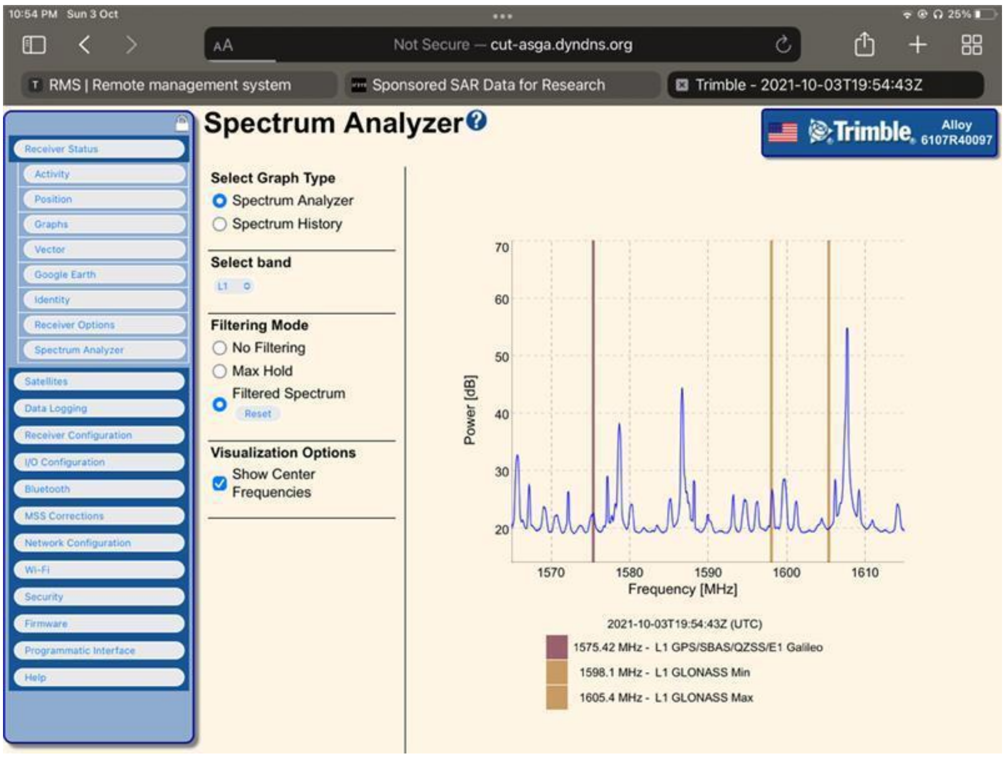

Figure (a) Recent case of interference recorded by the CyCLOPS strategic research infrastructure unit in Cyprus

Acknowledgements: The CyCLOPS project is co-funded by the European Regional Development Fund and the Republic of Cyprus through the Research and Innovation Foundation

Assessing the Resilience of Flood Defense Structures via Radar MTI & Backscatter Analysis

Dimitris Kouhartsiouk[1] , Skevi Perdikou[1]

[1] Geofem Ltd., Cyprus

Keywords: DInSAR, MTI, PSI, Levee, Infrastructure

The challenge

Areas around the world are exposed to the increased risk of flooding, more so in the face of extreme weather events and climate change. The failure of flood protection systems, such as water barriers and levees, results in major economic, social, and environmental losses, with the integrity of these systems being critical for millions of people globally. For this purpose, flood defense infrastructure, and in particular aging structures, require monitoring in an efficient and cost-effective way. Knowing if, where, and when a failure will occur is a crucial issue to consider when it comes to safety. In this study, we demonstrate the use of satellite radar for addressing the challenge of monitoring the deformation rate of sections of the Dutch levee network as well as the temporal profile of surface moisture that may be linked to the observed instability.

Methodology

The first part of the methodology encompasses the employment of the Multi-temporal Interferometry (MTI) processing technique known as Persistent or Permanent Scatterers Interferometry or PSI. The technique is based on the analysis of point targets on the surface, natural or artificial, that exhibit consistent radar signal scattering characteristics i.e., strong temporal scattering using satellite Synthetic Aperture Radar (SAR) data. PSI enables the estimation of deformation time-series of points in an interferometric data stack with a coherent radar backscattering over time. PSI is considered ideal for application of levee deformation monitoring particularly in the case of man-made structures such as concrete and earth embankments being generally strong radar scatterers. For estimating the deformation within the study area, PSI was applied on a dataset comprised of Copernicus Sentinel-1 radar imagery to study the deformation rates along the Dutch levee network. The second part of the methodology deals with the calculation of the surface soil moisture of the levees, where soil moisture plays a key role in slope stability assessment, particularly in the presence of ground high in clay minerals and therefore most prone to expansion and swelling. For the purpose of estimating the soil moisture, the amplitude component of satellite radar was examined for the same period as in-situ soil moisture sensor data. Spatiotemporal filtering was then applied to match corresponding values from both datasets (in-situ sensor vs satellite), with the inclusion of vegetation descriptors derived from optical satellite imagery (Copernicus Sentinel-2) to account for varying surface roughness affecting the radar backscatter. A machine learning model for soil moisture estimation was used to simulate the relationship of radar backscatter (backscatter coefficient) to soil and ground properties (soil moisture and vegetation) based on the inversion of the semi-empirical Water Cloud Model (WCM)* , a widely used radar backscatter model applied to radar imagery to retrieve soil moisture over vegetated areas. * Gao, Q.; Zribi, M.; Escorihuela, M.J.; Baghdadi, N. (2017)

Synergetic Use of Sentinel-1 and Sentinel-2 Data for Soil Moisture Mapping at 100 m Resolution. Sensors, 17, 1966 2

Results

The results of the PSI analysis showed a clear identification of sites exhibiting high displacements with some exceeding 60mm over the study period. The analysis of PS targets has resulted in the identification of approximately 158,000 permanent scatterers / targets over the study area with a good density coverage of the levee network. A number of locations along the levee network exhibiting deformation corresponding to over 25mm in Line-Of-Sight displacement have been identified (sites A, B, C and D in Figure 1). The displacement observed over parts of the levee network is indicative of settlement, potentially associated to post-construction phase. Regarding the soil moisture data analysis, the two datasets (in-situ soil moisture vs radar backscatter) showed strong correlation between them with positive covariance (increasing backscattering signal with increasing soil moisture content and vice-versa).

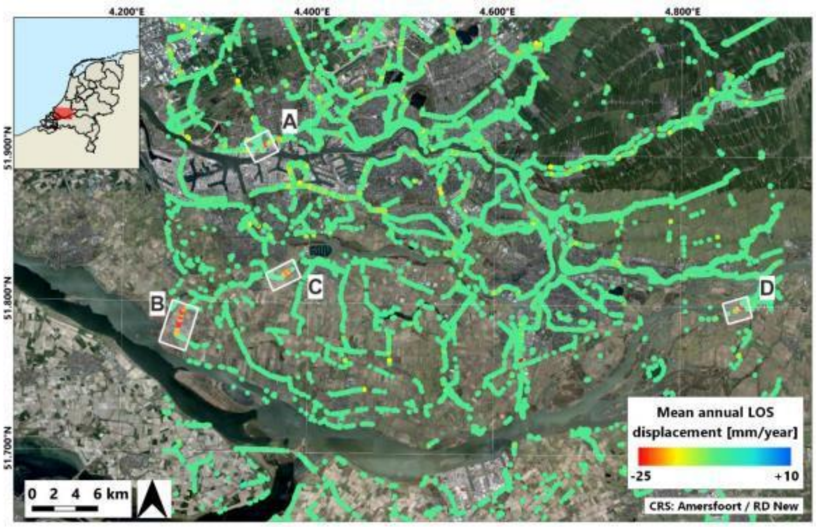

Figure 1 Line-of-Sight mean annual velocity over the levee network within the study area †. Results are preliminary.

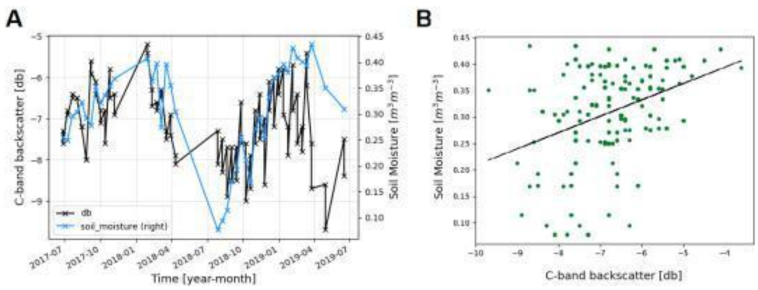

Figure 2 A: temporal profile of backscatter / σ^0 (db) and corresponding surface soil moisture over site A. B: correlation between soil moisture and backscatter (σ^0) via linear regression analysis (B). Results are preliminary.

Outlook for the future

The output and more particularly the calculated correlation between backscatter and surface soil moisture over bare soil conditions is potentially very important as calibration of the satellite radar backscattering via in-situ sensor measurements can provide wide coverage of satellite derived soil moisture measurements over large areas. This will enable the estimation of the soil moisture by the use of satellite derived means. The process of deriving surface soil moisture is still a complicated task and effects of land coverage, surface roughness and satellite specific parameters will also need to be accounted for to enable the development of a soil moisture algorithm. Further work is underway for this, also including a larger dataset, combined with further adjustments of parameters for ML training expected to further improve the correlation. This will enable the measurement of satellite-based soil moisture which, combined with the displacement measurements via satellite data, can provide a robust solution for non invasive assessment of ground structures and particularly with regards to levee resilience and safety.

Combined use of InSAR and FEA for the monitoring of landslides

Egli Michailidou[1] , Styliana Stavrou[1], Christakis Lereidis[1], Iordanis Aloupas[1], Skevi Perdikou[1]
[1] Geofem Ltd, Cyprus

Keywords: DInSAR, PSI, Landslide, FEA, Pianello

The challenge

Slow-moving landslides, move with low velocities over long periods of time and occur in many places worldwide. Even if they are considered as non-catastrophic, they can cause damages and transform to catastrophic fast-moving landslides due to triggering mechanisms. Therefore, the monitoring of landslideprone regions and the detection of the acceleration of active landslides is crucial. Differential Interferometric Synthetic Aperture Radar (DInSAR) techniques allow the systematic monitoring of structural and ground movements, and also enable a historical analysis that can provide indications of precursory deformation signals before catastrophic landslides. The combination of DInSAR with geotechnical Finite Element Analysis (FEA) provides valuable information for the monitoring and the identification of the possible causal factors of the landslides. In this paper an example of monitoring the temporal evolution of the Pianello landslide is presented, in the Bovino town in Southern Italy.

Methodology

For the monitoring of the Pianello landslide, Sentinel-1 data are used, for the period 2020 to 2022 in both ascending and descending orbits. The most suitable DInSAR technique for monitoring the slow-moving landslide, that affects the residential area of the town of Bovino, was considered to be Persistent Scatterer Interferometry (PSI). PSI provides the velocity of temporally coherent point targets in the satellite line-ofsight (LOS) direction in mm/year and the combination of the velocities in both directions ascending and descending can provide information about the vertical and horizontal (Earth-West) velocity of the points. In addition to the use of satellite data, this paper also presents the estimation of ground movements by the means of FEA. The predicted displacements by the FEA were compared to measured displacement both from in-situ monitoring and satellite data. The FEA model was developed using available information on the site geometry, soil stratigraphy and properties, water levels and construction sequence to approximate the stress history and field conditions. The soil stratigraphy is described by thick clay layers of Faeto Flysch characterized by poor mechanical properties which can be considerably influenced by the varying water regimes during winter and summer periods.

Results

The PSI results showed several point targets exhibiting significant displacements over the town of Bovino within the limits of the Pianello landslide. The displacements acquired from the descending geometry (westward LOS) are positive indicating movement towards the sensor, whereas the results from the ascending geometry (eastward LOS) are negative indicating movement away from the sensor. The decomposed results show vertical and horizontal movements in the east direction, as expected considering the ground sloping to the east. The slope movement rate is characterized by an almost linear trend and in the horizontal east direction there are velocities of around 30 mm/year and total displacement of 60 mm over the two-year study period. The FEA results showed to be in good agreement 2 with identified developed landslide bodies of existing literature studies. The predicted safety of the slope was found to be moderate which did not indicate a sudden large landslide event but correlated with a slow-moving landslide, agreeing with reports of the area. The predicted horizontal displacements were also showing similar trends to ones measured using satellite data which is approximately 30mm/yr. The results of the analysis did not show any signs of reduction in the rate of movement, which makes the monitoring of the landslide very important.

Outlook for the future

The next steps include a parametric analysis that will combine the results retrieved from the DInSAR and FEA analyses, in order to identify the sensitivity of each parameter contributing to the landslide event. Therefore, an identification of the triggering factors will follow, that together with the monitoring of the progress of the landslide movement and the understanding of the structural behaviour will lead to the better monitoring of the behaviour of this landslide while demonstrating the powerful use of combined DInSAR and geotechnical FEA methods.

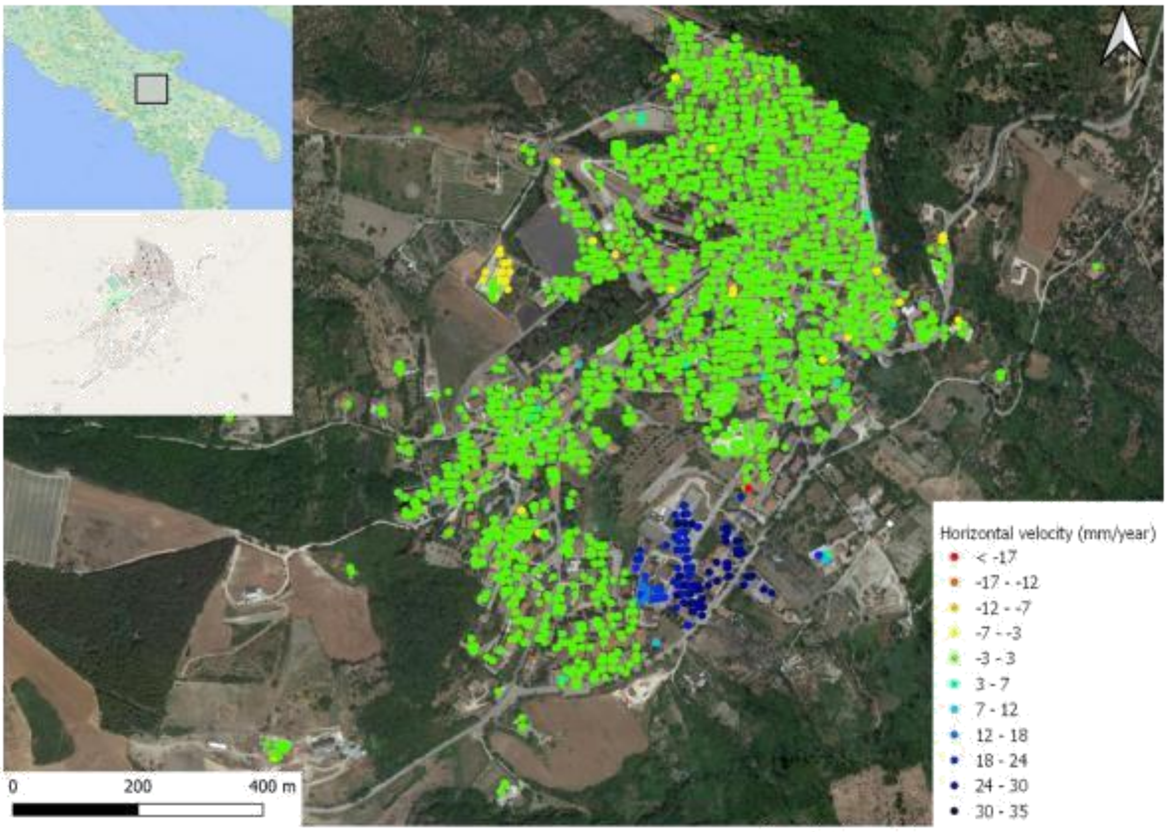

Figure 1. Horizontal mean annual velocity over the Bovino town

Slide-Map – a platform for landslide risk mapping in near-real time

Ionuț Șandric[1,2], Viorel Ilinca[3,2], Radu Irimia[1,2], Zenaida Chițu[4,5,2]

[1]University of Bucharest, Faculty Of Geography, Romania
[2] University of Bucharest, Institute For Research (Icub)
[3] Geological Institute of Romania, Caransebeş Street, No. 1, Bucharest, Romania
[4] National Meteorological Administration, 013686 Bucharest, Romania
[5] National Institute of Hydrology And Water Management, 013686 Bucharest, Romania

Keywords (5): landslides, artificial intelligence, UAV, risk assessment

The challenge

Artificial intelligence is successfully applied in landslide studies from mapping susceptibility or hazard to vulnerability and risk assessments and regional and local scales. The current paper presents the Slide-Map platform, designed to take one step further the landslides studies by implementing tools used to detect and map landslides features and do a rapid risk assessment with a minimum effort from the user's side. The platform is integrated into the ArcGIS system and provides the user with complete workflows from planning a UAV flight to the automatic detection of landslide features to assess the risk induced by landslides. The main challenges tackled by the Slide-Map platform are related to the detection and mapping of landslide features, the elements exposed to risk and creating a preliminary risk assessment report by using aerial imagery derived products, oblique aerial imagery and full-motion videos, mapping.

Methodology

The Slide-Map platform makes use of the latest developments in the field of deep learning by implementing several algorithms used in object instance segmentation and pixel classification. For the landslide fissures and cracks detection and mapping, it makes use of the Mask RCNN model, and for the landslide bodies, detection and mapping use the U-net model, both implemented in ArcGIS For Python API. The platform is developed on top of ArcGIS Pro. Based on the best practices in terms of maintainability, the integration with third-party software was developed using proxy components that implement each components' SDK or API, making these external solutions easy interchangeable. The first module presented in the paper covers the integration of the UgCS flight planning solution. Near-real time detection and mapping are performed on full-motion video streamed from the UgCS to the ArcGIS Pro.

Results

The platform has been implemented and tested within the Romanian Subcarpathians. A number of eight different case studies have been selected, and for each case study, at least one UAV flight has been flown. A few thousand samples were collected as training and validation datasets and used to train deep learning models for mapping the landslide features and the elements exposed to risk. Accuracies of 0.77 and 0.70, estimated from the Intersect over Union metric, have been achieved for the landslide fissures, cracks and bodies detection. Higher accuracies of 0.86 have been achieved for mapping roads located in the vicinity of the landslides, and even higher accuracies of 0.96 have been achieved for the detection of houses and other constructions. A slight decrease in the validation accuracy was observed when the images were collected on older landslides compared to recent landslides. Overall, the detection of fissures and fractures using deep learning and UAV aerial imagery proved reliable if the UAV flights are flown quickly after the landslide occurrence or after recent rainfalls. For the risk assessment, the platform uses the landslides features, the roads, and the houses previously detected and estimates the degree of risk based on the distance between the exposed elements and the landslide location. Further, if available, it estimates the areas that could be isolated in the case of a road failure caused by the landslide evolution.

Outlook for the future

The Slide-Map platform will be further developed to account for new functionality in the near future. One of the objectives is to integrate new sensors mounted on UAVs, like LiDAR and multispectral, to enhance landslide features detection and mapping. Another objective is to implement new algorithms for the precise mapping of the landslides features and vulnerable elements from only oblique aerial imagery and/or full-motion videos. Other aspects related to mapping the landslide dynamics and rapid assessment of landslide volumes are planned to be developed and integrated into the Slide-Map platform.

Poster(s)

The utilisation of DInSAR for the monitoring of the Shuibuya's concreteface rockfill Dam (CDRF) in China

Styliana Stavrou[1] , Egli Michailidou[1], Skevi Perdikou[1]

[1] Geofem Ltd, Cyprus

Keywords: InSAR, Dam, Monitoring, Settlement, PSI

The challenge

The monitoring of the civil structures' behaviour at different operational stages to ensure their safety and their good condition during their entire lifecycle is crucial. Dams are examples of structures that in a possible collapse, claim lives and cause great damage to the surrounding areas. In the case of high concrete-face rockfill dams (CFRD), their monitoring with traditional approaches is limited, especially in remote locations. Hence, Differential Interferometric SAR (DInSAR) techniques can be used effectively for the deformation monitoring of the dams and to provide information about any signs of problems. In this paper, the monitoring of the Shuibuya Dam located on the Qingjiang River in Badong County, Enshi, Hubei Province in China with a height of 233.5 m is presented. It was constructed in January 2022 for the purposes of serving a hydroelectricity production plant.

Methodology

Concrete-face rockfill dams like Shibuya's dam are suitable for being monitored via the satellite multi-temporal interferometry techniques of Persistent Scatterers (PSI) and / or Small Baseline Subset (SBAS), as they form good scattering surfaces that can provide high density of detected targets. PSI provides the mean annual velocity of temporally coherent point targets in the lineof-sight (LOS) direction in mm/year. For the monitoring of the dam in this project, a dataset of 86 ascending Single Look Complex (SLC) images from January 2019 to December 2021 were used. Man-made features such as roads, buildings, or natural ones like rocks, form coherent targets exhibiting consistent signal, while the loss of coherence is often associated with vegetation. This dam shows strong coherence due to its wide area of concrete surface. The geology of the wide area consists of rock materials, which increases the stability of the dam's surroundings. According to the literature and previous research, an embankment may settle to a level where it is overtopped by water and failure will occur.

Results

The results extracted from the PSI analysis showed a continuous movement away from the satellite with signs of stabilisation over time. As this displacement concerns a dam, the anticipated movement is mainly vertical, and therefore settlement is observed. The analysis showed that the range of the LOS mean annual velocity on the dam is between 0 and -11 mm/year. The output also indicated that the largest settlement occurred in the upper and middle parts of the dam, while the sides and the bottom of the dam presented relatively small or no changes. Long-term settlements of the dam are expected especially when it concerns 2 such a huge concrete-face rockfill dam like Shibuya's dam. Deformation is caused by loading from gravity, the reservoir water level, and the characteristics of the rockfill. Overall, the results and the monitoring points suggest that the absence of anomalies in the temporal evolution of settlement, such as a significant displacement, is a common behaviour for this type of dam and shows that the Shuibuya's dam is well-constructed and operated.

Outlook for the future

After construction was completed (October 2016) a period of a sharp and continuous increase of settlement followed that was reduced over time. Due to the soil properties and the aquifers that are able to change the conditions of the whole construction, the dam might not stabilize completely. It is therefore important to continue its monitoring using DInSAR methods, to avoid unpredictable and big-scale displacements. In this way, excessive movements could be detected and identified early on, for the appropriate interventions to take place and prevent catastrophes, while ensuring the dam remains in good condition.

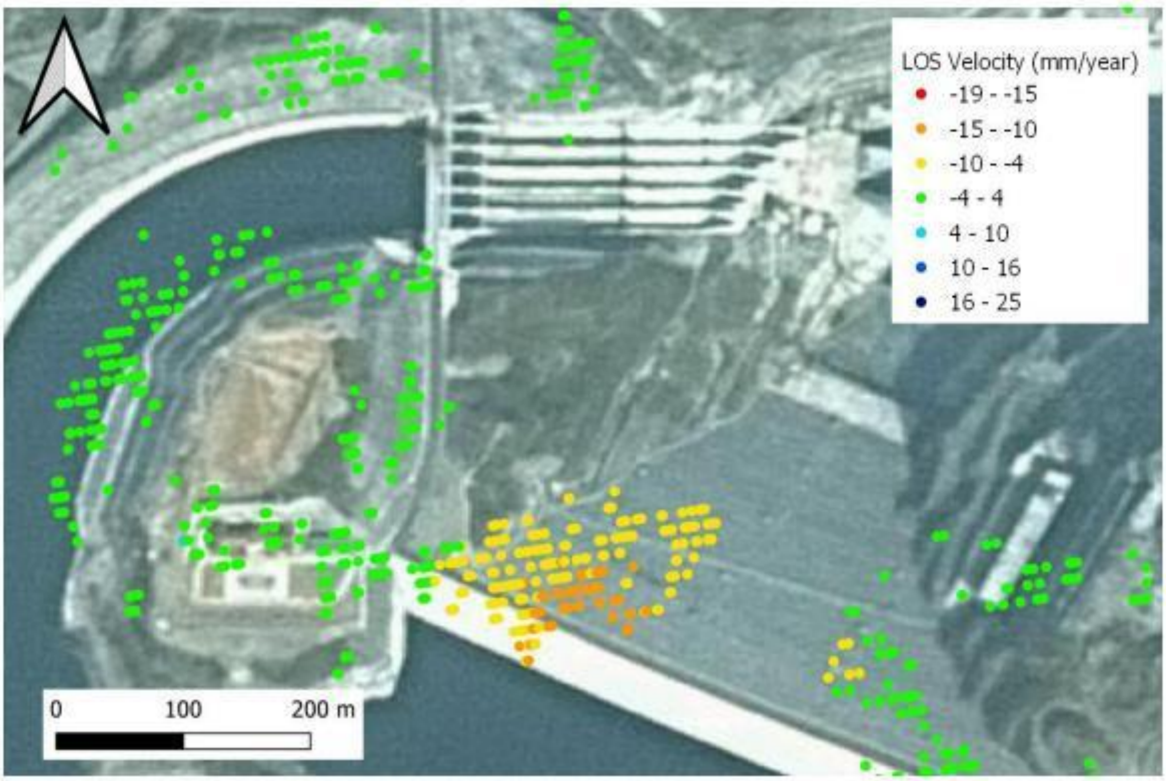

Figure 1: Line of Sight velocity over the Shibuya dam.

Mapping Exposure to Landslides by Means of Artificial Intelligence and UAV Aerial Imagery in the Curvature Subcarpathians, Romania

Zenaida Chitu[1], Ionut Sandric[2], Viorel Ilinca[3], Radu Irimia[4]

[1]Institute for Research (ICUB), University of Bucharest, Romania

[2] Faculty of Geography, University of Bucharest, Romania

[3] Institute for Research (ICUB), University of Bucharest, Romania

[4] Faculty of Geography, University of Bucharest, Romania

Keywords (5): risk assessment, aerial images, automatic detection, landslides, infrastructure elements.

The challenge

Curvature Subcarpathians is one of Romania's most complex geological and geomorphic areas, frequently affected by landslides. The juxtaposition of snowmelt and spring rainfalls triggers significant damage to roads and buildings every few years (2018, 2021). In this context, accurately delineating the most affected areas becomes critical for evaluating landslide exposure.

Methodology

Aerial images have begun to be used more for different risk assessment phases to detect natural phenomena spread and damaged infrastructure elements. In this study, we use a fully automatic detection of the landslide body and infrastructure elements (intact or collapsed buildings and roads) to support Regional Civil Protection Agencies in disaster intervention decision support. Our methodology is based on deep learning techniques for automatic detection, mapping and classification of landslide and infrastructure elements. A U-Net model was trained to detect the landslide body, and several Mask RCNN models were trained to detect the landslide features and infrastructure elements.

Results

The training accuracy for the U-Net model used for landslide body mapping is 0.86, and the validation accuracy is 0.80. The training accuracy of the Mask RCNN models is 0.76 for landslide cracks, 0.82 for roads and 0.92 for buildings. Some confusion between landslide cracks and local roads without asphalt is often seen in rural areas. The models are run on high-resolution aerial imagery collected with Unamend Aerial Vehicles after a landslide event. The data obtained from the deep learning models are further integrated with information from various sources such as aerial/satellite imagery, online GIS resources, weather forecasts, and spatial analysis techniques for providing a helpful tool to emergency management specialists.

The tools have been integrated into a GIS platform that acts as a decision support system, and it can be used from a graphical user interface without the need to have programming skills.

Outlook for the future

Even though this tool was demonstrated only in two study areas located in Prahova County, where road infrastructure is exposed to landslide occurrence, we intend to extend its usability at the level of the Civil Protection Agency in Romania.

S_InnT: Innovative Technologies in Remotely Sensed & In-situ Data

Chair(s): Prof. Andreas Anayiotos, Maria Zoran

UAV-based glacier monitoring: GNSS kinematic track post-processing for accurate reconstruction in challenging environments

Valeria Belloni[1], Davide Fugazza[2], Martina Di Rita[3], Mattia Crespi[4]

[1] Sapienza University of Rome, DICEA, Rome, Italy
[2] University of Milan, Department of Environmental Science and Policy, Milan, Italy
[3] Leica Geosystems AG, Heerbrugg, Switzerland
[4] Sapienza University of Rome, DICEA - Sapienza School for Advanced Studies, Rome, Italy

Keywords: UAV photogrammetry, UAV kinematic track post-processing, Glacier monitoring

The challenge

Over the past decades, different approaches have been investigated to identify the best method to monitor glacier morphology changes. Among them, UAV campaigns have proven to be ideal candidates since they enable data collection over wide areas in a reasonable time. Also, following best practices for data acquisition and processing, UAVs and SfM allow reconstruction of the 3D surface with good accuracy. Nowadays, many UAVs offer GNSS RTK capabilities that can improve the accuracy of reconstructions. However, there are circumstances in which accurate RTK solutions cannot be achieved in the field. For this reason, the post-processing of UAV kinematic tracks could represent a powerful tool for improving 3D models. The present work aims to investigate UAV track post-processing for improving the accuracy of 3D models in complex glacier environments. The impact of UAV track post-processing is investigated using direct georeferencing to demonstrate that it can compensate for the loss of RTK.

Methodology

UAV GNSS track post-processing represents an interesting topic since in challenging environments such as glaciers, RTK connections can be unavailable or lost during the acquisition, due to occlusions or long distances between the UAV and the reference station. Also, UAV GNSS track post-processing could greatly improve glacier reconstructions when Ground Control Points (GCPs) are scarce or not available. In the present work, the Leica Infinity software is used to investigate the potential of its new tool for UAV track post-processing, released in the 3.6.1 version. This tool is dedicated to improve image positioning accuracy and derive the best 3D models. The study area is Forni Glacier (Central Italian Alps) and the used UAV is a DJI Phantom 4 RTK. During the campaign, performed in August 2021, UAV images and 3D point coordinates were acquired. The data were firstly processed following a standard photogrammetric workflow based on direct georeferencing, without UAV track post-processing and using camera precalibration. The image orientation was computed with SfM integrated with bundle block adjustment to generate the 3D model of the glacier and an accuracy assessment was performed using the 3D points. Then, independent processing was carried out including UAV track post-processing to assess its impact on improving the accuracy of the reconstruction. An accuracy assessment was performed as in the first test. Finally, the Dense Point Cloud (DPC) of the glacier was generated.

Results

This section presents the results of image orientation, DPC generation and glacier loss computation using Leica Infinity. Table 1(a) shows the assessment of the standard photogrammetric approach based on direct georeferencing. The results highlight residuals on the Check Points (CPs) of 0,56 m, 0,74 m and 1,27 m in Easting, Northing and Orthometric Height, respectively. The errors are due to the shift between the coordinate system of the CPs and the UAV images which is caused by the RTK signal loss and the inaccurate position of the UAV drone station. Table 1(b) shows the results of the approach based on UAV track post-processing and direct georeferencing. The results highlight CP residuals below 0,04 m in Easting, Northing and Orthometric Height, demonstrating that UAV track post-processing can improve the accuracy in challenging environments and compensate for inaccurate in-situ measurements and RTK loss. It also demonstrates the possibility of generating accurate 3D models without GCPs, if the camera is pre-calibrated. This is an interesting result since the GCP setup is usually complex and a sub-optimal target distribution can highly affect the results.

CP id	ΔE (m)	ΔN (m)	ΔH (m)	Mean Reproj. Error (px)	Images Marked n.
A001	-0,59	0,76	1,30	23,1	10
A003	-0,77	0,89	1,33	83,0	6
0000A	-0,50	0,72	1,25	32,7	9
0000B	-0,51	0,71	1,33	60,2	4
0000E	-0,53	0,75	1,26	23,2	10
0000G	-0,51	0,73	1,28	32,6	10
0000I	-0,52	0,72	1,24	31,0	10
000L	-0,55	0,71	1,22	32,7	10
0000F	-0,55	0,69	1,27	38,3	10
0000H	-0,69	0,75	1,24	36,3	10
Red Dot	-0,51	0,74	1,24	35,3	10
001	-0,54	0,74	1,26	26,8	10
0014	-0,52	0,71	1,27	34,0	10
Mean	**-0,56**	**0,74**	**1,27**	**37,6**	**-**
SD	**0,08**	**0,05**	**0,03**	**16,4**	**-**
RMSE	**0,57**	**0,74**	**1,27**	**40,8**	**-**

(a)

CP id	ΔE (m)	ΔN (m)	ΔH (m)	Mean Reproj. Error (px)	Images Marked n.
A001	0,00	0,00	0,04	0,4	10
A003	0,01	0,00	0,03	1,0	6
0000A	0,00	0,00	0,01	0,4	9
0000B	-0,02	-0,01	0,04	0,7	4
0000E	-0,02	0,01	0,04	0,6	10
0000G	0,00	0,01	0,03	0,5	10
0000I	-0,01	0,00	0,01	0,5	10
000L	0,00	-0,01	0,01	0,4	10
0000F	0,00	-0,02	0,00	0,7	10
0000H	0,00	-0,02	0,04	0,8	10
Red Dot	-0,01	0,02	-0,01	0,7	10
001	-0,01	-0,01	0,00	0,4	10
0014	0,01	0,01	0,01	0,7	10
Mean	**0,00**	**0,00**	**0,02**	**0,6**	-
SD	**0,01**	**0,01**	**0,02**	**0,2**	-
RMSE	**0,01**	**0,01**	**0,02**	**0,6**	-

(b)

Table 1 Assessment without (a) and with (b) UAV GNSS track post-processing

Figure 1(a) shows the glacier DPC generated using UAV track post-processing. Figure 1(b) presents a preliminary comparison between the generated 2021 DPC and a previous 2016 DPC. The comparison highlights an average glacier height loss of 30 m in five years with a maximum value of 50 m.

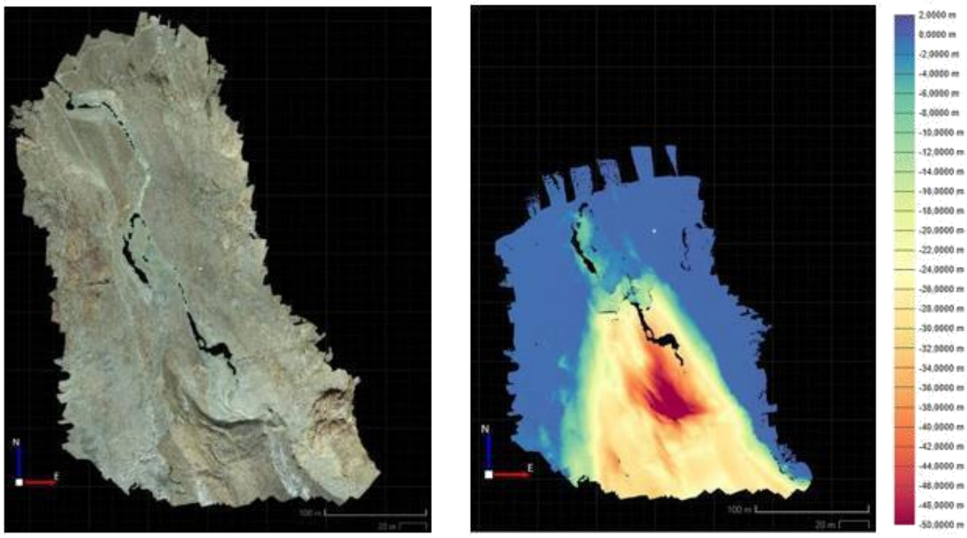

(a) (b)

Figure 1 Forni Glacier 3D model (a) and height loss (2016-2021) (b)

Outlook for the future

In future works, the aim is to evaluate the loss of the glacier using a multi-temporal differencing approach of glacier DSMs. Specifically, the DSM from the 2021 campaign will be compared to the generated DSMs of Forni Glacier corresponding to 2014, 2016, 2018, 2019 and 2020, to evaluate the glacier loss over a period of seven years. The comparison will be entirely performed with Leica Infinity software that allows height and volume loss computation between DSMs through the available *Comparison map* and *Volume* computation tools. Also, to improve loss computation, co-registration methods will be investigated in case the shifts between the DSMs are not neglectable. As already mentioned, preliminary results of a comparison between the 2016 and 2021 DPCs showed that the glacier lost around 30 m (with a peak of 50 m) in height in five years. However, further detailed analyses will be performed to better understand the evolution of the glacier over time and the impact of climate change.

Assessment Of COVID-19 Impacts On Satellite-Observed Aerosol Loading Over Few European Metropolitan Cities

Dan Savastru[1], Maria Zoran[1], Roxana Savastru[1], Marina Tautan[1]

[1]National Institute of R&D for Optoelectronics, ITC Department, Bucharest- Magurele, Romania

Keywords: Aerosol Optical Depth (AOD), COVID-19, MERRA-2, MODIS.

The challenge

Under COVID-19 pandemic period, with the progress of air pollution control in European Community countries, the concentrations of particulate matter PM2.5 and PM10 at the ground level have decreased. However, the issue of the complex air pollution in metropolitan cities has become more severe, posing a serious threat to environment. Aerosols emitted in the European densely populated and industrialized metropolitan cities have a high impact on air quality, radiative forcing and local and regional climate system, with a significant risk to human public health, especially during viral pandemic periods like as COVID-19. This remote sensing-based study aims to investigate the spatiotemporal variations of MODIS-derived Aerosol Optical Depth (AOD) and Modern-Era Retrospective analysis for Research and Applications (MERRA-2) data during January 2019 - November 2021(covering four COVID-19 waves) over six metropolitan cities in Europe (London, Berlin, Paris, Madrid, Milan, and Bucharest).

Methodology

Satellite aerosol products are available from several moderate spatial resolution sensors and provide information on the spatial and temporal dynamics of aerosol concentration. Satellite-based AOD retrievals are validated against in-situ AOD measurements from three AERONET ground stations located in urban/land, rural/ coastal, and ocean surfaces. This paper used the Modern-Era Retrospective analysis for Research and Applications (MERRA-2) derived total aerosol optical depth (AOD) product provided by NASA and Copernicus Atmosphere Monitoring Service (CAMS). As a measure of the aerosol column concentration over a large urban area, AOD represents the attenuation of sunlight by aerosols being a fundamental variable used to study aerosol loading in the atmosphere. Have been analyzed temporal patterns of observational data of the total AOD at 550 nm in the period before the outbreak of the epidemic and during the implementation of preventive measures and control of COVID-19, as well as compared it with the data obtained in the same period of 2015-2019 years. Cross-correlation analysis was used to evaluate the similarity between two-time series data of daily climate observables (Planetary Boundary Layer heights, air temperature and relative humidity, wind speed, surface solar irradiance and daily AOD levels, under different synoptic meteorological conditions.

Results

The results of the analysis showed that the COVID-19 lockdown improved air quality in the short term, but as soon as coal consumption at power plants and refineries returned to normal levels due to the resumption of their work, pollution levels returned to their previous level. One of the key results of this research underlines a significant reduction of the AOD levels over metropolitan cities (mostly for Milan and Bucharest cities) during the first COVID-19 wave from spring 2020 total lockdown period as compared to the long-term average AOD level (2015–2019) for the same periods of the year (**Fig.1**). Seasonal variation of AOD over the investigated metropolitan cities during analyzed COVID-19 pre- and pandemic period demonstrated clear annual course with maxima in spring and summer and minimum in autumn and winter. High AOD values can be attributed to hygroscopic growth of aerosols, formation of secondary aerosols and pollutants as a result of agricultural biomass combustion after crop harvesting in the periurban areas, which entails pollutants accumulation in this region. In spring season, the whole areas of the Southern European metropolitan cities (Madrid, Paris, Milan and Bucharest) are exposed to increased dust concentrations, which comes from the transboundary sources like Saharan intrusions leading to increase of AOD values.

Outlook for the future

The results further highlight the urgent need of moving towards air pollution approach linkage with pandemic viral infections research under atmospheric emissions reduction and global warming. This study highlights the imperious need to better monitor and understand how the chemical responses of secondary pollutants to emission change under complex meteorological conditions, along with climate change and socio-economic drivers may affect future air quality in large urban areas. The implications for regional and global policies for air quality improvement based on geospatial information are also significant, as our study clearly indicates that AOD levels would not likely meet the World Health Organization guidelines in many European metropolitan cities, despite the drastic reductions in mobility. Consequently, are well required revisions of air quality regulations with more ambitious targets that are specific to the different regions of the European metropolitan cities.

Acknowledgements: This work was supported by the Romanian Ministry of Research, Innovation and Digitalization, through Program 1- Development of the national research-development system, Subprogram 1.2 - Institutional performance - Projects to finance the excellent RDI, Contract no. 18PFE/30.12.2021, and Program NUCLEU Contract 18N/ 08.02.2019 Act Adit. Nr. 15 /2022

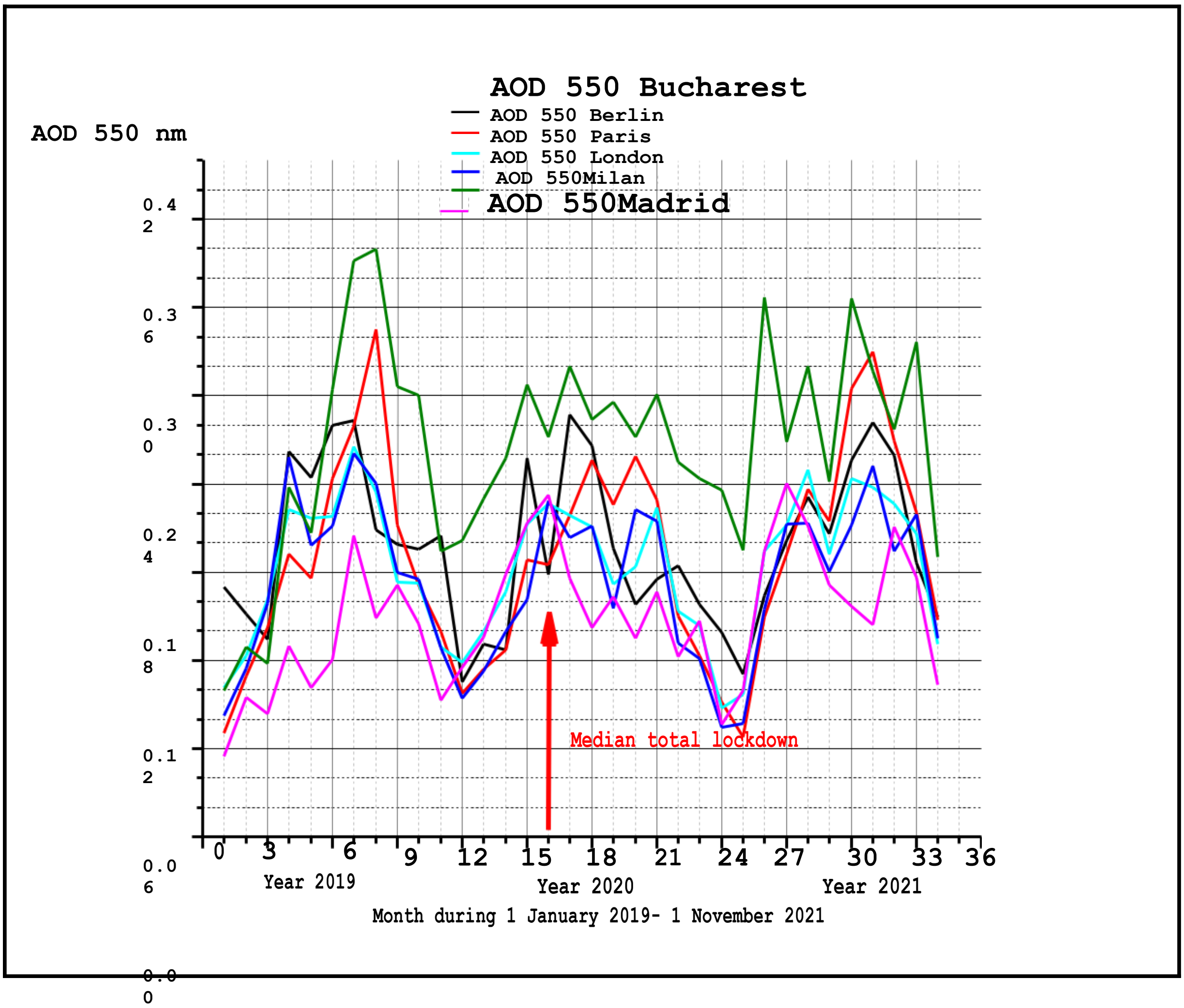

Figure 1. Aerosol Optical Depth at 550 nm temporal patterns between 1 January 2019- 1 November 2021 for Madrid, Paris, Milan, London, Berlin, and Bucharest European metropolitan cities.

Landsat 9 Data and GEE For Estimating Land Surface Albedo Over Southern Italian Cities

Carlo Barletta[1], Alessandra Capolupo[1], Eufemia Tarantino[1]

[1] Department of Civil, Environmental, Land, Construction and Chemistry (DICATECh), Politecnico di Bari, via Orabona 4, 70125 Bari, Italy

Keywords: Open satellite data, cloud-computing, Climate Change (CC), sustainable development, Copernicus UrbanAtlas

The challenge

Land surface albedo is a relevant factor to tackle climate changes issue as it drives the energy balance of the Earth surface. To safeguard our planet from the main global threats, the United Nations defined 17 Sustainable Development Goals (SDGs). Monitoring albedo is essential to assess climate changes impacts, which put at risk the achievement of sustainable development [**Error! Reference source not found.**-5]. For this purpose, open satellite data and cloud platforms, like Google Earth Engine (GEE), are very suitable [**Error! Reference source not found.**-**Error! Reference source not found.**]. Moreover, the launch of Landsat 9 mission in 2021, offers new opportunities, not yet explored, in retrieving albedo maps with an improved quality than Landsat 8. The aim of this study is to test the Silva *et al*. algorithm, introduced for Landsat 8 data in 2016 [**Error! Reference source not found.**], for estimating albedo from Landsat 9 data. To meet such a purpose, a proper code in GEE environment was developed. The methodology was tested over some areas in Southern Italy, selected as pilot sites.

Methodology

Figure 1 shows the operative workflow applied in this study to retrieve land surface albedo from Landsat 9 satellite data over the territories of Cagliari and Palermo cities, in Southern Italy. Once the selected Landsat 9 scenes were collected, the images were masked from clouds and then, processed in the GEE platform by developing and implementing a proper JavaScript code in order to apply the Silva *et al*. (2016) algorithm [**Error! Reference source not found.**]. A similar code was set also to process date close Landsat 8 images. After obtaining surface albedo maps for both study areas, a statistical analysis and a comparison between Landsat 8 and Landsat 9 outcomes were performed to verify the applicability of the above-mentioned algorithm from Landsat 9 data, characterized by the same geometric and spectral resolutions, as well as an improved radiometric resolution than 12-bit Landsat 8 data [**Error! Reference source not found.**]. Firstly, the analysis was carried out on the whole territory of both case studies, and then, on each land use/land cover (LU/LC) class, provided by Copernicus UrbanAtlas 2018 [**Error! Reference source not found.**]. In particular, statistical metrics such as scatterplots, Mean (μ), Correlation Coefficient (ρ), Standard Deviations (SD), Median (m), and Root Mean Square Error (RMSE) were computed.

Results

As a preliminary work, this research shows promising results. Landsat 9 data seem, in fact, to provide improved land surface albedo estimations, thanks to its highest radiometric resolution. However, no significant improvements in terms of spatial and spectral resolutions were detected. Indeed, all the bands of Landsat 9 OLI-2 sensor, have the same geometric and spectral resolutions than those of OLI sensor on board of Landsat 8 satellite. Therefore, results are consistent in both study areas. Comparing the values obtained from Landsat 8 and Landsat 9 images, the differences in terms of μ, SD and m are on the order of 10^{-3} for both case studies and the RMSE is 0.020 and 0.024 for Palermo and Cagliari, respectively. The correlation is also very strong. Indeed, it is equal of 0.972 and 0.942 for Palermo and Cagliari (Figure 2). Furthermore, the results concerning Palermo are not influenced by the LU/LC classes, extracted from UrbanAtlas 2018, (RMSE < 0.025 and ρ > 0.91), while some issues have been identified in Cagliari. "Wetlands" category, absent in Palermo, is the most critical (RMSE = 0.034 and ρ = 0.392).

GEE cloud platform turned out to be of great potentialities for estimating an environmental variable, such as land surface albedo, from newly Earth observation data. GEE, in fact, allowed to process Landsat 9 and Landsat 8 satellite data optimizing acquisition and operational times, thanks to the presence of both datasets in its catalogue and the cloud technology.

Outlook for the future

This study paves the way for future works such as:

1. the application of Silva *et al*. (2016) [**Error! Reference source not found.**] method over different study areas to explore its potentialities in estimating land surface albedo from Landsat 9 data considering different environmental context;

2. the development of an *ad hoc* algorithm for extracting the land surface albedo from the new available medium-resolution data provided by Landsat 9 in order to take advantages of its improved radiometric calibration.

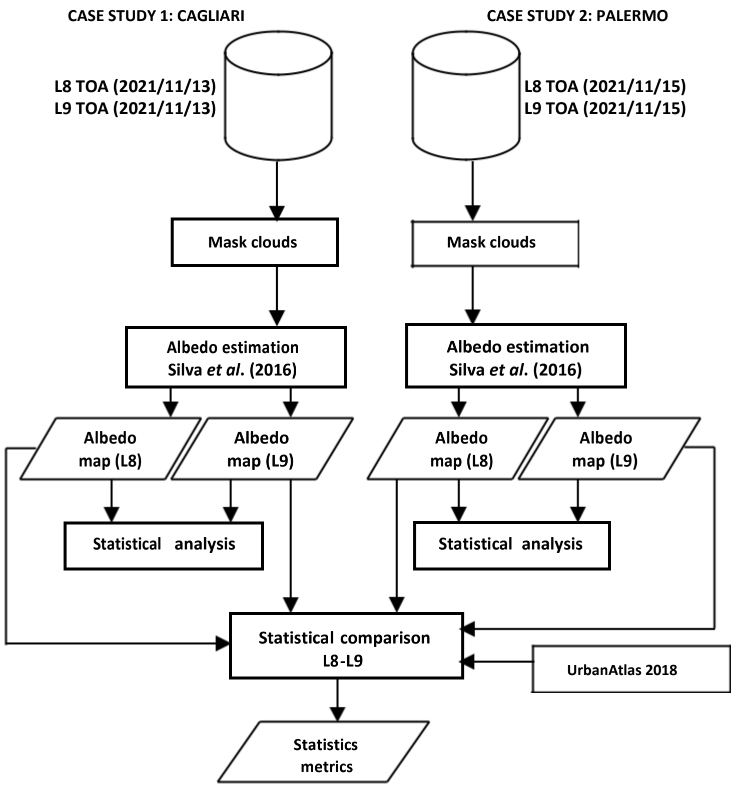

Figure 1 Operative workflow

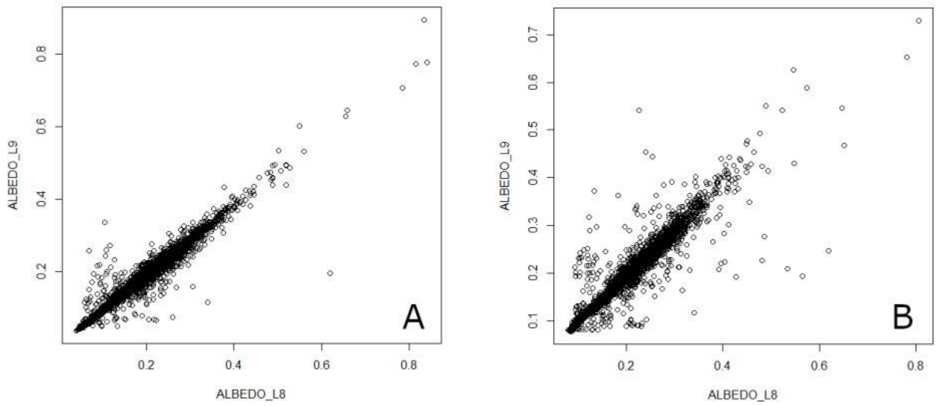

Figure 2 Scatterplots between Landsat 8 and Landsat 9 albedo estimations for Palermo (A) and Cagliari (B) study areas

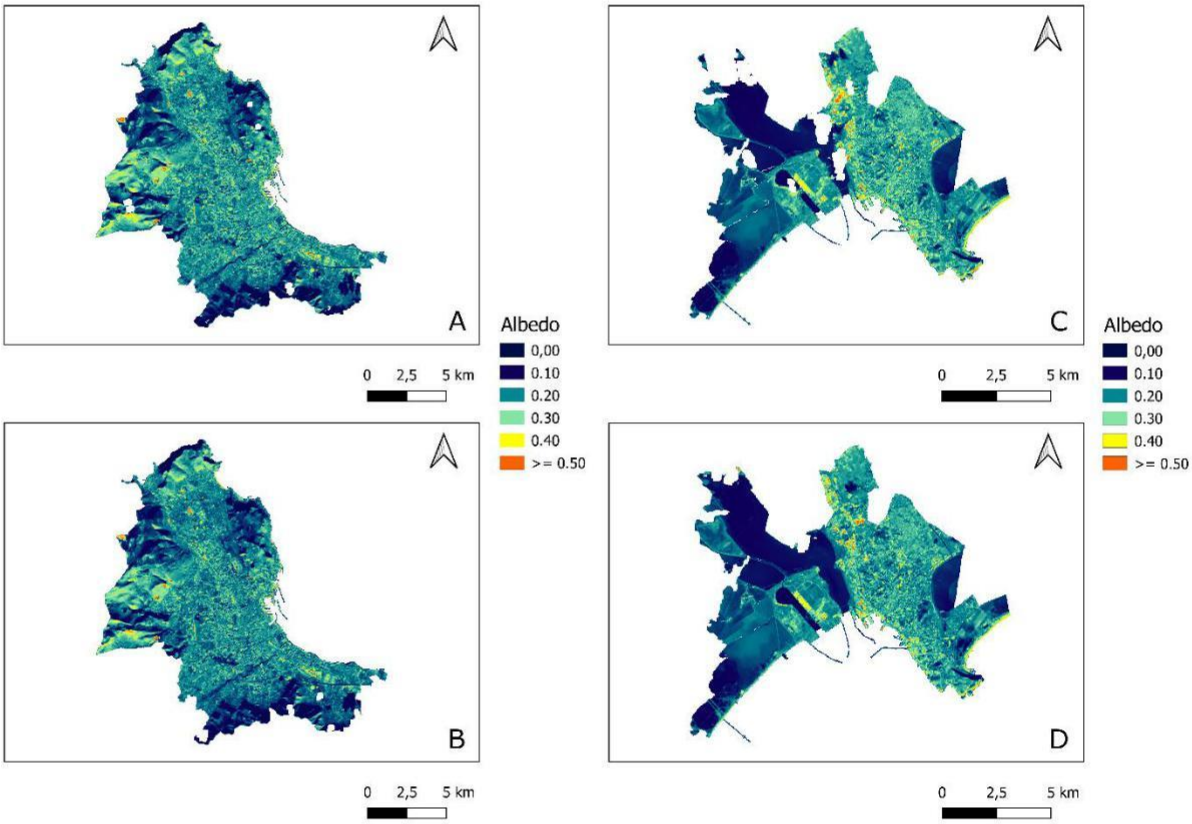

Figure 3 Land surface albedo maps of Palermo (on the left) and Cagliari (on the right). Such maps were generated by handling Landsat 8 (A and C) and Landsat 9 (B and D) images, respectively

Poster(s)

Reference target extraction for point cloud intensity normalization in Scan to BIM

Rabia Rashdi[1,2], Zhouyan Qiu[1,2], Pedro Arias[1], Joaquín Martínez Sánchez[1]

1 Applied Geotechnologies Group, School of Mining and Energy Engineering, University of Vigo, Vigo, 36310, Spain
2 ICT & Innovation Department, Ingeneria Insitu, Vigo, 36310, Spain

Keywords: Calibration, extraction, Mobile laser scanning, BIM, smart cities

The challenge

Transport infrastructure and Building Information Modelling (BIM) play a valuable role in creating smart cities, to make the environment more efficient, safe and secure. Mobile laser scanning (MLS) has become an important tool for surveying the environment. It provides rich 3D point clouds with geometric and radiometric details which is useful in detecting road inventories. Despite its increasing demand for detailed 3D representation, some drawbacks are associated with MLS data. First, MLS point clouds produce billions of points, resulting in a massive volume of data. Furthermore, MLS point clouds have a high spatial resolution, capturing unwanted objects and noise in the scene such as moving objects. MLS cannot capture complete coverage of the scene beyond the roadways because of the occlusions affected by buildings and trees. Data acquired from multiple laser scanners at different timings, with varying point densities make point cloud processing challenging. Hence, the need to normalize point cloud intensity is necessary to have a uniform value, which can be utilized in various scenarios.

Methodology

This paper proposes an approach for intensity calibration and extraction of target surfaces for the application of Scan to BIM framework, which can be further used for intensity normalization of the point clouds in transport infrastructure. The proposed method consists of four major parts: (1) Intensity calibration; (2) calculating normal vectors; (3) calculating angles by normal vectors; and (4) clustering the point clouds by distance. The proposed workflow is illustrated in Figure 1. Firstly, the entire point cloud was captured with an intensity calibration process. Each measurement was taken at different distances and angles. The resulting point clouds contained irrelevant information such as moving people, trees, and ground surfaces. Normal vectors were calculated by fitting the nearest LiDAR points within a particular distance in a plane to remove unnecessary information and extract the reference target points. Further, the point clouds were filtered by calculating angles by normal vectors. Finally, for the segmentation of the reference target, point clouds were divided into clusters using a minimal Euclidean distance between points in distinct clusters.

Results

Optech LYNX mobile mapping system was used for the data collection. This system provides a radiometric resolution of the intensity of 12 bits. The measuring range of Optech LYNX is more than 100 meters to a target with a reflectivity of 20%. A wooden target was used as a calibration target. For the reference target, measurements were carried out between distances from 1 meter to 12 meters, while keeping the mobile mapping system static. The performance of the target surface extraction before and after the processing was analyzed. The entire scene of the experiment is shown in Figure 2 (a). The total amount of points collected was 89,802,204. For the segmentation of the target's planar surface, normal vectors were computed and grouped using a minimum Euclidean distance between points. The extracted reference clustered-colored points as shown in Figure 2(c), which will further help to detect the reflectance value of the reference target for the correction and normalization of the intensity data.

Outlook for the future

The aim of this study was to propose a method as a pre-processing step for intensity normalization of the point clouds using mobile laser scanning data, based on angle and distance effects. The approach emphasizes applications such as transport infrastructures and smart cities Our methodology will create unique approaches for incorporating normalized point clouds into typical BIM processes like as segmentation, classification, and object identification. Methods to normalize different point clouds with uniform features are important such that they are unaffected by environmental effects and varying densities. In the future, a standard process for intensity normalization based on segmentation and object detection will be implemented which can be a great solution for creating BIM models and digital twins.

Figure 1 Workflow of the proposed research

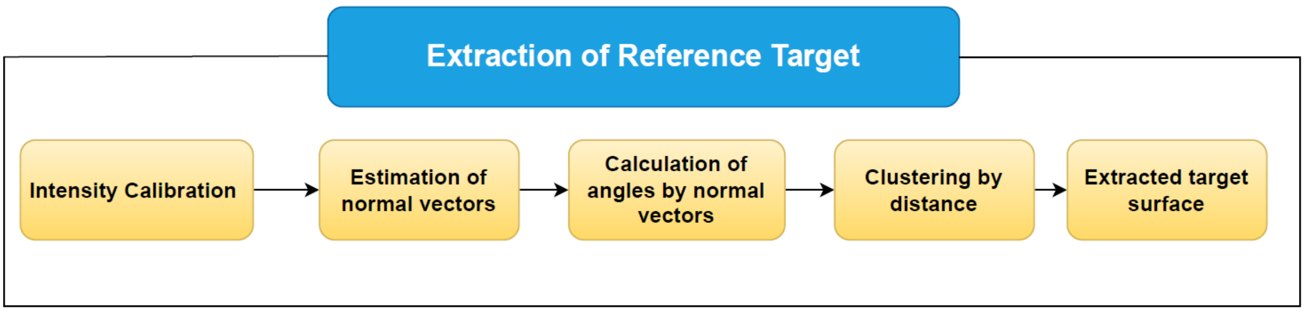

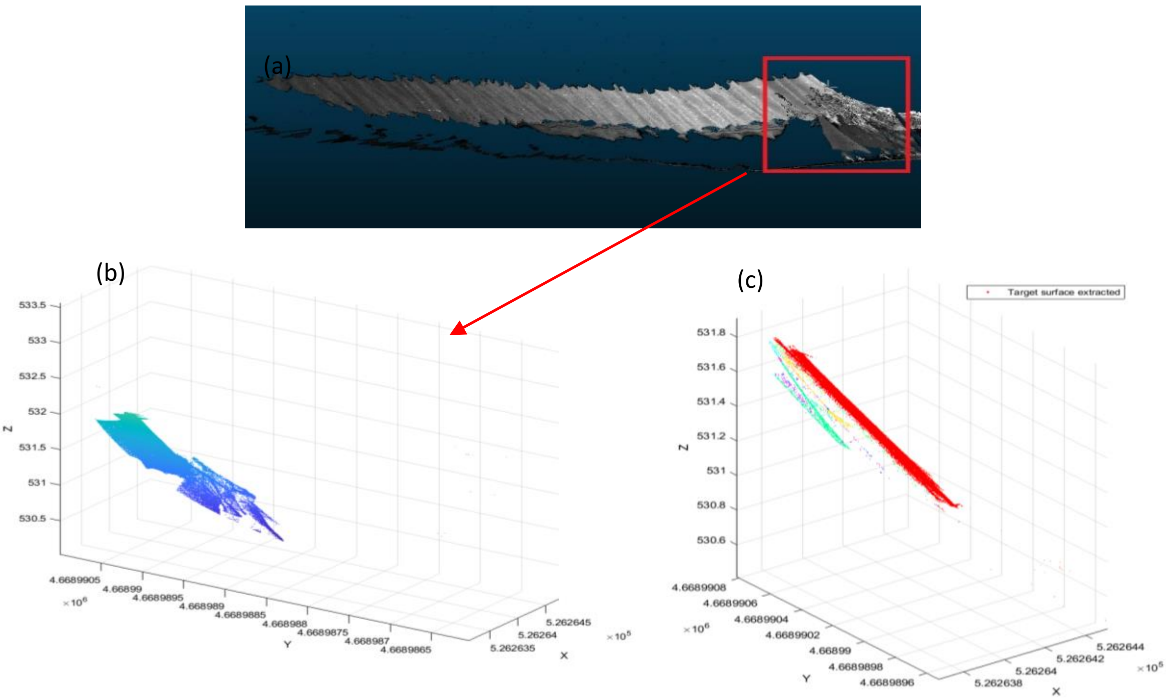

Figure 2 (a) Raw point cloud, (b) segmented point cloud (1.5-2.5 m) and (c) extracted target surface

Novel Radargrammetric Approach for Capella Space Imagery

Karlheinz Gutjahr[1], Can Atalay[2], Roland Perko[1], Hannes Raggam[1], Janik Deutscher[1], Mathias Schardt[1,3] and Umut Gunes Sefercik[4]

[1] Joanneum Research, DIGITAL - Institute for Information and Communication Technologies, Austria
[2] Zonguldak Bülent Ecevit University, Turkey
[3] Graz University of Technology, Austria
[4] Gebze Technical University, Turkey

The challenge

Capella Space recently launched the first US-based commercial SAR satellite constellation in X-band providing high resolution imagery with very short revisit times. In contrast to existing SAR missions like TerraSAR-X, Cosmo-SkyMed or Radarsat, Capella operates in different orbital planes which for the first times allows 3D mapping from cross-orbital acquisitions based on stereo radargrammetry. Therefore, multiple Spotlight data sets were tasked for a selected test site in Austria, including polar and equatorial acquisitions from Capella-2 and 3, both launched in 2020. This paper reports on 2D and 3D accuracy assessments based on those novel data sets, followed by dense surface model generation which are qualitatively validated w.r.t. airborne LiDAR reference data. The study uniquely shows that radargrammetry can be successfully applied on Capella Space images both on co- and cross-orbital data with accuracies comparable to those known from TerraSAR-X.

Methodology

To allow the investigation of the 3D mapping potential of Capella Space SAR data, three left looking Spotlight products acquired at different off-nadir viewing angles and two ascending orbit inclinations have been collected for an Austrian test site where reference airborne LiDAR data exists with 1m GSD. This rural area shows flat to slightly hilly terrain, the ellipsoidal heights ranging from 270 to 440 m a.s.l., and represents agricultural as well as various forest types. In Spotlight mode, single-look complex (SLC) data resolution is limited to 0.5 m, however amplitude-only multi-looked spotlight provides a higher resolution up to 0.3 m with superior speckle suppression. Thus, this study focusses on a novel radargrammetric approach based on the amplitude-only products which are already ellipsoidal geocoded (GEC). To fit the standard epipolar radargrammetry pipeline an inverse geocoding procedure is proposed to transform the GEC amplitude to the SLC geometry. In order to make an initial assessment of the 2D geo-location as well as of the 3D stereo mapping accuracy, ground control points (GCPs) were manually measured in the images. Then, a fully automatic workflow was applied to the Capella Space stereo pairs and the triplet in order to generate DSMs with 1m spacing (using the Remote Sensing Software Package (RSG) by Joanneum Research), which were finally validated w.r.t. the LiDAR reference data (using the BundLe block adjustment of the University of Hannover (BLUH)).

Results

Point residuals between measured image coordinates and those resulting from backward point transformation were calculated in azimuth and range for the individual images. RMS and mean values of these residuals are given in Table 1, where a distinct bias is inherent to these residuals (mean values), especially in range direction. Thus, the range offset was refined using least squares adjustment.

Image / Look angle / Orbit inclination / Date / Satellite	GCPs	RMS initial [pxl]		Mean initial [pxl]		RMS adjusted [pxl]	
		Az	*Rg*	*Az*	*Rg*	*Az*	*Rg*
ASC1 / 39° / 97° / 2022-01-13 / Capella-3	25	1.80	4.37	-0.50	-3.48	1.73	2.65
ASC2 / 39° / 45° / 2022-01-17 / Capella-2	25	2.80	3.88	1.08	-2.70	2.59	2.79
ASC3 / 26° / 97° / 2022-01-19 / Capella-3	25	2.02	2.37	-0.82	-0.52	1.84	2.32

Table 1. 2D geo-location accuracy given in pixels.

In order to determine a-priori estimates for the 3D mapping accuracy being feasible from Capella Space stereo pairs, the stereo image measurements were used to calculate 3D ground coordinates of the GCPs by least-squares spatial point intersection and compared to the manual ground coordinate measurements. In this concern, individual stereo pairs, as well as image triplets, were analyzed. The RMS values of the 3D point residuals are summarized in Table 2.

Model	Stereo Angle	GCPs	RMS [m]			
			East	*North*	*Height*	*Length*
ASC1 – ASC2	53.3°	25	1.05	0.71	0.85	1.52
ASC2 – ASC3	45.2°	25	1.04	0.78	0.60	1.33
ASC1 – ASC3	13.2°	25	2.09	0.96	1.22	2.60
ASC triplet	all	25	1.04	0.69	0.62	1.39

Table 2. 3D geo-location accuracy given in meters.

The DSMs resulting from the individual stereo pairs as well as from the triplet are shown in Figure 1. Those DSMs include gaps which are caused by rejection of unreliable matching results, depicted in Table 3 which also reports the bias and RMS of the DSMs. There, the amount of the gaps is drastically reduced when using the image triplet (1.8% versus 50% or more). Bias and RMS values are also lowest for the triplet. The different qualities of co- and cross-orbital pairs can be traced back to the small intersection angles. Overall, the resulting accuracies of the polar-pair is in the expected range known from TerraSAR-X imagery.

Model	Stereo Angle	Bias [m]	RMSZ [m]	Rejected Pixels [%]
ASC1 – ASC2	53.3°	0.78	4.37	59.7
ASC2 – ASC3	45.2°	-1.51	6.05	62.8
ASC1 – ASC3	13.2°	0.63	4.08	50.8
ASC triplet	all	-0.60	3.83	1.8

Table 3. Statistical values of height differences w.r.t. LiDAR given in meters.

Outlook for the future

Overall, this work for the first times reports the radargrammetric mapping potential of Capella Space data also tackling cross-orbital stereo configurations. The novel approach reprojects the multi-looked GEC products into SLC geometry to benefit from this inherent speckle suppression. Based on this initial study on radargrammetric 3D mapping from the Capella Space constellation the following topics are highly relevant as future work: (1) Evaluation of

SLC vs. GEC based radargrammetry, (2) further investigations on the range offsets, (3) ascending and descending fusion, (4) more optimal intersection angle properties at about 25°,

(5) in depth analysis on co- and cross-orbital stereo configurations and their influence on specific applications such as forest assessment or ice monitoring, and (6) direct comparison to the results achievable from other very high resolution SAR satellite constellations, in particular TerraSAR-X and Cosmo-SkyMed.

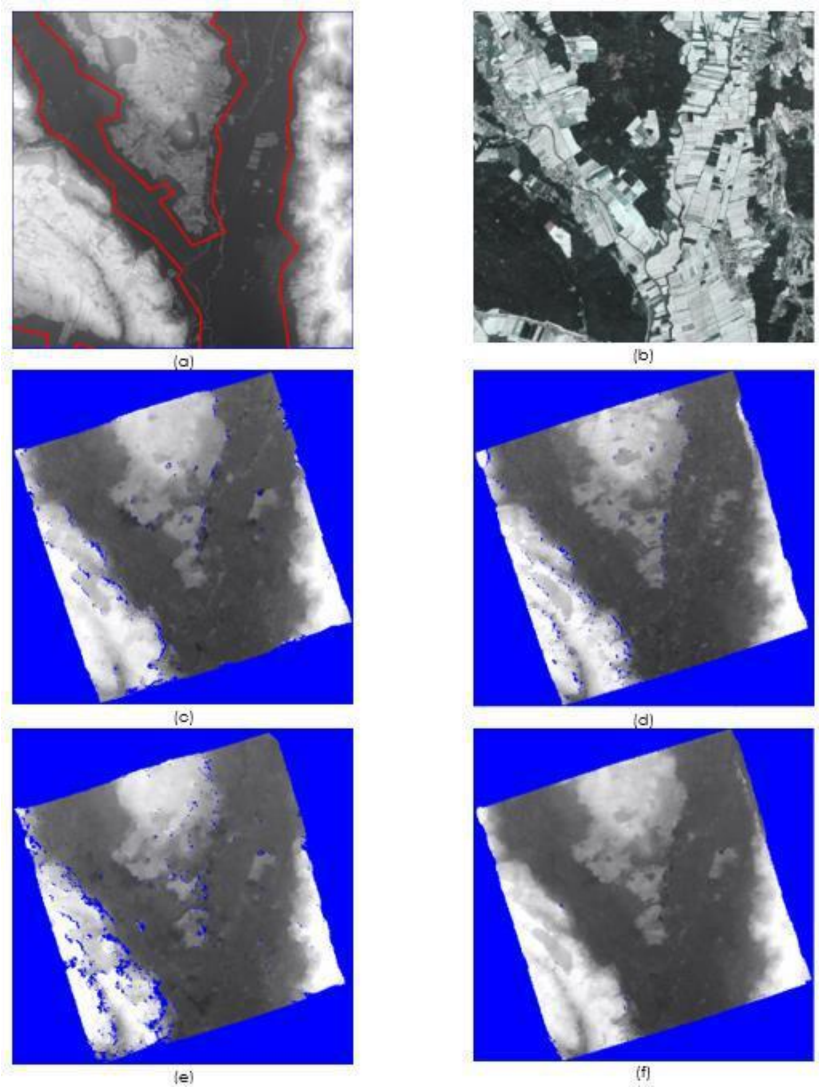

Figure 1. Comparison of digital surface models:(a) LiDAR reference DSM superimposed by the validation region shown in red, (b) orthophoto, (c) DSM ASC1-ASC2, (d) DSM ASC1-ASC3, (e) DSM ASC2-ASC3, and (f) DSM triplet.

Using the VENµS Super-Spectral Camera for Detecting Moving Vehicles

Arnon Karnieli, Manuel Salvoldi, Aviv Cohen-Zada

The Remote Sensing Laboratory, Jacob Blaustein Institutes for Desert Research, Ben Gurion University (Israel)

Keywords: object detection, spectral change detection, normalized difference moving object index (NDMOI), speed and orientation determination

The challenge

Monitoring transportation for planning, management, and security purposes has become a growing interest for various stakeholders. Despite the apparent advantages of using air- or drone-borne systems for vehicle detection, several methods have been introduced over the last two decades that utilize spaceborne very-high-resolution (VHR) imagery with one-meter to sub-meter resolutions. For detecting moving vehicles, two sensor capabilities have been extensively utilized: (1) a stereo mode through either a satellite constellation or tilting capabilities; and (2) a gap in the acquisition time between the push broom detector sub-arrays. These capabilities allow the observation of changes in the location of moving objects between image pairs or across spectral bands, respectively. However, both methods require overcoming differences in ground sampling distance and/or prerequisite spectral analyses to identify suitable bands for change detection. The current study demonstrates a proof of concept for the VENµS satellite's capability to detect moving vehicles in a single pass with a relatively low spatial resolution.

Methodology

The VENµS Super-Spectral Camera has a unique stereoscopic capability since two spectral bands (numbers 5 and 6), with the same central wavelength and width (620 nm and 40 nm, respectively), are positioned at the extreme ends of the focal plane (Fig. 1 and 2). This design allows a 2.7-sec difference in observation time between these bands (Fig. 3) and, therefore, is highly useful for change detection applications within a very short time interval. In order to distinguish a moving vehicle from its background, the normalized differenced moving object index (NDMOI) can be calculated as:

$$= \frac{6 \quad - 5}{\overset{+}{6 \qquad 5}} \tag{2}$$

where B6 and B5 correspond to the VENµS bands 6 and 5, respectively Each moving vehicle candidate in the NDMOI image is represented by a pair of pixel clouds, one local maximum with high index values (i.e., bright pixels) and one local minimum with low NDMOI values (dark pixels). Background pixels are typically grey-scale (around zero) and imply static objects or unchanged pixels (Fig. 4). Fig. 5 shows the process flow diagram of this approach. The first step is to identify the pixel clouds C1, C2 and Cm, corresponding to every potential dynamic object, based on a threshold-based methodology. Cloud 1 (C1) represents the vehicle location detected in B5, C2 represents the object location in B6 (after 2.7 sec) and Cm is the object detected in B7 (middle of the focal plane). The last step consists of filtering false dynamics objects to identify the pixel clouds corresponding to the same vehicle and to determine the speed intensity and orientation. The methodology used to match the C_1 and C_2 polygons that identify the same vehicle is depicted in Fig. 6. The $(C_2)_j$ and $(C_m)_k$ polygons belong to the same vehicle identified by $(C_1)_i$ because the difference of their orientations $_{OK}$ (with respect to the north) is lower than a threshold .

Results

Fig. 7a, b depicts the results obtained by the threshold-based algorithm for two sections of the Israeli highway. Fig. 7c, d shows the moving vehicles with the corresponding velocity vector fields (cyan arrows). In these two sections of the highway, nine and seven moving vehicles were identified, respectively. Fig. 7c, d also shows that most of the C1 and C2 polygons detected in the threshold-based step of the algorithm were eliminated because they were considered false moving objects. The methodology was also applied to open agricultural areas in order to identify vehicles on dirt off-unpaved roads or open fields. Fig. 8a shows two vehicles that were detected on a located dirt road where the estimated speed of both vehicles is around 29 km/h. Fig. 8b shows a possible machine working in an agricultural field on 08 March 2020, with an estimated speed of 26 km/h. As an application example, the number of moving vehicles was assessed during the Covid-19 pandemic closures. The developed methodology was demonstrated with the 23-km-long section of the Israeli highway for 32 free-cloud VENµS images available in 2020. A time series of moving vehicles is depicted in Fig.

9. This year, the Israeli government imposed two complete lockdowns just before the national holiday of Passover (between 08 and 16 April) and the High Holy Days (from 18 to 20 September and from 2 to 9 October). The first lockdown started on 9 April 2020 and the second on 18 September 2020. The estimation of moving vehicles shows that during the holidays (including Saturdays) and during the lockdowns, there was a consistent drop in the number of moving objects on the selected road. On 13 April, just after the beginning of the first complete lockdown, there was a peak in the number of cars. This is related to the fact that the end of Passover was on 14 April 2020, so many people violated the lockdown to go to their families for the holiday. Nevertheless, these results show the effectiveness of the proposed methodology.

Outlook for the future

Future work emanating from this study is planned in two directions. The first is to improve the vehicle identification stage of the algorithm, and the second is to assess the algorithm performance better and compare it to other methods. There are possibilities of improving the vehicle identification step, including (1) using artificial intelligence to match the C1 and C2;

(2) taking advantage of the information retrieved from the other bands between B5 to B6; and (3) utilizing the DEM capabilities of VENµS for a more precise evaluation of the movement information, as well as extracting vertical movement data.

A better assessment of the algorithm's performance may involve (1) applying a sensitivity analysis for the algorithm's parameters and various scenarios; (2) applying other moving vehicle detection methods on VENμS images; and (3) applying the DMOI algorithm on a VHR image. While the first two options are available and can be conducted soon, the third option is currently restricted solely to the upcoming L2 products of VENμS with a 4-m GSD. Since this spatial resolution is still insufficient for vehicle identification, it will be intriguing to see what a VHR sensor with unique settings, such as those of the VSSC, can accomplish for vehicle detection applications.

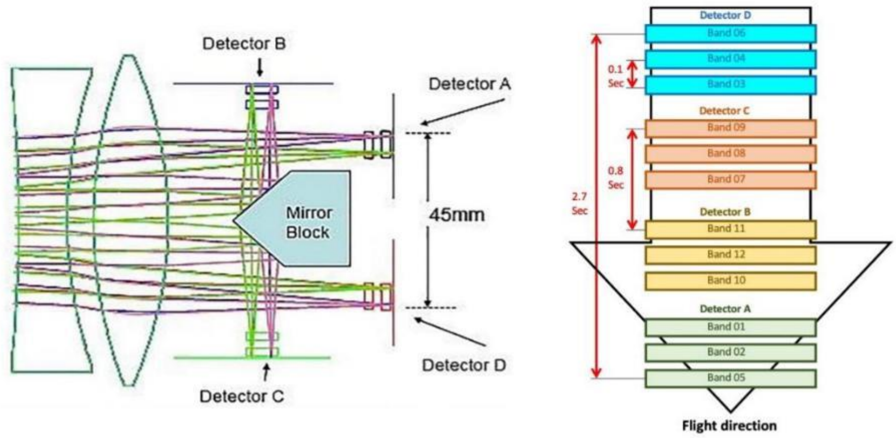

Figure 1. VSSC focal plane and detector arrangement.

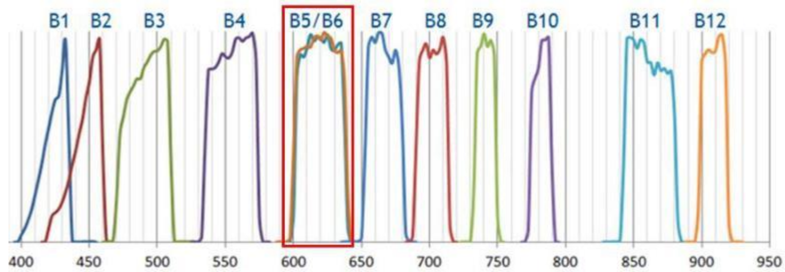

Figure 2. VSSC spectral bands.

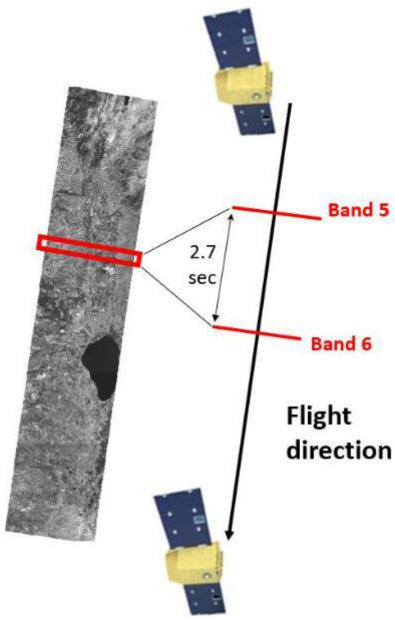

Figure 3. Bands 5 and 6 acquisition time gaps.

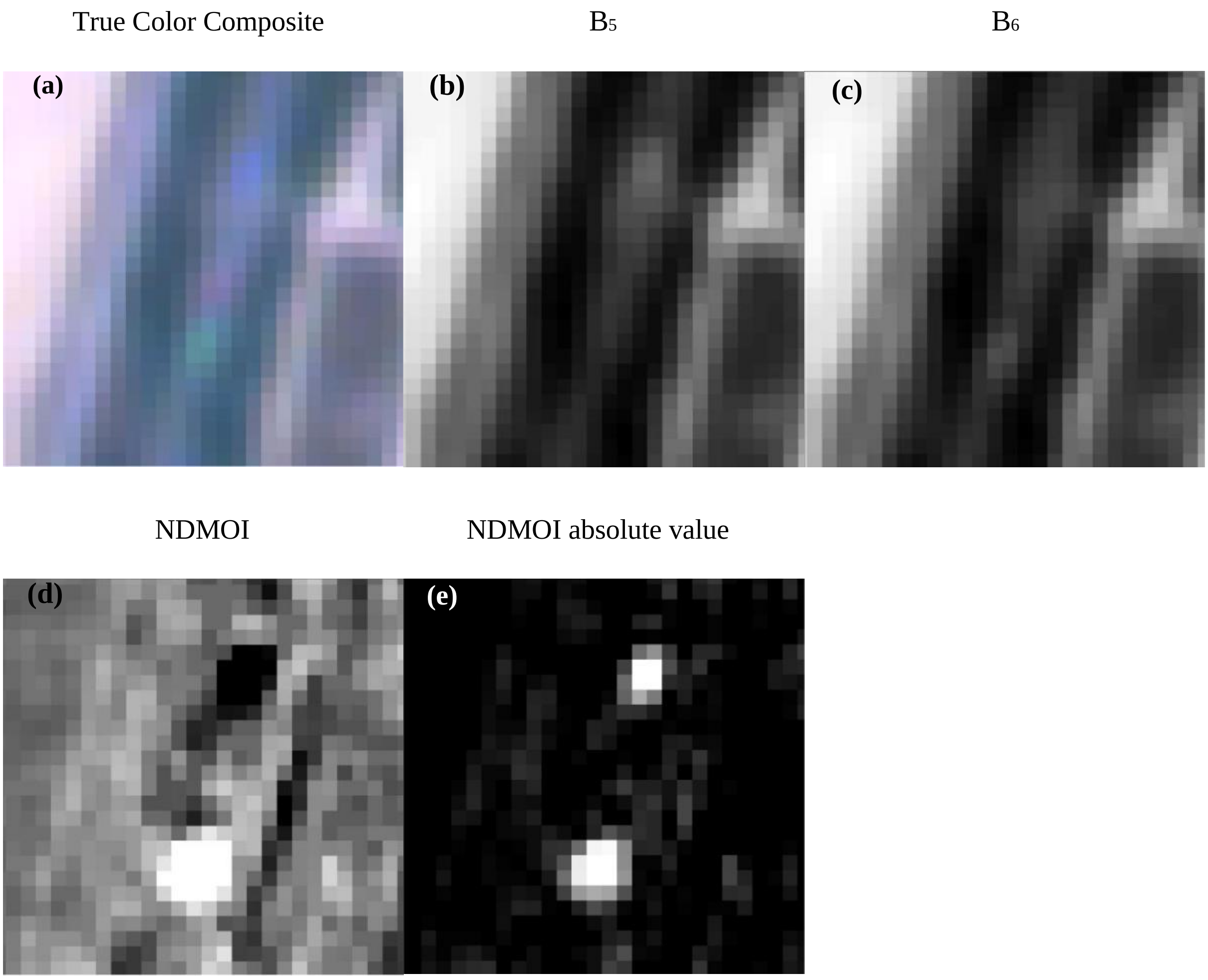

Fig. 4. Comparison of moving vehicle indices. (a) True-color (RGB = 666, 555, 447 nm) VENμS image acquired on 26 October 2020; (b) and (c) grey-scale bands 5 and 6 of the same scene; (d) NDMOI image; (e) NDMOI absolute value image. The maximum displacement distance can be observed in the B_5 and B_6 images. The absolute value of the NDMOI masks the background as dark pixels, highlighting the location of the moving vehicle in both B_5 and B_6 as bright pixels.

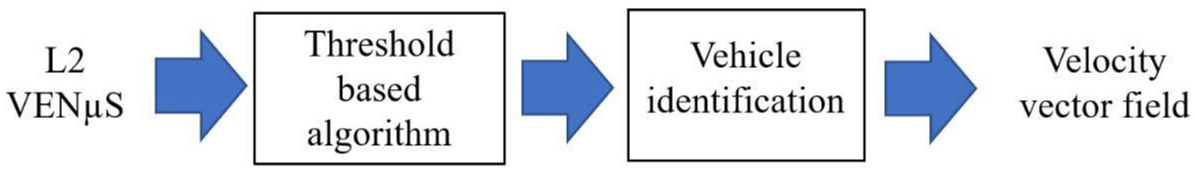

Fig. 5. Process flow of the moving vehicle detection algorithm proposed in this study

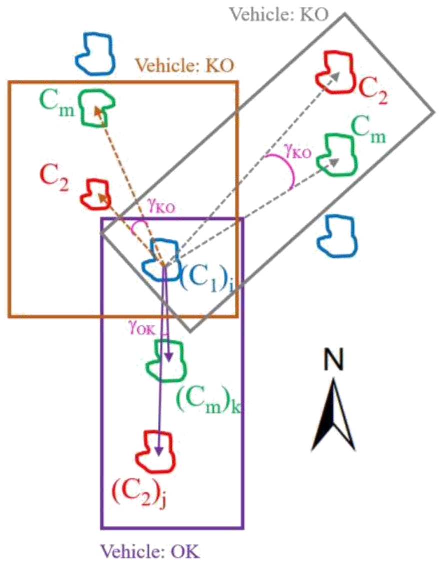

Fig. 6 Vehicle identification algorithm

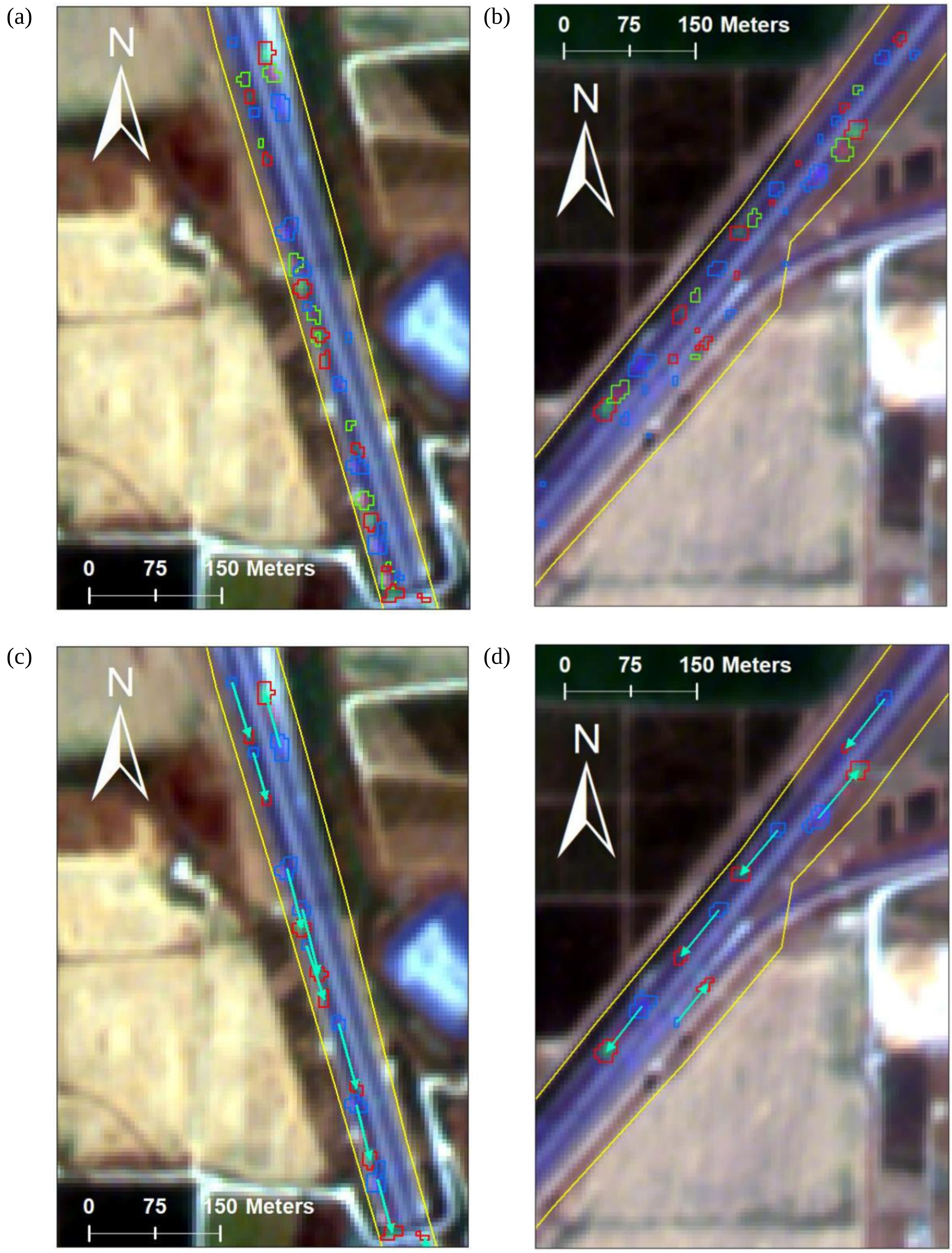

Fig. 7. True-color (RGB = 666, 555, 447 nm) VENµS image with C_1, C_2, and C_m polygons detected on a section of a highway. (a) Image acquired on 02 July 2019 on Section I; (b) image acquired on 02 July 2019 on Section II. (c) Corresponding velocity vector field of section I of the highway on 02 July 2019 (d) section II of the highway on 02 July 2019. Note that the algorithm detected the small moving object (the polygon C_1 is composed of two pixels) in the south-north exit from the highway.

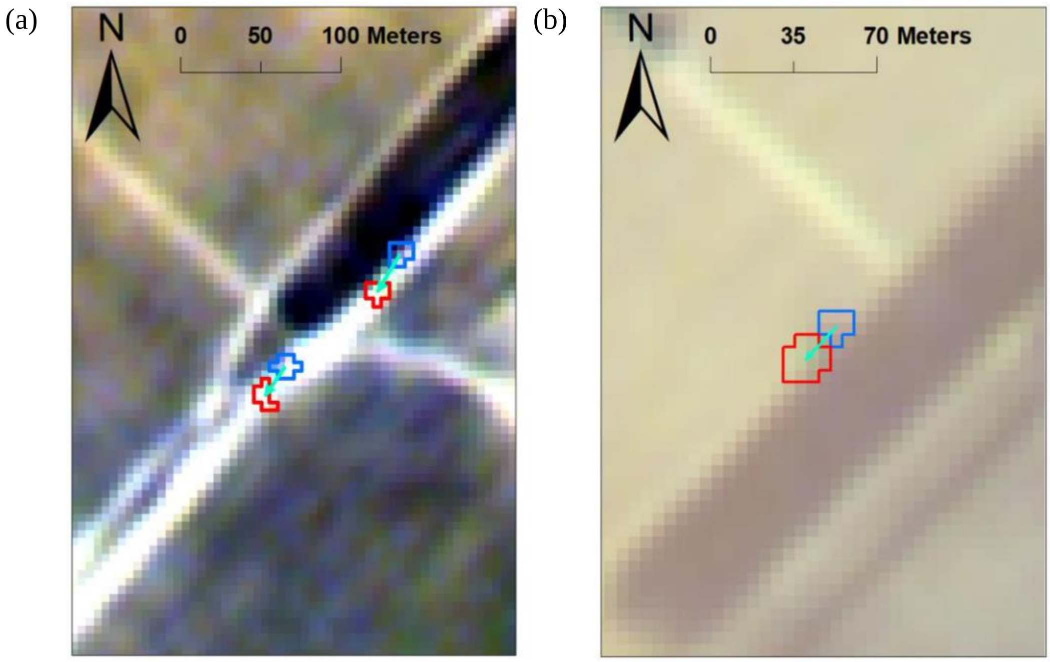

Fig. 8. (a) True-color (RGB = 666, 555, 447 nm) image acquired on 26 October 2020 with two vehicles detected on a dirt off-road; b) image acquired on 08 March 2020 with a machine detected on an agricultural field.

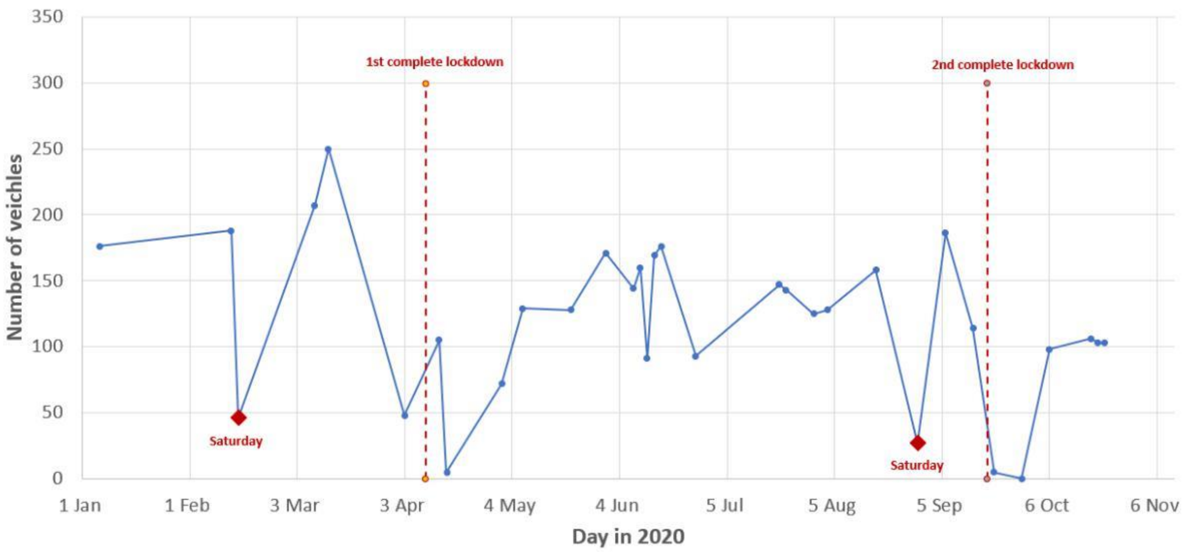

Fig. 9. Estimation of the moving vehicles detected in 2020 inside the 23-km-long section of Israeli Highway.

In situ topsoil sensing system to support environmental performance monitoring

Konstantinos Karyotis[1,2], Nikolaos L. Tsakiridis[1,3], Nikolaos Tziolas[1], Eleni Kalopesa[1], Periklis Chatzimisios[4] and Georgios Zalidis[1]

[1]Aristotle University of Thessaloniki, Laboratory of Remote Sensing, Spectroscopy and GIS, Department of Agriculture, Greece
[2]International Hellenic University, Department of Science and Technology
[3]Aristotle University of Thessaloniki, Automation and Robotics Laboratory, Department of Electrical and Computer Engineering, Faculty of Engineering, Greece
[4]International Hellenic University, Department of Information and Electronic Engineering, Greece

Keywords: Citizen science, Soil Spectroscopy, Transfer Learning, Crowdsourcing, Artificial Intelligence

The challenge

The modernized Common Agricultural Policy 2023–2027 in the European Union highlights the need for Paying Agencies to perform checks on a much thinner timescale and to quantify the impact of various practices on natural ecosystems. The introduction of participatory sensing and smart sensors enable the cost-effective establishment of an additional data layer to complement, validate and enhance the predictive performance of critical agro-environmental –related parameters. In particular, the advent of low-cost, portable, and handheld spectrometers operating in the infrared domain of electromagnetic spectrum and realized using microelectromechanical systems enables the rapid and non-destructive measurement of a soil's reflectance spectrum that can be transformed to soil properties through employing AI techniques. To this end, we propose a methodology based on a set of handheld Short-wave infrared (SWIR) soil spectrometers for real time in situ estimation of soil properties, leveraging existing Soil Spectral Libraries (SSLs) and efficient deep learning techniques.

Methodology

The proposed sensing system was tested under real field conditions in 80 fields during the summer of 2021. The device is portable, employing a Fabry–Pérot interferometer that operates at SWIR region of electromagnetic spectrum (1750 – 2150 nm), with built in LED illumination. A collection of 120 distinct topsoil samples distributed in three different regions in Cyprus was measured under both in situ and laboratory conditions. A group of soil surveyors without prior expertise were equipped with the handheld spectrometers, and after a hands-on demonstration of the usage protocol, they collected spectral measurements and physical topsoil samples of the indicated locations. The sampling locations were carefully selected by employing the Conditional Latin Hypercube Selection algorithm over Sentinel-2 imagery which was pre-processed to derive only the pixels resembling exposed soil. The field activities took place in Summer 2021, and only after consecutive dry intervals of at least one week. For the laboratory case, sample pre-processing (air-drying and passing through a 2 mm sieve) for ambient factors' effects removal was performed. The acquired spectral signatures formed two sets; a Convolutional Neural Network has been developed, aiming to eliminate the effects to the spectral signatures caused by moisture, shadow, or by the existence of non-soil materials. To this end, the CNN mapped the in situ spectral signatures (model input) to the ones acquired after laboratory pre-treatment (model output). The spectral signatures that resulted after this mapping formed a regional SSL which was augmented after spiking local samples from open SSLs (LUCAS 2015 and GEO-CRADLE). The Wylie Bay and Lucky Bay Internal Soil Standards as proposed by IEEE P4005 “Standards and Protocols for Soil Spectroscopy” where used to harmonize the existing and developed SSLs, and more specifically, for the standardization of LUCAS, a calibration transfer function was developed over the national subset of the survey. The spectral values then acted as predictors for the estimation of Soil Organic Carbon (SOC) which was evaluated over a randomly selected independent test set containing 20% of total samples.

Results

We performed a one-to-one comparison between the spectral signatures of the two datasets with measurements obtained with a full range, high resolution, NIR spectroradiometer (Spectral Evolution, PSR+3500). The applied transformation induced a correction to the spectra acquired in situ that results to a significant spectral distance drop, which can be reflected as a reduction of Mean Absolute Error from 0.20% to 0.025%, which was calculated over an independent set (Figure 1a). After thoroughly assessing a set of widely used AI algorithms, the Random Forest presented the highest performance and was applied in both cases. The dataset containing the “transformed” spectra exhibited enhanced accuracy in terms of SOC predictive performance compared to the model developed using as predictors the original in situ spectra. More concretely, this transformation unveiled the correlations between spectra and SOC and enabled the accurate estimation of SOC content, by improving the calculated accuracy metrics (R^2 = 0.71 and RMSE = 0.20% - Figure 1b) compared to the ones corresponding to the original in situ spectral signatures (R^2 = 0.19 and RMSE = 2.11%). This technique minimizes the effects of ambient factors to the spectral signatures and helps the development of a new dataset of “transformed” spectra, which can be used to extract useful information about the soil’s characteristics.

Outlook for the future

The proposed approach broadens the possibilities of merging collections of in situ spectra with existing SSLs and further highlights the need for development of a universally accepted sensing protocol. Furthermore, SOC or other soil properties that can be monitored with diffuse reflectance spectroscopy can be easily scaled up and act as bridge to Earth Observation data in terms of a bottom-up approach and in support of the Copernicus in situ component, under the hypothesis of reliable estimations of the targeted soil quality indices. The proposed framework is considered modular and hence it can be adjusted to different, environmental observations and soil spectrometers to radically transform the environmental monitoring approaches.

(a)

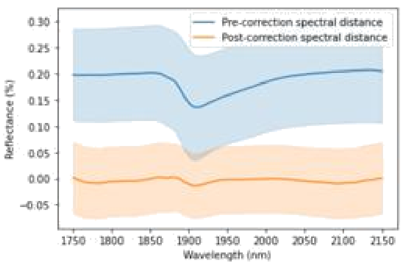

(b)

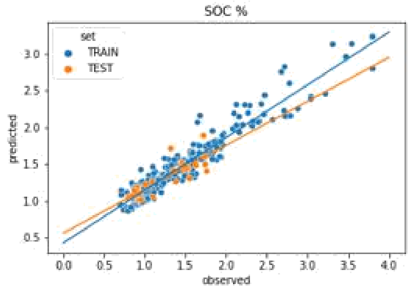

Figure 1 (a) Mean difference and between in situ spectra and the transformed spectra to laboratory reference spectral values (The transparent ribbon represents the 95% confidence interval of differences) (b) Scatterplot of measured and predicted values for SOC content

S_EOC: Earth Observation Challenges: Open Science, Open Innovation, Digital Innovation Hubs, Sustainable Development Goals (SDGs)

Chair(s): Dr. Prof. Mattia Crespi, Prof. Andreas Anayiotos

Global Monitoring of Inland Water Surface With GEDI Geo Big Data Using Google Earth Engine: Preliminary Analysis, Potentials and Issues

Alireza Hamoudzadeh[1], Roberta Ravanelli[1], Isabel Cocozza[1], Virginia Coletta[1], Mattia Crespi[1,2]

[1] Sapienza University of Rome, DICEA, Geodesy and Geomatics Division, Italy

[2] Sapienza School for Advanced Studies, Sapienza University of Rome, Italy

Keywords: GEDI, inland surface water monitoring, Google Earth Engine, accuracy assessment, outliers detection and removal

The challenge

Inland surface water is the source for about two-thirds of the freshwater consumed by humans and a key component of the hydrological cycle, thus its monitoring is fundamental to understand climatic changes and their impact on humans and biodiversity. The availability of new global data is thus crucial to carry out this monitoring at a global scale, provided that a proper assessment is performed to evaluate its accuracy.

In this respect, Google Earth Engine (GEE) is known as a reliable, and real-time cloud-based computation platform, capable of integrating a high variety of up-to-date geospatial datasets with powerful analysis tools. GEE has recently added the Global Ecosystem Dynamics Investigation (GEDI) dataset [1,2] to its already wide archive. The GEDI dataset is a geo big data archive of laser-ranging observations of the Earth's surface collected by a LiDAR instrument mounted onboard the International Space Station.

The available literature highlights that the accuracy of GEDI data is variable and impacted by several factors (e.g., latitude, time of the observation); also, even a preliminary data inspection evidences that gross errors are rather frequent. Therefore, to fully understand the potential of GEDI data for inland water surface level monitoring, and possibly design and implement a global processing methodology within GEE, three primary objectives have to be pursued: outliers detection and removal, biases identification and estimation, measurement noise evaluation and stochastic modeling.

This work focuses on a preliminary analysis of GEDI data, with the goal of outliers detection and removal. A procedure is proposed and implemented in GEE to prepare a cleaner data set for inland surface water monitoring. The effectiveness of the procedure is tested on some lakes where a ground truth constituted by continuous hydrometric water levels is available.

Methodology

The proposed outlier detection procedure consists of three different steps. The first level compares the "MERIT Hydro: Global Hydrography Datasets" with water surface level measured by GEDI: high anomalies between the two datasets make it possible to detect suspicious footprints to be removed. The usage of external data increases reliability and prevents errors caused by GPS shifts in GEDI footprints.

The second step of the outlier detection procedure is based on other GEDI features. Specifically, the “quality_flag” indicates if the considered footprint has an invalid waveform (1=valid, 0=invalid), due to anomalies in the energy, sensitivity, amplitude, etc of the signal. The “degrade_flag” indicates the degraded state of pointing (the saturation intensity of the returned photons might reduce the accuracy of the measurement) and/or positioning information (GPS data gap, GPS receiver clock drift).

The third step of the outlier detection procedure relies on the robust version of the standard 3σ-test, in which every GEDI water level that is not within five NMADs (Normalized Median Absolute Deviation) from the median is removed (Figure 1 shows an example for Lake Garda, the largest lake in Italy).

First results and further developments

To assess the implemented outlier detection procedure and to preliminarily evaluate the accuracy of the GEDI data, we computed the differences between the water levels inferred by GEDI data cleaned from outliers and the (as much as possible) contemporary water levels collected by the hydrometric stations at four major lakes (Garda, Maggiore, Como, Iseo) in Northern Italy obtained from “Enti regolatori dei grandi laghi” website [3].

The values of the main statistical parameters of the differences for Lake Garda over the period 07/2019 – 07/2021 are reported in Table 1.

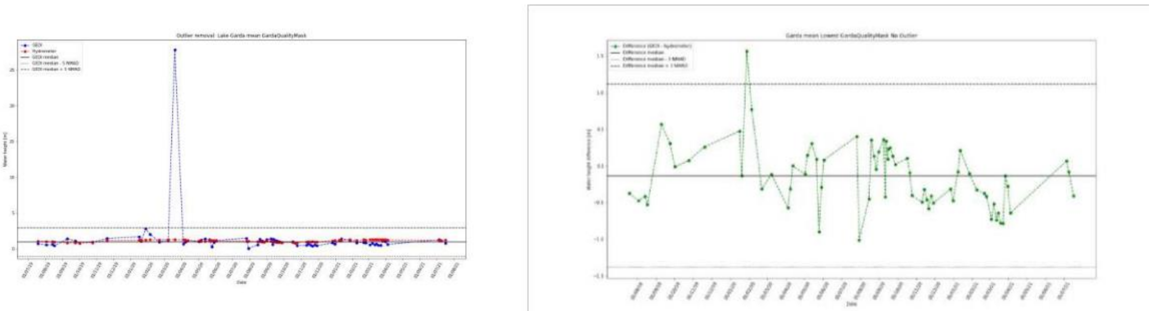

Figure 1- Comparison between the GEDI derived water levels and the contemporary water levels before and after the outlier detection for Lake Garda over the period 07/2019 – 07/2021

Mean [m]	Median [m]	Standard deviation [m]	NMAD [m]
-0.14	-0.13	0.43	0.42

Table 1- Main statistical indices of the differences between cleaned GEDI data and reference hydrometric data for Lake Maggiore over the period 05/2019 – 08/2021

Further developments of the proposed procedure, considering spatio-temporal interpolation techniques, are presently ongoing to address additional possible biases due to asynchronous and not co-located reference measurements when the water level is not stationary. Moreover, other altimetric data (e.g. ICESat-2) will be used as an additional reference.

Comparison of Copernicus Urban Atlas and HRL Imperviousness enhanced by administrative data in urbanization studies.

Wojciech Łachowski

Institute of Urban and Regional Development, Poland

Keywords (5): Urban Atlas, imperviousness, urbanization, administrative data

The challenge

Due to their availability and time scope, data from the Copernicus Program are a reliable source of information about changes in land use and land cover (LULC) in the area of European cities. These data, however, present a slightly different type of information, which means that the possibilities of their use are also different. However, Copernicus data can be combined with administrative data, which allows for a much wider knowledge of urbanization processes. As part of this study, several possibilities of using High Resolution Layers Imperviousness (HRL IMD) and Urban Atlas (UA) data, enhanced by registers such as: 1) population distribution (number of people registered at a given address), 2) issued building permits (geocoded to registration plots). The aim of the study was therefore to compare HRL IMD and UA data enhanced by administrative data for the study of urbanization processes. The analysis was made on the example of Silesia in Poland.

Methodology

As part of the research, the comparative characteristics of both data sets were prepared. The assessment was based on the following criteria against which datasets usefulness can be assessed in terms of urbanization studies:

1. Accuracy and precision in determining the extent of urban land cover and land use
2. Possibility to analyze the level of land investment
3. Possibility of isolating urban fabric and its changes
4. Possibility to designate the urban core, rural areas and transition zones
5. Possibility of studying the relationship between the distance from the urban core and the growth of urban fabric

For the purposes of assessing the possibility of using datasets, several operations and analyzes were performed consisting in combining Copernicus data with administrative data, including:

1. Imperviousness changes in inhabited areas (HRM IMD + population)
2. Population density on urban fabric (UA + population)
3. Changes in the range of the urban core, transition zone and rural areas (UA + HRL IMD + population)
4. Current investment activity in the light of LULC changes (UA + HRL IMD + building permits).

Results

One of the criteria taken into account when comparing the above-mentioned data sources is the accuracy and precision of determining the extent of urban land cover and land use areas. In this case, the most significant factors influencing the evaluation of both data sets are their format and the accuracy of the data producer's classification. It is worth noting that in the case of the preparation of HRL IMD data for 2018, they omit fewer objects than the Urban Atlas. On the other hand, when classifying the Urban Atlas for the previous years, the collected information was more detailed. In terms of overall investment level, HRL data combined with construction permit data is more useful than UA. This is due to the possibility of a more precise determination of the area of human activity. In the case of HRL IMD data without additional data sources, it does not enable detection urban fabric. Only the fusion with population data (e.g. geocoded cenzus data) and data aggregation allow for the designation of inhabited impervious areas. However, is not the same as housing development. The Urban Atlas data is therefore much more precise when it comes to detecting residential complexes. It is worth noting that for the designation of the city core, both data sets can be used. However, only the UA can be used without additional data. Fusion with population data or building permits results in better accuracy of the designated core and transition zone and opens up new possibilities e.g., the prediction of further spatial development and thus the characteristics of the directions of urbanization. Delimitation of the urbanized core with the use of HRL IMD data is possible only after fusion with population data. The precision of determining the number of the population to address points means that additional data aggregation is necessary. As a result, the detail of the obtained results is lower than in the case of UA data. The UA are therefore better suited for determining the urban core. In the case of the correlation of urban fabric growth and distance to the core, both datasets suffer from disadvantages. HRL allows the calculation of surface changes, but it is difficult to distinguish settlements. On the other hand, UA allows for the identification of settlement, but it is only possible to obtain information about the area of building complexes, not the built-up area.

Outlook for the future

UA and HRL IMD have a very large, still untapped potential in terms of urbanization research. An opportunity to use this potential may come from initiatives aimed at opening up data in cities, making administrative data more widely available. For this reason, it is worth knowing for what purposes the data from the Copernicus program are most useful.

Poster(s)

Crowdsourced observations and geospatial data for the modelling of butterfly distribution using MAXENT in Styria, Austria

Daniel Kulmer [1], Manuela Hirschmugl [1,2]

[1] University of Graz, Institute for Geography and Regional Sciences, Austria
[2] Joanneum Research, Institute DIGITAL, Graz, Austria

Keywords (5): Maxent, Crowd sourcing, land use, biodiversity, species distribution

The challenge

The use of crowdsourcing data for scientific purposes has gained much attention in the past years due to the increased number of crowd sourcing apps available to everybody. Compared to expert-based in-situ assessments, crowd-sourcing data has several potential disadvantages: first, the observation quality; second, the irregular location, number and distribution of the observations and third, the absence of non-observations. In our case, the quality (i.e. the type of butterfly observed) is relatively high, as observations are regularly checked and confirmed by experts. The location accuracy together with the irregular number and distribution of observations as well as the missing non-observations are the main challenges in this study. Distribution modelling is hampered by observations clustered in and around human settlements, leisure destinations and main hiking routes. The aim of this study therefore is to create an unbiased map of relative abundance of the butterfly family Nymphalidae as a basis for further research and better biodiversity protection and/or restoration with regard to SDG15.

Methodology

In terms of data, we use a set of existing geospatial data sets: land use information from the national cadastral land registration; agricultural use from the land parcel information system (LPIS); a map of biotopes from the federal environmental agency and meteorological data of the climate atlas Styria. All data was calculated to a grid of 500 x 500m. The in-situ observations of butterflies have been collected using two different crowdsourcing apps: “Blühendes Österreich” and GBIF.org. We merged the data from both sources to have the maximum amount of observations available for our analysis. Due to the above mentioned absence of non-observations, we use the “Maxent” (Maximum Entropy) tool for distribution modelling. Absence of non-observations means that we only get the observations of existence from the crowdsourcing apps, but do not know where no individuals of a species exist. In a first evaluation step, we use the quality parameter “area under the curve (AUC)” readily built-in within Maxent. First evaluation of the resulting data showed a high bias towards the settlements, which needs to be corrected. We used several options to calculate a bias layer: building density, observation density and a combination of both. The bias layer is used to factor out the bias from the result.

Results

Variable contribution can be determined by the increase in training gain (Feature contribution) or by permuting a variable and measuring the resulting drop in AUC (Permutation importance). From the input features used, the “Area Share Urban” and “Area Share Traffic” layers are the most important ones. This was to be expected, as most observations are done where many people live (bias). When employing a bias layer in the model, the dominance of these two layers is significantly reduced, e.g. for Areas Share Urban from 54.9 to 45,4 measured by permutation importance (building density as bias layer, see Table 1).

Table 1: Feature contribution (FC) and permutation importance (PI) values in percent with or without bias layer(s)

Bias layer ⍰	Without bias layer		observation density as bias layer		building density as bias layer		additive combination of observation & building	
	FC	PI	FC	PI	FC	PI	FC	PI
Area Share Urban	68.4	54.9	46.2	51.6	45.0	42.3	40,9	45,4
Area Share Traffic	11.0	12.1	18.3	27.2	14.0	24.2	21,2	24,7
Biotopes	1.7	1.9	1.2	2.8	5.9	3.6	6,1	8,5
Area Share Land Use Extensive	3.2	7.9	4.2	6.1	4.7	8.3	4,6	4,8
Temperature July	3.7	3.6	10.4	0	6.4	0	4,2	0

The results show a relatively stable model with AUC values around 0.7 regardless of the selection of input data (not shown for brevity) or of bias layer (see Fig. 1, ‘model data’). For more accurate and independent quality assessment, we divided the input data into training and evaluation data by random division in 90/10%. This is not the model-inherent split into training and testing data; instead, the validation data was completely left out of the modelling process. We consider the model best, if the mean probability value of the training data is highest, the standard deviation is smallest and the mean probability of the evaluation data is not significantly smaller than the one of the training data. The results in Figure 1 (a) show, that the use of a bias layer increases the mean probability by about 5 % and decreases the standard deviation. Based on this result, using observation and combined bias layer show slightly better results than building bias layer. Figure 1(b) depicts the distribution map without applied bias layer and using the combined bias layer in comparison.

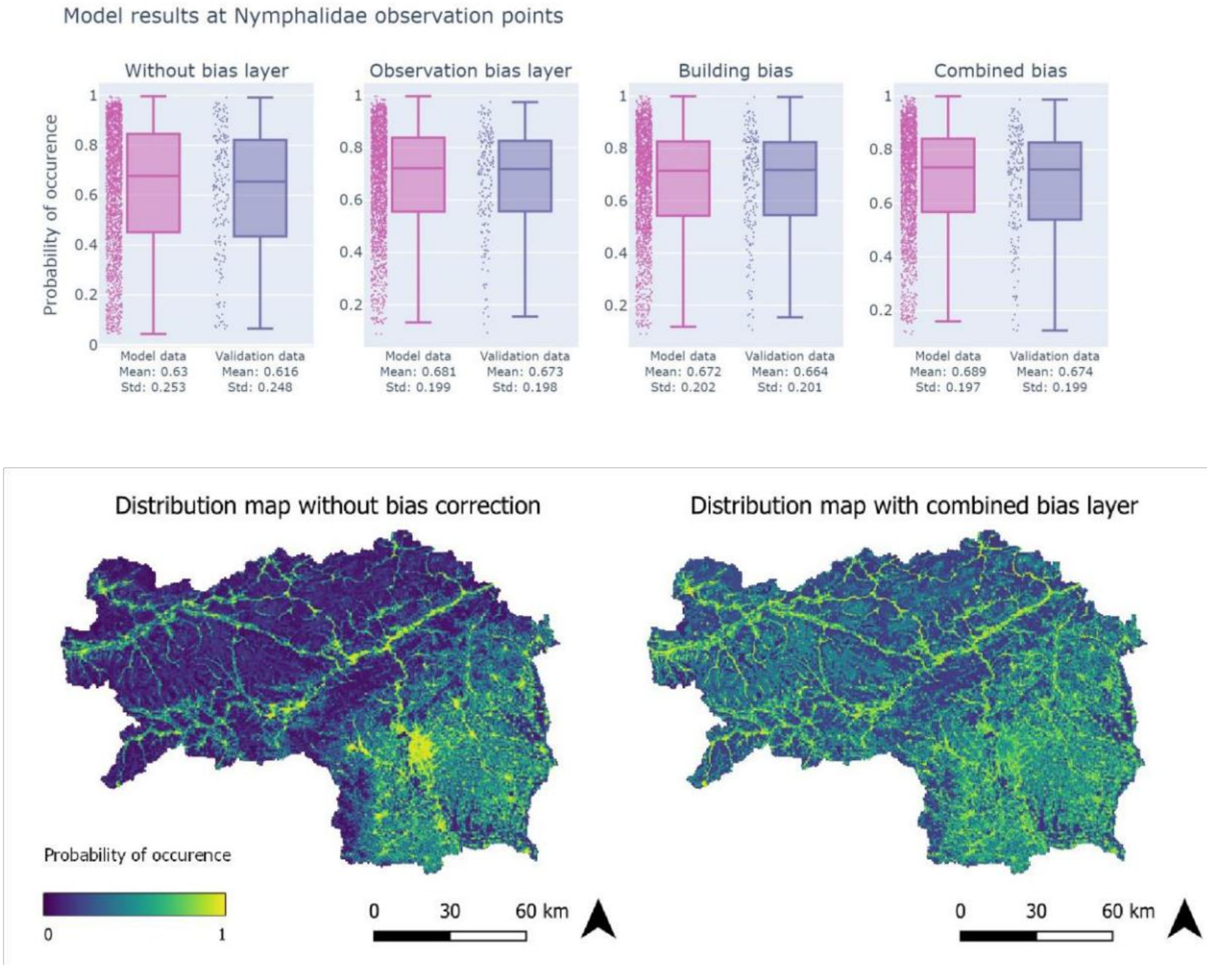

Figure 1 (a) Comparison of model and validation data without and with different bias layers **(b) Comparison of resulting distribution maps without and with combined bias layer**

Outlook for the future

Future work can comprise the use of alternative geospatial data sources, such as time series data of Sentinel-2 for dynamic land use information. Further, these model results should be employed in identifying hotspots to generate "stepping stone" areas for insect distribution. More work is also needed in the further development of the model, dealing with bias layers and the missing no-occurrence of species.

Estimation of solar radiation at ground level using SENTINEL 3 data and machine learning techniques: a case study in Cyprus.

Diofantos Hadjimitsis[1,2], George E. Georghiou[3], Silas Michaelides[1], Maria Prodromou[1,2], Argyro Nisantzi[1,2], Konstantinos Fragkos[1], Christiana Papoutsa[1,2], Rodanthi Mamouri[1,2], Eleni Loulli[1,2], Marina Pekri [1,2] Spyros Theocharides[3], Javier Lopez-Lorente[3], George Makrides[3]

[1] Eratosthenes Centre of Excellence, Limassol, Cyprus
[2] Cyprus University of Technology, Department of Civil Engineering and Geomatics, Limassol, Cyprus
[3] PV Technology Laboratory, FOSS Research Centre for Sustainable Energy, Department of Electrical and Computer Engineering, University of Cyprus, Nicosia, 1678, Cyprus

Keywords (5): Cyprus, machine learning, photovoltaic, remote sensing, solar radiation.

The challenge

The two main factors affecting the performance of renewable solar energy, namely the Land Surface Temperature (LST) and solar radiation, can be measured using satellite thermal bands. It is increasingly important that satellite-based estimations are validated against ground-based observations to ensure the availability of accurate and reliable data for energy yield and performance estimations. This study introduces an approach to estimating the surface downwelling global horizontal irradiance (GHI) using radiances datasets acquired from the Top of Atmosphere (ToA) via a machine learning model, specifically XGBoost, which is an optimized distributed gradient boosting model. The study comprises results from a ground station at the FOSS Research Centre of Sustainable Energy of the University of Cyprus (UCY) in Nicosia, Cyprus, and the current satellite mission (Sentinel-3).

Methodology

The process and analysis of Sentinel-3 data, for the period from June 2017 until December 2021, were implemented by using the Google Earth Engine web platform. In this platform, the open-source images acquired by several satellites are accessible and can be efficiently imported and processed in the cloud without the necessity of downloading the data to local computers. Time series of the radiances from the Level 1B data of the OLCI sensors onboard Sentinel-3 were created for the aforementioned period.

Measurements of the GHI are performed at the FOSS Research Centre using a thermopile pyranometer with a flat spectral response from 285 to 2800 nm. To ensure the highest reliability of the retrieved data all operational and maintenance procedures were complaint with the IEC 61724-1 standard. The sampling rate was 1-second, and 15-min averages were acquired through a data-acquisition platform. These data were used for the assessment of the estimated GHI derived from the combined use of Sentinel 3 data and machine learning techniques.

The methodology followed to develop the GHI estimation from the ToA radiance included the construction of an eXtreme Gradient Boosting (XGBoost) machine learning model. The training dataset for the model was randomly selected with a split train-test of 70-30%.

Moreover, the model's hyperparameters were tuned with a search algorithm and cross-validation. The input features or predictors used, were the 21 radiance spectral bands available in the Sentinel-3 OLCI, which range from the visible to the near-infrared spectra, and the mean solar zenith angle during the observation period. The field data used were those matching the timestamp of the satellite observations. Figure 1 shows a conceptual overview of the methodology.

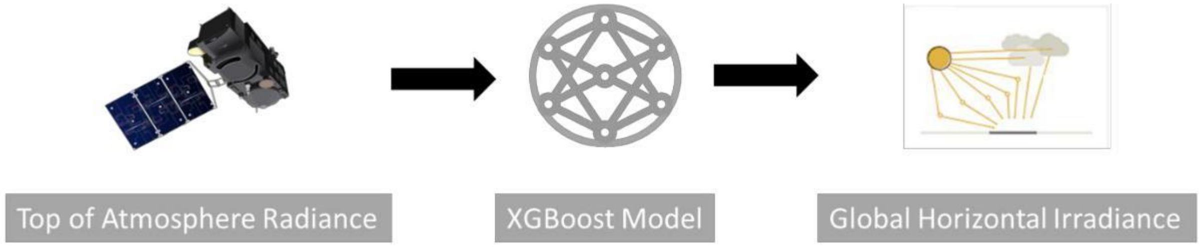

Figure 5 Methodology overview for the calculation of GHI using ToA radiance.

Results

The optimal XGBoost model, which resulted from 500 combinations of hyper-parameters, consisted of a Max. depth of 10, a learning rate of 0.2, the number estimators of 500, and a linear function booster. The model can estimate GHI with a 6.59% (45.3 W/m^2) mean absolute error (MAE) and minimal mean bias error (MBE) of 0.23% (1.55 W/m^2) and a coefficient of determination (R^2) of 0.88 as presented in Table 1. In addition, the agreement between the metrics of the train and test stages, which are close and slightly smaller in the training dataset, demonstrates that the model's tuning and cross-validation in the construction of the optimal model was able to deal with under- and over-fitting of the model.

Table 4 Performance Evaluation Results of the Training and Testing Sets.

Performance Metric	**Training**	**Testing**
R-squared (R^2)	0.86	0.88
MBE (W/m^2)	-0.05	1.55
MAE (W/m^2)	43.35	45.30
MBE (%)	-0.007%	0.23%
MAE (%)	6.23%	6.59%

Finally, Figure 2 shows the scattering of the estimated GHI data as calculated by the XGBoost model against the ground measurements of FOSS for the test dataset. It can be observed the high agreement reported by the performance metrics in Table 1. Based on the data fitting it can be concluded that the XGBoost model is able to model the attenuation of ToA radiance occurring in the atmosphere until reaching ground level with high agreement, minimal bias, and low error rates.

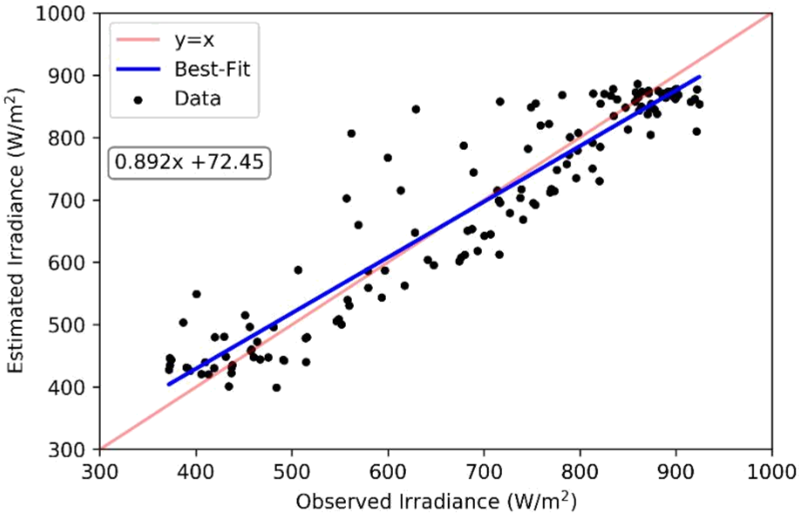

Figure 6 Scatter plot of Estimated against the Measured GHI for the test dataset.

Outlook for the future

The proposed methodology for the estimation of the ground level GHI using satellite data and XGBoost illustrates the possibility to apply machine learning models and avoid the modelling of the atmosphere's attenuation of solar radiation until ground level. The benefit of using Sentinel-3 data compared to other satellite missions is its increased spatial resolution of 300 m. Levering machine learning and this increased spatial resolution can bring additional insights and facilitate the assessment of solar radiation at ground level for multiple applications, from renewable energy to agriculture. Future work could investigate how the estimated GHI and other relevant variables such as LST can be utilised to derive the estimated PV power and compared against actual measurements or evaluate GHI estimations across small geographical areas that leverage the increased spatial resolution of the Sentinel-3 mission. Finally, the case studies could be expanded to other locations and climate conditions.

Acknowledgements

The authors acknowledge the 'EXCELSIOR': ERATOSTHENES: EXcellence Research Centre for Earth Surveillance and Space-Based Monitoring of the Environment H2020 Widespread Teaming project (www.excelsior2020.eu). The 'EXCELSIOR' project has received funding from the European Union's Horizon 2020 research and innovation programme under Grant Agreement No 857510, from the Government of the Republic of Cyprus through the Directorate General for the European Programmes, Coordination and Development and the Cyprus University of Technology.

S_OT: Other Topics

Chair(s): Maria Prodromou, Eleni Loulli

Detection of nature interventions in Sentinel-2 images of Norway using U-Net

Øivind Due Trier[1], Arnt-Børre Salberg[1], Ragnvald Larsen[2], Ole T. Nyvoll[2]

[1] Norwegian Computing Center, Section for Earth Observation, Norway
[2] Norwegian Environment Agency, Norway

Keywords: Undisturbed nature, road detection, deep learning, digital terrain model, gradient image.

The challenge

This paper presents a new method for automated detection of nature interventions in Sentinel-2 satellite images. The Norwegian Environment Agency is maintaining a map of undisturbed nature: areas 1 km or more from major infrastructure developments, such as roads, railways, built-up areas, power lines, hydropower dams and wind power plants. The main source for updating the map of undisturbed nature is the regular update of the national digital map series, based on aerial photography followed by manual photo interpretation. For urban areas, the update cycle is 1-3 years, but for rural areas, forests and mountain areas, the update cycle may be more than five years. Thus, alternative sources for updating the map of undisturbed nature were sought. The Sentinel-2 satellites provide weekly coverage of Norway in the form of multispectral images at 10 m resolution. Visual inspection of such images indicated that forest roads and construction roads may be detected by automatic methods.

Methodology

In recent years, deep neural networks are being used as the preferred method in many image detection tasks in remote sensing. The hypothesis in this study was that U-Net could be trained to detect new roads in Sentinel-2 images. U-Net is used in several image detection problems on remote sensing images. U-Net is a convolutional neural network originally developed for biomedical image segmentation in images with only one spectral band. We modified the U-Net architecture to accept input images with 10 spectral bands. The U-Net was trained and tested on cloud free Sentinel-2 image tiles of southern Norway from 2018-2021, and the months April-September. Images with snow covered roads were not used. The detection method was then implemented in an automatic pilot service. Each evening, new Sentinel2 images covering southern Norway, and with less than 10% cloud cover, were downloaded from https://scihub.copernicus.eu/dhus/. The pilot service was run during the summer of 2021 from 1 June until 1 October, both to demonstrate the usefulness of an automatic detection service and to identify necessary improvements. We wanted to investigate if the detection results could be improved by adding an extra input band derived from a digital terrain model (DTM). A DTM of Norway in 10 m resolution and in UTM zone 33N was downloaded from https://hoydedata.no. The DTM is derived from airborne lidar data with 2-10 points per m^2. From the DTM, a gradient image G was obtained by using Sobel's edge detectors. Then, in order for the gradient image to have roughly the same value range as the spectral bands, a scaling was needed.

We used $0.1\sqrt{}$.

Results

By running a few different variations of the method on the test data, which were not seen during training, the best results were obtained when U-Net was trained on all roads except tractor roads, and DTM gradient was added as an extra input band to U-Net. The true positive rate was 61 %, with 39 % false negative rate. The false positive rate was 23 %. However, the main purpose of the detection method was not to find existing roads, but to find new roads, built after 1 January 2018, not present in the current vector data. Since a correct ground truth for new roads was not available, it was only possible to do a visual inspection of predicted roads in the satellite images. In tile T32VMN, there were several predictions of new roads that seemed to be correct (Figure 1a-b). However, there were also predictions that were wrong (Figure 1c-d). Small creeks that were not included in the water mask were often mistaken as small roads (Figure 1c). Also, ridges of bare rock and gravel landslides were sometimes mistaken as roads, if they were long and narrow (Figure 1d). In tile T32VNR, there were also many predictions of new roads that appeared to be correct (Figure 1e-h). In one of these (Figure 1f), only parts of the new road were predicted. However, by using another image acquisition date, almost all parts of the new road were predicted. Several of the new roads were construction roads for wind power turbines (Figure 1g-h).

Outlook for the future

The false negative rate of the proposed method was high (39 %) when applied on individual image acquisitions. However, it was observed that a missing road at one acquisition date could be predicted at another date. Thus, a possible improvement of the method could be to accumulate road predictions from several image acquisition dates. The false positive rate (23 %) seemed to be high. A possible improvement could be to remove predictions that are clearly not connected to the existing road network, since building a new road in isolation is impractical for a number of reasons. Thus, predicted new roads that are, say, more than 200 m from the nearest existing road could be discarded. The 200 m gap may be needed since it may happen that parts of a new road is missing from a predicted new road. In conclusion, we have demonstrated that automated detection of new roads, for the purpose of updating the map of undisturbed nature, is possible. The method seems to work but needs considerable improvement before being applicable for the intended purpose.

Acknowledgements

We thank Jon Prøis Rustand, Asplan Viak, for providing vector data.

Comparison of Digital Elevation Models by Chernoff faces

José Rodríguez-Avi[1], Francisco José Ariza-López[2]

[1] University of Jaén, Department of Statistics and Operational Research, Spain
[2] University of Jaén, Department of Cartographic Engineering, Geodesy and Photogrammetry, Spain

Keywords (5): Chernoff faces, Basin morphometry, Morphometric analysis, Quality, graphics.

The challenge

The quality is based on the comparison of a product with a reference or pattern. In the case of Digital Elevation Models (DEM), it is possible to compare them using a large number of parameters (multivariate perspective) (e.g. slope, aspect, elevation, positional accuracy, etc.). A special case is the morphological comparison, where it is usual to use more than ten variables (e.g. stream length and ratio, form factor, drainage frequency, density and texture, bifurcation, elongation and circularity ratios, etc.). However, the use of numerous parameters makes it difficult to understand these comparisons. In addition, as indicated in numerous works, the quality of the product is not well understood in these cases. Our challenge is to propose a graphic form, close and understandable by users, to represent the results of a quality assessment. Our proposal is based on using Chernoff faces (JASA 1973, 68(342) pp 361-368), which consists of identifying each variable with a facial feature so that high values of the variable correspond to more outstanding features (better in the sense of interpretation of the variable considered).

Methodology

In this case, the methodology has been oriented towards several lines of work. Frist, a well-defined use case of DEM comparison has been sought. For this, a bibliographic search was carried out on the evaluation and comparison of several DEMs. As a result of this search, it was identified that morphological comparisons between DEMs are common and that there is an extensive set of morphological variables that are used very frequently. Second, a search focused on multivariate graphic representation techniques was also carried out. As a result of this search, it was decided to consider the use of Chernoff faces due to their expressiveness. Two additional lines of work that need to be worked on are, on the one hand, the selection of the variables to be considered. This is so because the Chernoff faces allow the representation of a certain number of variables. In this line, based on the analysis of references, it is intended to establish an order according to their frequency of use, in such a way that the first 14 will be considered as a general information mechanism. On the other hand, and no less complex, is the process of assigning the variables to the different features (for instance, mouth, eyes, nose, ears, etc.) that uses the Chernoff face-based representation. Expert users on the subject will be consulted here.

Results

The data comes from the work of Jain et al (doi: 10.1007/s10668-020-00652-x) in which four DEMs from satellites (SSRTM-GL1, AW3D30, GDEM-V2, CartoDEM-V3.1) are compared with a DEM derived from a map by digitizing contour lines and which is considered the reference. To adjust the information, the differences in each variable with respect to the reference base is considered. In this way, the best value is 0, and from here, the worse the value compared to the reference cartography. The assignment of morphological variables to the features of the face appears in the Table 1, whereas the graphical representation appears on Figure 1. This is a very expressive way to report the result of the comparisons. The reference face (labeled SOI Topo sheet) has been included and indicates the ideal case. The other faces must be interpreted in relation to this one.

Modified item	**Variable**
height of face	Watershed area
width of face	Perimeter
structure of face	Basin length
height of mouth	Total number of streams
width of mouth	Stream Length
smiling	Relief
height of eyes	Ratio bifurcation
width of eyes	Stream Length ratio
height of hair	Drainage density
width of hair	Stream frequency
style of hair	Drainage texture
height of nose	Circulatory ratio
width of nose	Relief (basin morphometry
width of ear	Ruggedness number

Table 5: Relation between variables and face's features

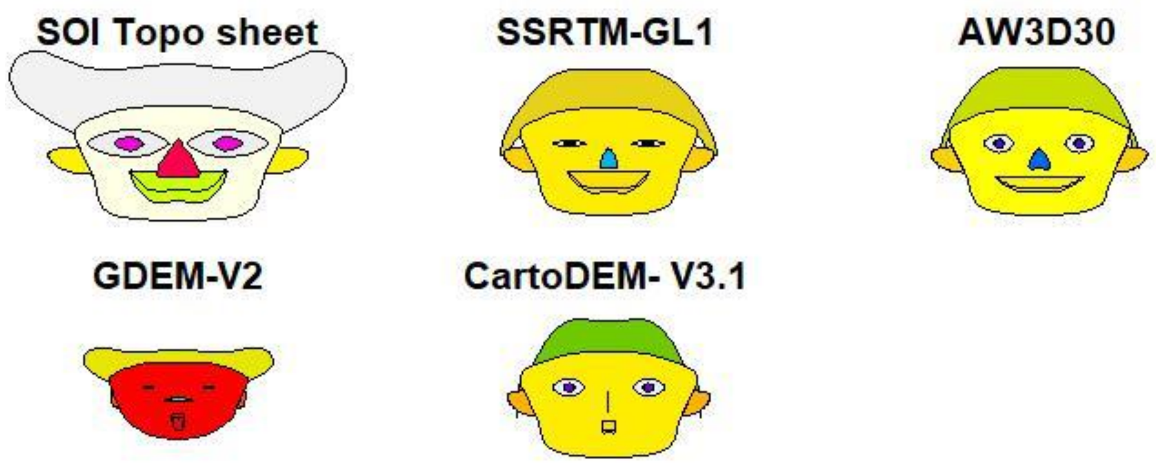

Figure 7: Chernoff faces for each DEM model.

Given that the variables in Table 1 have been ordered from worst (highest differences with respect to the reference) to best (smallest differences), the interpretation of the faces corresponds to the best presence of the features. Thus, the more prominent it is a feature, the better that model is for the associated variable relative to the others (remark that the optimal model is the labeled SOI Topo set, which is the reference, so all errors are 0)

Outlook for the future

In this document we have presented the idea and some initial results that we consider very interesting due to their ability to transmit the idea of quality in a simple and fast way. As indicated in the methodology, the selection of the variables to be used and the assignment to the features of the face are still to be developed. We have indicated that we intend to do this on a scientific basis and taking user feedback into account. The robustness of these two processes is key for us, as our goal is to establish a standard that facilitates comparability between DEM and the understanding of its quality through a graphic report. The example shown in this work is based on morphological aspects, but our interest is to apply it to other cases, such as positional accuracy and other quality components in DEMs. The use of asymmetric Chernoff faces or different faces for the same comparison is also another task that requires more research work in the future.

Topographic Position Index and height error of Digital Elevation Models

José Rodríguez-Avi[1], Francisco José Ariza-López[2], Juan Francisco Reinoso-Gordo[3].

[1] University of Jaén, Department of Statistics and Operational Research, Spain
[2] University of Jaén, Department of Cartographic Engineering, Geodesy and Photogrammetry, Spain
[3] University of Granada, Department of Architectural and Engineering Graphic Expression, Spain

Keywords (5): Topographic Position Index, height, error, DEM, PROXCAL MDS

The challenge

When determining errors in Digital Elevation Models (DEM), a variable that can influence their magnitude and distribution is the type of terrain. In this work we analyze the possible influence of the terrain landform classification generated by the Topographic Position Index (TPI) on the height error magnitude. A big drawback of the TPI calculation is that it depends on several parameters (minimum distance, maximum distance, and the neighborhood analysis area). This paper will analyze whether the different terrain classes derived from the TPI algorithm with different parameters generate similar error distributions between them. This could allow a better understanding of the height error distribution as well as the interest of these categories for the vertical accuracy assessment of DEMs.

Methodology

Two DEMs datasets of a mid-mountain area around the town of Allo in Navarra (Spain) are used: the DME02 product (reference) which has 2x2 meters of resolution, and the DME05, which has 5x5 meters resolution. The error is determined as error = MDE05 - MDE02. Through the TPI algorithm with different minimum and maximum distances (Dmin and Dmax) and a fixed circular neighborhood the following ten land form classes are generated: T1 (V-shape river valleys); T2 (Lateral midslope incised drainages); T3 (upland incised drainages); T4 (U-shape valleys); T5 (broad flat areas); T6 (broad open slopes); T7 (fat ridge tops, mesa tops); T8 (local ridge/hilltops within broad valleys); T9 (lateral midslope drainage divides); T10 (high narrow ridges, mountain tops). This classification is made in 14 scenarios generated by several combinations of Dmins and Dmaxs distances. For each landform class, the error distribution function is calculated. To compare them, a distance matrix is calculated, based on the Kolmogorov-Smirnov distance, of the errors of all classes against all classes, so that matrices (one for each scenario) of order 10x10 are obtained. To analyze the proximity of the zones in relation to the errors in height, a multidimensional scaling is carried out using a PROXCAL procedure for multiple input matrices. This allows to obtain a graphic representation of the differences between the different landforms and an aggrupation between the classes according to their proximity.

Results

Starting from the 14 scenarios considered, a total of 14 distance matrices of dimension 10x10 have been obtained. These matrices are the input for an individual differences PROXCAL procedure, which allows an analysis of both the difference between scenarios (SRC1 to SRC 14 in Figure (b)) and the relative position of the land form types in total and for each one of the scenarios. In the global analysis of the 14 cases, a regularity is observed in the obtained graphs, with certain significant groupings. In addition, it is observed that the best explanation in terms of STRESS is obtained mainly for the 3-dimensional analysis. The Table shows the coordinates obtained by selecting three dimensions (according to the STRESS criterion) for the individual differences model, while the corresponding graphical representation is shown in Figure (a).

Final coordinates: MDS for individual differences

	Dimension		
	1	2	3
T1	-0,137	-1,679	-1,616
T2	0,125	-0,550	-0,710
T3	-1,181	0,398	-1,232
T4	0,913	-1,048	1,647
T5	2,381	0,529	1,474
T6	-0,568	2,008	0,164
T7	0,284	-0,284	0,632
T8	-0,865	-0,598	-0,045
T9	0,003	0,361	-0,102
T10	-0,956	0,863	-0,212

Once the dimension of the analysis is selected, numerical coordinates are obtained for each landform in each scenario, and cluster analyses are performed to determine the way in which the types of terrain can be grouped. Finally, a comparison is made between the results of each type to analyze the stability of the solutions.

Outlook for the future

In this work, a statistical procedure is proposed that allows the analysis of DEM's errors and relate them to the landforms of the represented terrain. This opens possibilities to improve these analyses, on the one hand, by selecting other different zones to study the consistency of the clusters detected and/or proposing new allocation algorithms and scenarios. On the other hand, it can be used to compare different data acquisition methods and even propose versions where, in addition to the elevation error, other associated variables can be included, such as slope or orientation.

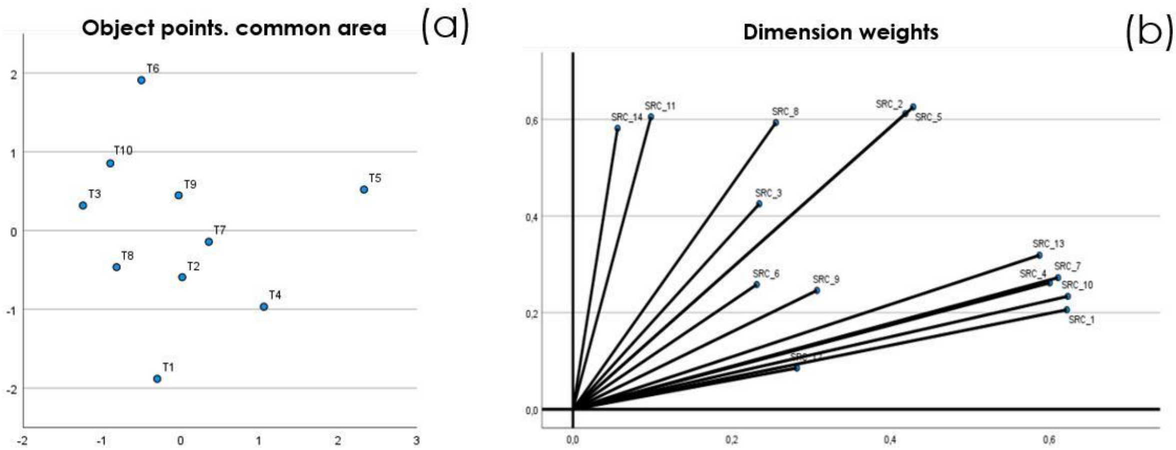

Figure 1 (a) Stimuli map (b) Dimension (scenarios) weights. Individual differences

What do the male and female testimonials from the Women in Copernicus survey tell?

Marine Nyssen[1], Caroline Closon, Nathalie Stéphenne[2], Barbara Riedler[3], Marie Jagaille[4] , Eleni Loulli[5,6]
(Style: Authors, presenting author underlined)

[1] University of xxx, Department of xxx, Belgium
[2] Service Public de Wallonie – SPW-, Geomatic Department, Belgium
[3] University of Salzburg, Austria
[4] University of Rennes, France
[5] ERATOSTHENES Centre of Excellence, Limassol, Cyprus
[6] Department of Civil Engineering and Geomatics, Faculty of Engineering and Technology, Cyprus University of Technology, Limassol, Cyprus

Keywords (5): Copernicus, Earth Observation, Gender equality, GIS, Gender bias

The challenge

Because of gender imbalance in STEM (science, technology, engineering, mathematics) education, gender inequalities are frequent in most STEM jobs and highest in Information Communication Technologies (ICT). Only 22% of AI programmer are women[7]. The space sector presents this bias gender pattern. From upstream (satellite development and space exploration) to downstream (use of Earth Observation data in Geoinformation analysis – EO&GI), women are present in this Copernicus ecosystem. Based on this assumption, the Women in Copernicus project aimed to make them more visible. The survey in 2020 gathered more than 450 answers from women and gave them a voice and even a face (see the website). However, their experience and their comments demonstrate barriers and feelings in their education and their everyday job life.

Methodology

The survey carried out in 2020 has been updated in 2022 to enlarge the audience. These surveys have been addressed to people working or having worked with Copernicus data or in the Copernicus domain of activities. The first one, translated in 7 languages, was divided 6 sections (demographics, background and career, barriers, facilitators, education choices and final). It has been disseminated on social media (LinkedIn and Twitter) and mailing lists and newsletters from more than 7 organisations including EARSC, NEREUS and EURISY.

In 2022, the second survey aimed to involve men in this gender analysis of the Copernicus sector. This second version included questions about qualities attributed to men and women to better understand the stereotypes. An Arabic translation has been added to increase the global audience. Quantitate answers and analyses of the first survey have been presented on the website and at several scientific events.

This paper focuses on the thematic analysis of the qualitative comments shared by the survey participants. we performed an analysis of each comment, identifying the theme they are

[7] https://eur-lex.europa.eu/legal-content/EN/TXT/PDF/?uri=CELEX:52020DC0152&from=EN

referring to. Then, we grouped these comments into categories and identified the most representative. Even if the WIC project was highly visible during these two years, the second survey gather really few new participants. Despite a men focus in the dissemination, it ends up with only 100 male participants. Moreover, the male participants proposed much less information in the qualitative comments

Results

This analysis defines and highlights some negative commonalities in the participants experiences expressed in terms of considering the profession as masculine and having issues in seeing a woman working in those fields. Women mention the lack of role models in the positions and in the organizations they work for. Women also regret the lack of good mentors in their career and the lack of recognition they suffer from their manager. Women also mention the male culture which can, in the worst cases, end up with harassment from their male coworkers. Mother who responded mentioned the fact that motherhood can impact their careers and can affect the balance between private and professional life. And finally, some of them suffer from lack of confidence.

The facilitators were less mentioned by women but is largely made of the support from family, friends and colleagues to follow their path. They also put forward support among women who can give confidence, help each other, inspire each other. They also identify the importance of role models in their life and career. Finally, for many participants the best facilitator is herself.

Outlook for the future

These results highlight that the realities presented in STEM domains are also found for women in EO&GI settings. Future studies should question how to change the situation of gender inequality in STEM. Studies and actions should involve men and women together in the fight for gender equality and change the education pattern to bring more girls and women into the sector. To reach the economic and sustainable Development Goal on gender8, men and women must lower gender imbalance. While men are also suffering from genre stereotypes, such as a strong masculinity request, this survey demonstrated that they are too few to be engaged to change the bias. We still must convince that we all can gain from more equality. Improvements in gender equality would lead to an additional 10.5 million jobs in 2050, which would benefit both women and men.9 The space-education for tomorrow can find some inspiration in WIC testimonials.

---

8 Progress on the Sustainable Development Goals: The gender snapshot 2021 | Digital library: Publications | UN Women – Headquarters

9 Economic Benefits of Gender Equality in the EU | European Institute for Gender Equality (europa.eu)

Figure 1 keywords occurrences in WOC testimonials

S_AI: Artificial Intelligence and Big Earth Data

Chair(s): Dr. Nektarios Chrysoulakis, Dr. Ioannis Varvaris

Machine And Deep Learning Tools Exploiting Earth Observation for Airport Geodata Production

Benjamin Beaumont[1], Dimitri Graur[1], Eric Hallot[1]

[1]Remote Sensing and Geodata Unit, Institut Scientifique de Service Public (ISSeP), Liège, Belgium

Keywords: Land Cover, Object Detection, Change Detection, Airport Management, Earth Observation

The challenge

The management of flows (aircrafts, service vehicles, goods, passengers...) within the complex environment of an airport requires accurate and up-to-date geodata. The SmartAirports project aims to develop GIS-based tools for optimizing flows, minimizing rotation time on apron side and smoothing real-time airport operations. Airport congestion can indeed result in passenger delays, additional in-flight and ground time, increased fuel consumption and emissions of harmful greenhouse gases. Multi-sensor Earth observation (EO) data can help to create reliable geodata and to dynamically monitor a whole series of airport elements.

Methodology

This paper proposes 4 approaches for extracting geodata applied to 4 EO datasets: Worldview-3 SUPERPIXEL (spat.res.15cm), aerial orthophotos (25cm), Pleaides (50cm), and Sentinel (1&2) time series. It assesses the robustness of these approaches on distinct geographical contexts: Belgian & Qatar airports.

(1) VHR data should theoretically allow for very high quality manual digitalization of many airport objects. The extraction of cartographic information on two classes of objects, water surfaces and vegetation, can benefit from an index thresholding approach (NDVI, NDWI), which limits manual work.

(2) An open-source OBIA processing chain (GRASSGIS7.8, R4.1.1, Python .9.5 & JupyterLab) is used to map airports' land cover features, using the VHR datasets. Main processing steps include import, preprocessing, segmentation, training, segment statistics, supervised classification and validation, among which only sampling remains manual.

(3) The third approach consists in building a robust aircraft object detector working on VHR data. We use the scaled YOLOv4-P7 model trained using the Rareplanes and AIRBUS public

datasets. A secondary objective is to reveal the contextual location of the detected planes (stands, runway) by combining the detection results with the ones from approaches 1 and 2.

(4) With short revisit times and an open access policy, Sentinel data are emerging as relevant data for change detection. A workflow running on the Terrascope platform automatically provides change indicators (Pruned Exact Linear Time method and threshold-based classification) to detect significant changes in the airport and its environment.

Results

On the Al Hamad airport (±20km², Doha, Qatar), the digitalization (approach (1)) of more than 550 objects by one operator requires approximately 4 hours. The following classes are digitized with high confidence (fig. (a)): runway, taxiway, apron, blastpad, aircraft, aircraft stand, building, car parking, painted centreline and runway exitline. The resulting data is the ideal ground truth for the training and validation of the more automated approaches.

Whether the OBIA processing chain (approach (2)) is applied to Qatar or Belgium airports, with any of the VHR data as input, the results do not differ significantly. In all cases, the overall accuracies range from 83.5% for a 10 classes map (fig. (b)) to 90.0% for a 5 classes map (ground artificial surface/vegetation/building/bare soil/water).

The results obtained from the deep learning model (approach (3); fig. (c)) can be summed up in several metrics: Precision: 96%; Recall: 100%; mAP@.5: 0.99; mAP@.5:.95: 0.89. By carefully analysing the results, the model makes mistakes only when aircrafts are not entirely visible within the 512x512 tiles, which could be corrected by varying the analysis window (overlap).

Approach 4 has the advantage of being fully automated and can detect significant conversions between four land cover categories: vegetation, water, building and soil. This detection is a good indicator to identify areas that need to be updated by the more precise approaches 1 & 2, and for example to initiate the programming of VHR data acquisition.

Outlook for the future

This research highlights the value brought by space-based data to airports management. Through the 4 tested approaches, integrating various machine and deep learning solutions, we demonstrate the added and combined value of each of them. Given the limited spatial extent of the sites studied, manual digitizing is a relevant solution when VHR data are available. Traditional machine learning approaches are still marred by manual creation of the training set and an error rate of over 10%. Deep learning, applied here to aircraft detection, demonstrates its efficiency equivalent to the quality of a digitization work, while being automatic. This technology is thus positioned as an unbeatable tool for the provision of high quality geodata at low cost.

Our first perspective is to apply deep learning to the detection of new objects (vehicles, containers...). Secondly, several semantic segmentation models will be tested in order to replace the machine learning based classification methods. This could help overcoming the high error rate of these approaches. Finally, all the tools will be integrated into an ORACLE-based infrastructure that can be transposed to any airport.

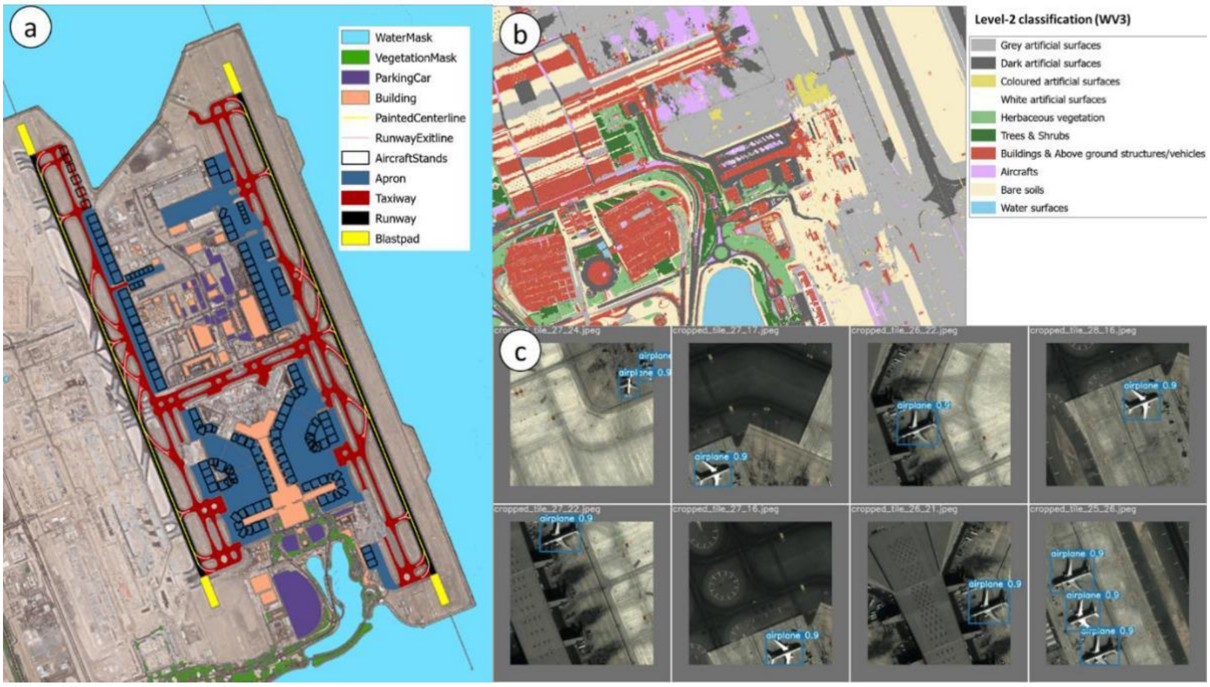

Figure. On the Al Hamad airport (Doha, Qatar), (a) results of the digitalization process, (b) automated land cover mapping (10 classes) and (c) aircrafts detection with confidence level.

Exploring The Potential of Future Satellite Imagers: Assessing the Hyperspectral Sensors' Soil Organic Carbon Predictive Capacity

Stylianos Kokkas[1], Nikolaos Tziolas[1], Nikolaos L. Tsakiridis[1,2], Konstantinos Karyotis[1], Georgios Zalidis[1]

[1]Aristotle University Of Thessaloniki, Laboratory Of Remote Sensing, Spectroscopy And Gis, Department Of Agriculture, Greece

[2]Aristotle University Of Thessaloniki, Automation And Robotics Laboratory, Department Of Electrical And Computer Engineering, Faculty Of Engineering, Greece

Keywords (5): Remote Sensing, Deep Learning, Soil modelling, CNN, AI

The challenge

The potential of spaceborne data is unveiled day after day through the development of Earth Observation (EO) based digital services. Over the next few years, it has been announced that the spectral satellite imagers fleet will be expanded with a set of hyperspectral sensors to be put into orbit. Each active mission can be employed for various applications, but when it comes to mapping soil physical and chemical properties, fine spectral and spatial resolution can play a significant role in calibrating robust models. This work describes an effort to present the capacities for Soil Organic Carbon (SOC) modeling of two existing multispectral optical imagers (Landsat 8 and Sentinel-2A) and explore the potential of the two soon to be operable hyperspectral missions, EnMAP (launched on the 1^{st} of April, 2022) and CHIME (to be launched on 2029), based on the spectral data of Land Use and Coverage Area frame Survey 2015 (LUCAS) soil spectral library (SSL) which was simulated to each of the above-mentioned sensors.

Methodology

Two state-of-the-art Artificial Intelligence (AI) algorithms, the commonly used Random Forest (RF) and a recently developed Convolutional Neural Network (CNN) were assessed in terms of their performance for SOC prediction based on LUCAS spectra. For the selection of optimal values of RF hyperparameters, a grid search on a five-fold cross-validation was conducted while for the CNN case, the proposed network is arranged in a series of five different types of layers, namely: (i) the input layers, through which the spectral signatures are provided as input to the network; (ii) the convolutional layers, which filters input and extracts information from specific spectral regions by through the convolution operation; (iii) the pooling layer, used to reduce the resolution of the spectral dimension; (iv) the flattening layer, converting the multichannel filters into a single continuous vector; (v) the dense layer, which connects all outputs of the previous layer through a series of fully-connected layers to the network's output. The LUCAS 2015 dataset, which contains 8917 topsoil spectral signatures (3 to 1 ratio cal val) from croplands and SOC laboratory analysis, was resampled to the spectral resolution of each sensor, centered to each sensor's band and was used for model calibration. For the multispectral sensors we employed the associated spectral response functions for the resampling, while on the other hand, for EnMAP and CHIME Gaussian functions were utilized. Further to the abovementioned cases, a full resolution modeling round was conducted, representing the SOC modeling through hyperspectral data ideal case scenario

Results

The estimation of SOC across the mineral-cropland soil samples of the LUCAS 2015 Soil Spectral Library are notable since the SOC was predicted with an RMSE of 8.71 g kg^{-1} and R^2 reaching a value of 0.58 using the RF model and an RMSE of 6.40 g kg^{-1} and R^2 = 0.77 with the proposed CNN. In comparison with the predictive performance values of the competing algorithms the CNN model significantly improved the performance predictions (R^2 = 0.74, RPD = 1.97) and decreased the RMSE to 6.67 g kg^{-1} for CHIME compared to the second-best performing algorithm (RF, R^2 = 0.57, RPD = 1.49 and RMSE = 8.77 g kg^{-1}). This performance increase is consistent also in the case of the second hyperspectral sensor (EnMAP) where the RMSE drops from 8.77 g kg^{-1} to 6.43 and the R^2 increases from 0.56 to 0.76 when comparing RF with CNN. SOC estimation with multispectral data showed poor performance results (R^2 0.21 for Landsat 8 and 0.23 for Sentinel-2A) but again, the CNN presented an increase in terms of accuracy metrics similar to the hyperspectral cases (R^2 = 0.40 for Landsat 8 and 0.39 for

Sentinel-2A respectively). As expected, the performances of the forthcoming hyperspectral imagers are significantly better than those of multispectral imagers for both AI models, and in terms of modeling techniques comparison, in all the cases the CNN model outperformed the RF approach. The modeling results for the prediction of SOC across the mineral-cropland soil samples of the LUCAS 2015 SSL are summarized in Table 1, where the performance metrics are given. These are notable results considering the distribution of the LUCAS 2015 dataset. The findings can be explained due to the multi-input architecture's potential to combine effectively the complementary information contained in the various spectral transformations that are used as input channels; a discreate feature that cannot be extracted by simple machine learning models. Compared with the resampled spectra LUCAS 2015 dataset, the accuracy of predictive models generally decreased when using resampled spectra for multispectral imagers. However, the performance metrics obtained from full-spectrum data for SOC estimation were similar to those obtained with the resampled hyperspectral spectra. Concretely, no significant differences were observed between full-spectrum (RMSE = 6.40 g kg^{-1}) and the two hyperspectral imagers (RMSE = 6.43 and 6.67 g kg^{-1} for EnMAP and CHIME, respectively).

Outlook for the future

The comparison of full-spectrum modeling for SOC prediction to hyperspectral imaging promises that the capacity of the forthcoming sensors starts converging to their full potential in terms of spectral resolution. This can be further explored to a wider set of key soil properties and minerals, since further to SOC, a broad set of parameters has proven to have observable correlations with Vis-NIR-SWIR reflectance. Since the soil ecosystem is very complex, constituting comprised of multiple variables, part of which evolve in time, there rises the need not only for optimizing the sensors' spectral resolution but also spatial and temporal as well. EnMAP marches towards this direction by providing a 4-day revisiting time which is a slight improvement compared to Sentinel's constellation of 5 days, but the current spatial coverage of 30 m might not be sufficient when it comes to small parcel monitoring. Due to these developments in hyperspectral imaging that will arise in the future, modeling should adapt efficiently. The aforementioned CNN could be converted from single output to multi-output, covering the range of important variables that the new Satellite missions will provide.

Table 1: Performance metrics of the AI algorithms of SOC prediction for the resampled multispectral and hyperspectral sensors

	RF			**CNN**		
LUCAS 2015	**R^2**	**RMSE g/kg**	**RPD**	**R^2**	**RMSE g/kg**	**RPD**
Full spectrum	0.58	8.71	1.50	0.77	6.40	2.03

CHIME	0.57	8.77	1.49	0.74	6.67	1.97
EnMAP	0.56	8.82	1.49	0.76	6.43	2.05
Sentinel-2A	0.23	11.56	1.14	0.40	10.17	1.29
Landsat 8	0.21	11.71	1.12	0.39	10.24	1.28

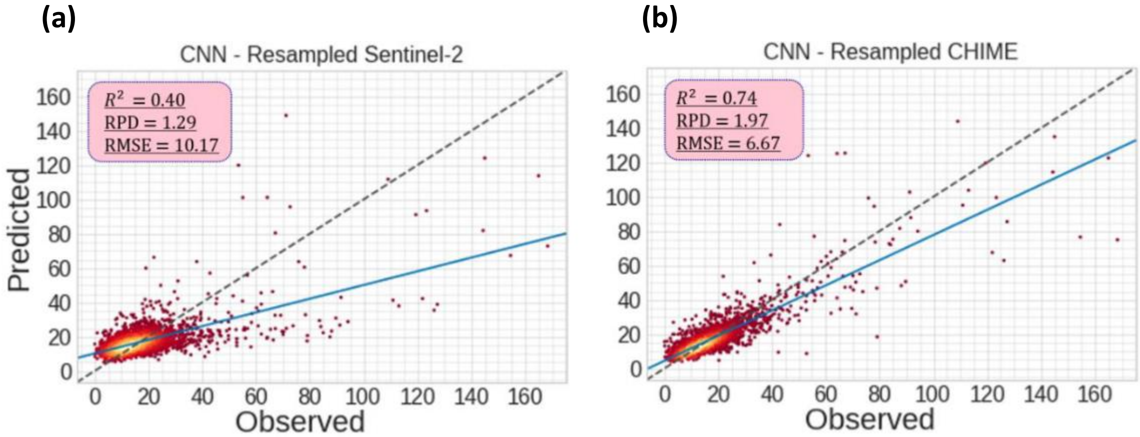

Figure 1: Goodness of fit indicating the relationship between observed and predicted SOC of the proposed CNN model using as inputs the resampled (a) Sentinel-2 and (b) CHIME

dataset of LUCAS 2015 SSL

Optimizing ground-based observations of global precipitation patterns

Johannes Bühl[1], Martin Radenz[1], Patric Seifert[1], Argyro Nisantzi[2], Rodanthi Mamouri[2], Ulla Wandinger[1], and Albert Ansmann[1]

[1] Leibniz Institute for Tropospheric Research (TROPOS), Leipzig, Germany

[2] ERATOSTHENES Center of Excellence, Limassol, Cyprus

Keywords (5): Cloud radar, precipitation, Cloudnet, global observations, principal component analysis

The challenge

Precipitation formation is a key process in Earth's hydrological cycle (Schneider et al, 2017). It keeps ecosystems running and is hence a major concern of current weather and climate research (Adler et al., 2017). Recent shifts in global precipitation patterns were pinned down with the help of large-scale measurement data (O'Gorman et al., 2015) and with numerical modeling (Lehmann et al., 2015). Still, the origins of these changes are obscure, because precipitation formation is complex and involves a large diversity of ice and liquid processes (Heymsfield et al., 2020).

The precipitation initiation temperature (PIT) at cloud top is critical for the kind of processes taking place inside of clouds during precipitation formation and the further evolution of the cloud system. For a given PIT, certain processes will not be active, while others will strongly influence precipitation formation. Observing and understanding of all these processes is necessary for keeping track of current changes and projecting future developments of precipitation formation (Koren et al., 2005; Rosenfeld et al., 2008; Myagkov et al., 2016; Bühl et al., 2019).

Precipitation originating from the ice phase is mostly initiated at cloud top and precipitation particles fall downwards through the whole temperature profiles of the clouds. Cloud properties relevant for precipitation formation like liquid water path, ice nucleation processes, ice crystal growth and the efficiency of secondary ice formation and ice multiplication are all dominated by ambient temperature (Korolev et al., 2020). Most of these processes are restricted to a certain temperature interval (e.g., -3…-8 °C for secondary ice formation) or have a distinct onset temperature (e.g., -26 °C for deposition freezing). Convective precipitation including warm rain is not tied strongly to the actual cloud top but the cloud top temperature is still an important parameter in these processes (Senf et al., 2017). However, the difficult differentiation between warm or cold precipitation events from spaceborne observations is out of focus of the current paper (Mülmenstädt et al., 2015).

Methodology

The distribution of global precipitation initiation temperature is analyzed with a data-driven approach based on data from the cloud profiling radar aboard of CloudSat satellite. A principal component analysis technique is applied to identify regions with similar precipitation characteristics. 'Similarity' between long-term histograms of precipitation initiation temperature for two given locations on Earth is mathematically defined via their Pearson correlation coefficient. The method is subsequently used to analyze the sensitivity of ground-based remote-sensing networks to patterns of precipitation initiation temperature globally. Gaps in the observation capabilities of current ground-based remote-sensing networks are identified and tentative suggestions for optimizing the global sensor distribution are made.

Results

Networks of ground-based networks are found to be capable to measure a representative picture of global precipitation characteristics, if sensors are suitably distributed. The present study quantifies this effect in terms of a correlation coefficient and suggests that about six additional stations would allow a significant increase in coverage of precipitation patterns world-wide.

Outlook for the Future

The present study indicates that it is sensible to add new permanent cloud-observing capabilities in certain areas of Africa, South America and South-East Asia to the existing ACTRIS-Cloudnet network. The ECoE on Cyprus could help hereby serve as a role model for founding of novel stations.

Copernicus for Urban Resilience in Europe: Intermediate results from the CURE project

Nektarios Chrysoulakis[1], Zina Mitraka[1], Mattia Marconcini[2], David Ludlow[3], Zaheer Khan[3], Brigitte Holt Andersen[4], Tomas Soukup[5], Mario Dohr[6], Alessandra Gandini[7], Jürgen Kropp[8], Dirk Lauwaet [9], Christian Feigenwinter[10]

[1]FORTH, Institute of Applied and Computational Mathematics, Remote Sensing Lab, Greece

[2]DLR, Deutsches Zentrum für Luft- und Raumfahrt, Germany

[3]University of the West of England, Bristol, United Kingdom

[4]CWare ApS, Denmark

[5]Gisat S.R.O., Czech Republic

[6] GeoVille Informationssysteme und Datenverarbeitung GMBH, Austria

[7]TECNALIA, Fundacion Tecnalia Research & Innovation, Spain

[8] PIK, otsdam Institut fuer Klimafolgenforschung, Germany

[9] VITO, laamse Instelling voor Technologisch Onderzoek N.V., Belgium 10 Universitaet Basel, Switzerland

Keywords: Urban Resilience, DIAS, Thermal Comfort, Air Quality and Health, Urban Flood and Subsidence Risks

The challenge

A major challenge for the urban community is the exploitation of the Copernicus products in dealing with the multidimensional nature of urban sustainability towards enhancing urban resilience. The H2020-Space project CURE (Copernicus for Urban Resilience in Europe) aims to synergistically exploit Copernicus Core Services to develop an umbrella cross-cutting application for urban resilience at several European cities. CURE is expected to provide the urban planning community with spatially disaggregated environmental information at local scale. It uses DIAS (Data and Information Access Services) to develop a system integrating this application, capable of supporting operational applications and downstream services across Europe in the future. Furthermore, CURE is expected to provide scenarios on how the developed system could potentially be integrated into the existing Copernicus service architecture addressing also its economic feasibility.

Methodology

The innovation potential of CURE lies on the exploitation of the Copernicus offer in the domain of urban resilience. CURE develops cross-cutting applications combining products from CLMS (Copernicus Land Monitoring Service), CAMS (Copernicus Atmospheric Service), C3S (Copernicus Climate Change Service) and EMS (Copernicus Emergency Service) with third-party data, and a system for integrating these applications, enabling its incorporation into operational applications and downstream services across Europe in the future. An active co-creation process, involving potential users, enables an effective and dynamic knowledge exchange to ensure that demands and needs are addressed. 11 cross-cutting applications reflecting specific urban sustainability dimensions (climate change adaptation and mitigation, healthy cities and social environments, energy and economy) are developed, as parts of the CURE umbrella cross-cutting application. These are based on state-of-the-art methods developed in past projects, which are improved and adapted to Copernicus in CURE. Each application is developed and evaluated for one or more of the CURE front-runner cities (Berlin, Copenhagen, Sofia and Heraklion). The CURE system is developed as a DIAS Service, including the hardware components set-up (processing units and storage), and the software design (interaction between those components, information provided by the platform and the deployed applications in a cloud computing environment).

Results

The WEkEO platform has been selected for the development of the CURE system as a DIAS Service. The baseline design of the CURE system is shown in the following Figure. This includes the set-up of hardware components, such as processing units and storage, as well as the software design and the interaction between those components, the information provided by the platform and the deployed applications in a cloud environment. The CURE system was built on two sub services: the CURE Master and the Application Nodes. A container-based approach was applied, where each step of the workflow was provided by an encapsulated Docker container. Eleven cross-cutting applications between CLMS, CAMS, C3S and EMS were dockerized and integrated in the Application Nodes of the CURE system. They are considered as parts of an umbrella cross-cutting application on urban resilience and they are based on state-of-the-art methods that have been developed in past projects. However, in CURE, these methods were improved and adapted to the above Copernicus Core Services. More specifically, they concern: AP01 - Local Scale Surface Temperature Dynamics; AP02 - Surface Urban Heat Island Assessment; AP03 - Urban Heat Emissions Monitoring; AP04 - Urban CO2 Emissions Monitoring; AP05 - Urban Flood Risk; AP06 - Urban Subsidence, Movements and Deformation Risk; AP07 - Urban Air Quality; AP08 - Thermal Comfort; AP09 - Urban Heat Storage Monitoring; AP10 - Nature Based Solutions; and AP11 - Health Impacts (socioeconomic perspective). Each method is separately given below, explaining how each application (AP01 - AP11) makes use of products derived from at least two Copernicus Core Services.

Outlook for the future

CURE is expected to lead to more efficient routine urban planning activities with obvious socioeconomic impact, as well as to more efficient resilience planning activities related to climate change mitigation and adaptation, resulting in improved thermal comfort and air quality (societal benefit), as well as in enhanced energy efficiency (economic benefit). In a broader context, mitigation and adaptation actions that enhance the resilience of cities need to be based on a sound understanding and quantification of the drivers of urban transformation and vulnerability, as defined in SDGs and the New Urban Agenda. An ever-growing number of European cities is putting environmental sustainability at the core of their urban development strategies (e.g., Covenant of Mayors). Local authorities benefit from the development of tools such as the CURE system, to streamline environmental data collection and management and to facilitate the exchange of information and best practices at all levels. Therefore, CURE is able to support the implementation of these polices, because it provides analysis at different scales, facilitating the comprehension of the underlying mechanisms that drive environmental problems in cities. This will benefit from a site level perspective and thus support the identification of priorities for policy intervention at the city level.

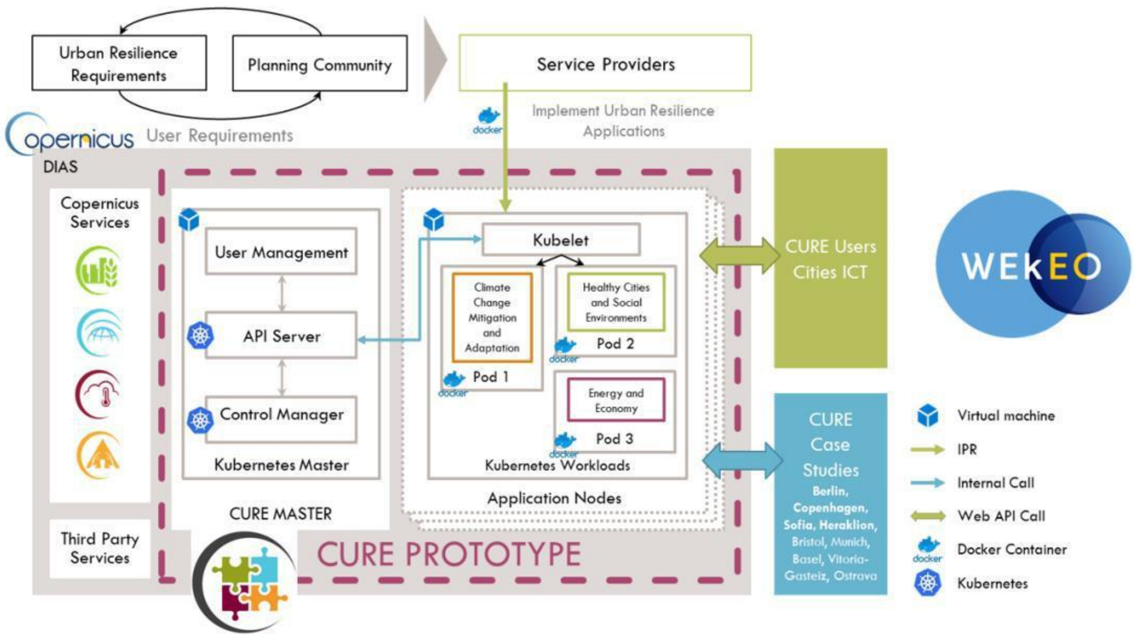

Figure Baseline design of the CURE system